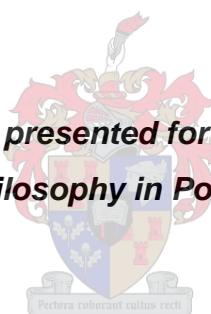


**SYNTHESIS AND CHARACTERIZATION OF TWO NOVEL
URETHANE MACROMONOMERS AND THEIR
METHACRYLIC/URETHANE GRAFT COPOLYMERS**

by

Abubaker Alshuiref

*Dissertation presented for the degree of
Doctor of Philosophy in Polymer Science*



at the

University of Stellenbosch

Promoter: Prof R. D. Sanderson

March 2010

DECLARATION

I, the undersigned hereby declare that the work contained in this thesis is my own original work and has not previously, in its entirety or in part, been submitted at any university for a degree.

Signature:

Date:

ABSTRACT

Polymethacrylates are well known adhesives and can carry specific functionality, but have the disadvantage that their flexible backbones impart limited thermal stability and mechanical strength. Polyurethanes (PUs) are finding increasing application and use in many industries due to their advantageous properties, such as a wide range of flexibility combined with toughness, high chemical resistance and excellent weatherability. PUs do however have some disadvantages, for instance, PU is considered an expensive polymer, especially when considered for solvent based adhesives. the focus of this study was to consider a largely unstudied area of PU chemistry, namely combining PUs with polymethacrylates.

Two types of linear urethane macromers (UMs) UM1 and UM2 were synthesized by the polyaddition polymerization of 4,4'-methylenediphenyl diisocyanate (MDI) with ethylene glycol (EG), and MDI with neopentylglycol (NPG), via a pre-polymer method, followed by termination with 2-hydroxy ethylacrylate (2-HEA) and methanol (MeOH) to yield UMs having specific urethane chain lengths, and which have to be predominantly monofunctional. Structural identification of the UMs was verified by MALDI-TOF-MS, FTIR, ^{13}C -NMR and ^1H -NMR spectroscopy.

Various percentages of the respective UMs (0-55 wt % of methacrylate monomers) were then incorporated into polymethyl methacrylate (PMMA) and poly n-butyl methacrylate (PnBMA) backbones via solution free-radical copolymerization. The resulting methyl methacrylate-g-urethane and n-butyl methacrylate-g-urethane copolymers were characterized by ^1H -NMR, ^{13}C -NMR, FTIR, SEC with double detectors (UV and RI), light scattering, UV-Vis, HPLC, TGA, DSC, DMA and TEM. Weight percentages of UM incorporated into the methyl methacrylate-g-urethane copolymers were calculated using FTIR, UV-Vis and ^1H -NMR techniques. Phase separation which occurred between the urethane segment and methacrylate segment in the graft copolymerization products was investigated by DMA, DSC and TEM analysis.

Microphase separation occurred in all PMMA-g-UM1 and PnBMA-g-UM1 copolymers: two glass transitions temperatures corresponding to the PMMA or PnBMA and UM1 fractions, respectively, were observed. On the other hand, DMA and DSC results showed that in most graft copolymer products the two respective component parts PMMA-g-UM2 or PnBMA-g-UM2 were compatible, because only one T_g was observed. Two glass transitions occurred for PMMA or PnBMA and UM2 when the amount of UM was increased to 55 wt % during copolymerization and microphase separation was evident in DSC, DMA and TEM measurements.

Thermal stability and storage modulus (stiffness) of all the synthesized PMMA-g-urethane and PnBMA-g-urethane copolymers increased as the concentration of urethane macromonomer in the copolymerization feed increased, as confirmed in TGA and DMA results. The surface and adhesive properties of the synthesized graft copolymer were studied by measuring the static contact angle and peel strength. Adhesion increased as the content of UMs increased in the graft copolymer. The graft copolymers prepared using a high UM2 feed for both PMMA and PnBMA showed improved in adhesion compared to the pure methacrylate polymers. The adhesion was better for both leather and for vinyl.

OPSOMMING

Polimetakrilate is bekende kleefstowwe. Hulle het egter die tekortkoming dat hulle buigbare ruggraat beperkte termiese en meganiese stabiliteit besit. Poliuretane (PUs) word deesdae al hoe meer gebruik in baie nywerhede as gevolg van hulle baie voordele, insluitend hul wye buigsaamheid tesame met sterkte, hoë chemiese weerstand en uitstekende weerbaarheid. PUs het egter 'n paar nadele: hulle is baie duur, veral wanneer hulle gebruik word in oplosmiddel-gebaseerde kleefstowwe. Die doel van hierdie studie is om die kombinerings van PUs met polimetakrilate te bestudeer, 'n onderwerp wat tot dusver baie min aandag-getrek het.

Twee tipes liniêre uretaanmakromere (UMs), UM1 en UM2, is gesintetiseer deur gebruik te maak van poliaddisiepolidimerisasie van 4,4'-metileendifeniel diisosianaat (MDI) met etileenglikol (EG), en MDI met neopentielglikol (NPG), via 'n prepolimeermetode, gevolg deur terminering met 2-hidroksiëtielakrylaat (2-HEA) en metanol (MeOH). Die produk hiervan is UMs met spesifieke kettinglengtes (hoofsaaklik monofunksioneel). Die samestelling van die UMs is met behulp van die volgende gevorderde analitiese tegnieke bepaal: MALDI-TOF-MS, FTIR, ^{13}C -NMR en ^1H -NMR.

Verskillende hoeveelhede van die UMs (0-55 gewling% metakrylaatmonomere) is dan in die polimetielmetakrylaat (PMMA) en poli-n-butielmetakrylaat (PnBMA) ruggrate geïnkorporeer deur middel van oplossing-vryradikaalpolimerisasie. Die samestelling van die kopolimeerprodukte, metiel-metakrylaat-g-uretaan en n-butielmetakrylaat-g-uretaan, is met behulp van die volgende gevorderde analitiese tegnieke bepaal: ^1H -NMR, ^{13}C -NMR, FTIR, SEC met dubbele detektors (UV en RI), ligverstrooiing UV-Vis, HPLC, TGA, DSC, DMA en TEM. Die hoeveelheid UM geïnkorporeer in die metielmetakrylaat-g-uretaan kopolimere is bereken deur gebruik te maak van FTIR, UV-Vis en ^1H -NMR data. Die faseskeiding wat plaasgevind het tussen die uretaansegment en die metakrylaatsegment in die produkte van die entpolimerisasie is met behulp van DMA, DSC en TEM ondersoek.

In alle PMMA-g-UM1 en PnBMA-g-UM1 kopolimere het mikrofaseskeiding plaasgevind: twee verskillende glasoorangstemperature vir die PMMA of PnBMA en UM1 fraksies is waargeneem. Hierteenoor het DMA en DSC resultate getoon dat in die meeste entkopolimeerprodukte (PMMA-g-UM2 of PnBMA-g-UM2) was die twee komponente verenigbaar, aangesien net een T_g waargeneem is. In die geval van die kopolimere waar die hoeveelheid UM in die kopolimerisasiereaksies tot 55 gew% verhoog is, is twee glasoorangstemperature vir PMMA of PnBMA, en UM2 waargeneem. Mikrofaseskeiding is met behulp van DSC, DMA en TEM bewys.

Termiese stabiliteit en stoormodulus (styfheid) van alle gesintetiseerde PMMA-g-

uretaan en PnBMA-g-uretaan kopolimere het toegeneem namate die uretaankonsentrasie in die kopolimerisasie-reaksie toegeneem het soos deur middel van TGA en DMA resultate bewys is. Die oppervlakte- en kleefeienskappe van die bereide entkopolimere is bestudeer deur die statiese-kontakhoek en skilkrug te meet. Adhesie het toegeneem namate die UM-inhoud toegeneem het. Die entkopolimere berei met hoër PMMA en PnBMA inhoud het uiteindelik beter adhesie getoon as die suiwer metakrilaatpolimere. Die adhesie was beter vir beide leer en viniel.

Dedicated to my wife and my parents

Acknowledgments

I would like to extend my thanks to Prof. R.D. Sanderson who has been a determined guide and consultant throughout my study.

I would also like to thank the Libyan International Center for Macromolecular Chemistry and Technology (Tripoli) for their financial support and giving me the opportunity to study in this field.

I would like to thank the Institute of Polymer Science at the University of Stellenbosch who welcomed me and provided me with the opportunity to further my studies. I feel very fortunate to have been able to attend lectures and conferences with this extraordinary department.

I would like to thank Dr. M.J. Hurndall, for patiently assisting me with my English and scientific writing of the thesis.

I would like to thank the all the staff and students at Polymer Science for their assistance and encouragement.

I would like to thank Plascon Research Center for the use of their analytical laboratory.

I would also like to extend my gratitude to my wife and my parents for their guidance and unwavering support throughout my life. They were behind me at every step in my life, even when I didn't really know where I was going and helped to show me where I should always find my direction. I can only hope to show the same kind of dedication and love to them.

Table of contents

Chapter 1

Introduction and objectives	1
<i>1.1 Introduction</i>	<i>1</i>
<i>1.2 Aim</i>	<i>4</i>
<i>1.3 Objectives</i>	<i>4</i>
<i>1.4 Layout of thesis</i>	<i>5</i>
<i>1.5 References</i>	<i>6</i>

Chapter 2

Theoretical background	9
<i>2.1 Polyurethanes</i>	<i>9</i>
2.1.1 History and application of polyurethanes.....	10
2.1.2 Basic reagents used for the preparation of linear polyurethanes	12
2.1.2.1 Isocyanates	12
2.1.2.2 Polyols.....	18
2.1.2.3 Catalysts.....	18
2.1.3 Methods of preparation of polyurethanes.....	18
2.1.3.1 The melt-dispersion process.....	18
2.1.3.2 The solution process	18
2.1.3.3 The prepolymer process.....	19
2.1.3.4 The ketimine and ketazine process.....	19
2.1.4 Health aspects of isocyanates.....	19
<i>2.2 Polyacrylates</i>	<i>20</i>
2.2.1 Introduction.....	20
2.2.2 Preparation of polyacrylates	21
2.2.2.1 Solution polymerization.....	21
2.2.2.2 Emulsion polymerization	22
2.2.3 Applications of polyacrylates.....	22
2.2.4 Urethane acrylate oligomers	22
<i>2.3 Graft copolymers</i>	<i>23</i>
2.3.1 Synthesis of graft copolymers	25

2.3.1.1	Grafting from	25
2.3.1.2	Grafting onto	26
2.3.1.3	Grafting through.....	26
2.3.2	Macromonomers	27
2.3.2.1	Synthetic methods leading to the preparation of well defined macromers.....	27
2.4	<i>Free radical polymerization</i>	28
2.4.1	Free radical copolymerization	28
2.4.2	Reactivity of macromonomers in homopolymerization and copolymerization reactions.....	30
2.4.3	Polymer-polymer phase separation	31
2.4.4	Examples of interpenetrating polymer network and copolymers with linear polyurethanes (acrylic-polyurethane copolymers)	33
2.5	<i>References</i>	35

Chapter 3

Analytical methods	43	
3.1	<i>Fourier transform infrared spectroscopy</i>	43
3.2	<i>Matrix-assisted laser desorption/ionization</i>	44
3.3	<i>Nuclear magnetic resonance spectroscopy</i>	44
3.4	<i>Size exclusion chromatography</i>	45
3.5	<i>Light scattering</i>	45
3.6	<i>High-performance liquid chromatography</i>	45
3.6.1	Gradient elution liquid chromatography.....	46
3.7	<i>Ultraviolet/visible spectroscopy</i>	46
3.8	<i>Dynamic mechanical analysis</i>	46
3.9	<i>Dynamic thermogravimetry</i>	47
3.10	<i>Transmission electron microscopy</i>	47
3.11	<i>Differential scanning calorimetry</i>	47
3.12	<i>References</i>	48

Chapter 4

Synthesis and characterization a of novel urethane macromonomer (UM1) and
methacrylic/urethane graft copolymers

50

4.1	Introduction.....	50
4.2	Synthesis of urethane macromonomer (UM1).....	50
4.2.1	Introduction.....	50
4.2.2	Reagents	51
4.2.3	Experimental setup	51
4.2.4	Urethane macromonomer formulations.....	52
4.2.5	Experimental procedure	52
4.3	Synthesis of methacrylic-urethane graft copolymers	54
4.3.1	Introduction.....	54
4.3.2	Experimental	54
4.3.3	Choice of solvent	54
4.3.4	Materials	54
4.3.5	Purification of the monomers.....	55
4.3.6	Methacrylic-urethane copolymer formulations.....	55
4.3.7	Experimental procedure	56
4.4	Characterization of UM1 and methacrylate-g-urethane copolymers	57
4.4.1	Fourier transform infrared spectroscopy.....	57
4.4.2	Matrix-assisted laser mass spectrometry.....	58
4.4.3	¹ H-NMR	58
4.4.4	¹³ C-NMR	58
4.4.5	Size exclusion chromatography.....	58
4.4.6	Light scattering	58
4.4.7	Gradient polymer elution chromatography.....	59
4.4.8	Ultraviolet/visible spectroscopy.....	59
4.4.9	Thermogravimetric analysis.....	59
4.4.10	Dynamic mechanical analysis.....	60
4.4.11	Differential scanning calorimetry	60
4.4.12	Transmission electron microscopy.....	60
4.5	Results and discussion	60
4.5.1	Formation of urethane macromonomer (UM1)	60
4.5.1.1	FTIR analysis.....	61
4.5.1.2	Matrix-assisted laser mass spectrometry	62
4.5.1.3	¹ H-NMR analysis.....	74

4.5.1.4	¹³ C-NMR analysis	76
4.5.1.5	SEC analysis	77
4.5.2	Methacrylic-urethane graft copolymer formation	77
4.5.2.1	SEC analysis	77
4.5.2.2	Extraction of unreacted macromonomer	80
4.5.3	Characterization of graft copolymers after extraction.....	82
4.5.3.1	SEC analysis	82
4.5.3.2	GPEC analysis.....	83
4.5.3.3	Light scattering	88
4.5.3.4	FTIR analysis.....	89
4.5.3.5	UV-Vis spectroscopy analysis.....	93
4.5.3.6	¹³ C-NMR analysis	95
4.5.3.7	¹ H-NMR analysis.....	96
4.5.4	Thermal and mechanical analysis.....	100
4.5.4.1	Thermogravimetric analysis	100
4.5.4.2	Dynamical mechanical analysis	107
4.5.4.3	Differential scanning calorimetry	113
4.5.5	Transmission electron Microscopy.....	115
4.6	<i>Conclusions</i>	116
4.7	<i>References</i>	117

Chapter 5

Synthesis and characterization of a novel urethane macromonomer (UM2)

methacrylic/urethane

graftcopolymers..... 121

5.1	<i>Synthesis of urethane macromonomer (UM2)</i>	121
5.1.1	Introduction.....	121
5.1.2	Raw materials.....	121
5.1.3	Experimental setup	122
5.1.4	Urethane macromonomer formulations.....	122
5.1.5	Experimental procedure	122
5.2	<i>Synthesis of methacrylic-urethane graft copolymers</i>	
5.2.1	Methacrylic-urethane copolymer formulations.....	124
5.3	<i>Characterization methods</i>	124
5.4	<i>Results and discussion</i>	124
5.4.1	Urethane macromonomers (UM2)	125
5.4.1.1	Fourier-transform infrared spectroscopy	125

5.4.1.2	MALDI-TOF-MS.....	126
5.4.1.3	¹ H-NMR analysis.....	131
5.4.1.4	¹³ C-NMR analysis	132
5.4.1.5	SEC analysis	134
5.4.2	Methacrylic-urethane graft copolymer formation	135
5.4.2.1	Extraction of unreacted macromonomer	136
5.5	<i>Characterization of graft copolymers after extraction</i>	137
5.5.1	SEC analysis	137
5.5.2	Gradient elution HPLC	139
5.5.2.1	GPEC of PMMA-g-UM2 copolymers	139
5.5.2.2	GPEC of PnBMA-g-UM2 copolymers.....	142
5.5.3	Light scattering	144
5.5.4	FTIR analysis.....	144
5.5.4.1	PMMA-g-UM2 copolymers	144
5.5.4.2	PnBMA-g-UM2 copolymers.....	146
5.5.4.3	Effect of the UM2 content on copolymerization.....	148
5.5.5	UV-Vis spectroscopy analysis.....	149
5.5.6	¹³ C-NMR analysis	151
5.5.6.1	PMMA-g-UM2 copolymers	151
5.5.6.2	PnBMA-g-UM2 copolymers.....	152
5.5.7	¹ H-NMR of methacrylic-urethane graft copolymers.....	152
5.5.7.1	PMMA-g-UM2 copolymers	153
5.5.7.2	PnBMA-g-UM2 graft copolymers	153
5.5.7.3	Determination of the percentage UM2 in the graft copolymers using a ¹ H-NMR technique	154
5.6	<i>Thermal and mechanical analysis</i>	156
5.6.1	Thermogravimetric analysis.....	156
5.6.1.1	Thermal stability of urethane macromonomer (UM2).....	156
5.6.1.2	PMMA-g-UM2 copolymers	157
5.6.1.3	PnBMA-g-UM2 copolymers.....	159
5.6.2	DMA analysis.....	161
5.6.2.1	PMMA-g-UM2 copolymers	162
5.6.2.2	PnBMA-g-UM2 copolymers.....	164
5.6.3	Differential scanning calorimetry	167
5.7	<i>Transmission electron microscopy</i>	169
5.8	<i>Conclusions</i>	170
5.9	<i>References</i>	171

Surface and adhesion properties of methacrylic/urethane graft copolymers 174

6.1	<i>Introduction</i>	174
6.2	<i>Surface properties</i>	175
6.2.1	Introduction.....	175
6.2.2	Theoretical background.....	177
6.2.3.1	Materials.....	177
6.2.3.2	Optical contact measurement.....	177
6.2.3.3	Surface energy measurement.....	177
6.2.3	Results and discussions	178
6.3	<i>Adhesive properties</i>	181
6.3.1	Introduction.....	181
6.3.2	Theoretical background.....	181
6.3.3	Experimental	183
6.3.3.1	Adhesive preparation.....	183
6.3.3.2	Peel tests	183
6.3.4	Results and discussion	183
6.4	<i>Conclusions</i>	185
6.5	<i>References</i>	185

Chapter 7**Conclusions and recommendation for future work 187**

7.1	<i>Conclusions</i>	187
7.2	<i>Recommendation and future work</i>	189

List of Figures

Figure 4.1: FTIR spectrum of UM1	61
Figure 4.2: MALDI-TOF-MS of UM1 prepared using Method 1.....	64
Figure 4.3: Enlarged region of MALDI-TOF-MS of UM1 (a) in the m/z region 700-1800 (b) experimental isotopic distribution of UM1 in m/z region 1988-2006.....	66
Figure 4.4: Comparison by MALDI-TOF-MS between four different methods that were used to reduce the side reactions.....	68
Figure 4.5: MALDI-TOF- MS shows the comparison between four different methods that were used to reduce the side reactions	69
Figure 4.6: MALDI-TOF- MS of UM1 prepared using method 4.....	70
Figure 4.7: Enlarged region of mass spectra of UM1 (a MALDI-TOF- MS of UM1 in the m/z region 700-1800 and n changed from n=1 to n=4 (b) MALDI-TOF-MS of UM1 in the m/z region 1800-3000 and n changed from n=4 to n=8.....	71
Figure 4.8: MALDI-TOF-MS of UM1, showing the experimental isotopic distribution (top) and the theoretical (bottom) corresponding to structures (A, B, C).....	74
Figure 4.9: Spectrum of UM1 dissolved in deuterated-DMSO.	75
Figure 4.10: Spectrum of UM1 dissolved in deuterated-DMSO.	76
Figure 4.11: SEC trace of UM1.....	77
Figure 4.12: SEC traces of UM1, PnBMA and PMMA (UV detector).	79
Figure 4.13: SEC traces of unextracted graft copolymer PMMA-g-UM1.	80
Figure 4.14: SEC traces of unextracted graft copolymer PnBMA-g-UM1.....	80
Figure 4.15: MALDI-TOF-MS (a) before using UM1 in free radical copolymerization (b) extracted unreacted UM1 after free radical copolymerization	81
Figure 4.16: SEC traces of PMMA-g-UM1 illustrating the UM1 distribution.....	82
Figure 4.17: SEC traces of PnBMA-g-UM1 illustrating the UM1 distribution.	83
Figure 4.18: Example of gradient elution profiles considered for the separation of PMMA-g-UM1 copolymer: stationary phase: Nucleosil C18; 100Å, eluent: chloroform/DMF.	85
Figure 4.19: HPLC elution plots of UM1 and PMMA homopolymer	85
Figure 4.20: Gradient HPLC chromatogram of the PMMA-g-UM1 copolymer.	86
Figure 4.21: Gradient elution profiles considered for the separation of PnBMA-g-UM1.....	87

Figure 4.22: HPLC elution plots of UM1 and PnBMA homopolymer	87
Figure 4.23: Gradient HPLC chromatogram of the PnBMA-g-UM1 copolymer before extract unreactated UM1 and PnBMA homopolymer	88
Figure 4.24: Gradient HPLC chromatogram of the PnBMA-g-UM1 copolymer after extract unreactated UM1 and PnBMA homopolymer	88
Figure 4.25: FTIR spectra of PMMA-g-UM1 and PMMA homopolymer.....	90
Figure 4.26: FTIR spectra of PnBMA-g-UM1 and PnBMA homopolymer.....	91
Figure 4.27: Calibration curve of (a) PMMA and (b) PnBMA mixed with different amounts of UM1	92
Figure 4. 28: UV/Vis spectrum: (A) UM1 (B) PMMA and (c) PnBMA	93
Figure 4.29: UV/Vis spectra of UM1 copolymerized with different amounts of acrylate (a) PMMA and (b) PnBMA	93
Figure 4.30: Calibration curve for the determination of the percentage of UM1 incorporated into PMMA or PnBMA.....	94
Figure 4.31: Spectra of PMMA-g-UM1 copolymer and PMMA homopolymer dissolved in DMSO....	95
Figure 4.32: ¹³ C-NMR spectra of PnBMA-g-UM1 copolymers and PnBMA homopolymers dissolved in DMSO.....	96
Figure 4.33: Spectra of PMMA-g-UM1 copolymer, PMMA homopolymer and UM1 dissolved in DMSO.	97
Figure 4.34: spectra of PnBMA-g-UM1 copolymer, PnBMA homopolymer and UM1 dissolved in DMSO.....	98
Figure 4.35: TGA thermogram of UM1 and its derivative curves	101
Figure 4.36: TGA thermograms and their derivative curves of MMA copolymerized with different amount of UM1.....	103
Figure 4.37: TGA thermograms and their derivative curves of n-BMA copolymerized with different amount of UM1	107
Figure 4.38: Tan δ traces of PMMA, UM1 and the PMMA-g-UM1 copolymers.....	110
Figure 4.39: Loss modulus of the PMMA-g-UM1 copolymer.....	110
Figure 4.40: Storage modulus traces of PMMA and PMMA-g-UM1 copolymers.	111
Figure 4.41: Tan δ traces of PnBMA and the PnBMA-g-UM1 copolymers.	112
Figure 4.42: Storage modulus traces of PnBMA and the PnBMA-g-UM1 copolymers.....	113
Figure 4.43: DSC of PMMA-g-UM1 copolymer	115
Figure 4.44: DSC of PnBMA-g-UM1 copolymer	115

Figure 4.45: Typical TEM image of PMMA-g-UM1 copolymer	116
Figure 4.46: Typical TEM image of PnBMA-g-UM1 copolymer.....	116
Figure 5.1: FTIR spectra of UM2	126
Figure 5.2: Enlarged region of MALDI-TOF-MS of UM2.....	127
Figure 5.3: Enlarged region of mass spectra of UM2 (a) MALDI-TOF-MS of the UM2 in the m/z region 700-1800 Da and n changed from n=1 to n=3 (b) MALDI-TOF-MS of the UM2 in the m/z region 1800-300 Da and n changed from n=4 to n=7	129
Figure 5.4: ¹ H-NMR spectrum of urethane macromonomer (UM2) dissolved in DMSO.....	131
Figure 5.5: ¹³ C-NMR spectrum of urethane macromonomer (UM2) dissolved in DMSO.	134
Figure 5.6: SEC chromatogram of UM2.....	135
Figure 5.7: SEC traces of unextracted graft copolymer (a) PMMA-g-UM2 and (b) PnBMA-g-UM2..	137
Figure 5.8: SEC trace of (a) PMMA-g-UM2 and (b) PnBMA-g-UM2 (RI detector) showing the efficiency of the extraction procedure	137
Figure 5.9: Example of SEC traces of PMMA-g-UM2 illustrating the UM2 distribution.	138
Figure 5.10: Example of SEC traces of PnBMA-g-UM2 illustrating the UM2 distribution.....	138
Figure 5.11: Gradient HPLC profiles used for chemical composition for the separation of PMMA-g-UM2 copolymers.....	140
Figure 5.12: Gradient HPLC plots of UM2 and PMMA homopolymer	140
Figure 5.13: Gradient HPLC chromatogram of the PMMA-g-UM2 copolymer before extraction of the unreacted UM2	141
Figure 5.15: Gradient HPLC profiles used for chemical composition separation.....	142
Figure 5.16: Gradient HPLC plots of UM2 and PnBMA homopolymer	142
Figure 5.17: Gradient HPLC chromatogram of the PnBMA-g-UM2 copolymers) before extraction of unreacted UM2 and PnBMA homopolymer.....	143
Figure 5.18: Gradient HPLC chromatogram of the PBMA-g-UM2 copolymers after extraction of the unreacted UM2 and PnBMA homopolymers.....	143
Figure 5.19: FTIR spectra of PMMA-g-UM2 copolymers and PMMA homopolymer.....	146
Figure 5.20: FTIR spectra of PnBMA-g-UM2 copolymers and PnBMA homopolymer.	147
Figure 5.22: UV/Vis spectrum of UM2.....	149
Figure 5.23: UV/Vis spectra of UM2 copolymerized with different quantities of acrylate (A) PMMA and (B) PnBMA.....	149

Figure 5.24: Calibration curve for the determination of the percentage of UM2 incorporated into PMMA or PnBMA.....	150
Figure 5.25: ¹³ C-NMR spectra of PMMA-g-UM2 copolymers and PMMA homopolymer dissolved in DMSO.....	151
Figure 5.26: ¹³ C-NMR spectra of PnBMA-g-UM2 copolymers and PnBMA homopolymer dissolved in DMSO.....	152
Figure 5.27: ¹ H-NMR spectrum of PMMA-g-UM2 copolymer dissolved in DMSO	153
Figure 5.28: ¹ H-NMR spectrum of PnBMA-g-UM2 copolymer (G55B) and PnBMA homopolymer dissolved in DMSO.	154
Figure 5.29: TGA thermogram of UM2 and its derivate curve.....	156
Figure 5.30: TGA thermograms and their derivate curves of MMA copolymerized with different amounts of UM1	159
Figure 5.31: TGA thermograms and their derivate curves n-BMA copolymerized with different amounts of UM2	161
Figure 5.32: Tan δ traces of PMMA, UM2 and PMMA-g-UM2 copolymers.....	163
Figure 5.33: Storage modulus traces of PMMA and PMMA-g-UM2 copolymers	163
Figure 5.34: Loss modulus of PMMA-g-UM2 copolymer	164
Figure 5.35: Tan δ traces of PnBMA, UM2 and PnBMA-g-UM2 copolymer.....	165
Figure 5.36: Loss modulus of PMMA-g-UM2 copolymer	165
Figure 5.37: Storage modulus traces of PnBMA and PnBMA-g-UM2 copolymers	166
Figure 5.38: DSC trace of PMMA-g-UM2 copolymer.....	168
Figure 5.39: DSC trace of PnBMA and PnBMA-g-UM2 copolymer.....	169
Figure 5.40: TEM image of PMMA-g-UM2 copolymer.....	170
Figure 5.41: TEM image of PnBMA-g-UM2 copolymer.....	170
Figure 6.1: Image of a water drop showing the height and radius used in determination of the contact angle θ	177
Figure 6.2: Contact angles of water vs feed ratio of urethane macromonomer.	179
Figure 6.3: Typical graphs showing results of a peel strength test.....	182
Figure 6.4: Schematic view of T-peel test for the measurement of peel strength.	182
Figure 6.5: Peel strength of (a) PMMA-g-UM2 and (b) PnBMA-g-UM2 versus UM2 content.....	184

List of Schemes

Scheme 2.1: Formation of a linear polyurethane.....	9
Scheme 2.2: Formation of isocyanate prepolymer macromolecules.	10
Scheme 2.3: Formation of a polyurethane	10
Scheme 2.4: Resonance structures of the isocyanate group.	12
Scheme 2.5: Resonance structures of the aromatic isocyanate	13
Scheme 2.6: TDI isomers.	13
Scheme 2.7: 4,4'-Diphenylmethane diisocyanate.....	13
Scheme 2.8: 1,6-Hexamethylene diisocyanate.	14
Scheme 2.9: Formation of carbamic acid derivatives.	14
Scheme 2.10: Urethane formation from reaction with alcohol.....	15
Scheme 2.11: Urea formation from reaction with amine.	15
Scheme 2.12: Reaction between water and isocyanate.	15
Scheme 2.13: Reaction of carboxylic acid with isocyanate.....	16
Scheme 2.14: Formation of allophanate and biuret.....	16
Scheme 2.15: Dimerization of isocyanate.	17
Scheme 2.16: Trimerization of isocyanate.	17
Scheme 2.17: The ketimine and ketazine process.	19
Scheme 2.18: General formula of an acrylate ester.	21
Scheme 2.19: General formula of a graft copolymer.	23
Scheme 2.20: Representation of different types of block copolymers.....	24
Scheme 2.21: Schematic representation of the synthesis of graft copolymers.....	25
Scheme 2.22: Representation of the synthesis of well-defined macromonomers.....	27
Scheme 2.23: Representation of the synthesis of macromonomers.	28
Scheme 2.24: Propagation reactions in free radical polymerization.....	29
Scheme 2.25: Synthesis of polyurethane–acrylate dispersion.....	35
Scheme 4.1: <i>formation of urethane macromonomer (when 2-HEA reacts at one side and MeOH at the other side of the UM1.....</i>	53

Scheme 4.2: Reaction products shows 2-HEA reacts on both sides of the UM1.....	53
Scheme 4.3: Reaction product shows methanol reacts on both sides of the UM1, to form unreactive urethane macromer.....	54
Scheme 4.4: Formation of methacrylic-urethane graft copolymer.....	57
Scheme 4.5: Reaction products when 2-HEA reacts on side and isopropanol reacts from an other side.....	63
Scheme 4.6: Repeat unit (δ) of UM1.....	69
Scheme 5.1: Formation of urethane macromonomer (when 2-HEA reacts at one side and MeOH at the other side of the UM2)	123
Scheme 5.2: Repeat unit (δ) of UM2.....	127

List of Tables

Table 4.1: Reagents used for synthesis of UM1	51
Table 4.2: Formulations used for the preparation of UM1	52
Table 4.3: Formulations used for the preparation of PMMA-g-UM1 and PnBMA-g-UM1 copolymers	55
Table 4.4: Effect of the concentration of initiator on yield of graft copolymers	56
Table 4.5: FTIR peak assignment of the UM2	62
Table 4.6: Possible UM1 structures that might be created during synthesis of UM1.....	65
Table 4.7: Abbreviations of main urethane macromer chains detected by MALDI-TOF-MS	70
Table 4.8: Summary of monoisotopic masses of the ion peak series observed in MALDI-TOF-MS.....	73
Table 4.9: Number average molecular weight (M_n) and polydispersity (M_w/M_n) of the UM1 of different chain lengths, as determined by SEC.....	77
Table 4.10: Formulation and characterizations of graft copolymers	78
Table 4.11: The number average molar mass and weight average molar mass of the graft copolymers obtained via SEC-MALLS	89
Table 4.12: Weight percentages of UM1 incorporated into the graft copolymers, as calculated from FTIR data	92
Table 4.13: UV data for the determination of the weight percentages of UM1 incorporated into PMMA or PnBMA.....	94
Table 4.14: Percentage UM1 incorporated into graft copolymers, as determined by $^1\text{H-NMR}$	99
Table 4.15: Thermal data obtained from TGA scans for PMMA-g-UM1	104
Table 4.16: Thermal data obtained from TGA scans of PnBMA-g-UM1	106
Table 4.17: DMA results for PMMA-g-UM1 and PnBMA-g-UM1 copolymers at varying UM1 ratio in polymerization feed.....	113
Table 4.18: DSC results for PMMA-g-UM1 and PnBMA-g-UM1 copolymers at varying UM1 ratio in polymerization feed.....	114
Table 5.1: Reagents used for PU formulations.....	121
Table 5.2: Formulations used for the preparation of polyurethane macromonomers	122
Table 5.3: Formulations used for the preparation of PMMA-g-UM2 and PnBMA-g-UM2 copolymers.....	124

Table 5.4: FTIR peak assignment of the UM2	125
Table 5.5: Abbreviations of main urethane macromonomers chain detected by MALDI-TOF-MS.....	128
Table 5.6: Summary the monoisotopic masses of the ion peak series observed in MALDI-TOF-MS	130
Table 5.7: peak assignments for UM2.....	133
Table 5.8: Number average molecular weight (M_n), and polydispersity (M_w/M_n) the UM2 of different chain lengths, as determined by SEC.....	135
Table 5.9: Formulation and characterizations of graft copolymer	136
Table 5.10: The number average molar mass and weight average molar mass of the graft copolymers obtained via SEC- MALLS.	144
Table 5.11: IR absorption data for PMMA-g-UM2 copolymer.....	145
Table 5.12: IR absorption data for PnBMA-g-UM2 copolymer	147
Table 5.13: Percentages UM2 incorporated into the graft copolymers as calculated from FTIR data	148
Table 5.14: UV/Vis data for the determination of the percentage of UM2 incorporated into PMMA or PnBMA.....	150
Table 5.15: Percentage UM2 incorporated into graft copolymers, as determined by $^1\text{H-NMR}$	155
Table 5.16: Thermal data obtained from TGA scans for PMMA-g-UM2.....	158
Table 5.17: Thermal data obtained from TGA scans for PnBMA-g-UM2.....	160
Table 5.18: DMA results for PMMA-g-UM2 and PnBMA-g-UM2 copolymers at varying UM2 ratio in polymerization feed.....	166
Table 5.19: DSC results for PMMA-g-UM2 and PnBMA-g-UM2 copolymers at varying UM2 ratios in polymerization feed.....	168
Table 6.1: Contact angle values of methacrylic-urethane graft copolymer	178
Table 6.2: Contact angles and surface tensions for methacrylic-urethane graft copolymer.....	180
Table 6.3: Peel energy of commercial vinyl and leather for methacrylic-urethane graft copolymer containing different amount of UM2.....	185

List of Abbreviations

AIBN	2,2' Azobis (isobutyronitrile)
BA	Butylacrylate
¹³C-NMR	Carbon nuclear magnetic resonance spectroscopy
DMA	Dynamic mechanical analysis
DMAc	Dimethylacetamide
DMF	Dimethylformamide
DMSO	Dimethylsulfoxide
DSC	Differential scanning calorimetry
EG	Ethylene glycol
ELSD	Evaporative laser light scattering detector
FTIR	Fourier transform infrared spectroscopy
g	Graft
GPEC	Gradient polymer elution chromatography
¹H-NMR	Proton nuclear magnetic resonance spectroscopy
2-HEA	2-Hydroxyethyl acrylate
2-HEMA	2-Hydroxyethyl methacrylate
HPLC	High-performance liquid chromatography
KTFA	Potassium trifluoro acetate
MALDI-TOF-MS	Matrix-assisted laser desorption/ionization time of flight mass spectroscopy
MDI	Methylene diphenyldiisocyanate
MEK	Methyl ethyl ketone
MeOH	Methanol
MMA	Methyl methacrylate
M_n	Number average molecular weight
M_w	Molecular weight
n	Urethane average chain length
n-BMA	n-Butyl methacrylate
NPG	Neopentylglycol
OCA	Optical contact angle analysis
PAS	Photo acoustic spectroscopy
PMMA	Poly(methyl methacrylate)
PnBMA	Poly(normal butyl methacrylate)
PnBMA-g-UM1	n-Butyl methacrylic-urethane graft copolymers
PnBMA-g-UM2	n-Butyl methacrylic-urethane graft copolymers
PMMA-g-UM1	Methyl methacrylic-urethane graft copolymers
PMMA-g-UM2	Methyl methacrylic-urethane graft copolymers
Pu	Polyurethane
RI	Refractive index
SEC	Size exclusion chromatography

SFE	Surface free energy
TDI	Toluene diisocyanate
TGA	Thermal gravimetric analysis
TEM	Transmission electron microscopy
THF	Tetrahydrofuran
PU	Polyurethane
UM1	Urethane macromonomer based on 4,4-diphenylmethane diisocyanate and Ethylene glycol
UM2	Urethane macromonomer based on 4,4-diphenylmethane diisocyanate and neopentylglycol
UMs	Urethane macromonomers
UV-Vis	Ultraviolet/visible spectroscopy

Chapter 1

Introduction and objectives

1.1 Introduction

Polyurethanes (PUs) are finding increasing application and use in many industries¹⁻⁴ due to their advantageous properties, such as a wide range of flexibility combined with toughness, high abrasion resistance, high chemical resistance, high acid etch resistance, excellent weatherability, and very low temperature cure. These features make PU one of the most widely used and one of the fastest growing types of polymers in the world. PUs do however have some disadvantages, for instance: PU is considered an expensive polymer, especially the isocyanate component, and PU production presents many problems, especially with respect to the high reactivity of the isocyanate group towards impurities such as water, etc.⁵ Today, however, side reactions have been largely reduced, from being a problem to now being under control. PUs require a higher boiling solvent, which can be as exotic as (NMP) Here the solvent is mostly evaporated, the urethane heated and the two surfaces joined. This is a difficult high-tech glue to use, not generally accepted for household use.

Historically, polyacrylates have found extensive use as adhesives and coatings.⁶ Most polyacrylates generally have a low glass transition temperature (T_g), which makes them suitable to handle, process, and purify. In addition, the wide range of available acrylate monomers allows the physical properties of their polymers to be tailored. Polyacrylates are less expensive than PUs. However, a problem associated with polyacrylates is that their flexible backbones impart limited thermal stability and mechanical strength.

It is known that the favorites general purpose adhesives, are: the monomeric acrylates, such as super glue, which cure from monomer to polymer, solution based acrylics,⁷ polyurethane in solvent^{8,9} or a moisture curing grade of polyurethane; two-part epoxy resins^{10,11} and emulsion based polyvinyl acetates,¹² commonly known as wood glue.¹³ The major market is however, solvent based adhesives and is dominated by acrylics using a low temperature solvent such as a (MEK) solvent mixture.

Two phases can be chosen to make either phase continuous, but it is preferable for price to have a continuous acrylic phase with micro inclusions of Pu, which means that either the acrylic or the urethane phase can associate with the surface to be glued. This has been proved in rolled steel research, by mixing three urethanes with different functionality and

finding enrichment of the correct one at the adhesive phase and enrichment of the correct one at the surface phase and modulus improvement of the entire adhesive film by enrichment of the high modulus component in between these.¹⁴

A motivation for the present study was to use low cost PUs as grafts in polyacrylates to study property improvements that may in future impact on binder or adhesive product properties.

Properties and applications of polymers can be extended by copolymerization with other polymers to give new materials with tailored properties and performances.¹⁵ The ability to produce polymers with well defined and controlled structures has led to the study of structure-property relationships in polymer materials. An understanding of this relationship is essential in predicting polymer properties and in designing materials with new properties.

Branched polymers are distinguished by the presence of the branch points as well as the presence of more than two chain end groups per molecule. The presence of these branches has an effect on various polymer properties such as crystallinity, glass transition temperature, viscoelastic properties, and viscosity.

The introduction of polymerizable end groups into a polymer chain can be achieved by, for example anionic polymerization techniques.^{16,17} Functional initiation or electrophilic termination are the main ways to include the active groups. These types of polymers with precisely controlled functionality can be used as macromonomers, which can undergo further reactions to afford branch polymers.¹⁸

Many researchers have studied creating specialized copolymers of various architectures, for offering new properties.¹⁹⁻²³ One of the most attractive copolymers is graft copolymers, which contain polymer units that are incorporated as side chains on a backbone polymer, and which cause that polymer to exhibit good phase separation.^{24,25} Graft copolymers have been used for a variety of applications, such as impact-resistant plastics, thermoplastic elastomers, compatibilizers, polymeric emulsifiers, hydrogels, drug delivery polymers, and gas permeation membranes.²⁶⁻²⁸ Graft copolymers are generally prepared by three general methods: the grafting-onto, grafting from, and the macromonomer method.^{16,29}

The “grafting onto” method involves a coupling reaction between the backbone and the branches, which are prepared separately by living polymerization methods.³⁰ Functional groups are distributed along the chain backbone, and can react with the living branches. In the “grafting from” method, active sites are required along the main chain backbone that are able to initiate the polymerization of the second monomer, resulting in the formation of

branches and the final graft copolymer. In the macromonomer method, polymer chains having polymerizable end groups, known as “macromonomers”, are copolymerized with another monomer in order to produce the graft copolymer.¹⁸

Macromonomers are very important for the preparation of various kinds of graft copolymers with a different number and length of branch segments.³¹⁻³⁴ Macromonomers are usually linear polymeric species having one or more reactive end groups that can participate in polymerization reactions. Such end groups include acrylic, vinylic, allylic, propenylic, or isopropenylic functionality,^{35,36} so the macromonomers can either homopolymerize to give regular comb-shaped polymers or copolymerize with conventional monomers to give graft copolymers.³⁷

Macromonomers have been widely and successfully used as building blocks for the synthesis of various branched polymer architectures (also on a commercial scale). Macromonomers can be readily copolymerized with conventional monomers to afford graft copolymers with well defined structures. The structure of the polymer chain of the macromonomer affects the properties of the graft copolymer while the polymerizable end group controls the reactivity during polymerization. Many functional groups with chemical reactivity have been studied for various types of polymerizations, including conventional free radical,³⁸ group transfer,³⁹ anionic,⁴⁰ cationic,⁴¹ controlled free radical,⁴² and ring-opening metathesis⁴³ polymerizations.

The macromonomer method is generally the most efficient method for producing well defined graft copolymers.⁴⁴ There are several reasons for this: the wide variety of macromonomers and comonomers available makes possible the synthesis of graft copolymers with properties that can be selected, and the length of their branches can be controlled since the molecular weight of the macromonomer and its distribution can also be pre-selected.

To our knowledge this is the first report concerning monofunctional urethane macromonomers. In previous reports, a linear type vinyl-terminated bifunctional urethane macromonomers was first synthesized and applied to the dispersion polymerization of methylmethacrylate in ethanol.⁴⁵ However, in the styrene monomer system, the vinyl urethane macromonomer was verified as a reactive stabilizer owing to the ¹H-NMR spectra, the high molecular weight and the thermal properties of macromonomer-grafted PS.⁴⁶ The macromonomers consisting of different molecular weights of PEG and various terminal groups were synthesized and the role of the macromonomers in the dispersion polymerization of styrene was reported as a reactive stabilizer and grafting agent.⁴⁷

The telechelic macromonomer cross-linkable stabilizer (TMCS) was proposed and the evidence of crosslinking was confirmed from the viewpoints of the thermal properties or levels of solubility in organic solvents.⁴⁸ Recently, the structure of the macromonomer was modified from a linear-type to a cross-type by designing PEG in the tail part between two vinyl end groups to reduce the main chain length. The cross-type vinylurethane macromonomers (C-VUM) were successfully synthesized using trimethylolpropane (TMP) as a crosslinking-agent, and applied to the dispersion polymerization of styrene in ethanol as a reactive stabilizer and grafting agent.⁴⁹ Linear-type vinylurethane macromonomers (L-VUM) in the dispersion polymerization of styrene have also been investigated.⁵⁰

Urethane macromonomers can be synthesized by two methods: the prepolymer method and the 'one-shot' method.⁵¹ In the 'one-shot' process the monomers are added together in one step, whereas in the prepolymer process (which will be used in this study) the monomers are added in intervals. The prepolymer process holds more advantages over the one-shot process as it offers more control over the reaction, thereby resulting in polymers with smaller molecular mass distributions and better polymer morphology.⁵²

1.2 Aim

The aims of the study were to synthesis different types of predominantly monofunctional urethane macromonomers using grafting through technique via the pre-polymer method then various concentrations of urethane macromonomers were copolymerized with various amounts of MMA, and with various amounts of n-BMA, respectively, using solution free radical copolymerization. The synthesized graft copolymers were then be tested as solvent based adhesives.

1.3 Objectives

The overall objective of this study was the synthesis of methacrylic/urethane graft copolymers using the macromonomer technique, and their characterization. Specific objectives included the following:

1. Synthesize two types of linear UMs by the polyaddition polymerization of 4,4'-methylenediphenyl diisocyanate (MDI) with ethylene glycol (EG) and MDI with neopentylglycol (NPG) via the pre-polymer method, followed by termination with 2-hydroxy ethylacrylate (2-HEA) and methanol (MeOH) to yield UMs having specific urethane chain lengths and be predominantly monofunctional.
2. Screen the addition of reagents for synthesis and optimize by a further set of conditions to synthesize UMs will optimum clarity in their structure using MALDI-TOF-MS.

3. Characterize the urethane macromonomers by FTIR, $^1\text{H-NMR}$, $^{13}\text{C-NMR}$, SEC, TGA, DMA and, where possible, MALDI-TOF-MS.
4. Incorporate various percentages of the respective UMs into both methyl methacrylate and into normal butyl methacrylate, in solution polymerization via free radical copolymerization. The percentages of urethane macromonomer to be incorporated in the feed range between 0% and 55% by weight (according to MMA and n-BMA monomers).
5. Characterize the obtained methyl methacrylate/urethane graft copolymers and normal butyl methacrylate/urethane graft copolymers thus obtained by $^1\text{H-NMR}$ and $^{13}\text{C-NMR}$, FTIR, UV, SEC, UV-VIS and HPLC.
6. Calculate the weight percentages of UM incorporated into methacrylic/urethane graft copolymers using FTIR, $^1\text{H-NMR}$, and UV/Vis techniques.
7. Study the thermal behaviour of synthesized graft copolymers as a function of UM percentage UM incorporation using TGA analysis.
8. Study the mechanical properties of synthesized methacrylate/urethane graft copolymers as a function of percentage UM incorporation.
9. Investigate the possible phase separation between the urethane segment and methacrylate segment in the yield of graft copolymerization products by using DMA, DSC and TEM.
10. Investigate the surface and adhesive properties of synthesized graft copolymers using surface tension and T-Peel test studies.

1.4 Layout of thesis

Chapter 1: Introduction and objectives

This chapter gives a very brief insight into why branch polymers are important. It also contains a brief introduction to the major areas pertaining to this research, which include the synthesis of graft copolymers, macromonomers, polyurethanes, polyacrylates, and a brief introduction to what work has been done by other researchers in urethane–acrylate copolymers polymerization. Finally it includes the objectives of the research project.

Chapter 2: Historical and theoretical background

This is a review of the historical and theoretical aspects related to this research project that have been carried out by other researchers to date.

Chapter 3: Analytical techniques

This chapter gives an overview of the analytical techniques used during the synthesis and characterization of urethane macromonomer and its graft copolymers with acrylates monomers.

Chapter 4: Synthesis and characterization of urethane-acrylate graft copolymers

This chapter covers the synthesis of copolymers, material and chromatographic techniques that were used in this research. This chapter also takes a closer look at the results obtained for the various techniques used to analyze the prepared UM1, PMMA-g-UM1 and PnBMA-g-UM1 copolymers as well as thermal and mechanical properties and characterize the morphology by TEM analysis. These results are then also discussed to give more insight into the characteristics of the graft copolymer.

Chapter 5: Synthesis and characterization of urethane-acrylate graft copolymers

This chapter covers the synthesis of copolymers, material and chromatographic techniques that were used in this research. This chapter also takes a closer look at the results obtained for the various techniques used to analyze the prepared UM2, PMMA-g-UM2 and PnBMA-g-UM2 copolymers as well as thermal and mechanical properties and characterize the morphology by TEM analysis. These results are then also discussed to give more insight into the characteristics of the graft copolymer.

Chapter 6: Surface and adhesion properties of methacrylic/urethane graft copolymers

This chapter describes some surface and adhesion properties of synthesized methacrylic /urethane graft copolymers using surface tension T-peel test.

Chapter 7: Conclusions and recommendations

General conclusions to the study, and recommendations for future work are given.

1.5 References

1. Oertel, G., *Polyurethane Handbook*, 2nd ed. Hanser: New York, 1993.
2. Dounis, D.; Wilkes, G. *Polymer* **1997**, 38, 2819.
3. Weiss, K. *Prog. Polym. Sci.* **1997**, 22, 203.
4. Mahkam, M.; Sharifi, N. *Polymer* **2003**, 80, 199.
5. Seboa, S. PhD dissertation, University of Stellenbosch, South Africa, December 2002.

6. Elvers, B.; Hawkins, S.; Schulz, G., *Ullmann's Encyclopedia of Industrial Chemistry*. John Wiley and sons: New York, 1992; Vol. 21A, p 158.
7. Dunky, M.; Pizzi, A. *Appl. Surf. Chem.* **2002**, 23, 1039.
8. Somani, K.; Kansara, S.; Patel, N.; Rakshit, A. *Int. J. Adhes. Adhes.* **2003**, 23, 269.
9. Desai, S.; Patel, J.; Sinha, V. *Int. J. Adhes. Adhes.* **1990**, 10, 225.
10. Raftery, G.; Harte, A.; Rodd, P. *Int. J. Adhes. Adhes.* **2009**, 29, 580.
11. Davis, G. *Int. J. Adhes. Adhes.* **1990**, 10, 263.
12. Haaga, A.; Geeseya, G.; Mittleman, M. *Int. J. Adhes. Adhes.* **2006**, 26, 177.
13. Frihart, C. R., *Hand book of Wood Chemistry and Wood Composites*, CRC: USA, 2005; p 216.
14. Mequanint, K. MSc thesis, University of Stellenbosch, South Africa, December 1997.
15. Al-Malaika, S.; Kong, W. *Polym. Degrad. Stab.* **2005**, 90, 197.
16. Pitsikalis, M.; Pispas, S.; Mays, J.; Hadjichristidis, N. *Adv. Polym. Sci.* **1998**, 1, 135.
17. Hadjichrisridis, N.; Latrou, H.; Pispas, S.; Pitsikalis, M. *Curr. Org. Chem.* **2002**, 6, 155.
18. Ito, K. *Prog. Polym. Sci.* **1998**, 23, 581.
19. Frèchet, J. M. *Science* **1994**, 263, 1710.
20. Webster, O. W. *Science* **1991**, 251, 887.
21. Hedrick, J. L.; Miller, R. D.; Hawker, C. J.; Carter, K. R.; Volksen, W.; Yoon, D. Y.; Trollsas, M. *Adv. Mat.* **1998**, 10, 1049.
22. Beyer, F. L.; Gido, S. P.; Buschl, C.; Latrou, H.; Uhrig, D.; Mays, J. W. *Macromolecules* **2000**, 33, 2039.
23. Donnell, P. M.; Brzezinska, K.; Powell, D.; Wagener, K. B. *Macromolecules* **2001**, 34, 6845.
24. Dobrynin, A. V.; Erukhimovich, I. Y. *Macromolecules* **1993**, 26, 276.
25. Shinoda, S.; Miller, P. J.; Matyjaszewski, K. *Macromolecules* **2001**, 34, 3186.
26. Rempp, P.; Franta, E.; Masson, P.; Lutz, P. *Prog. Colloid. Polym. Sci.* **1986**, 72, 112.
27. Ito, K.; Kawaguchi, S. *Adv. Polym. Sci.* **1999**, 142, 129.
28. Sanda, F.; Hitomi, M.; Endo, T. *Macromolecules* **2001**, 34, 5364.
29. Hadjichristidis, N.; Pitsikalis, M.; Pispas, S.; latrou, H. *Chem. Rev.* **2001**, 101, 3747.
30. Yousi, Z.; Donghai, L.; Lizong, D.; Jinghui, Z. *Polymer* **1998**, 39, 2665.
31. Schulz, G. O.; Milkovich, R. *J. Polym. Sci. Part A: Polym.Chem.* **1984**, 22, 1633.
32. Kennedy, J. P.; Lo, C. Y. *Polym. Bull.* **1985**, 13, 343.
33. Rempp, P.; Lutz, P.; Masson, P.; Chaumont, P.; Franta, E. *Macromol. Chem. Suppl.* **1985**, 13, 47.
34. Cameron, G. G.; Chisholm, M. S. *Polymer* **1986**, 27, 1420.
35. Henschke, O.; Neubauer, A.; Arnold, M. *Macromolecules* **1997**, 30, 8097.
36. Shiho, H.; Desimone, J. *J. Polym. Sci. Part A: Polym. Chem.* **2000**, 38, 1139.
37. Se, K.; Inoue, N.; Yamashita, M. *Polymer* **2005**, 46, 9753.

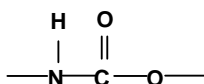
38. Roos, S.; Muller, A.; Matyjaszewski, K. *Macromolecules* **1999**, *32*, 8331.
39. Ishizu, K.; Kuwahara, K. *Polymer* **1994**, *35*, 4907.
40. Sanda, F.; Hitomi, M.; Endo, T. *Macromolecules* **2001**, *34*, 5364.
41. Yamada, K.; Miyazaki, M.; Ohno, K.; Fukuda, T.; Minoda, M. *Macromolecules* **1999**, *32*, 290.
42. Nomura, K.; Takahashi, S.; Imanishi, Y. *Polymer* **2000**, *4*, 4345.
43. Nagasaki, Y.; Ukai, R.; Kato, M.; Suruta, T. *Macromolecules* **1994**, *27*, 7236.
44. Langlois, V.; Vallee-Rehel, K.; Peron, J.; Borgne, A.; Walls, M.; Guerin, P. *Polym. Degrad. Stab.* **2002**, *76*, 411.
45. Shim, S. E.; Jung, H.; Lee, K.; Lee, J. M.; Choe, S. *J. Colloid Interface. Sci* **2004**, *279*, 464.
46. Jung, H.; Kim, S. Y.; Lee, K.; Lee, B. H.; Shim, S. E.; Choe, S. *J. Polym. Sci. Part A: Polym. Chem.* **2005**, *43*, 3566.
47. Kim, S. Y.; Lee, K.; Jung, H.; Shim, S. E.; Lee, B. H.; Choe, S. *Polymer* **2005**, *46*, 7974.
48. Lee, K.; Shim, S. E.; Jung, H.; Kim, S. Y.; Choe, S. *Macromolecules* **2005**, *38*, 2686.
49. Lee, K.; Jung, H.; Kim, S. Y.; Lee, B. H.; Choe, S. *Polymer* **2006**, *47*, 1830.
50. Liu, Z.; Xiao, H.; *Polymer* **2000**, *41*, 7023.
51. Renault, B.; Tassaing, T.; Cloutetl, E.; Cramail, H. *J. Polym. Sci. Part A: Polym. Chem.* **2007**, *45*, 5649.
52. Saunders, J.; Frisch, K., *Polyurethane Chemistry, Part I*. Wiley-Interscience: New York, 1962.

Chapter 2

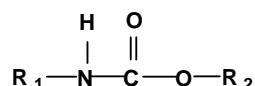
Theoretical background

2.1 Polyurethanes

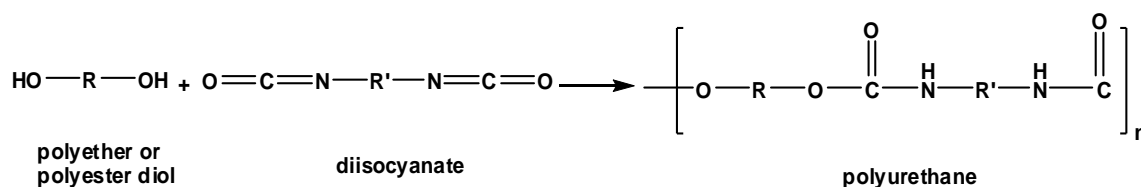
Polyurethanes (PUs) is the collective name for large group of polymers with very different compositions and a variety of property profiles that have the urethane group in common. A urethane group is essentially a carbamic acid ester, i.e. an ester-amide derivative of carbonic acid, and characterized by the following linkage:



Linear PUs are polymers in which the principal chain structure is composed of aliphatic or aromatic sections R_1 and R_2 fixed together with polar urethane groups.



where R_1 is an aliphatic or aromatic group derived from an isocyanate monomer, and R_2 is a more complex group derived from the polyol component (generally, polyether or polyester). There are a number of methods available for the preparation of PUs, but the most widely used is the step-wise addition reaction of di- or poly-functional hydroxyl compounds, such as hydroxyl-terminated polyether or polyesters with di- or poly-functional isocyanates. This step-wise addition polymerization does not eliminate any by-products like step wise addition polymerization does. When only difunctional reactants are used, linear PUs are produced, as shown below:

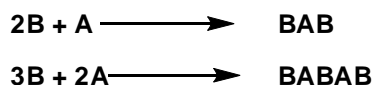


Scheme 2.1: Formation of a linear polyurethane.

The presence of multifunctional components, e.g. triisocyanates, or the use of branched hydroxylpolyols, will yield Pus with a three-dimensional crosslinked structure.

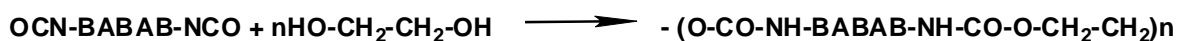
In particular, the structure of PU chains produced by the polyaddition process can be formed by the relative sequence of charging the individual feeds. It is a common practice that a prepolymer^{1,2} is synthesized initially and an excess amount of one component is used, e.g. too much diisocyanate (B) in relation to polyol (A). When the polyol component is added to

diisocyanate, the molar ratio of the reacting substances determines the size of the isocyanate prepolymer macromolecule:



Scheme 2.2: Formation of isocyanate prepolymer macromolecules.

The synthesized urethane–isocyanate prepolymer BAB or BABAB can be further extended in the next reaction step using a low molecular weight diol, ethylene glycol (EG) or other compound which has active hydrogen atom(s) in its structure. High molecular weight PUs are produced in this way, and the size of the final macromolecule, when there are no diffusion constraints, is controlled by the molar ratio of the reacting functional groups:



Scheme 2.3: Formation of a polyurethane.

It is also possible to synthesize Pus in a single-stage or “one shot” process.³ The molar ratios of the diisocyanate, polyol and extender should then be carefully selected. The chain structure will however not be as accurately defined as in the prepolymer process. PU chains will not contain only urethane structures but also aromatic groups from the isocyanate and ether groups and ester groups derived from polyols will be present. In the “one shot” method, in addition to the formation urethane bonds other groups can be present in small amounts such as urea groups, biuret groups, allophanate groups, carbodiimide groups, aromatic hydrocarbon rings, azaheterocyclic (isocyanurate) or oxazolidone structures, and even ionic groups in some cases.³

2.1.1 History and application of polyurethanes

PU plastics were first synthesized by Bayer.⁴ The first PU was obtained in 1937, from the reaction of 1,6-diisocyanatohexane and 1,4-butanediol.¹ PU products were introduced into the market in the late 1940s and they quickly established a strong position there, mostly as elastomers and foamed materials. It was however only in the 1950s that the first PU coatings were developed, when toluene diisocyanate (TDI) was manufactured on a large scale.⁵ Fast progress followed and in the 1970s PU coatings were introduced for motor vehicle applications.^{6,7} Despite some business depressions, the world’s PU market has shown remarkable growth through the 1980s and 1990s, reaching about 6.6 million tons of isocyanates and polyols in 1995.⁸

The very wide applicability of PUs results from the fact that their performance properties can be widely modified by selecting appropriate raw materials and catalysts, by employing

various production methods, and/or by employing various methods for further processing and/or for shaping the final products. Resulting from their specific micro-phase structure, which is formed by rigid chain segments and flexible chain segments, PUs offer very good elasticity with simultaneously reasonably high mechanical strength and abrasion resistance, and also controllable hardness.⁹ PUs can be available both as relatively rigid plastomers and as flexible elastomers with compact or foamed structures. There are two inhibiting factors that portion of the applicability of polyurethanes: their limited stability at temperatures above 90 °C, and their flammability, particularly the foamed Pus.

PUs are produced in the form of foamed plastics, structural elastomers, coating elastomers, adhesives and leather-like materials. Flexible cellular PU elastomers are used especially in furniture making and the automotive industry. On the other hand, rigid foamed PUs can be converted into lightweight elements with structural stability and superior thermal insulation performance (closed-cell foams) and/or acoustic insulation performance (open-cell foams). Thermoplastic elastomers (PUT) are also available, they can be processed as typical thermoplastics due to H-bonding of their allophanate groups.^{5,7,8,10,11}

A newer trend in the application of PUs is the production of biodegradable ionomers. These make the feed stocks for aqueous dispersions which need no external emulsifiers, and which find their outlets as environmentally friendly lacquers.¹² The combination of emulsions of PU ionomers and emulsions of other polymers, like poly(vinyl alcohol), yields interpenetrating polymer networks (the so-called semi-IPNs) with very good adhesion to metallic and ceramic substrates, and with improved resistance to water.¹³

Another interesting application is the production of typical interpenetrating polymer networks (IPNs) of PUs and other chain polymers, like poly(methyl methacrylate),¹⁴ polystyrene,¹⁵ or with condensation polymers, like unsaturated polyesters,¹⁶ epoxy resins,¹⁷ and polysiloxanes,¹⁸ with no covalent bonds between the IPN components. The use of vegetable raw materials: starch,¹⁹ natural rubber,²⁰ lignin, wood flour, molasses, cellulose, glucose, fructose or saccharine makes it possible to obtain relatively easily biodegradable PUs. The exceptional combination of physical properties, hydrolytic stability as well as low in vitro protein adsorption and platelet adhesion to PUs enables some medical applications for PUs where the contact with body fluids, e.g. plasma and blood, is required.^{21, 22}

PUs generally offer good performance properties, are easily processed, and show good resistance to water, atmospheric conditions, organic solvents, dilute acid and alkali. Non-aromatic PUs are also resistant to photo-oxidative ageing. It is therefore clear that PUs are used in numerous fields of technology and in everyday life.^{23, 24}

2.1.2 Basic reagents used for the preparation of linear polyurethanes

The basic pool of feeds applicable to the manufacture of PUs comprises diisocyanates, polyether polyols or polyester polyols, small diols diamines (used as low molecular weight extenders of isocyanate prepolymer chains), catalysts for the polyaddition process of diisocyanates and compounds with unstable hydrogen atoms (water, alcohols, amines), and auxiliary substances selected for specific processes, e.g. blowing agents for foamed polyurethanes, multi-functional amines or isocyanates as cross-linking agents, or organophosphorus antipyrene compounds (which are widely used in foamed PUs). The choice and use of many of these materials are discussed in detail in numerous review papers that describe production processes of individual polyurethane products.²⁵ Only the isocyanates, polyols and catalysts will be described here.

2.1.2.1 Isocyanates

Isocyanates, esters of isocyanic acid, were first synthesized by Wurtz in 1848 (as reported by Chen and Hsu).¹ These compounds have one or several –NCO groups. Isocyanates are generally characterized by high and versatile reactivity. Aliphatic and aromatic monoisocyanates are widely used as building blocks for agricultural chemicals. Their use is mainly prompted by the unique capability of the isocyanate to undergo nucleophilic addition reactions.

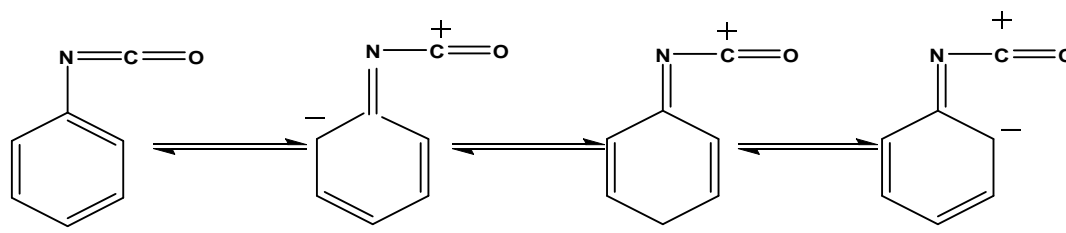
Reactivity of the isocyanate group

The high energy content and polarizability of the double bonds in an isocyanate group permit multiple reactions. The reactivity of an isocyanate toward nucleophilic agents is mainly due to the pronounced positive character of the C atom in the cumulative double bond sequence consisting of nitrogen, carbon and oxygen, especially in aromatic systems.²⁶ The electronic structure of the isocyanate group can be represented by several tautomeric resonance structures, which are illustrated Scheme 2.4



Scheme 2.4: Resonance structures of the isocyanate group.

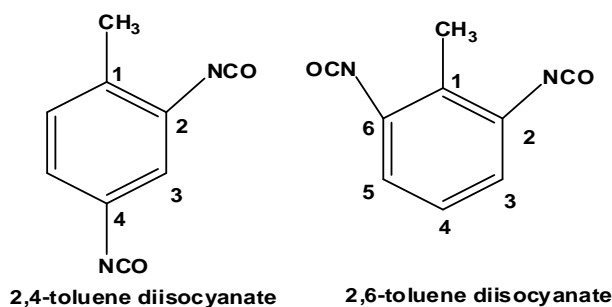
From the resonance structures, the positive charge at the C atom is obvious. On the other hand, the negative charge can be delocalized onto the oxygen atom, the nitrogen atom, and the R group. If R is an aromatic group, then the negative charge can be delocalized, as illustrated in Scheme 2.5. This explains why an aromatic isocyanate has a distinctly higher reactivity than an aliphatic isocyanate.²⁷ Furthermore, the reactivity of an isocyanate group can vary significantly, even for the same class of isocyanates. The structure, substituents, and steric effect can all influence reactivity.^{25,26}



Scheme 2.5: Resonance structures of the aromatic isocyanate

Types of isocyanates

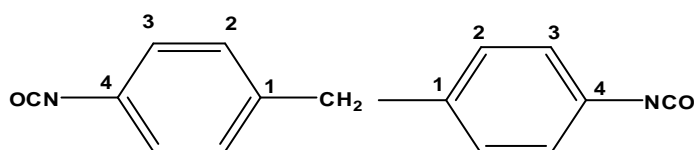
More than 90% of PUs are still produced from aromatic polyisocyanates.²⁸ The most commonly used aromatic isocyanates are TDI, and 4,4'-methylenediphenyl diisocyanate (MDI). TDI consists of a mixture of 80% 2,4- and 20% 2,6-toluene diisocyanate isomers (Scheme 2.6).



Scheme 2.6: TDI isomers.

The commercially available TDI is a mixture of these two isomers, in various ratios, although the pure 2,4- compound is also available commercially. TDI is a colorless liquid with a boiling point of 120 °C at 10 mm Hg.

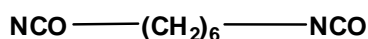
MDI is a solid with a melting point of 37 °C. It tends to dimerize at room temperature, and should therefore be stored below 0 °C as a solid, or between 40 and 45 °C as a liquid, to minimize the dimerization. MDI is normally produced as the 4,4'- isomer (Scheme 2.7) (98%); the 2,4'- and 2,2'- isomers are present in trace amounts. MDI is used in the production of rigid foams, elastomers, and some coatings.¹



Scheme 2.7: 4,4'-Diphenylmethane diisocyanate (MDI).

There are other aromatic diisocyanates that have some important applications, such as 1,5-diisocyanatonaphthalene (NDI), toluidine diisocyanate (TODI) and p-phenylene diisocyanate (PPDI).²⁹

Aliphatic isocyanates can be made from the corresponding aliphatic diamines via the phosgenation process. Cyclic aliphatic diamines are, in many cases, available through ring hydrogenation of the corresponding aromatic amines, such as the hydrogenation of diamino diphenyl methane (MDA) to give diamino dicyclohexyl methane.³⁰ The most important aliphatic isocyanates are 1,6-hexamethylene diisocyanate (HDI) (Scheme 2.8) and 4,4-diisocyanate dicyclohexylmethane (H₁₂MDI).



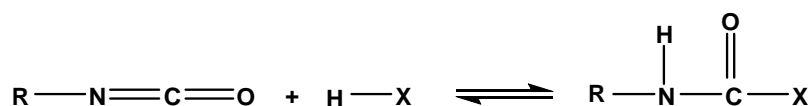
Scheme 2.8: 1,6-Hexamethylene diisocyanate(HDI).

These aliphatic isocyanates, or their modified forms, are widely used in the coatings industry.³¹ HDI is a colorless liquid with a boiling point of 127 °C at 1.33 kPa. HDI is less reactive than TDI and MDI. The reactivity of HDI can be increased by tertiary amines or tin compounds, to equal to or better than the NCO reactivity in TDI.³²

General reactions of isocyanates

1) Nucleophilic addition reactions

The most important reaction of isocyanates is the formation of carbamic acid derivatives (Scheme 2.9) by the addition of nucleophilic reactants across the C=N double bond.



Scheme 2.9: Formation of carbamic acid derivatives.

With increasing nucleophilic character of HX, the reaction proceeds at lower temperatures.³³ However, the above reaction product decomposes at higher temperatures to regenerate the starting material, i.e. free –NCO, since the reaction is a genuine equilibrium.²⁷

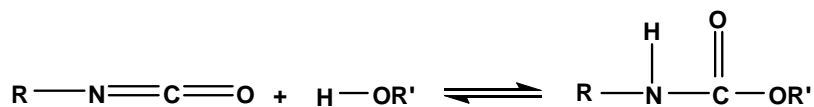
2) Primary reactions

Primary reactions require only low temperatures compared to the secondary reactions. Primary reactions are based on the increased relative reaction velocity.

i) Reactions with alcohols

The reaction between an alcohol and an isocyanate (Scheme 2.10) is an exothermic reaction.³³ These reactions are usually catalyzed by bases, mainly tertiary amines or organic metals. Reactivity is influenced by the structure of the amines. Primary, secondary and

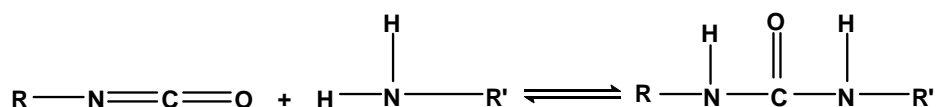
tertiary hydroxyls have decreasing reactivity due to the neighbouring methyl group causing steric hindrance. Amines exert a strong catalytic effect on isocyanate reactions.³² Hydroxylated compounds with tertiary amino groups (like triethanolamine) also exhibit a catalytic effect.³²



Scheme 2.10: Urethane formation from reaction with alcohol.

ii) Reactions with amines

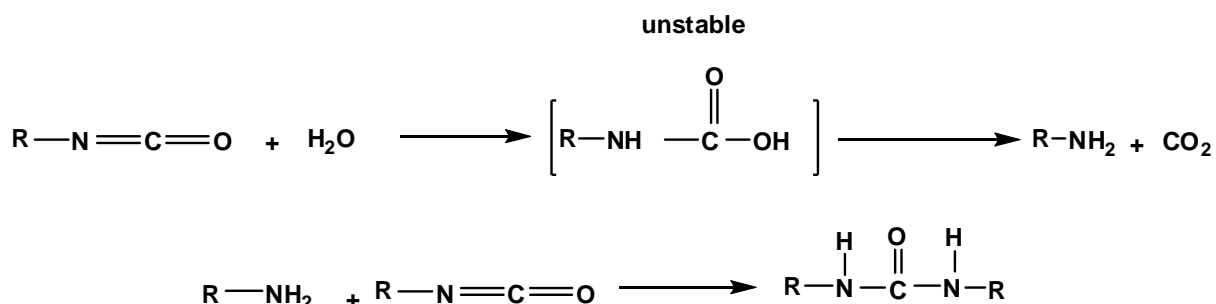
Reactions of isocyanates with amines to form polyureas (Scheme 2.11) are very fast and do not require catalysis. Aliphatic amines react more quickly than aromatic amines. The highly reactive aliphatic amines are used as chain extenders in the preparation of polyureas.



Scheme 2.11: Urea formation from reaction with amine.

iii) Reaction with water

The reaction between an isocyanate and water is a special case of an alcohol/isocyanate reaction. Here the primary product is the carbamic acid. It is not stable and will decompose to the corresponding amine and carbon dioxide. The amine formed will then react immediately with the isocyanate group in the system of polyurea structure, as illustrated in Scheme 2.12.

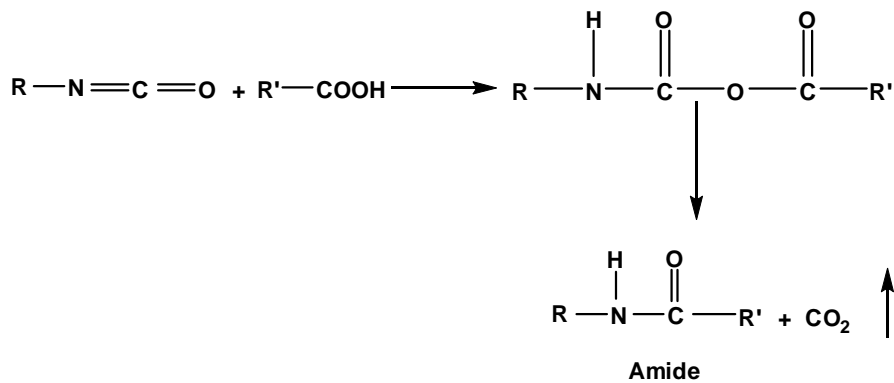


Scheme 2.12: Reaction between water and isocyanate.

This reaction is very important for the formation of Pu foam, since the carbon dioxide acts as a blowing agent. However, this reaction can also create problems in the storage of isocyanate. Moreover, to obtain high molecular weight, linear, thermoplastic Pus, it is essential to completely exclude water from the reaction system.^{34,35}

iv) Reaction with carboxylic compounds

The reaction of isocyanates with carboxylic acids affords intermediate carbamyl anhydrides. These are generally not stable and decompose to form amides and CO₂.

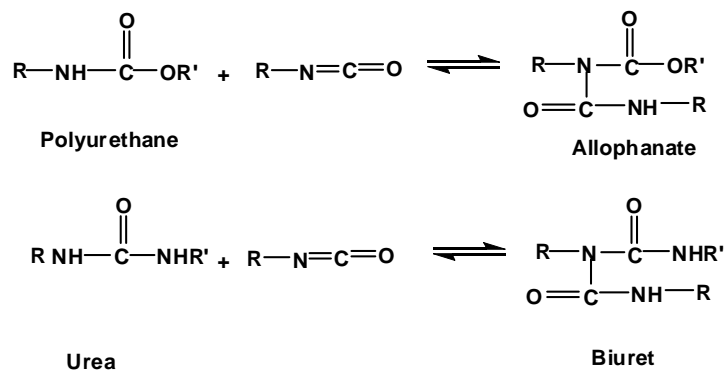


Scheme 2.13: Reaction of carboxylic acid with isocyanate.

The structure of the isocyanate and the carboxylic acid, and the reaction conditions, have a great influence on the decomposition of these carbamyl anhydride derivatives.⁶

3) Secondary reactions

The urethane and urea formed from the primary reactions still contain moderately active hydrogen. Although the reactivities of amide hydrogen and urea hydrogen are lower than the starting reagents, alcohol and amine, they are still capable of nucleophilic attack by the isocyanate, which results in an allophanate and a biuret. Allophanates are usually formed between 120 °C and 150 °C, and biurets between 100 °C and 150 °C.³⁵ Due to their low thermal stability, allophanates and biuret will dissociate into the starting components above 150 °C, as shown in Scheme 2.14 by equilibrium arrow designation.



Scheme 2.14: Formation of allophanate and biuret.

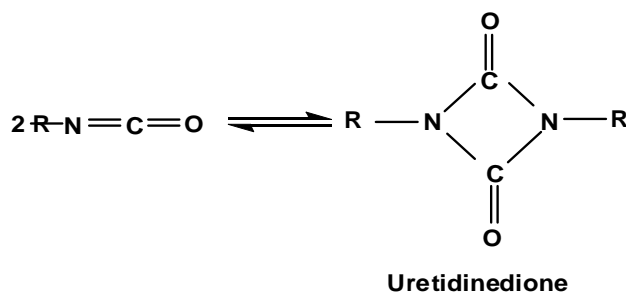
The formation of allophanates and biuret will probably result in the Pu crosslinking. Since these bonds dissociate at elevated temperatures, a small amount of excess isocyanate functionality is often used in the polymerization to promote crosslinking, while the polymer can still be melt processed.

4) Self-addition reactions

The highly unsaturated character of the NCO groups, under specific conditions, allows dimerization.

i) Dimerization

The dimerization reaction is shown in Scheme 2.15. Dimerization is limited to aromatic isocyanates and it is inhibited by ortho substituents.³⁶ For example, 2,4- and 2,6-TDI dimerize very slowly due to the hindering effect of the methyl group attached to the aromatic radical, while MDI dimerizes reasonably at room temperature, even without a catalyst. Moreover, dimerization is also a readily reversible reaction above 150 °C. However, the isocyanates, which can be formed by heating both aliphatic and aromatic isocyanates, are very stable and the dimerization reaction cannot be easily reversed.³⁷

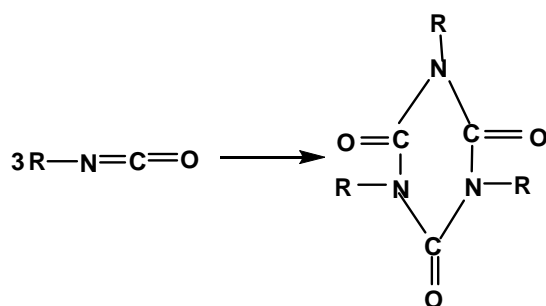


Scheme 2.15: Dimerization of isocyanate.

The dimerization reactions proceed at ambient temperature in highly polar solvents, such as DMF, with alkaline catalyst. The product depolymerizes readily and hence the reaction is of no technical use. Due to this splitting, dimerization of aromatic isocyanates is restricted to only a thermal window.³⁸

ii) Trimerization

Trimerization of isocyanate to form stable triazol rings is shown in Scheme 2.16. Trimerization is usually catalyzed by strong bases. After a given degree of trimerization, the reaction has to be terminated with *o/p*-toluene-sulphonic acid–methyl ester to avoid brittle polycyclic and crosslinked structures.³⁸



Scheme 2.16: Trimerization of isocyanate.

Aliphatic and cycloaliphatic isocyanates can either be trimerized alone or mixed with aromatic polyisocyanates. The isocyanates are mainly used for light-stable and weather-resistant coatings.³⁸

2.1.2.2 Polyols

Polyols commonly include α - ω hydroxy-terminated polyesters, and polyethers, polyolefins and glycols. The properties of any PU depend on the chemical composition and the molecular mass of the polyols used for its production. Typically, long-chain, high molecular weight polyols are preferable in elastomers synthesis.

2.1.2.3 Catalysts

The catalytic activity in the reaction of isocyanates and compounds with unstable hydrogen atom(s) (i.e. alcohols, amines, water, carboxylic acids, malonates, etc.) is known by tertiary amines and organometallic compounds, and among the latter the most important compounds are those of Sn, Pb and Fe. The most popular amine catalyst is 1,4-diazabicyclo-[2.2.2]-octane (DABCO), and the most widely used tin catalysts are: dibutyltindilaurate (DBTDL) and dibutyltindioctanate (DBTDO). These two types of compounds form the basis for very specific catalytic systems that have been developed, and which offer a high selectivity with respect to polyol components with different molecular weights and with primary, secondary or tertiary hydroxyl groups, and also with respect to small amounts of water possibly present in polyol feeds (or added for some specific purpose). These catalysts are used in the liquid form in most cases, and as solutions in glycol(s) or polyol(s), which are used commercially for the so-called polyol masterbatches. Catalytic salts of Bi, Fe, Ti, Co, Cd and Zn are used less frequently. Iron (II) acetoacetate, trialkylphosphines and compounds such as N-methylmorpholine and piperidine are also useful, and are therefore of some significance. Catalysts used for the preparation of PUs have been widely studied and reported in many papers.^{25,38-44}

2.1.3 Methods of preparation of polyurethanes

A number of techniques are available to prepare high molecular mass PUs: the melt-dispersion process, solution process, pre-polymer process, and the ketimine and ketazine processes.

2.1.3.1 The melt-dispersion process

Prepolymers containing NCO end groups can be synthesized in the melt by polycondensation of a polyester diol or polyether diol, a diisocyanate, and a diol containing an ionic group. Reducing the pH causes polycondensation, affording a high molecular mass PU urea. This process has many advantages, e.g. the reaction can be accelerated by increasing the temperature, no solvent is used, and a high volume-time yield is possible.^{28,45}

2.1.3.2 The solution process

In this process the reaction between an isocyanate and any hydroxyl-bearing compound occurs at low temperatures (20-120 °C, depending on the nature of the isocyanate used, and whether or not a catalyst is used). The lower reaction temperature means that at high

molecular mass the viscosity of the reaction medium is too high to permit good mechanical agitation and ease of handling. To obtain good processing, the viscosity must be reasonably low. This is achieved by adding polar low-boiling solvents such as acetone, methyl ethyl ketone or tetrahydrofuran to reduce the viscosity.⁴⁶

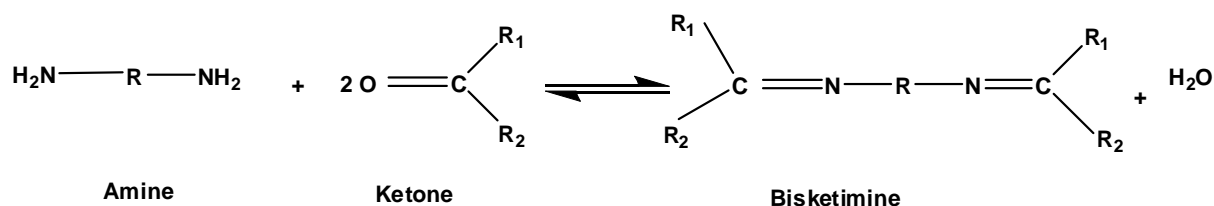
Besides reducing the viscosity of the mixture, the solvents also act as heat sinks, since the reaction between –NCO and –OH is highly exothermic. Reaction progress is measured by determining the isocyanate value. After a suitable degree of reaction, the pendant functional groups are neutralized by means of a suitable tertiary amine. Water is then added slowly, under moderate shear, followed by the addition of the chain extender to increase the molecular mass. The resulting dispersion is a binary colloidal system in which a discontinuous PU phase is dispersed in a continuous aqueous phase. In the last step the solvent is removed under vacuum.^{26,27}

2.1.3.3 The prepolymer process

Most PU dispersions are produced by this method. In this process the polyol component and isocyanate in excess in quantities are reacted to give PU prepolymer chain with an excess –NCO content. This can be confirmed by the disappearance of the –OH peak of the polyol component, as determined by infrared spectroscopy (IR), or by the volumetric titration value. Then the excess of –NCO in the prepolymer can be extended by adding diamines or short glycols in the presence traces of water, to form a high molecular mass PU dispersion.^{47,48}

2.1.3.4 The ketimine and ketazine process

In this process all the reactants, including the chain extender, are charged in the presence of ketones as solvents. Ketones react reversibly with amines (extenders) to form ketimine or ketazine. The highly reactive aliphatic diamine, ethylene diamine, reacts slowly with the isocyanate group if the medium is acetone.



Scheme 2.17: The ketimine and ketazine process.

Addition of water results in dispersion and release of the amine, and polyaddition occurs. This process requires only very small quantities of solvent, or no solvent at all.⁴⁹

2.1.4 Health aspects of isocyanates

Isocyanates have an inherent toxicity and harmful effects follow the inhalation of free isocyanate groups in vapour, mists and particles, or eye/skin contact with liquid or vapour of

all isocyanates. HDI and TDI are amongst the cheapest isocyanates, with the highest vapour pressure, making them the most dangerous. In view of HDI's extremely hazardous nature, its usage is very limited. In relatively high concentrations, isocyanates have a strong irritant effect on the respiratory tract in the most people, as discussed in various articles.⁵⁰⁻⁵²

Some people may develop bronchial sensitivity to isocyanates, and if these people are later exposed to even very low concentrations of isocyanates, which may even be below the exposure standard, they react by developing asthma-like symptoms, such as chest tightness, cough, wheeze and shortness of breath. Such attacks may occur up to several hours after cessation of exposure (for example, during the night), although, if the person is particularly sensitive, the attack may occur earlier.

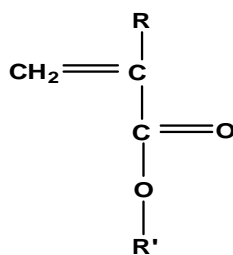
Asthmatic people are more prone to sensitization and other adverse reactions. People with a history of hay fever, atopic condition, asthma, recurrent acute bronchitis, interstitial pulmonary fibrosis, pulmonary tuberculosis, occupational chest disease and impaired lung function should be advised against exposure to isocyanates.

2.2 Polyacrylates

2.2.1 Introduction

Acrylic acid (AA) and acrylate esters have been known since the middle of the nineteenth century. A systematic investigation of acrylate esters was published as long ago as 1901 by Von Pechmann and Rohm.⁵³ A process for the industrial production of acrylate esters was developed in 1928 by H. Bauer and H Rohm.⁵⁴ Poly(methylmethacrylate) (PMMA) has been produced by solution polymerization since 1927, first by Rohm and Haas. Emulsion polymers were first developed on an industrial scale in 1930 by Von Pechmann.⁵³ The use of polyacrylate in many fields of applications increased rapidly with the development of new methods for producing acrylic acids and acrylate esters.

Acrylate and methacrylate esters are derivatives of the corresponding acids. They are the simplest members of the family of polymers of unsaturated carboxylic acids. Polyacrylates, formed by a head-to-tail addition process, have a hydrocarbon backbone with a pendent ester group. Polymethacrylates also have a pendant and methyl group on the same carbon atom. The acrylate polymers are characterized by having hydrogen attached to the carbon-carbon double bond (C=C in Scheme 2.18), and therefore have more rotational freedom than the methacrylate. The substitution of methyl (CH₃) for the hydrogen atom, producing a methacrylate polymer, restricts the freedom of rotation of the polymer and thus produces harder polymers with higher tensile strength and lower elongation than the acrylate counterparts.⁵⁴



Scheme 2.18: General formula of an acrylate ester.

where, R = H for acrylate or R = CH₃ for methacrylate, and R' is generally an alkyl group.

2.2.2 Preparation of polyacrylates

Acrylates can be polymerized very easily because their carbonyl groups activate the vinyl group. Polyacrylates are produced predominantly by radical polymerization. Conventional radical formers (e.g. peroxides and other per compounds) or azo compounds are used as initiators (controlled free radical reactions are also possible).

2.2.2.1 Solution polymerization

Solution polymerization involves heating the monomer and initiator in the presence of a solvent. At the end of the polymerization the solvent may be removed by distillation or a spray-drying technique. Aromatic hydrocarbons such as benzene and toluene are used as suitable solvents for the polymerization of acrylates of long-chain alcohols, while esters and ketone can be used for the polymerization of acrylates of short-chain alcohols. If the solvent boils at the temperature used for polymerization, a large amount of the heat of polymerization can be removed by evaporative cooling (latent heat of boiling). The solvent may act as chain transfer modifier in solution polymerization, hence it is very important to take this into consideration when choosing a solvent. The lower the transfer constant is, the higher is the molecular mass of the polymers, and the higher the viscosity will be. The latter has a negative effect on the mixing of the reactor contents and the removal of the heat of polymerization.⁵⁴ Soluble azo compounds, peroxides, or hydroperoxides are used as initiators, in concentrations of 0.01–2.00 wt % relative to the monomer.⁵³

Solution polymerization can be carried out by two methods: (i) the all-in-one, or 'one-shot', process, which involves charging the monomer, solvent initiator and modifier all at once into the reaction vessel and heating to the reaction temperature, or (ii) the 'drip-feed', or continuous process, which involves feeding the monomer and initiator separately into the solvent at the reaction temperature. Factors influencing solution polymerization include reaction temperature, monomer concentration, type of solvent, concentration of initiator and chain-transfer agents.⁵³

2.2.2.2 Emulsion polymerization

The basic components of an emulsion polymerization are water, acrylic monomer, surfactant, initiator, modifier and buffer.⁵⁵ The characteristic properties of a polymer are influenced by the conditions of polymerization, such as the catalyst used, the reaction time and temperature, and monomer concentration. All of these factors can be adjusted to change the molecular weight of the polymer and ultimately the polymer properties.

Acrylic emulsions are used in large volumes for many products, such as coatings, sealants and adhesives, and as cement modifiers. Polymer composition and structure can be tailored to meet the required application. Emulsions are easier to handle and are non-hazardous compared with polymers in solution.

2.2.3 Applications of polyacrylates

Polyacrylates are used in many applications, such as coatings, textiles, papers, oil additives, paints, and adhesives.⁵⁵ Polyacrylates can be soft or hard, for example: PMMA is a hard polymer, and because of its high hardness, it tends to be used for making shaped objects, while polybutyl methacrylate (PnBMA) is much softer and tends to find use in applications that require flexibility or extensibility. The ease of handling polyacrylates and the ease of copolymerizing softer acrylates with harder methacrylate, styrene, and vinylacetate, permit the manufacture of products that range from soft rubbers to hard film-forming polymers.

2.2.4 Urethane acrylate oligomers

Coatings that consist of an oligomer, a monomer and a photo-initiator can be cured by UV. The most commonly used UV-curable formulations contain unsaturated acrylates. The main types of acrylic oligomers include epoxy acrylates, polyester acrylates, polyether acrylates, urethane acrylates and silicone acrylates. Among the oligomers used for UV-curable coatings, the urethane acrylate oligomers (UAO) offer a wide range of excellent application properties, such as high impact and tensile strength, abrasion resistance and toughness, combined with excellent resistance to chemicals and solvents.⁵⁶ Hence urethane acrylates are used extensively in wood coatings, overprint varnishes, printing inks and adhesives applications.

UAO are commercially available with molecular weights ranging from 600 to 6000 g/mol and functionalities ranging from 2 to 6. They provide either a hard or flexible coating depending on molecular weight, functionality and chemical structure.⁵⁷

Pu derivatives are obtained by the reaction of a polyol with a diisocyanate, whereas polyurethane acrylate (PUA) oligomers are generally prepared by a two-step synthesis.⁵⁷ An excess of diisocyanate can react with a polyol, and only then with an hydroxyl-terminated

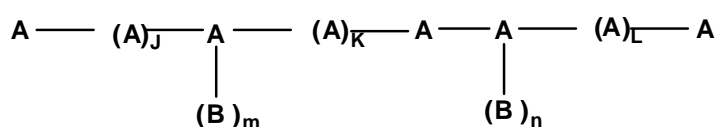
acrylate.⁵⁸ In another procedure a diisocyanate, in excess, first reacts with a monoalcohol acrylate and then with the polyol, as reported by Fibril et al.⁵⁹ Finally, as recently described by Chen et al.⁶⁰, a one-step synthesis can also be performed by exothermic control or by using 2-methyl-2-propenoyl isocyanate. Most of these urethane acrylate macromonomers are multi-functional, i.e at least difunctional and afford crosslinked coatings.

2.3 Graft copolymers

Graft copolymerization is a common technique by which to modify the chemical and physical properties of polymers.⁶¹ Graft copolymers consist of two different types of polymer, which are usually incompatible or immiscible. The incompatibility between the main chain and the branch makes graft polymers similar to polymer blends, but in the case of graft polymers the immiscible phases are joined by covalent bonds. These show micro-phase separations and can exhibit remarkable thermal and mechanical properties, and subsequently advanced applications. Graft copolymers are often prepared in order to modify polymer properties.⁶² This is because the main chains are usually thermodynamically incompatible. Most graft copolymers can be classified as multiphase polymers in the solid state, similar to polymer blends, block copolymers, and polymer networks. Microphase-separated graft copolymers can display many of the unique thermal and mechanical properties observed in block copolymers, including thermoplastic elasticity. Since the morphology of heterophase polymers can be affected by the casting solvent and the nature of its interaction with the polymers blocks, the physical properties are also expected to depend on the casting solvent.⁶³

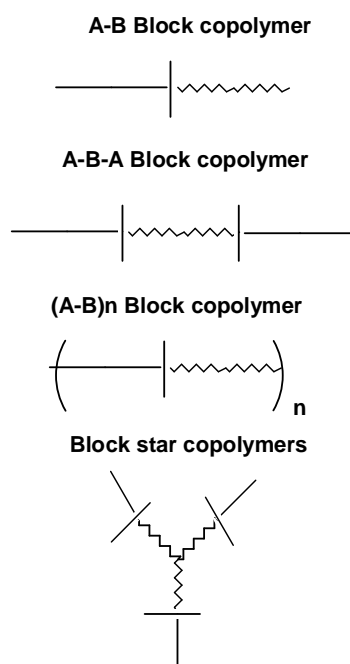
Newer areas of interest are nanophase-separated graft copolymer systems.⁶⁴ This occurs when the grafts are too short to form a large domain which (in this case) can then change the bulk properties to portray both phases independently.

Graft polymers can be used as surfactants, compatibilization agents in polymer blends, additives in high-impact materials, adhesives, and thermoplastic elastomers.⁶¹ They exhibit enhanced tensile strength, improved metal adhesion, controlled wettability, and surface modification.⁶⁵ The simplest case of a graft copolymer is represented by the structure in Scheme 3.1, where A is the main polymer chain; J, K, L are repeat units; and B_n and B_m are the side chain grafts made from monomer B.



Scheme 2.19: General formula of a graft copolymer.

The extent of polymerization in B_n and B_m grafts contributes to the degree of grafting (grafting yield), which is gravimetrically determined as a percentage of the mass increase.⁶⁶ Both the backbone and side chain grafts can be either homopolymers or copolymers, with different chemical compositions. Branching in one or more stages and crosslinking may occur, and these branches are usually randomly distributed along the polymer backbone.⁶⁷ Linear block copolymers comprise chemically different segments, much like grafts. They can be arranged as a copolymer of two differing monomeric units, such as A-B, with only two distinct segments, or in a triblock fashion, such as A-B-A, with three segments, or as multiblocks of the structure $(A-B)_n$, comprising many segments, as shown in Scheme 2.20.



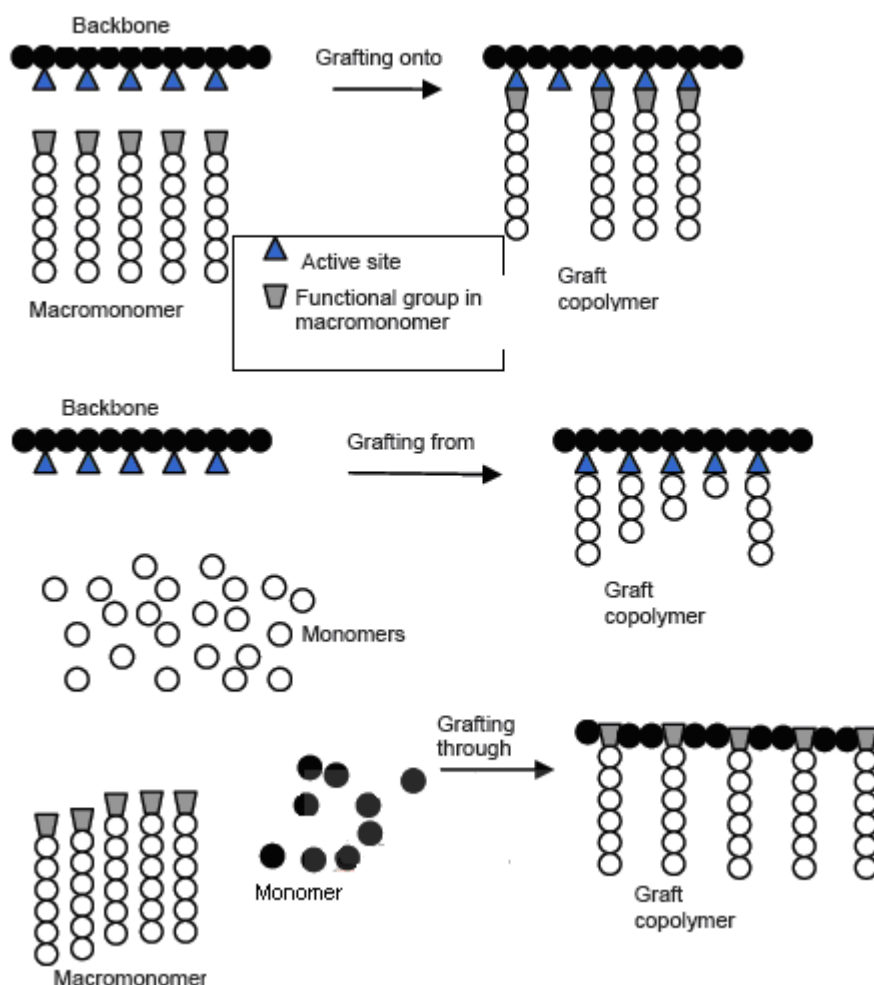
Scheme 2.20: Representation of different types of block copolymers.

In block copolymers, like graft copolymers, both A and B sequences may be homopolymers or copolymers, as long as the A sequence is different from the B sequence.

Another, less common configuration is the star block copolymer, with arms that radiate from a central core of a chemical makeup that is different to that of the arms.⁶⁸ Graft copolymerization takes place as a result of the formation of active sites on the polymer backbone. The active sites may be functional groups, free radicals or ionic groups, which initiate the polymerization reaction. The creation of active sites on the polymer backbone can be carried out by several methods, such as synthetically, or by postmodification with plasma treatment, ultraviolet or light radiation, decomposition of chemical initiator and high energy radiation.⁶⁹ The free radical polymerization method is the oldest and most widely used procedure for the synthesis of graft polymers because it is relatively simple.⁶⁸ However, it usually yields heterogeneous materials that are difficult to characterize and may be complicated by crosslinking.

2.3.1 Synthesis of graft copolymers

The preparation of graft polymer structures has been achieved by three different methods,⁷⁰ as outlined in Scheme 2.21.



Scheme 2.21: Schematic representation of the synthesis of graft copolymers by the: grafting onto, grafting from and grafting through methods.⁷⁰

"Grafting through", is when a macromonomer is copolymerized with an oligomeric comonomer; "grafting from", is when the polymerization of a second monomer is initiated by sites located on the main polymer chain; and "grafting onto", is when a polymeric species reacts with functional groups located on the chain of another polymer. These synthetic routes have been adapted from techniques mostly used to prepare comb-branched polymers.⁷¹

2.3.1.1 Grafting from

In the "grafting from" method, after or during the preparation of the polymer backbone, active sites are produced along the main chain and these are able to initiate the polymerization of the second monomer. Polymerization of the second monomer results in the formation of the branches and the final graft copolymers. The number of branches can be controlled by the number of active sites generated along the backbone, assuming that each one of them

initiates the formation of one branch. The isolation and characterization of each part of a graft copolymer in this case is almost always impossible, because knowledge of precursor molecular characteristics is limited to knowledge of the backbone and the grafts need to be severed from the backbone for their characterization⁷²⁻⁷⁴.

2.3.1.2 Grafting onto

The "grafting onto" method is most commonly used for the preparation of graft polymers with a tailored structure and topology. In the "grafting onto" method the polymer backbone and the arms are prepared separately, by a living polymerization mechanism. The backbone bears functional groups, distributed along the chain, which can react with living branches. Upon mixing the backbone and the branches in the desired quantity and under the right experimental conditions, a coupling reaction takes place in the final comb-shaped polymers.⁷⁵⁻⁷⁷ The branching sites can be introduced into the backbone either by a homopolymerization reaction or by copolymerization of the main backbone monomer(s) with a suitable comonomer with the desired functional groups.⁷⁸

2.3.1.3 Grafting through

The "grafting through" approach to the preparation of graft polymers consists of two steps.⁷⁹ First, a linear polymer bearing a terminal polymerized end group is prepared. This species is referred to as a macromonomer. Second, copolymerization of the macromonomer with a suitable comonomer is carried out, generally by radical polymerization. The most common methods by which to incorporate a polymerizable group at the chain end are functional initiation or reactive termination (end capping). Since the macromonomer is prepared separately, it can be fully characterized. The radical copolymerization of the macromonomer and monomers leads to the formation of the backbone. The number of branches per backbone can generally be controlled by the ratio of the molar concentration of the macromonomer to that of the comonomer. Several other factors have to be considered, among them the copolymerization behaviour of the macromonomer and the comonomer forming the backbone. Numerous examples of comb-branched graft copolymers prepared by this approach have been reported.^{78,80-86}

Grafting through offers several advantages for the synthesis of well-defined graft copolymers: (a) a wide variety of macromonomers and monomers are available, and all the possible polymerization techniques can be employed, leading to very large number of graft copolymers that can be synthesized; (b) the chain length of the side chains can be controlled by the synthesis of the macromonomers; (c) the backbone length can be also controlled when a living polymerization method is used for the copolymerization reaction; (d) the number of graft chains per backbone can be controlled by the molar ratio of the macromonomer and the comonomer, and by the reactivity ratios of the components of the

copolymerization system. However, there are several limitations that characterize the macromonomer method for the synthesis of graft copolymers. The most important is the lack of control over the spacing of the graft chains along the backbone. The spacing distribution is determined by both the reactivity ratios of the macromonomer and the comonomer and their concentrations. Phase separation depends on this spacing distributions and graft length.

2.3.2 Macromonomers

Macromonomers (a combination of a macromolecular chain and a polymerizable end group) have been widely used for the synthesis of many branched macromolecular architectures.⁸⁷ This is a consequence of (a) the vast range of macromonomers that have been prepared and (b) the different polymerization processes employed for their homo- and copolymerization (conventional free radical, group transfer, anionic, cationic, controlled free radical, ring opening metathesis, metallocene and late transition metal catalyzed polymerizations) with either low-molecular-weight monomers or other macromonomers. These branched structures are well-defined since: (a) the length of the branches is fixed by the molecular weight of the macromonomer, which is known, and can be predetermined using a living polymerization method for the synthesis of the macromonomer, (b) the size of the main chain of the branched structure can be controlled using a living polymerization method, and (c) the distribution of the branches can be controlled by the composition of the copolymerization mixture and the reactivity ratio of the macromonomers.

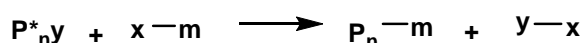
2.3.2.1 Synthetic methods leading to the preparation of well-defined macromonomers

Three general synthetic methods have been used for the synthesis of well-defined macromonomers P_n-m, where P_n is the polymeric chain and m the polymerizable (monomer) functional group:

- (a) reaction of a living polymer with a linking reagent containing the polymerizable functional group m
- (b) initiation of living polymerization with an initiator containing the functional group m
- (c) post-polymerization transformation of the neutralized polymeric chain in order to introduce the polymerizable functional group m.

(a) Reaction of living polymer with a reagent containing the polymerizable group m

The general reaction scheme is shown below:



Scheme 2.22: Representation of the synthesis of well-defined macromonomers.

P_n^{*} is the living chain, and x-m the linking agent with the polymerizable group. Only a few representative examples are given in the literature.⁸⁸⁻⁹⁴

(b) Initiation of living polymerization with an initiator containing the polymerizable group m

The general reaction scheme is given below:



Scheme 2.23: Representation of the synthesis of macromonomers.

m-y is the initiator bearing the polymerizable group m. In this case each chain has a polymerizable group (functionality 100%).⁹⁵⁻¹⁰¹ The synthesis of polymacromonomers can be accomplished by almost all the available polymerization methods: conventional free radical,¹⁰²⁻¹¹³ controlled/living free radical,^{97, 114-116} ring opening metathesis,^{95,117-126} anionic,^{104, 127-131} cationic,¹³² condensation,¹³³⁻¹³⁵ and metallocene polymerization.^{136,137}

2.4 Free radical polymerization

A free radical is basically a molecule with an unpaired electron. The tendency for this free radical to add an additional electron in order to form a pair makes it highly reactive, so that it will attack the bond on another molecule by removing an electron, leaving that molecule with an unpaired electron. Free radicals are often created by the splitting of a molecule into two fragments along a single labile bond (initiator). After a reaction has been initiated, the propagation reaction takes place. The entire propagation reaction of a single chain usually takes place within a fraction of a second and then by electron transfer or termination reaction the chain ends. In general, termination occurs in two ways: by combination or by disproportionation. Combination occurs when the polymer's growth is terminated by free electrons from two growing chains that join and form a single chain. Disproportionation occurs when a free radical removes a hydrogen atom from an active chain and leaves behind an unsaturated chain.

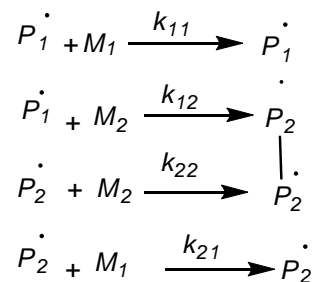
2.4.1 Free radical copolymerization

Copolymerization is the polymerization of two or more different monomers simultaneously. The rate of addition of the monomer to the growing chain depends on the nature of the end group of the radical chain. In the case of macromonomers, polymerization and copolymerization are characterized by several factors.^{108,138,139}

- Because of the high viscosity of the polymerization medium the polymerization of macromonomers is sensitive to the diffusion-controlled step of the polymerization reaction, which is affected by entanglement formation.
- The concentration of the polymerizable reactive end group is low.
- The propagation step includes the addition of macromonomer to the growing grafted radical.

- High segment density or a multi-branched structure around the propagation radical site leads to a slow rate termination constant k_t and a less reduced rate propagation constant k_p compared to the case with conventional monomers.

The copolymerization kinetic behaviour of many different macromonomers has been treated according to the terminal model through the Mayo-Lewis equation.¹⁴⁰ Mayo-Lewis formulated a model of copolymerization in which the rate constants for the addition of each monomer are assumed to be dependent on the terminal unit on the growing chain. If two monomers M_1 and M_2 are involved in the copolymerization with two propagation radicals \dot{P}_1 and \dot{P}_2 then four different reactions will be involved¹⁴¹:



Scheme 2.24: Propagation reactions in free radical polymerization.

According to the terminal model, the disappearance rate of monomers can be described by the following equations:

$$\frac{-d[M_1]}{dt} = k_{11} [\dot{P}_1][M_1] + k_{21} [\dot{P}_2][M_1] \quad (2.1)$$

$$\frac{-d[M_2]}{dt} = k_{12} [\dot{P}_1][M_2] + k_{22} [\dot{P}_2][M_2] \quad (2.2)$$

where $[M_1]$ and $[M_2]$ are the monomer feed concentrations, and $[\dot{P}_1]$, $[\dot{P}_2]$ are the concentrations of the growing radicals for M_1 and M_2 , respectively.

Dividing equation 2.1 by 2.2 gives:

$$\frac{d[M_1]}{d[M_2]} = \frac{k_{11} [\dot{P}_1][M_1] + k_{21} [\dot{P}_2][M_1]}{k_{12} [\dot{P}_1][M_2] + k_{22} [\dot{P}_2][M_2]} \quad (2.3)$$

Under steady state conditions the termination of the radicals is equal to their generation, thus:

$$k_{21}[\dot{P}_2][M_1] = k_{12}[\dot{P}_1][M_2] \quad (2.4)$$

Equation 2.5 allows the elimination of the radical concentration from equation 2.4 and the copolymer composition becomes

$$\frac{d[M_1]}{d[M_2]} = \frac{[M_1] ([M_1]r_1 + [M_2])}{[M_2] ([M_1] + [M_2]r_2)} \quad (2.5)$$

where r_1 and r_2 are the reactivity ratios of M_1 and M_2 , respectively.

$$r_1 = \frac{k_{11}}{k_{12}} \quad \text{and} \quad r_2 = \frac{k_{22}}{k_{21}}$$

The reactivity of macromonomers is the same as for small monomers. However, there are some deviations have been reported.⁶⁸

2.4.2 Reactivity of macromonomers in homopolymerization and copolymerization reactions

The homopolymerization of macromonomers affords comb-shaped structures, polymacromonomers or molecular brushes, with an extremely high density of branching, since each monomeric unit bears a polymeric chain as a side group. Depending on the graft length and degree of polymerization, the polymacromonomers may adopt several conformations in solution, such as star-like, comb-like, bottle-brush, or flower-like. The copolymerization of a macromonomer with another conventional monomer results in the formation of graft copolymers.

Use of different combinations of macromonomers and comonomers in several proportions, and the ability to use diblock macromonomers or more than one macromonomer in the same copolymerization mixture, lead to a rich variety of structures differing in chemical composition, and the number of branches and conformations. Furthermore, the use of difunctional macromonomers may lead to the formation of networks with controlled crosslink density. Other more complex architectures, like well-defined star polymers, palm-tree, and dendritic polymers, may also be prepared by using macromonomers as intermediate building blocks.

Despite their numerous synthetic advantages, the use of macromonomers is accompanied by several drawbacks, such as: (a) increase in viscosity during solution polymerization, (b)

the concentration of the polymerizable end groups is very low, (c) the polymerization proceeds via the interaction between polymer chains and, (d) the steric hindrance of the active center of the developing polymer chain increases during addition of macromonomer. All of these features may lead to products of increased compositional and chemical heterogeneities. Hence it is important to study the reactivity of the macromonomers and compare it with the reactivity of low-molecular-weight monomers

As the macromonomers combine the properties of a polymer chain and a monomer in the same molecule, it is a matter of continuing interest to define the influence of the macromolecular chain on the reactivity of the polymerizable end group. The most important factors affecting the reactivity of the macromonomers are the following: (a) the chemical nature of the comonomer and the macromonomer's polymerizable end group, which determines the inherent reactivity of the system; (b) the diffusion and the kinetic excluded volume, which determines the size of the macromonomer; and (c) the potential incompatibility between the macromonomer and the growing copolymer structure. This may lead to phase separation and thus to products characterized by compositional and chemical heterogeneity. A combination of several characterization techniques is required to determine whether the obtained structures are well-defined or not.^{138,142-147}

Among these factors, the most important is the reactivity of the macromonomer which lower than the reactivity of low molecular weight monomer. Consequently, during the polymerization the increased incompatibility between the macromonomer and the growing polymer chain may dramatically reduce the reactivity of the macromonomer. During free radical polymerization the excluded volume of macromonomers can inhibit the approach of the active center of the growing polymer chain to the polymerizable end group of the macromonomer. Since the above factors reduce the reactivity of the macromonomers it can be concluded that during "one shot" copolymerization with a low molecular weight comonomer the graft structure will be very poor in branches in the initial stages of the copolymerization (high reactivity of the comonomers), whereas in the later stages of the copolymerization the structure will be richer in branches (excess of the unreacted macromonomers over the low-molecular-weight monomer). Therefore, in most cases, the final product will have a heterogeneous distribution of branches along the backbone. The influence of the solvent becomes important when it is selective either for the macromonomer or for the growing backbone of the branched structure, leading to the formation of micellar structures, and in a few cases, to acceleration of polymerization.^{148,149}

2.4.3 Polymer-polymer phase separation

The microphase-separated structures of block copolymers are controlled by the delicate competition between the interaction energy between the blocks and the chain stretching

energy. The repulsion between the chemically different fragments drives the system to undergo phase separation, however, because the incompatible blocks are chemically connected the system exhibits microphase separation and self-organizes into various ordered structures. For the simplest diblock copolymer melt, the ordered structures include lamellae, hexagonally packed cylinders, and body-centered cubic spheres. These equilibrium morphologies can be tailored by varying the copolymer composition and the segregation degree between the two blocks. Because of the ongoing interest in novel macromolecular organization, well-defined nonlinear copolymers with complex architectures such as graft, star-block, multi-arm, and hyperbranched copolymers have been studied experimentally.¹⁵⁰⁻¹⁵⁸

It has been found that the molecular architecture is an important factor for tailoring the morphologies, phase behaviour, and material properties of copolymers. Among the copolymers with complex architectures, considerable attention has been paid to the microphase separation of graft copolymers because of their unique material properties and their applications as interface compatibilizers, thermoplastic elastomers, and viscosity modifiers.^{159,160} Well-ordered lamellar, cylindrical, and spherical morphologies are observed. The morphologies of graft copolymers and domain spacing of ordered structures depend on the molecular architecture of graft copolymers, such as the number of grafts and the distribution of junctions. There is a dramatic shift in the phase boundaries of graft copolymer melts compared with diblock copolymers melts at a given segregation degree.¹⁶¹⁻¹⁶³

Whereas as the architecture of copolymers changes from diblock copolymers to graft copolymers, the morphological behaviour depends not only on the composition and interaction energy, but also on the molecular architecture, such as the position of junctions and the number of branches. Systematic studies of the relationship between molecular architecture and morphology have been experimentally limited due to the unavailability of model graft copolymers with well-defined architectures.^{161,163-165}

The chain length of the macromonomer, which defines the length of branches in the graft copolymer, is predetermined and precisely controlled using living polymerization strategies. The choice of monomers and the order of monomer addition also control the composition of the branch and backbone upon subsequent copolymerization.⁸⁷

Occurrence of microphase separation depends on many factors, including segmental polarity difference; segmental length; crystallizability of either segment; intra- and inter-segment interactions, such as hydrogen bonding; overall composition; and molecular weight. The elasticity, toughness, and other physical properties of these materials are largely determined

by the size, crystallinity, and interconnectivity of the hard domains, as well as the nature of the domain interface and the degree of mixing and of hard segments in the soft segment phase.¹⁶⁶⁻¹⁷²

2.4.4 Examples of interpenetrating polymer networks and copolymers with linear polyurethanes (acrylic- polyurethane copolymers)

Poly(urethane-acrylate) copolymers are particularly noteworthy due to their ability to form waterborne dispersions, for environmentally friendly materials.¹⁷³ The powdered materials like corundum (Al_2O_3) or zirconium oxide (ZrO_2) can be blended with polyurethane-acrylate binders and then moulded in a one-axis pressing operation, and the obtained so-called green ceramics can be subjected to preliminary machining.^{174,175}

Another example of is the ceramic–polymeric (urethane-acrylate) copolymers, which can be processed in the tape casting process using the above inorganic to yield thin ceramic foils for electronics.¹⁷⁶ When the micro-structure of the block PU polymer itself is analyzed, considerable phase heterogeneity of that material is observed.¹⁷⁷ The particles will not agglutinate and after the drying operation they can be employed as environmentally attractive powder coatings.¹⁵⁸

Moreover, poly(urethane-acrylic) dispersions that have the characteristic of an interpenetrating polymer network (IPN) find use as carrier protective coatings.^{11,178} The IPN systems are characterized by interpenetration of linear macromolecules or independent spatial networks of a minimum of two polymer types, synthesized according to different mechanisms, e.g. acrylic polymers obtained in the free radical polymerization process and polyurethanes obtained in the linear polyaddition reaction of diisocyanates and polyols. In case of compositions, in which the linear structure is offered by one polymer only, e.g. poly (butyl acrylate); the system is called semi-IPN.

Basically, the chains of both polymers (PU and acrylic) should not be joined by any covalent bond but they should only be tangled by the actions of hydrogen bridges and dispersion forces.¹⁷⁹ This is the case when acrylic monomers contain no active hydrogen atoms and when they cannot react with the isocyanate prepolymer. Those monomers are subjected to polymerization in aqueous emulsion, in the presence of a dissolved initiator, e.g. hydrogen peroxide, and the dispersion of the PU ionomer (produced separately beforehand) is also present in the system as the emulsifier (that function is sometimes supported by an external surface active agent).^{179,180} Irrespective of this method, the networks created by both polymers can be fixed together when an unsaturated compound with the –OH group in its structure (e.g. 2-hydroxyethyl acrylate (2-HEA)) is used as one of the raw materials in the synthesis of polyurethanes, i.e. an extension compound for isocyanate prepolymer chains.

The poly(urethane acrylic) macro-anionomer product can be synthesized in a four-staged step-growth polymerization process, followed by free-radical copolymerization in aqueous emulsion.¹⁸¹ The chemical basis for the process is termination of the linear urethane-isocyanate chains by means of HEA.¹⁸² The urethane–acrylate macro-anionomer produced in that way is capable of forming aqueous dispersions and it can be subjected to emulsion copolymerization at further stages with typical acrylates (methyl acrylate and butyl acrylate) in a free-radical copolymerization process, yielding the poly(urethane-acrylic) macro-anionomer (the final product of this synthesis).

Research carried out in recent years has demonstrated the possibility of synthesizing “comb-like or star-like poly(urethane-acrylic) copolymers” using the controlled/living techniques of radical polymerization (ATRP) which can produce polymers with narrow polydispersity.¹⁸³ A “living polymer” can be formed in the reaction system by minimizing the irreversible chain termination reactions, so that the chain propagation reaction becomes controlled. The suitable oligourethane needs to be synthesized first, which – as the macroiniferter must be capable of forming simultaneously a stable radical. That urethane oligomer, after addition of vinyl chain radicals, will increase the modified hydrophobic performance, depending on the type of monomer and length of produced chains. The side chains should contain ionic groups, e.g. derived from methacrylic acid, if the obtained copolymer is required to be water-dispersible.

The urethane oligomer was used as the macroinifert in free radical polymerization;¹⁸⁴ it was synthesized in the reaction of the isocyanate prepolymer of MDI, poly(tetramethylene oxide) (PTMO) and an aromatic chain extender; 1,2-tetraphenylethane-2-diol (TPED). The aromatic structure of which compound makes possible the resonance stabilization in the created urethane macro-radical. The reaction that yields the polyurethane acrylate dispersion with the use of the urethane macroiniferter is shown in Scheme 2.25; the urethane remains difunctional and forms triblock copolymers.

13. Potoczek, M.; Heneczkowski, M.; Oleksy, M. *Ceram. Int.* **2003**, 259, 29.
14. Athawale, V.; Kolekar, S. *Eur. Polym. J.* **1998**, 34, 1447.
15. Chantarasiri, N.; Farkrachang, N.; Kawnamarit, K.; Eurpermkiati, A. *Eur. Polym. J.* **2000**, 36, 95.
16. Kro, I. P.; Wojturska, J. *J. Polym. Sci. Part A: Polym. Chem.* **2002**, 47, 6.
17. Lin, M. S.; Lee, S. T. *Polymer* **1997**, 38, 53.
18. Vlad, S.; Vlad, A.; Oprea, S. *Eur. Polym. J.* **2002**, 38, 829.
19. Desai, S.; Thakore, I. M.; Sarawade, B. D.; Devi, S. *Polym. Eng. Sci.* **2000**, 40, 1200.
20. Paul, C. J.; Nair, M. R.; Neelakantan, N. R.; Koshy, P. *Polymer* **1998**, 39, 6861.
21. Poussard, L.; Burel, F.; Couvercelle, J. P.; Merhi, Y.; Tabrizian, M.; Bunel, C. *Biomaterials* **2004**, 25, 3473.
22. Wang, J. H.; Yao, C. H. *J. Biomed. Mater. Res.* **2000**, 51, 761.
23. Frish, C. *Urethane Technol.* **1987**, 22, 108.
24. Woods, G., *The ICI Polyurethanes Book*. Wiley-Interscience: New York, 1987.
25. Oertel, G., *Polyurethane Handbook*. Hanser Publishers: Munich, 1994.
26. Mequanint, K. PhD dissertation, University of Stellenbosch, South Africa, Dec1997.
27. Mequanint, K. MSc thesis, University of Stellenbosch, South Africa, Feb 2001.
28. Zhu, Y.; Huang, Y.; Chi, Z.; Shen, H. *Eur. Polym. J.* **1994**, 30, 1493.
29. Schmitt, F.; Wenning, A.; Weiss, J. *Prog. Org. Coat.* **1998**, 34 227.
30. Fukuoka, S.; Masazumi, C.; Masashi, K. *J. Chem. Soc.* **1984**, 18, 399.
31. Weiss, K. *Prog. Polym. Sci.* **1997**, 22, 203.
32. Harjunalanen, T.; Lahtinen, M. *Eur. Polym. J.* **2003**, 39, 817.
33. Crawford, M.; Bass, R.; Haas, T. *Thermochim. Acta* **1998**, 323, 53.
34. Britain, J.; Ge, P. *J. Appl. Polym. Sci.* **1960**, 4, 207.
35. Douglas, A.; Zeno, W.; Wicks, J. *Prog. Org. Coat.* **2005**, 54, 141.
36. Bruins, P., *Polyurethane Technology*. Wiley-Interscience: New York, 1969; p 72.
37. Orzesek, H. *Appl. Catal. A* **2001**, 221, 303.
38. Wegener, G.; Brandt, M.; Duda, L.; Hofmann, J.; Kleszczewski, B.; Koch, D. *Appl. Catal. A, General.* **2001**, 221, 303.
39. Reegan, S. L.; Frisch, K. C., Catalysis in Isocyanate Reactions. *In: Advances in Urethane Science and Technology*. Technomic Publishing Co: Westport CT, 1971.
40. Saunders, J. H.; Frisch, K. C., *Polyurethanes: Chemistry and Technology, part I. Chemistry*. Kriger Publishing Co: USA, 1983.
41. Wirpsza, Z.; *Polyurethanes: Chemistry, Technology and Applications*. Ellis Horwood: New York, 1993.
42. Ratier, M.; Khatmi, D.; Duboudin, J. G. *Appl. Organomet. Chem.* **1992**, 6, 253.
43. Klotz, H.; Lassila, K.; Listemann, M. L.; Minnich, K. E.; Savoca, A. C. *J. Mol. Catal. A*,

- . *Chem.* **1997**, 120, 296.
44. Simons, K. *Catalyst* **2005**, 1, 2005.
 45. Chattopadhyay, D.; Sreedhar, B.; Raju, K. *Polymer* **2006**, 47, 3814.
 46. Randall, D.; Lee, S., *Polyurethane Handbook*. John Wiley and sons: New York, 2002; Vol. 78, p 68.
 47. Thomes, P., *Waterborne and Solvent Based Surface Coatings*. John Wiley and sons: New York, 1998; Vol. III, p 51.
 48. Jayakumar, R.; Nanjundan, S. *Eur. Polym. J.* **2005**, 41, 1623.
 49. Mahmood, N. PhD thesis, University of Halle-Wittenberg, Germany, 2005.
 50. Bernstein, D. I.; Cartier, A.; Cote, J.; Malo, J. L.; Boutlet, L. P.; Wanner, M.; Milot, J.; Respir, A. J. *Crit. Care Med.* **2002**, 166, 455.
 51. Mapp, E. C.; Fryer, A. A.; Marzo, N. D.; Mazro, N. D.; Pozzato, V.; Padoan, M.; Boschetto, P. *J. Allerg. Clin. Immunol.* **2002**, 109, 867.
 52. Lamba, N.; Woodhouse, K.; Cooper, S., *Polyurethane in Biomedical Applications*. CRS: Washington, USA, 1998.
 53. Elvers, B.; Hawkins, S.; Schulz, G., *Ullmann's Encyclopedia of Industrial Chemistry*. John Wiley and sons: New York, 1992; Vol. 21A, p 158.
 54. Wilks, E., *Industrial Polymer Handbook*. John Wiley and sons: New York, 1988; Vol. 1, p 578.
 55. Cunningham, M. *Prog. Polym. Sci.* **2002**, 27, 1039.
 56. Lee, B.; Kim, H. *Polym. Degrad. Stab.* **2006**, 91, 1025.
 57. Hanahata, H.; Yamazaki, E.; Kitahama, Y. *Polym. J.* **1997**, 29, 818.
 58. Oprea, S.; Vlad, S.; Stanciu, A.; Ciobanu, C.; Macoveanu, M. *Eur. Polym. J.* **1999**, 35, 1269.
 59. Burel, F.; Lecamp, L.; Youssef, B.; Bunel, C.; Saiter, J. *Thermochim. Acta* **1999**, 326, 133.
 60. Chen, J.; Pascault, J.; Taha, M. *J. Polym. Sci. Part A: Polym. Chem.* **1996**, 34, 2889.
 61. Fernandez-Garcia, M.; Luis, J.; Cerrada, M.; Madruga, E. *Polymer* **2002**, 43, 3173.
 62. Battared, H.; Treger, G., *Graft Copolymerization*. Wiley-Interscience: New York, 1967.
 63. Xie, H.; Xie, D. *Prog. Polym. Sci.* **1999**, 24, 275.
 64. Maynarda, D.; Lyub, S.; Fredricksona, G.; Wudla, F.; Chmelka, B. *Polymer* **2001**, 42, 7567.
 65. Ito, K.; Usami, N.; Yamashita, Y. *Macromolecules* **1980**, 13, 216.
 66. Miroslav, J.; Bohumil, M.; L.Toman; Latalova, P. V. P. *React. Funct. Polym.* **2003**, 57, 137.
 67. Salager, J.; Becker, P., *Encyclopedia of Emulsion Technology*. John Wiley and sons: New York, 1998; Vol. 3.
 68. Polk, W. D. PhD dissertation, University of Stellenbosch, Stellenbosch, July 2001.

69. Nasef, M.; Hegazy, S. *Prog. Polym. Sci.* **2004**, 29, 499.
70. Elhrari, W. MSc thesis, University of Stellenbosch, Stellenbosch, December 2006.
71. Schunk, T.; Long, T. *J. Chromatogr. A.* **1995**, 692, 221.
72. Beers, K.; Gaynor, S.; Matyjaszewski, K.; Moeller, M. *Macromolecules* **1998**, 26, 9413.
73. Kato, K.; Uchida, E.; Kang, E.; Uyama, Y.; Ikada, M. *Prog. Polym. Sci.* **2003**, 28, 209.
74. Park, E.; Lee, H.; Choi, H.; Lee, D.; Chin, I.; Lee, K.; Kim, C.; Yoon, J. *Eur. Polym. J.* **2001**, 37, 367.
75. Essel, A.; Pham, Q. *J. Polym. Sci. Part B: Polym. Phys.* **1970**, 8, 723.
76. Takaki, M.; Asarni, R.; Ichikawa, M. *Macromolecules* **1977**, 10, 850.
77. Quirk, R.; Zhuo, Q. *Macromolecules* **1997**, 30, 1531.
78. Frank, R.; Merkie, G.; Gauthier, M. *Macromolecules* **1997**, 30, 5397.
79. Hadjichrisidis, N.; Pitsikalis, M.; Pispas, S.; Latrou, H. *Chem. Rev.* **2001**, 101, 3747.
80. Altares, T.; Wyman, P.; Allen, R.; Meyersen, J. *Polymer* **1965**, 3, 131.
81. Asami, R.; Takaki, M.; Kyuda, K. *Polymer* **1983**, 15, 139.
82. Suzuki, T.; Okawa, T. *Polymer* **1988**, 2, 2095.
83. Norton, L.; McCarthy, J. *Macromolecules* **1989**, 22, 1022.
84. Uyama, H.; Kobayashi, S. *Macromolecules* **1991**, 24, 614.
85. DeClercq, R.; Goethals, J. *Macromolecules* **1992**, 25, 1109.
86. Charleux, B.; Pichot, C. *Polymer* **1993**, 34, 195.
87. Ito, K. *Prog. Polym. Sci.* **1998**, 23, 581.
88. Takaki, M.; Asami, R.; Tanaka, S.; Hayashi, H.; Esch, T. *Macromolecules* **1986**, 19, 2900.
89. Tsukahara, Y.; Tsutsumi, K.; Yamashita, Y.; Shimada, S. *Macromolecules* **1990**, 23, 5201.
90. Ito, K.; Hashimura, K.; Itsuno, S. *Macromolecules* **1991**, 24, 3977.
91. Ito, K.; Tomi, Y.; Kawaguchi, S. *Macromolecules* **1992**, 25, 1534.
92. Grande, D.; Six, J.; Breuning, S.; Heroguez, V.; Fontanille, M.; Gnanou, Y. *Polym. Adv. Tech.* **1998**, 9, 601.
93. Djalali, R.; Hungenberg, N.; Schmidt, M. *Macromol. Rapid Commun.* **1999**, 20, 444.
94. Batis, C.; Karanikolopoulos, G.; Pitsikalis, M.; Hadjichristidis, N. *Macromolecules* **2000**, 33, 8925.
95. Heroguez, V.; Breunig, S.; Gnanou, Y.; Fontanille, M. *Macromolecules* **1996**, 29, 13.
96. Mecerryes, D.; Dhan, D.; Lecompte, P.; Dubois, P.; Demonceau, A.; Noels, A.; Jérôme, R. *J. Polym. Sci. Part A: Polym. Chem.* **1999**, 37, 2447.
97. Yamada, K.; Miyazaki, M.; Ohno, K.; Fukuda, T.; Minoda, M. *Macromolecules* **1999**, 32, 290.
98. Shen, Y.; Zhu, S.; Zeng, F.; Pelton, R. *Macromolecules* **2000**, 33, 5399.

99. Ishizu, K.; Furukawa, T. *Polymer* **2001**, 42, 7233.
100. Shen, Y.; Zheng, F.; Zhu, S.; Pelton, R. *Macromolecules* **2001**, 34, 144.
101. Shen, Y.; Zhu, S.; Pelton, R. *Macromolecules* **2001**, 34, 376.
102. Hatada, K.; Kitayama, T.; Ute, K.; Masuda, E.; Shinozaki, T.; Yamamoto, M. *Polym. Bull.* **1989**, 21, 165.
103. Uyama, H.; Honda, Y.; Kobayashi, S. *J. Polym. Sci. Part A: Polym. Chem.* **1993**, 31, 123.
104. Ishizu, K.; Kuwahara, K. *Polymer* **1994**, 35, 4907.
105. Ishizu, K.; Sunahara, K. *Polymer* **1995**, 36, 4155.
106. Kawaguchi, S.; Winnik, M.; Ito, K. *Macromolecules* **1995**, 28, 1159.
107. Nugroho, M.; Kawaguchi, S.; Ito, K. *Macromol. Reports* **1995**, A32, 593.
108. Ito, K.; Kawaguchi, S. *Adv. Polym. Sci.* **1999**, 142, 129.
109. Schmidt, M.; Sheiko, S.; Prokhorova, S.; Möller, M. *Macromolecules* **1999**, 32, 2629.
110. Tsukahara, Y.; Yai, K.; Kaeriyama, K. *Polymer* **1999**, 40, 729.
111. Shiho, H.; Desimone, J. *J. Polym. Sci. Part A: Polym. Chem.* **2000**, 38, 1139.
112. Nakagawa, O.; Kitayama, T.; Hatada, K. *Polym. Bull.* **2002**, 48, 445.
113. Oishi, T.; Lee, Y.; Nakagawa, A.; Onimura, K.; Tsutsumi, H. *J. Polym. Sci. Part A: Polym. Chem.* **2002**, 40, 1726.
114. Wang, X.; Lascelles, S.; Jackson, R.; Armes, S. *Chem. Commun.* **1999**, 1817.
115. Haddleton, D. M.; Perrier, S.; Bon, S. A. F. *Macromolecules* **2000**, 33, 8246.
116. Wang, X.; Armes, S. *Macromolecules* **2000**, 33, 6640.
117. Feast, W. J.; Gibson, V. C.; Johnson, A. F.; Khosravi, E.; Moshin, M. A. *Polymer* **1994**, 35, 3542.
118. Breunig, S.; Héroguez, V.; Gnanou, Y.; Fontanille, M. *Macromol. Symp.* **1995**, 95, 151.
119. Héroguez, V.; Gnanou, Y.; Fontanille, M. *Macromol. Rapid Commun.* **1996**, 17, 137.
120. Feast, W. J.; Gibson, V. C.; Johnson, A. F.; Khosravi, E.; Moshin, M. A. *J. Mol. Cat. A: Chem.* **1997**, 115, 37.
121. Héroguez, V.; Gnanou, Y.; Fontanille, M. *Macromolecules* **1997**, 30, 4791.
122. Héroguez, V.; Six, J. L.; Gnanou, Y.; Fontanille, M. *Macromol. Chem. Phys.* **1998**, 199, 1405.
123. Héroguez, V.; Amédéo, E.; Grande, D.; Fontanille, M.; Gnanou, Y. *Macromolecules* **2000**, 33, 7241.
124. Imanishi, Y.; Nomura, K. *J. Polym. Sci. Part A: Polym. Chem.* **2000**, 38, 4613.
125. Nomura, K.; Takahashi, S.; Imanishi, Y. *Polymer* **2000**, 41, 4345.
126. Allcock, H. R.; Denus, C. R. d.; Prange, R.; Laredo, W. R. *Macromolecules* **2001**, 34, 2757.
127. Ishizu, K.; Shomomura, K.; Saito, R.; Fukutomi, T. *J. Polym. Sci. Part A: Polym.*

- Chem.* **1991**, 29, 923.
128. Kitayama, T.; Kishiro, S.; Hatada, K. *Polym. Bull.* **1991**, 25, 161.
 129. Shizu, I.; Yukimasa, S.; Saito, R. *Polymer* **1992**, 33, 1982.
 130. Hatada, K.; Kitayama, T. *Polym. Int.* **2000**, 49, 11.
 131. Pantazis, D.; Chalari, I.; Hadjichristidis, N. *Macromolecules* **2003**, 36, 3783.
 132. Sanda, F.; Hitomi, M.; Endo, T. *Macromolecules* **2001**, 34, 5364.
 133. Cianga, I.; Yagci, Y. *Polym. Bull.* **2001**, 47, 17.
 134. Cianga, I.; Yagci, Y. *Eur. Polym. J.* **2002**, 38, 695.
 135. Deimede, V.; Kallitsis, J. K. *Chem. Eur. J.* **2002**, 8, 467.
 136. Breitling, F.; Lahitte, J. F.; Peruch, F.; Plentz-Meneghetti, S.; Isel, F.; Lutz, P. J. *Polym. Prepr.* **2000**, 41, 1889.
 137. Lahitte, J. F.; Peruch, F.; Plentz-Meneghetti, S.; Isel, F.; Lutz, P. J. *Macromol. Chem. Phys.* **2002**, 203, 2583.
 138. Tsukahara, Y.; Mizuno, K.; Segawa, A.; Yamashita, Y. *Macromolecules* **1989**, 22, 1546.
 139. Kawaguchi, S. *Adv. Polym. Sci.* **1999**, 142, 129.
 140. Charleux, B.; Pichot, C.; Llauro, M. *Polymer* **1993**, 34, 4352.
 141. Herman, F.; Norbert, M.; Charles, G.; George, M.; Jacqueline, I., *Encyclopedia of Polymer Science and Engineering*. John Wiley and sons: New York, 1986; p 192.
 142. Ito, K.; Tsuchida, H.; Hayashi, A.; Kitano, T.; Yamada, E.; Matsumoto, T. *Polym. J.* **1985**, 17, 827.
 143. Cameron, G. G.; Chisholm, M. S. *Polymer* **1986**, 27, 1420.
 144. Tsukahara, Y.; Tanaka, M.; Yamashita, Y. *Polym. J.* **1987**.
 145. Tsukahara, Y.; Mizuno, K.; Segawa, A.; Yamashita, Y. *Macromolecules* **1989**, 22, 1546.
 146. Tsukahara, Y.; Tsutaumi, K.; Yamashita, Y.; Shimada, S. *Macromolecules* **1989**, 22, 2869.
 147. Chen, G.; Jones, F. N. *Macromolecules* **1991**, 24, 2151.
 148. Jacks, S. *Makromol. Chem.* **1972**, 161, 167.
 149. Vargas, J. S.; Franta, E.; Rempp, P. *Makromol. Chem.* **1981**, 182, 2063.
 150. Leibler, L. *Macromolecules* **1980**, 13, 1602.
 151. Semenov, A. *Physics* **1985**, 61, 733.
 152. Hamley, I. W., *The Physics of Block Copolymers*. Oxford University Press: New York, 1998.
 153. Bates, F. S.; Fredrickson, G. H. *Phys. Today* **1999**, 52, 32.
 154. Pitsikalis, M.; Pispas, S.; Mays, J.; Hadjichristidis, N. *Adv. Polym. Sci.* **1998**, 1, 135.
 155. Hadjichristidis, N.; Pispas, S.; Pitsikalis, M.; Iatrou, H.; Vlahos, C. *Adv. Polym. Sci.* **1999**, 142, 71.

156. Hadjichristidis, N.; Pitsikalis, M.; Iatrou, H. *Adv. Polym. Sci.* **2005**, 1, 189.
157. Hadjichristidis, N.; Iatrou, H.; Pitsikalis, M.; Mays, J. W. *Prog. Polym. Sci.* **2006**, 31, 1068
158. Hadjichristidis, N.; Iatrou, H.; Pitsikalis, M.; Pispas, S.; Avgeropoulos, A. *Prog. Polym. Sci.* **2005**, 30, 725.
159. Kennedy, J. P.; Delvaux, J. M. *Adv. Polym. Sci.* **1991**, 38, 141.
160. Gersappe, D.; Irvie, D.; Balazs, A. C.; Liu, Y.; Sokolov, J.; Rafailovich, M.; Schwarz, S.; Peiffer, D. G. *Science* **1994**, 265, 1072.
161. Gido, S. P.; Lee, C.; Pochan, D. J.; Pispas, S.; Mays, J. W.; Hadjichristidis, N. *Macromolecules* **1996**, 29, 7022.
162. Lee, C.; Gido, S. P.; Poulos, Y.; Hadjichristidis, N.; Tan, N. B.; Trevino, S. F.; Mays, J. W. *J. Chem. Phys.* **1997**, 107, 6460.
163. Lee, C.; Gido, S. P.; Poulos, Y.; Hadjichristidis, N.; Tan, N. B.; Trevino, S. F.; Mays, J. W. *Polymer* **1998**, 39, 4631.
164. Xenidou, M.; Beyer, F. L.; Hadjichristidis, N.; Gido, S. P.; Tan, N. B. *Macromolecules* **1998**, 31, 7659.
165. Beyer, F. L.; Gido, S. P.; Buschl, C.; Iatrou, H.; Uhrig, D.; Mays, J. W. *Macromolecules* **2000**, 33, 2039.
166. Sung, C. S.; Hu, C. B.; Wu, C. S. *Macromolecules* **1980**, 13, 111.
167. Sung, C. S.; Smith, T. W. *Macromolecules* **1980**, 13, 117.
168. John, A. M.; Kirk, K. S. *Macromolecules* **1985**, 18, 32.
169. Qin, Z. Y.; Macosko, C. W.; Wellinghoff, S. T. *Macromolecules* **1985**, 18, 553.
170. Lee, D.; Richard, A.; Yang, C. *Macromolecules* **1988**, 21, 998.
171. Koberstein, J. T.; Galambos, A. F.; Leung, L. M. *Macromolecules* **1992**, 25, 6195.
172. Tien, Y. I.; Wei, K. H. *Macromolecules* **2001**, 34, 9045.
173. Asif, A.; Huang, C.; Shi, W. *Colloid. Polym. Sci.* **2005**, 283, 721.
174. Besshi, T.; Sato, T.; Tsutsui, I. *J. Mater. Pro. Tech.* **1999**, 95, 133.
175. Kumar, D. B.; Reddy, M. R.; Mulay, V. N.; Krishnamurti, N. *Eur. Polym. J.* **2000**, 36, 1503.
176. Hotza, D.; Greil, P. *Mater. Sci. Eng.* **1995**, A202, 206.
177. Aneja, A.; Wilkes, G. L. *Polymer* **2003**, 44, 7221.
178. Radhakrishnan, B.; Chambon, P.; Cloutet, E.; Cramail, H. *Colloid Polym. Sci.* **2003**, 281, 516.
179. Hirose, M.; Zhou, J.; Nagai, K. *Progr. Org. Coat.* **2000**, 38, 27.
180. Lubczak, J. *J. Appl. Polym. Sci.* **1997**, 66, 423.
181. Kato, M. JP Patent, 2000351805, **2000**.
182. Moroshi, Y.; Inoue, T. JP Patent, 2001040311, **2001**.
183. Licht, U.; Bayer, K. S. DE Patent, 10020195, **2001**.

184. Kro, I. P.; Kro, I. B.; Pikus, S.; Skrzypiec, K. *Colloid Surf. A. Physicochem. Eng. Aspects* **2005**, 35, 259.

Chapter 3

Analytical Methods

The following analytical techniques were used in this study to analyze and characterize the UMs and its graft copolymers:

- Fourier-transform infrared spectroscopy (FTIR) and photo-acoustic spectroscopy (PAS)
- Matrix-assisted laser desorption/ionization mass spectrometry (MALDI-TOF-MS)
- Nuclear magnetic resonance spectroscopy (NMR)
- Size exclusion chromatography (SEC)
- Light scattering (LS)
- Ultraviolet/visible spectroscopy (UV-Vis)
- High-performance liquid chromatography (HPLC)
- Gradient elution liquid chromatography (GELC)
- Thermogravimetric analysis (TGA)
- Dynamic mechanical analysis (DMA)
- Transmission electron microscopy (TEM)
- Differential scanning calorimetry (DSC)

3.1 Fourier-transform infrared spectroscopy and photo-acoustic spectroscopy

FTIR provides information about the chemical bonding or molecular structure of materials, whether organic or inorganic.¹⁻³ It is often used in failure analysis to identify unknown materials present in a specimen.

The technique is based on the fact that bonds and groups of bonds vibrate at characteristic excitation frequencies. A molecule that is exposed to infrared rays absorbs infrared energy at frequencies that are characteristic to its specific bond structure. During FTIR analysis, a spot on the specimen is subjected to a modulated IR beam. The specimen's transmittance and reflectance of the IR rays at different frequencies is translated into an IR absorption plot consisting of reverse peaks. The resulting FTIR spectral pattern is then analyzed.

In PAS a modulated radiation is absorbed by a sample, which causes periodic temperature fluctuations within the optical absorption depth. This enables periodic heat transfer to an ambient gas. The PAS signal is a result of the periodic pressure fluctuations in the gas that are associated with the temperature modulation produced by the heat coming from the sample.⁴

FTIR was used to follow and characterize the disappearing and emerging peaks of the functional groups during the preparation of the UMs and the graft copolymers.

3.2 Matrix-assisted laser desorption/ionization

Traditionally, mass spectroscopy (MS) is applicable to the analysis of low molecular weight organic and inorganic compounds, given that they have to be converted into (intact) gas phase ions. However, the recent development of ingenious ionization techniques like MALDI-TOF-MS^{5,6} has extended the mass range that can be analyzed by this technique. Mass spectroscopy has since become a very popular tool for structural analysis of synthetic polymers. High resolution mass spectra can be obtained with MALDI coupled to a time-of-flight (TOF) detector with the associated use of other special technical features like delayed extraction.⁵ Peaks in a MALDI-TOF spectrum are generated from (intact) individual polymer chains, thereby enabling structural identification of the polymer. The mass of the end groups is obtained by subtracting the mass of the cationizing agent and that of the appropriate number of repeat units as inferred from the mass to charge ratio (m/z) of the intact macromonomer ion peak in the spectrum.⁵ With additional information from the synthetic procedure used and from other spectroscopic techniques, e.g. NMR, the end group structure can then be determined.

MALDI-TOF-MS is becoming an increasingly important technique for characterization of the average molecular weights, oligomer repeat units, and end groups of polymers.⁷ Currently, MALDI-TOF operating in the reflector mode with time lag focusing can yield isotopically resolved mass spectra, which are extremely rich in information, allowing detailed analysis of a variety of macromonomers.⁷

3.3 Nuclear magnetic resonance spectroscopy

NMR is a magnetic nuclei field applied electromagnetic (EM) pulse, which causes the nuclei to absorb energy from the EM pulse and radiate energy back out. The energy radiated back out is at a specific resonance frequency that depends on the strength of the magnetic field and other factors. This allows the observation of specific quantum mechanical magnetic properties of an atomic nucleus. The most important applications for the organic chemist are ¹H-NMR and ¹³C-NMR spectroscopy. In principle, NMR is applicable to any nucleus possessing spin. NMR provides information on the number and type of chemical entities (nuclei) in a molecule.

In this study ¹H-NMR and ¹³C-NMR will be used to determine the chemical composition of the macromonomers and the nature of the terminal groups, as well as to characterize the graft copolymers.

3.4 Size exclusion chromatography

SEC is a chromatographic method in which particles are separated based on their size or, in more technical terms, their hydrodynamic volume. It is usually applied to large molecules or macromolecular complexes such as proteins and industrial polymers. Typically, when an aqueous solution is used to transport the sample through the column, the technique is known as gel filtration chromatography, versus the name gel permeation chromatography, which is used when an organic solvent is used as a mobile phase. SEC is a widely used polymer characterization method because of its ability to provide good molecular mass (M_w) results for polymers. M_w sensitive detectors are available, such as a low angle light scattering (LALS) detector, a multi-angle laser light scattering (MALLS) detector, and differential viscometers.⁸⁻¹¹ A number of detectors can be used if the response factors of the detectors for the components of the polymer are sufficiently different: for example, a combination of UV and RI detection.¹¹⁻¹³

3.5 Light scattering

Since there is no correlation between molar mass and elution volume for complex polymers using SEC analysis, the determination of molar mass using molar mass sensitive detectors, such as a light scattering detector, is necessary. When a polarized, monochromatic laser beam passes through a solvent containing polymer, the excess light scattered by the molecules at an angle to the incident beam over that scattered by the solvent alone is directly proportional to the molecular mass (M_w). The measurement of scattered light passing through a cell at different angles, from 0 to 90 degrees, provides an accurate molecular mass and enables a calculation of the radius of gyration (R_g). The (excess) intensity $R\theta$ of the scattered light at the angle θ is correlated to the weight average of molar mass (M_w) of the dissolved macromolecules.^{14,15}

The molar mass determination requires knowledge of the specific refractive index increment dn/dc , which depends on the chemical composition of the copolymer. The dn/dc value of a copolymer can be determined for a chemically monodisperse fraction if the value of the weight fraction w_i and the dn/dc of the homopolymer are known

$$(dn/dc)_{copolymer} = \sum w_i (dn/dc)_i \quad 3.1$$

But, in some limited cases good interactions between the monomer units in the polymer chain could move the dn/dc values of the copolymer away from the summation fraction.¹⁶

3.6 High-performance liquid chromatography

HPLC technique is widely used in the separation of polymers according to chemical

composition.¹⁷ This technique allows the separation of block copolymer molecules from their respective homopolymers. This is achieved by varying the mobile phase solvent composition.

3.6.1 Gradient elution liquid chromatography

Gradient elution liquid chromatography (GELC) was first used for the separation and characterization of complex polymers and low molecular weight polymers (macromonomer), as reported in 1978 by Boiemond and Van.¹⁸ In gradient elution the activity of the stationary phase can be changed in a suitable manner, which offers a useful option for the analysis of different mixtures of molecules. Gradient elution (called the solvent gradient) involves the continuous variation of the composition of the eluting medium during a chromatographic run. The polymer is dissolved in a solvent that dissolves the polymer completely. This solution is injected into a chromatographic system under a thermodynamically poor condition (weak solvent), and complete retention of the polymer occurs on the top of the column. During gradient elution the solvent strength of the mobile phase increases from that of the weak solvent, which leads to gradual dissolution of the polymer. When the strength of the mobile phase is great enough the polymer starts to elute, and the separation occurs. Retention is influenced by solubility effects, size exclusion, and interaction between the polymer and the column packing.¹⁹

3.7 Ultraviolet/visible spectroscopy

An UV/visible (UV-Vis) spectrometer operates on the double-beam principle, with one beam passing through the sample and the other passing through a reference cell.²⁰ UV-Vis involves the spectroscopy of photons in the UV-visible region. This means it uses light in the visible and adjacent near ultraviolet (UV) and near infrared (IR) ranges. The absorption in the visible range directly affects the colour of the chemicals involved. In this region of the electromagnetic spectrum molecules undergo electronic transitions. This technique is complementary to fluorescence spectroscopy, in that fluorescence deals with transitions from the excited state to the ground state, while absorption measures transitions from the ground state to the excited state.

3.8 Dynamic mechanical analysis

Dynamic mechanical analysis (DMA) is an increasingly useful technique for the characterization of polymers and viscoelastic properties.²¹⁻²³ DMA measures the mechanical properties of a material, such as the modulus (stiffness) and damping (energy dissipation) as a function of temperature and frequency under periodic (oscillatory) stress. The properties that can be obtained by DMA are the glass transition temperature (T_g), damping characteristics, degree and rate of cure, and polymer morphology. DMA is the study of the

movement of polymer chains by the application of a sinusoidally varying total force programmed in milliNewton (mN) as applied to the polymer.²¹ The total force applied to the polymer is the sum of static force and dynamic force, at chosen frequency. The sample responds to the applied force with delayed oscillating amplitude of a phase lag (δ).

3.9 Dynamic thermogravimetry

Dynamic thermogravimetry analysis (TGA)^{22,23} is a test applied to samples to determine changes in weight in relation to change in temperature. This analysis relies on a high degree of precision in three measurements: weight, temperature, and temperature change. As many weight loss curves look similar, the weight loss curve may require transformation before results may be interpreted. A derivative weight loss curve can be used to determine the point at which weight loss is most apparent. Again, interpretation is limited without further modifications, and deconvolution of the overlapping peaks may be required.

TGA is commonly used in research and testing to determine characteristics of materials such as polymers, to determine degradation temperatures, absorbed moisture content of materials, the level of inorganic and organic components in materials, decomposition points of explosives, and solvent residues. It is also often used to determine the corrosion kinetics in high temperature oxidation.

3.10 Transmission electron microscopy

Transmission electron microscopy (TEM) is a microscopy technique whereby a beam of electrons is transmitted through an ultra thin specimen, preferably 100 nm and interacts with the specimen as it passes through. An image is formed from the interaction of the electrons transmitted through the specimen. The image is magnified and focused onto an imaging device, such as a fluorescent screen, on a layer of photographic film, or detected by an analytical sensor.

TEM is also an imaging technique whereby a beam of electrons is focused on a sample specimen. Differences in the electron densities of the sample are detected, developing an enlarged image of the focused area. This technique allows high resolution and magnification of sample morphology. Staining is usually required to obtain the image.

3.11 Differential scanning calorimetry

Differential scanning calorimetry (DSC)^{24,25} is a thermo analytical technique in which the difference in the amount of heat required to increase the temperature of a sample and reference is measured as a function of temperature. Both the sample and reference are maintained at nearly the same temperature throughout the experiment (within experimental

error). Generally, the temperature program for a DSC analysis is designed such that the sample holder temperature increases linearly as a function of time. The reference sample should have a well-defined heat capacity over the range of temperatures to be scanned.

The main application of DSC is in studying phase transitions, such as melting, glass transitions, or exothermic decompositions. These transitions involve energy changes or heat capacity changes which can be detected by DSC with great sensitivity. The rate of temperature occurring is important for accurate melting point data, in order to avoid melting and recrystallization during the scan.

3.12 References

1. Fuente, J.; Wilhelm, M.; Spiess, H.; Madruga, E.; Fernandez, M.; Cerrada, M. *Polymer* **2005**, 46, 4544.
2. Asha, S.; Thirumal, M.; Kavitha, A.; Pillai, C. *Eur. Polym. J.* **2005**, 41, 1343.
3. Otts, D.; Dutta, S.; Zhang, P.; Smith, O.; Thames, S.; Urban, M. *Polymer* **2004**, 45, 6235.
4. Kiland, B. R.; Urban, M. W.; Ryntz, R. A. *Polymer* **2000**, 41, 1597.
5. Montaudo, G.; Samperi, F.; Montaudo, M. S. *Prog. Polym. Sci.* **2006**, 31, 277.
6. Pasch, H.; Schrepp, W., *MALDI-ToF Mass Spectrometry of Synthetic Polymers*. Springer: Berlin, 2003.
7. Arnould, A.; Polce, M.; Quirk, R.; Wesdemiotis, C. *Int. J. Mass Spectrum.* 2004, 238, 245.
8. Konas, M.; Moy, T.; Rogers, M.; Shultz, A.; Ward, T.; McGrath, J. *Polym. Sci. Part B: Polym. Phys.* **1995**, 33, 1441.
9. Zammit, M. D.; Davis, T. P. *Polymer* **1997**, 38, 4455.
10. Pasch, H.; Trathnigg, B., *HPLC of Polymers*. Springer-Verlag: Berlin, 1997; p 58
11. Trathnigg, B., *Size-exclusion Chromatography of Polymers, Encyclopedia of Analytical Chemistry*. John Wiley: New York, 2000.
12. Lee, H. C.; Ree, M.; Chang, T. *Polymer* **1995**, 36, 2215.
13. Philipps, H. *J. Chromatogr. A.* **2004**, 1037, 329.
14. Wu, C. *Macromolecules* **1993**, 26, 3821.
15. Wen, J.; Arakawa, T.; Philo, J. *Anal. Biochem.* **1996**, 240, 155.
16. Pasch, H. *Adv. Polym. Sci.* **2000**, 150, 1.
17. Heinz, L.; Pasch, H. *Polymer* **2005**, 46, 12040.
18. Boiemond, J.; Van, M. *Chromatography* **1978**, 149, 539.
19. Pasch, H.; Trathnigg, S., *HPLC Of Polymers*. Springer-Verlag: Berlin, Heidelberg 1998; p 80.
20. Harwood, L.; Moody, C.; Percy, J. *Experimental Organic Chemistry*. Blackwell

Science: London 1999; p 356.

21. Tan, H.; Li, J.; Guo, M.; Du, R.; Xie, X.; Zhong, Y.; Fu, Q. *Polymer* **2005**, 46, 7230.
22. Chen, Y.; Zhou, S.; Yang, H.; Gu, G.; Wu, L. *J. Colloid Interface. Sci.* **2004**, 279, 370.
23. Yang, J.; Lin, H. *J. Membr. Sci.* **2001**, 187, 159.
24. Elvers, B.; Hawkins, S.; Russey, W., *Ullmann's Encyclopedia of Industrial Chemistry*. VCH Publishers: New York, 1993; Vol. B6, p 4.
25. Klingsberg, A.; Piccininni, R., *Encyclopedia of Polymer Science and Engineering*. Wiley-Interscience: New York, 1986; Vol. Supplement, p 702.

Chapter 4

Synthesis and characterization of novel urethane macromonomer (UM1) and methacrylic/urethane graft copolymers

4.1 Introduction

Graft copolymers with a backbone of one polymer and branches of other polymer exhibit material properties that are a combination of both homopolymer constituents. There are several reviews of graft copolymers.¹⁻⁴ The presence of long chain branching has a dramatic effect on the dynamic and rheological behaviour of well-entangled polymers.⁵⁻⁷

The macromonomer technique is the simplest way to prepare graft copolymers.⁸ Macromonomers are polymers end-capped with a polymerizable end group able to copolymerize with low molecular weight monomers, so the macromonomers can either homopolymerize to give a regular comb polymer or copolymerize with a suitable monomer to give a graft copolymer. These end-functional polymers can be prepared by modifying polymer end groups or, very conveniently, by using functional initiators in living/controlled polymerizations.⁹

To the best of the author's knowledge this is the first report on the use or synthesis of monofunctional urethane macromonomers. In this present study, urethane macromonomers (UM1) were synthesized to be predominantly monofunctional, and then the UM1 will be used as grafts in solution free-radical copolymerization with methacrylate monomers. The effects of the UMs on the phase separation, and thermal and mechanical properties of the graft copolymer, were then studied.

4.2 Synthesis of urethane macromonomer (UM1)

4.2.1 Introduction

The synthesis of UM1 requires that all monomer reagents, solvents and intermediates be free from moisture. Any moisture present during UM1 synthesis will react with the isocyanate, resulting in a number of competitive secondary side reactions that can lead to the formation of undesired crosslinked material. Such side reactions include the formation of dimers and trimers, acylurea, allophanate, and amide and carbamic acid derivatives. These can also be avoided by using a low reaction temperature.¹⁰

Polyurethanes can be synthesized by two methods: the pre-polymer method and the 'one-shot' method.¹¹ In the 'one-shot' process the monomers are added together in one step, whereas in the pre-polymer process (which will be used in this study) the monomers are

added in intervals. The prepolymer process holds advantages over the one-shot process as it offers more control over the reaction, thereby resulting in polymers with smaller molecular mass distributions and better polymer morphology.¹⁰

Macromonomers are low molecular mass polymer species with polymerizable end groups.¹² Polyaddition polymerization was used in this study to introduce a polymerizable functional group into the urethane polymer chain end.

The experimental procedures used to synthesize the urethane macromonomer are described here. The UM1 was synthesized according to formula 4.1 below:



where 2-HEA is 2-hydroxyethyl acrylate, EG is ethylene glycol, MDI is 4,4'-diphenylmethane diisocyanate, n is the chain length, and MeOH is methanol, which was used to terminate the chain end.

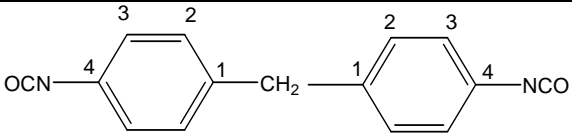
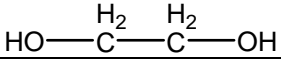
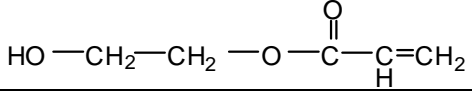
4.2.2 Reagents

The following reagents were dried as follows prior to use:

2-HEA, MeOH, EG and DMF were dried over a 4 Å molecular sieve (the molecular sieve was first dried in a vacuum oven for 24 h at 100 °C).

The raw materials used for the synthesis of the UM1 are tabulated in Table 4.1.

Table 4.1: Reagents used for synthesis of the UM1

Raw material	Chemical structure	Supplier
4,4'-diphenylmethane diisocyanate (MDI)		Sigma-Aldrich
ethylene glycol (EG)		Sigma-Aldrich
2-hydroxyethyl acrylate (2-HEA)		Sigma-Aldrich
methanol (MeOH)	CH ₃ OH	Sigma-Aldrich

4.2.3 Experimental setup

The following equipment was used for UM1 synthesis: a 250-ml three-neck flask, nitrogen gas inlet, oil bath, reflux condenser, temperature controller unit, magnetic stirrer, bubbler, glass syringe, packed column with molecular sieve, and calcium chloride to prevent any moisture entering the reactor vessel/flask.

4.2.4 Urethane macromonomer formulations

Formulations used for the preparation of the UM1 are tabulated in Table 4.2. The formulations were taken according to formula 4.1 assuming 100% conversion and average chain lengths $n = 5$

Table 4.2: Formulations used for the preparation of UM1

reagent	MDI	EG	2-HEA	MeOH	Total mass	Excess MeOH	[OH]/[NCO]
Weight (g)	15.32	3.17	1.18*	0.33*	20	0.16**	1.04
Weight (mol)	0.061	0.051	0.009	0.010	-	0.005	1.04

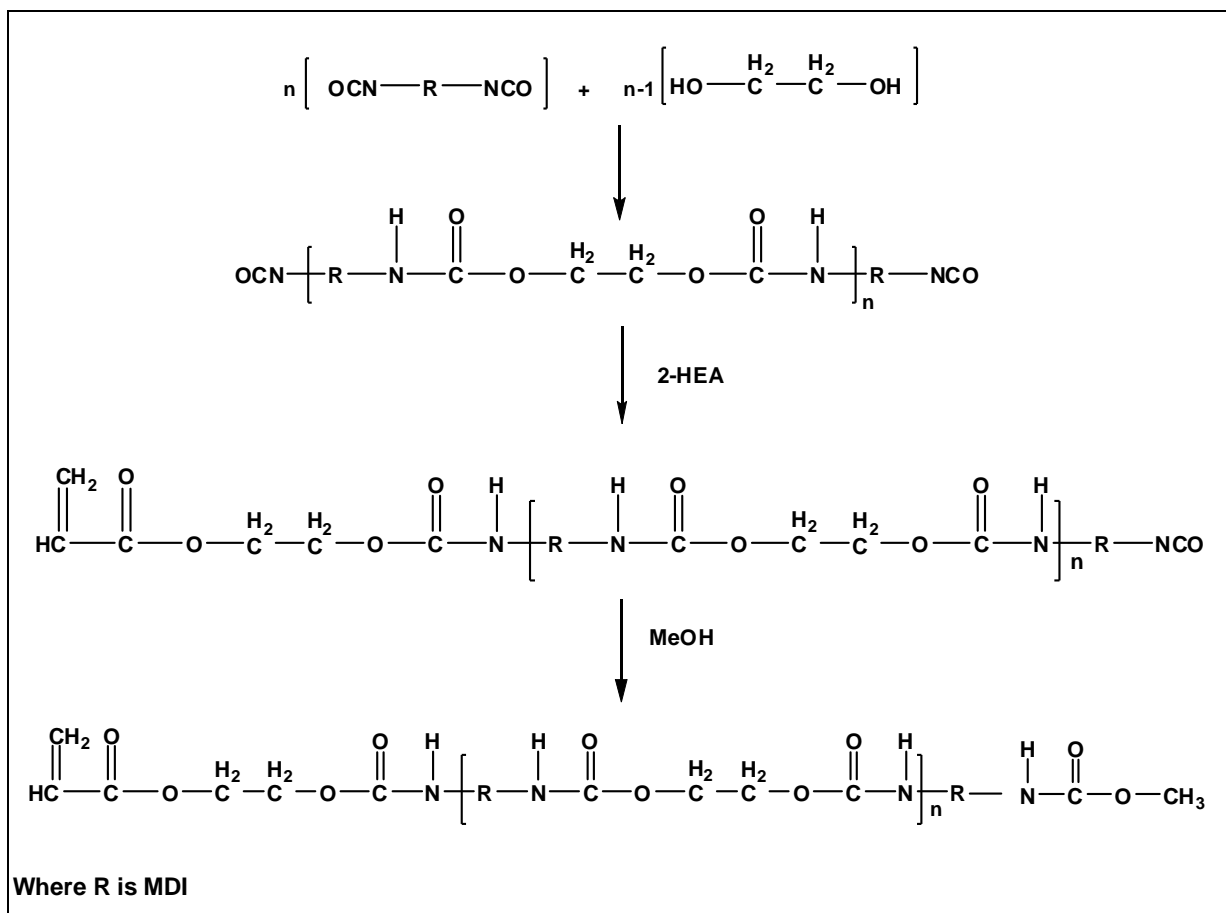
* The quantities of 2-HEA, MeOH, MDI and EG used to synthesize UMs were calculated as mole % according to the formula 4.1 at a [OH]/[NCO] mole ratio 1:1, in which 2-HEA was calculated as 40 mole % in the UM chain end and MeOH was calculated as 60 mole % in the UM chain end.

** An excess amount of MeOH was needed to ensure that all reactive NCO group were fully reacted. If not, then secondary reactions will take place, to ultimately form crosslinked structures (see section 2.1.2.1). Thus, the minimum quantities of excess MeOH were experimentally determined FTIR to be 0.15 moles, to ensure that all the NCO groups are fully reacted (Section 4.5.1). The excess helps to minimize difunctional acrylates.

4.2.5 Experimental procedure

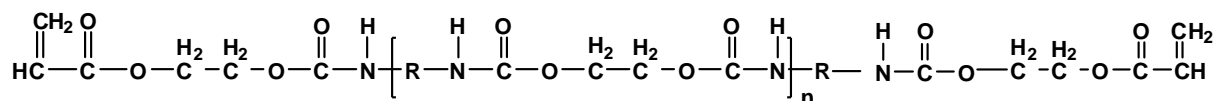
The synthesis of the UM1 was carried out under a nitrogen atmosphere. MDI and DMF were added to the flask and the reaction mixture cooled to below 10 °C. The reactor was then purged with nitrogen gas and sealed. This was followed by addition of the EG, under stirring (400-500 rpm). The temperature was increased to 15-18 °C and held there for 40-60 min. In the second step, the reaction temperature was increased to 20-40 °C and 2-HEA was added. The reaction was allowed to run for 60 min. In the final step, the reaction temperature was first increased to 40-45 °C, excess methanol was added, and then the reaction temperature was increased to 55 °C to ensure using IR spectroscopy that all previously unreacted isocyanate reacted. The degree of the reaction was verified by measuring the isocyanate group (2270 cm^{-1}) that disappears as result of reaction with hydroxyl groups.

The isocyanate group was no longer visible in the IR spectrum of the reaction product, as shown in Scheme 4.1. The obtained UM1 was dried in a vacuum oven at 45 °C for 24 hours and then stored in a desiccator until required for use in further polymerization.



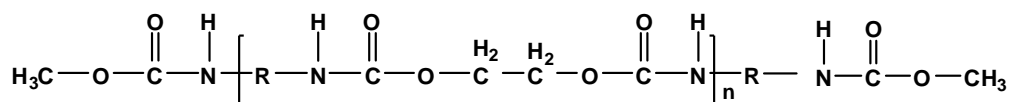
Scheme 4.1: Formation of urethane macromonomer (when 2-HEA reacts at one side and MeOH at the other side of the UM1).

Besides the desired UM1 with only one polymerizable end group, i.e. 2-HEA on one chain end and MeOH on the other, undesirable products can also be present. One such undesirable product occurs when 2-HEA reacts on both ends of the urethane pre-polymer (urethane chain with excess isocyanate).



Scheme 4.2: Reaction products of UM1 showing when 2-HEA reacts on both sides of the UM1.

The other possible structure that could form when methanol reacts on both chain ends of the urethane pre-polymer is shown in Scheme 4.3 This structure is also considered to be undesirable, as it will render the UM unreactive for further copolymerization with acrylic monomers due to no double bond being present on either of the chain ends. Thus it is very important to optimize reaction conditions in an attempt to maximize the yield of the desired product that has 2-HEA on one chain end and MeOH on the other.



Scheme 4.3: Reaction product of UM1 showing the product when the MeOH reacts on both sides of the UM1, to form an unreactive urethane macromer.

4.3 Synthesis of methacrylic-urethane graft copolymers

4.3.1 Introduction

Most graft copolymers are formed by the reaction of a parent polymer, containing reactive sites (macromonomer technique), with a second type of monomer. In this study UM1 was grafted with methyl methacrylate (MMA) and with normal butyl methacrylate (n-BMA) as the main chains respectively. The success of the grafting reactions was determined by characterizing the products by SEC, ¹H-NMR, ¹³C-NMR, UV-Vis, GPEC, FTIR, TGA, DMA, DSC and TEM.

4.3.2 Experimental

Various quantities of UM1 were copolymerized with various quantities of MMA, and with various quantities of n-BMA, respectively, using solution free radical copolymerization.

4.3.3 Choice of solvent

The choice of a good solvent for the acrylate and UM1 was done by trial and error. Many different solvents were tried, such as benzene, toluene, acetone, acetonitrile, methanol, ethanol, dimethylformamide (DMF) and dimethylsulfoxide (DMSO). Complete solubilization of the UM1 and acrylate was achieved by using DMF or DMSO. However, DMSO could not readily be used because it crystallizes at room temperature and needs to be heated before use. Therefore DMF was chosen as the solvent for all the copolymerization reactions of methacrylate and UMs.

4.3.4 Materials

n-BMA (Aldrich, 99%) and MMA (ICI Chemicals and Polymers, 99.9%) were washed with a 0.4 M potassium hydroxide solution (KOH, Associated Chemical Enterprises, 85%), followed by distillation under reduced pressure to remove the inhibitor. The monomers were stored for 24 hours at 0 °C over molecular sieve (4 Å). The following materials were also used: potassium persulphate (KPS, 99%), methanol (MeOH, 99.8%), dimethylformamide (DMF, 99.5%), distilled and deionized water (DDI, from a Millipore milli-Q purification system) and silicon oil (SA Silicones). 2,2'-Azobis(isobutyronitrile) (AIBN, Delta Scientific, 98%) was recrystallized from methanol. The urethane macromonomers (see Table 4.2) were synthesized as described earlier (Section 4.2.5).

4.3.5 Purification of the monomers

MMA and n-BMA monomers were first washed with 0.4 M KOH followed by distillation under reduced pressure to remove any other impurities using potassium persulfite. The monomers were first washed with 0.4 M KOH solution to remove the hydroquinone inhibitor. The distillation was carried out under reduced pressure and low heat (about 45 °C) to avoid self polymerization of the monomers. The distilled fractions were collected and dried over anhydrous magnesium sulfate to ensure a completely dry monomer. The monomers were stored at -8 °C prior to use.

4.3.6 Methacrylic-urethane copolymer formulations

Formulations used to prepare the different PMMA-g-UM1 copolymers and PnBMA-g-UM1 copolymers are shown in Tables 4.3

Table 4.3: Formulations used for the preparation of PMMA-g-UM1 copolymers and PnBMA-g-UM1 copolymers

Reagent	Mass of reagents used in various experiments			
	EXP.1* (g)	EXP.2* (g)	EXP.3* (g)	EXP.4* (g)
MMA	5.00	4.50	3.75	2.25
AIBN**	0.05	0.045	0.047	0.025
UM	0.00	0.50	1.25	2.75
DMF	35.00	35.20	35.45	35.00
n-BMA	5.00	4.50	3.75	2.25
AIBN**	0.05	0.045	0.047	0.025
UM	0.00	0.50	1.25	2.75
DMF	35.00	35.20	35.45	35.00

*The concentrations of the UM1 were between 0 and 55 wt % (relative to MMA or n-BMA), and the quantities of UM1 and MMA or UM1 and n-BMA in all copolymerization feeds were based on 5 g.

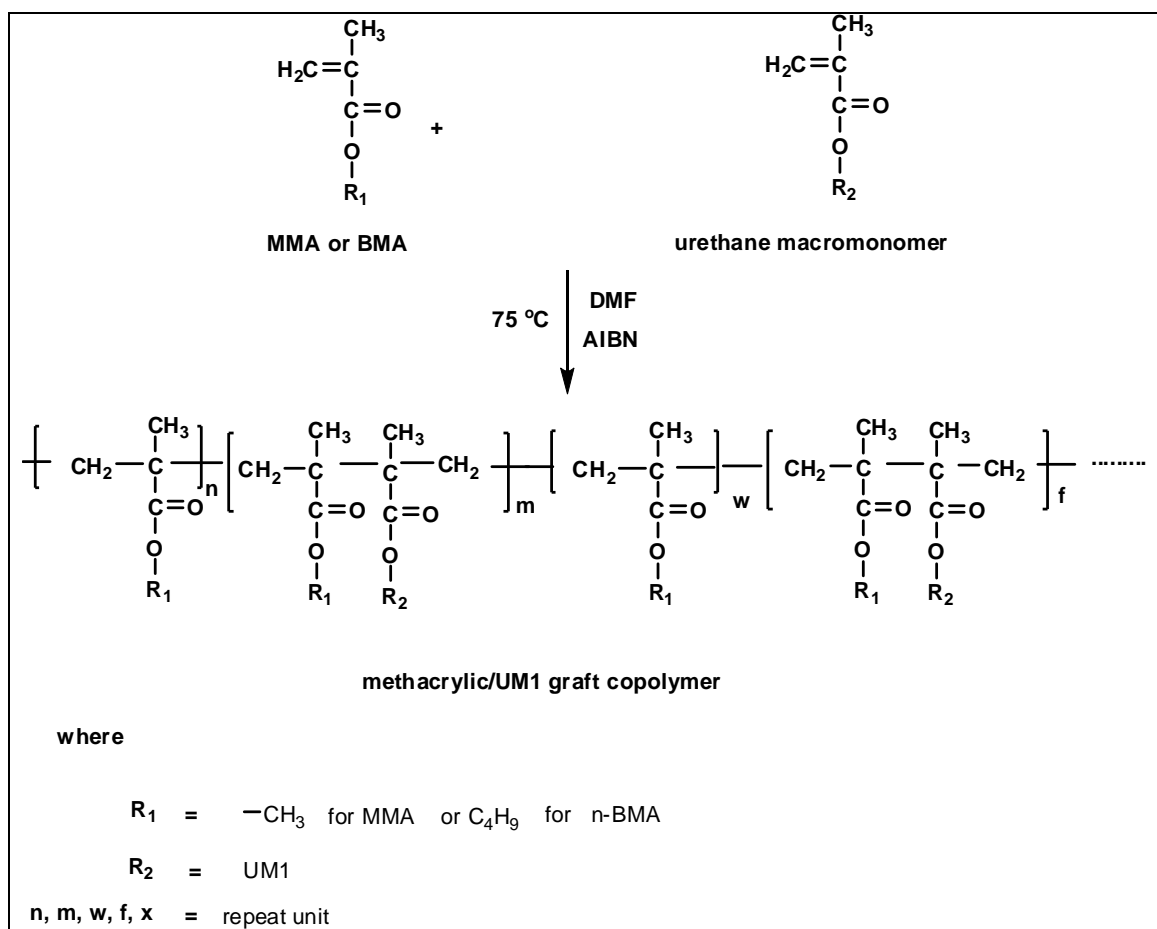
** The concentration of initiator (AIBN) was varied between 0.7 to 1% by weight according to n-BMA. (This is actually considered high, and will affect the molecular weight of graft copolymers). These concentrations of initiator were chosen because at low concentration of initiator the yield of graft copolymer is very low (as can be seen in Table 4.5) because of the high chain transfer constant to DMF, the solvent used.

Table 4.4: Effect of the concentration of initiator on yield of graft copolymers

Concentration of AIBN (wt %)	Feed polymerization			Graft yield from PMMA-g-urethane (g)	Graft yield from PnBMA-g-urethane (g)
	UM1 (g)	MMA (g)	nBMA (g)		
0.1	0.50	4.50	4.50	1.54	1.92
0.4	0.50	4.50	4.50	2.42	2.81
0.5	0.50	4.50	4.50	2.71	3.15
0.7	0.50	4.50	4.50	4.74	4.94
1	0.50	4.50	4.50	4.85	4.01
1.4	0.50	4.50	4.50	4.18	4.42

4.3.7 Experimental procedure

Solution free radical copolymerization was carried out in a 250-ml three-neck reactor with magnetic stirring, under a nitrogen atmosphere. Scheme 4.4 shows the synthesis procedure for the graft copolymers. DMF was first introduced into the reactor. MMA or n-BMA, and AIBN (1% wt relative to the monomer), were then charged into the reactor, followed by the UM. Various concentrations of UM1 were used: 0, 10, 25 and 55 wt % relative to MMA or n-BMA. The polymerization temperature was 75 °C and the reaction time was 24 h. The copolymers were precipitated in MeOH, then separated by filtration and dried under vacuum at room temperature overnight. The unreacted UM1 was removed by precipitation using DMF as solvent and THF and MeOH as nonsolvent. The removal of the unreacted macromonomer was tracked using SEC with UV and RI detectors (see Section 4.5.2.2).



Scheme 4.4: Formation of methacrylic-urethane graft copolymer.

4.4 Characterization of UM1 and methacrylate-g-urethane copolymers

Different techniques were used in this study to analyze and characterize the UM1 and methacrylate-g-urethane copolymers

4.4.1 Fourier-transform infrared spectroscopy (FTIR)

During the synthesis of the UM1, FTIR samples were prepared by extracting some polymer (dissolved in DMF) from the reactor at various time intervals. The samples were then run against a DMF background between sodium chloride discs. This was done to monitor the NCO content during the UM1 synthesis. Other IR analyses were performed on a Perkin Elmer Paragon 1000 FTIR instrument at 32 scans, using a photo-acoustic (PAS) cell, so eliminating sample preparation. FTIR spectra were recorded in the range $3500\text{-}500\text{ cm}^{-1}$, with a resolution of 4 cm^{-1} . Samples were prepared by grinding about 2-5 mg of the graft copolymer (after extraction) with 120 mg KBr, followed by pressing to form transparent disks.

4.4.2 Matrix-assisted laser mass spectrometry (MALDI-TOF-MS)

MALDI-TOF-MS were recorded on a Voyager-DE STR (Applied Biosystems, Framingham) equipped with a nitrogen 337 nm laser in the reflector mode, at 25 kV accelerating voltage, and with delayed extraction. The matrix was trans-2-[3-(4-tert-butylphenyl)-2-methyl-2-propenylidene] malononitrile (Aldrich) and potassium trifluoroacetate (KTFA) (Aldrich) was used as the cationizing agent. For each analysis, the analyte sample was prepared by first making up the following concentrations of the matrix, KTFA, and sample, in DMF, separately: 35 mg/mL matrix; 5 mg/mL KTFA; 1 mg/mL sample, before mixing them in the ratio of 4:1:4 and hand spotting on the target plate. One thousand laser shots were obtained for each spectrum. All the MALDI-TOF-MS results reported in this work were obtained as described here.

4.4.3 Proton NMR ($^1\text{H-NMR}$)

$^1\text{H-NMR}$ spectra were recorded in deuterated-DMSO, using a Varian Unity INOVA 400 MHz NMR instrument, and a Varian VXR 300 MHz NMR instrument. The NMR spectra were used to determine the chemical composition of macromonomer and to characterize the graft copolymers. All spectra were referenced to tetramethylsilane (TMS) at 0 ppm.

4.4.4 Carbon NMR ($^{13}\text{C-NMR}$)

$^{13}\text{C-NMR}$ spectra were obtained in the same manner as the proton $^1\text{H-NMR}$ spectra, but at a frequency of 600 MHz, using a Varian Unity INOVA NMR instrument. Long runs (overnight) were used.

4.4.5 Size exclusion chromatography (SEC)

Number average and weight average molecular mass (M_n) as well as polydispersity indices were obtained through the use of SEC with two concentration dependent detectors, UV and RI. The UV was adjusted to 254 nm, corresponding to the absorption of the aromatic ring. Therefore this detector only detects a response when there are aromatic rings in the sample, for example the urethane macromonomer. UM1 and methacrylate-g-urethane copolymers were dissolved in dimethylacetamide (DMAc) (5 mg/ml) and filtered through a 0.45- μm nylon filter. Analyses were carried out with a system comprising Waters 610 fluid Unit, Waters 410 differential refractometer at 30 °C, Waters 717plus auto sampler and Waters 600E system controller. Plgel columns 5 μm Mixed-C 300X7.5 mm (Polymer Laboratories) was used. The column oven was set at 30 °C. The DMAc solvent flow rate was 0.5 mL/min, and the injection volume was 100- μl . The system was calibrated with narrow polystyrene standards. Millennium 2005 was used for data acquisition and data analysis.

4.4.6 Light scattering (LS)

The dn/dc values of the graft copolymers were determined for pure graft copolymers, using a

Scan Ref monochromator instrument at a wavelength 633 nm. The dn/dc value for each graft polymer was determined by measuring the refractive indices of a series of prepared polymer samples in DMAc, of various concentrations, prepared from single stock solution (0.5 mg/mL, 1.0 mg/mL, 2.0 mg/mL, 3.0 mg/mL and 4.0 mg/mL). Samples of each graft (2.0 mg/mL) were injected in the SEC which is coupled to a multiangle light scattering (MALLS) detector, for the determination of the absolute molar mass of the graft copolymers.

4.4.7 Gradient polymer elution chromatography (GPEC)

HPLC is used to separate molecules under high pressure in a stainless steel column filled with a suitable matrix. The solvent/nonsolvent combination is an important parameter in gradient HPLC. The separation takes place with respect to the polarity of the different components. The nonpolar polymer elutes as the first component from the stationary phase; this is normally the acrylic homopolymers e.g. PMMA or PnBMA, if present. This component is followed by the graft copolymer, which is the most polar component in the product and which may contain unreacted urethane macromonomer as the second component.

The gradient HPLC system comprised a Waters 2690 separation module Alliance equipped with a Nucleosil CN column, pore size 100 Å, particle size 5µm, 12.5×4 (ID) cm. A constant column temperature of 40 °C was maintained through the use of an oven. The detector used was an evaporative light scattering detector (ELSD) PL-ELS 1000 from Polymer Labs, which was operated at 80 °C, with an N₂ carrier gas flow rate of 1 SLM (standard litres per min). Data collection and processing were performed using PSS Win SEC7 from Polymer Standards Service.¹³

Separation of a complex mixture with respect to the chemical composition distributions (CCDs) of the different species can be achieved by gradient HPLC. To determine the CCD of the graft copolymers CCl₃/THF or THF/DMF gradient was used as the mobile phases, and a cyano-modified silica gel (Nucleosil CN) as the polar stationary phase.¹⁴⁻¹⁶

4.4.8 Ultraviolet/visible spectroscopy (UV/Vis)

A Perkin Elmer UV/visible Lambda 20 Spectrometer was used to identify the UV absorption band of the aromatic ring bond in the structure of the urethane macromonomer. The data were analyzed with UV Winlab v.4.2 software. Quartz cuvettes (supplied by CND Scientific) with a 10 mm path length were used.

4.4.9 Thermogravimetric analysis (TGA)

TGA analyses of the UM1 and acrylate-UM1 graft copolymers were carried out using a TGA-50 SHIMADZU thermogravimetric instrument with a TA-50WSI thermal analyzer connected

to a computer. Samples (10-15 mg) were degraded in nitrogen or air (flow rate 50 ml/min) at a heating rate of 2.5 °C /min.

4.4.10 Dynamic mechanical analysis (DMA)

DMA was carried out on a Perkin Elmer DMA 7e using the thin-film extension mode. The frequency was 1 Hz and the heating rate was 5 °C/min. The sample was a 0.3-mm thick, solution-cast film, which was dried before testing.

4.4.11 Differential scanning calorimetry (DSC)

DSC was performed on a Du Pont DSC 913 or a Perkin Elmer Pyris instrument, depending on the samples. The glass transition temperatures were obtained from samples that had been pressed and secured in crimped aluminum pans. Scans were run at 5 °C/min and the reported T_g values were obtained from the second heat after a quench cool from the first run.

Three scans were performed, all at a standard 5 °C/min rate, for each sample. The samples were first heated to 220 °C and held isothermally for 5 min to remove all thermal history. The cooling cycle followed, with the sample cooled to -40 °C and then held at that temperature for 5 min. The temperature was then increased to 200 °C for the second heating cycle.

4.4.12 Transmission electron microscopy (TEM)

TEM images were recorded out at the University of Cape Town's electron microscopy unit. TEM was used to directly visualize the morphology of the acrylate-g-urethane copolymers. Bright-field TEM images were recorded on a JEM 200CX (JEOL Tokyo, Japan) TEM at an accelerating voltage of 120 kV. Prior to analysis, samples of urethane-acrylate graft copolymers were stained with OsO_4 , then embedded in epoxy resin and cured for 24 h at 60 °C. The embedded samples were then ultra-microtomed with a diamond knife on a Reichert Ultracut S ultra-microtome at room temperature. This resulted in sections with a nominal thickness of ~100 nm. The sections were transferred from water at room temperature to 300-mesh copper grids, which were then transferred to the TEM apparatus.

4.5 Results and discussion

4.5.1 Formation of urethane macromonomer (UM1)

A "prepolymer" method which comprises two successive steps was used in this study (see Scheme 4.1). In the first step, the reaction of a diisocyanate (in excess) and a diol afford a urethane chain with -NCO end functionality. The degree of polymerization was controlled by employing stoichiometrically unbalanced concentrations of reactants ([NCO] and [OH]). When a large excess of MDI is used a di-functional NCO prepolymer is formed, which is able

to further react, in a second step, with other additional functional groups, such as 2-HEA and MeOH.

4.5.1.1 FTIR analysis

FTIR analysis was used firstly to monitor the isocyanate (NCO group) consumption during the course of the UM1 synthesis, and secondly to characterize of the UM1 product.

(a) NCO content

The presence of the free NCO-group during the synthesis of the UM1 prepolymer is shown in Figure 4.1(a), represented by the NCO-peak at 2270 cm^{-1} . The absence of the characteristic NCO peak at 2270 cm^{-1} in Figure 4.1(b) indicates that all the isocyanate groups had reacted. This is very important, because if NCO-groups are present then in the presence of any trace of water in the reaction medium will result in the formation of a crosslinked structure.

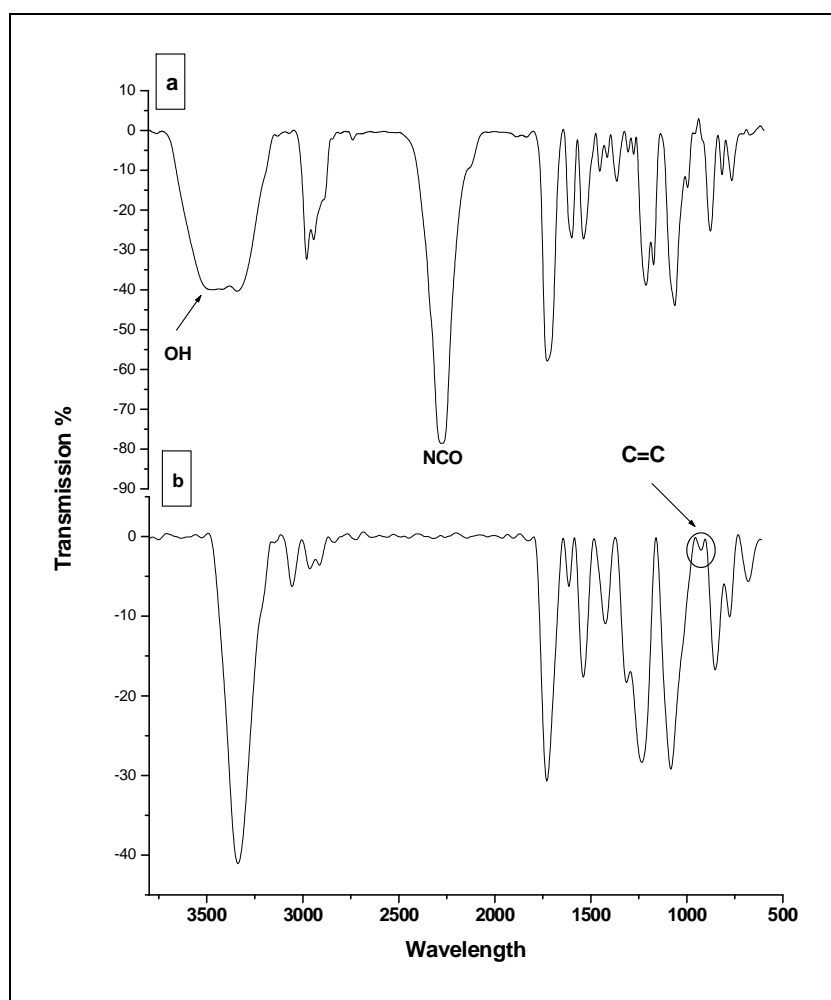


Figure 4.1: FTIR spectra of UM1 (a) during addition of EG, and (b) after addition of MeOH + 2-HEA.

(b) Characterization of the urethane macromonomers

FTIR analysis of the UM1 was carried out using a photoacoustic cell (PAS). Figure 4.1(b) shows the FTIR spectrum of the UM1 synthesized. The absorption band at 3518 cm^{-1} in the

FTIR spectrum in Figure 4.1 (a) represents the OH-groups of the UM1 prepolymer during the addition of EG. These OH- bands disappear in the UM1 as seen in the FTIR spectrum (Figure 4.1.b). There is a strong N-H stretching band of the urethane groups at about 3326 cm^{-1} .¹⁷ The absorption band at 1521 cm^{-1} is due to the N-H deformation vibration of urethane.^{18,19} The absorption band at 1602 is attributed to aromatic ring C-C of UM1.^{20,21} The absorption band at 936 cm^{-1} corresponds to C=C,^{22,23} indicating the formation of the urethane macromonomer. Assignments of the peaks are tabulated in Table 4.5.

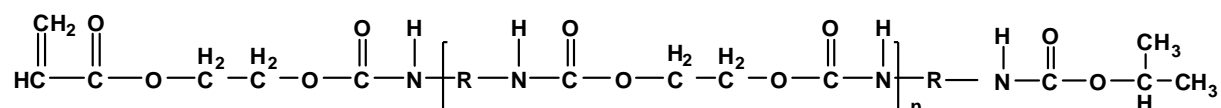
Table 4.5: FTIR peak assignment of the UM2¹⁴⁻²¹

Wavelength (cm^{-1})	Assignment	Reference
3326	Stretching vibration of the urethane N-H bond	2
3047, 2960 and 2897	Stretching vibration of the aliphatic C-H bond	1
1711	Amide I, stretching vibration of the of the ester C=O bond	4
1602	Stretching vibration of the aromatic ring C-C	5,6
1521	Amide II	1
1426	Stretching vibration of the benzene C-C	1
1410	Parallel vibration of C-H bond in CH_2 Symmetric deformation of aliphatic CH_4	1,2
1240	Twisting vibration of C-H in CH_2	1
1082	Symmetric stretching vibration of the CO-O-C	1
936	Out-of-the plane bending of CH in $\text{RCH}=\text{CH}$ Out-of-plane bending of CH in benzene ring	7
776	Vibration of aromatic CH	2
668	Vibration of aromatic CH	2

4.5.1.2 Matrix-assisted laser mass spectrometry (MALDI-TOF-MS)

The synthesis of UM1 yielded three fractions (see Section 4.2.5), which could not be separated by chromatographic techniques due to their similarity in structure. Hence the yield of each fraction could not be determined separately. Matrix-assisted laser desorption/ionization mass spectrometry (MALDI-TOF-MS) was used to characterize the structures of the UM1.

As it was discussed earlier in this chapter (Section 4.2.5), besides the desired UM1 with only one polymerizable end group, i.e. 2-HEA on one chain end and isopropanol at the other end (the isopropanol is later replaced by the use of MeOH, and the results of using the MeOH are seen later in this section), the obtained UM1 can also have undesirable by products.



Scheme 4.5: Reaction products when 2-HEA reacts on side and isopropanol reacts from the other side.

Three different methods were used to optimize the reaction conditions in efforts to obtain the desired product. After the polyurethane with excess isocyanate was prepared (Step 1 in Scheme 4.1) the temperature was decreased to 10 °C and then the following different procedures were followed:

1) Method 1: All of the 2-HEA was added at once at the start of the reaction and the temperature was held at 20-25 °C for 45-60 min to obtain a homogeneous mixture. This was followed by the addition of all the isopropanol. The reaction was allowed to proceed at 25-40 °C for a further 45-60 min.

2) Method 2: 2-HEA was added dropwise at 20 °C, and the reaction temperature was kept at 20-25 °C for 45-60 min. This was followed by the addition of all the isopropanol. The reaction was allowed to proceed at 40-45 °C for a further 45-60 min.

3) Method 3: 2-HEA and isopropanol were added together, in fractions, at 20 °C. The reaction temperature was kept at 20-40 °C and the reaction time was 60-90 min.

All comparisons between the three methods were made only after the free radical copolymerization of the synthesized UM1 and after the unreacted and unreactive UM1 were removed (as confirmed by SEC). Method 1 gave the highest yields of both PMMA-g-UM1 and PnBMA-g-UM1 copolymers prepared under similar copolymerization conditions. This also well documented in previous work.²⁴

The MALDI-TOF-MS method was employed to unambiguously identify individual compounds within the UM1. All MALDI-TOF-MS were recorded after it was made sure that no free isocyanate was still present in the products. This was done using the FTIR technique, as was shown in Figure 4.1 (b).

Figure 4.2 shows a typical MALDI-TOF-MS result for UM1 prepared by using Method 1. Mass spectrometry was carried out in reflection mode. The peaks in the mass distribution are at intervals of 312.35 Da mass units from each other, which corresponds to the molar mass of the UM1 repeat unit. Lithium chloride was added as the cationizing agent; hence all the chains in the spectrum in Figure 4.2 were cationized by lithium. This accounts for 3.15 Da of the experimental molar masses.

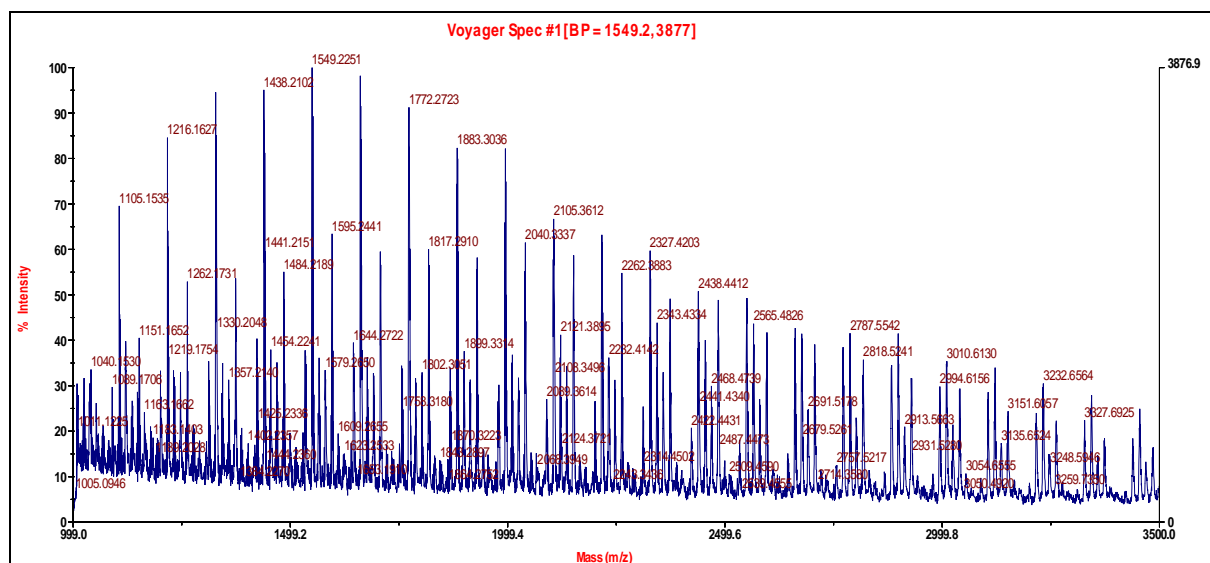


Figure 4.2: MALDI-TOF-MS of UM1 prepared using Method 1.

The MALDI-TOF-MS above shows that besides the three fractions of synthesized UM1, there are other side reactions that had taken place. This is due the reactive diisocyanate (isocyanate in excess, second step (scheme 4.1) during synthesis UM1) may be involved in a number of sides reactions below. Table 4.6 shows some possible UM1 structures that might form during the synthesis of UM1:

- a) Allophanate reactions (reaction with a urethane group)
- b) Biuret formation (reaction with a urea group)
- c) Carbodiimide formation (reaction with another diisocyanate)
- d) Cyclic reactions
- e) Urea linkage

Table 4.6: Possible UM1 structures that might form during synthesis of UM1

Chemical structure	Code*
	A
	B
	C
	D
	E
	F
	G
	H
	J
	K
	L

* Abbreviations used

Figure 4.3(a) is an example showing the m/z region 1700-2100, expanded for illustrative purposes, shows that the product of UM1 does not only have the three UM1 structures (A,B and C) were formed. However there are other side reactions that take place during the synthesis of UM1.

Figure 4.3(b), for illustrative purposes, shows that each peak in Figure 4.3(a) has six signals, of varying intensity, due to the natural abundances of the isotopes.

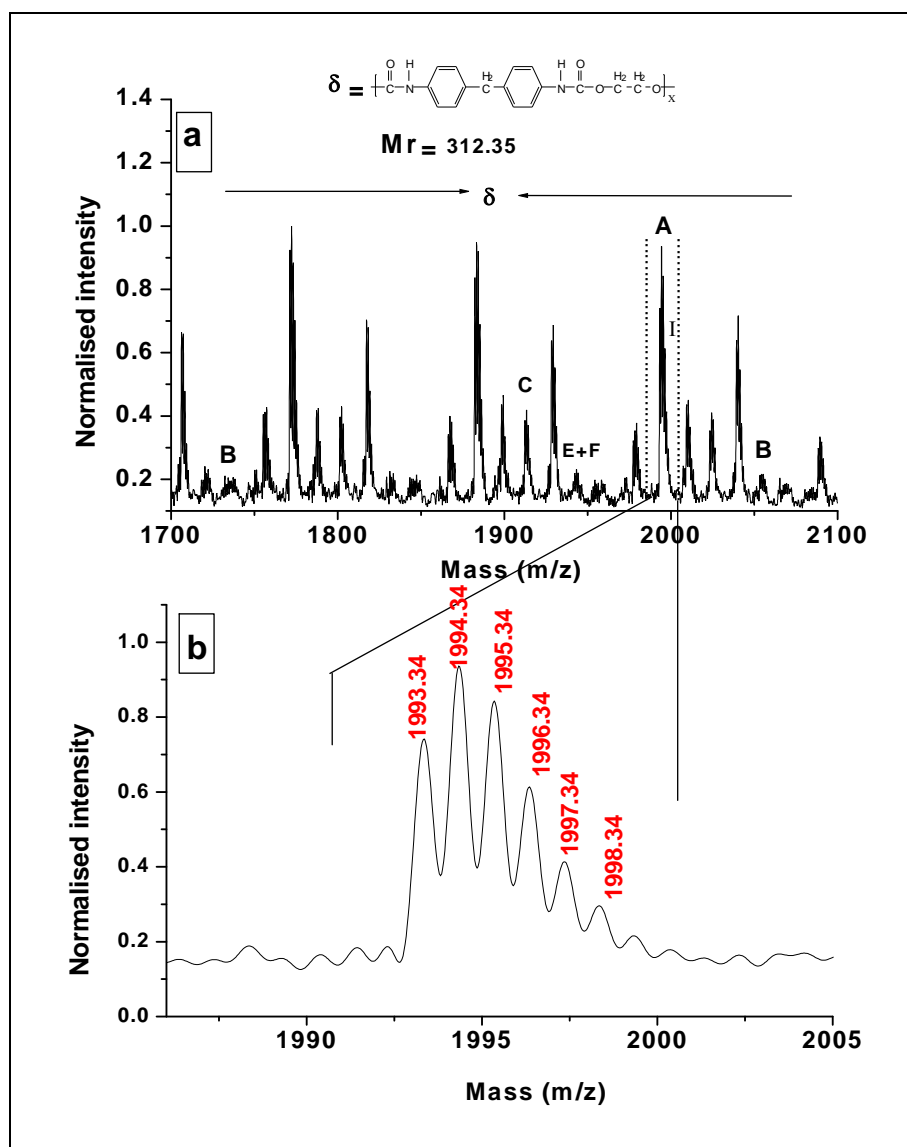


Figure 4.3: Enlarged region of MALDI-TOF-MS of UM1 (a) in the m/z region 700-1800 and (b) experimental isotopic distribution of UM1 in m/z region 1988-2005.

Four different methods were used to optimize the reaction conditions of UM1 that was synthesized by Method 1 in efforts to obtain higher yields % of the desired product and reduce the side reactions that take place during the synthesis of UM1.

- Method one: MDI in excess (2 molar excess) and dried DMF were added to the reaction flask and the mixture was heated to 50 °C. This was followed by addition of the EG, under stirring over 30 min. In the second step, the reaction temperature was reduced to 37 °C, 2-HEA was added all at once and the reaction was allowed to run for 60 min. In the final step, the isopropanol was added at 37 °C, the reaction was allowed to run 30 min, then the reaction temperature was increased to 55 °C to ensure that all the previously unreacted isocyanate reacted.

- Method two: MDI in large excess (5 molar excess) and dried DMF were added to the reaction flask and the mixture heated 50 °C. This was followed by addition of the EG, under stirring over 40 min. In the second step, the reaction temperature was reduced to 37 °C and 2-HEA was added all at once, and the reaction was allowed to run for 60 min. In the final step, the isopropanol was added at 37 °C, for 30 min, and then the reaction temperature was increased to 55 °C to ensure that all previously unreacted isocyanate reacted.
- Method three: MDI in excess (2 molar excess) and dried DMF were added to the reaction flask and the mixture heated to 70 °C. This was followed by addition of the ethylene glycol, under stirring over 40 min. In the second step, the reaction temperature was reduced to 37 °C and 2-HEA was added all at once, and the reaction was allowed to run for 60 min. In the final step, the isopropanol was added at 37 °C for 30 min, and then the reaction temperature was increased to 55 °C to ensure that all previously unreacted isocyanate reacted.
- Method four: MDI in excess (2 molar excess) and EG were added together dropwise to the reaction flask containing dried DMF, at 50 °C and stirred for 40-60 min. In the second step, the reaction temperature was reduced to 37 °C and 2-HEA was added all at once. The reaction was allowed to run for 60 min. In the final step, the isopropanol was added at 37 °C for 30 min, and then the reaction temperature was increased to 55 °C to ensure that all previously unreacted isocyanate reacted.

Figure 4.4 shows for comparison, typical full MALDI-TOF-MS for UM1 prepared using the four different methods. Mass spectrometry was carried out in linear mode. The peaks in the main distribution are at intervals of 312.35 Da mass units from each other, which corresponds to the molar mass of UM1 (the repeat unit). Lithium chloride was added as the cationizing agent, hence all the chains, in the spectrum in Figure 4.4, were cationized by lithium. This accounts for 3.15 Da of the experimental molar masses. When comparing these spectra with the spectra in Figure 4.2 it is noted that most of the side reaction that took place during the synthesis UM1 by Method 1 reduced in these spectra.

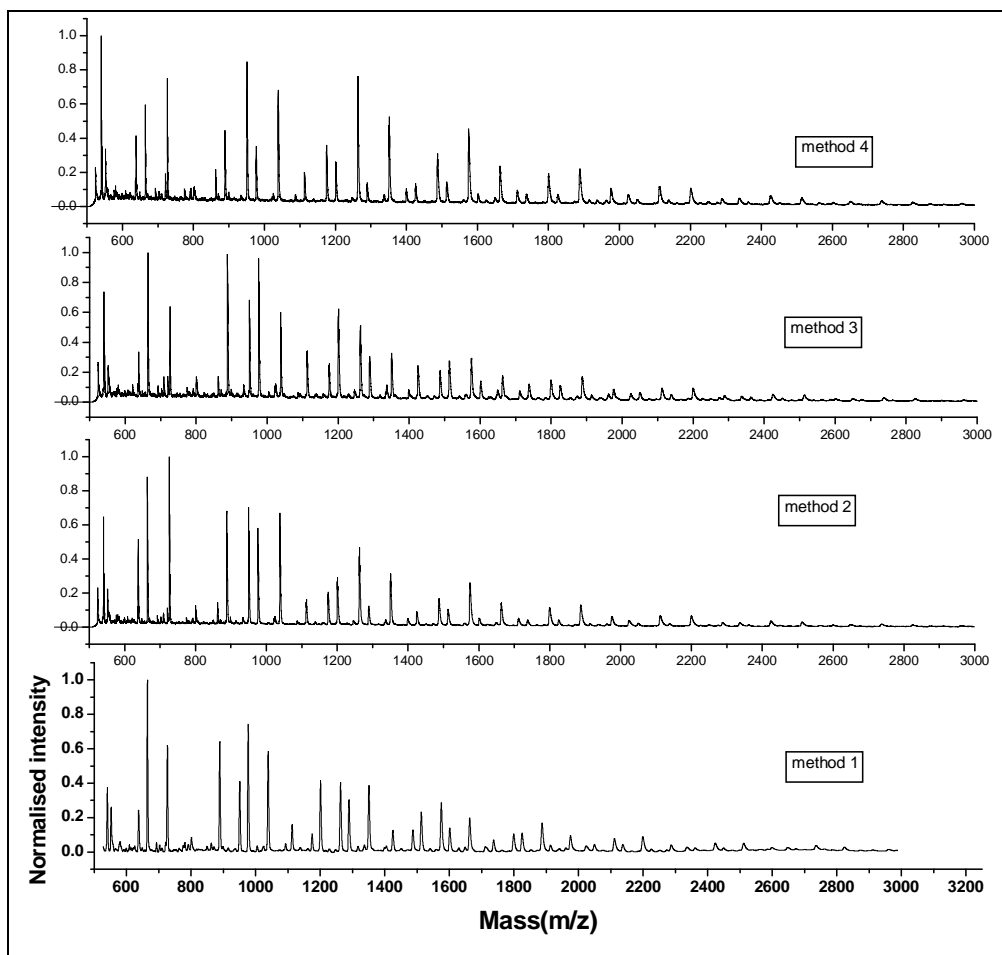


Figure 4.4: Comparison, by MALDI-TOF-MS between four different methods that were used to optimize the structure of UM1.

Figure 4.5 presents an example which shows the m/z region 1700-2100 expanded for illustrative purposes. This figure shows that method four afforded the least side reactions as compared to the other methods and it is shown that by working in a drier system, most of the side reactions could be avoided. Thus, this method will be used to synthesis urethane macromonomer (UM2) which is based on MDI and neopentylglycol (NPG), and to make our MALDI-TOF-MS more clear methanol has been used in this study instead of isopropanol which was used in previous work,²⁴ because the molecular weight of isopropanol is close to the molecular weight of EG which makes the MALDI-TOF-MS interpretation more troublesome.

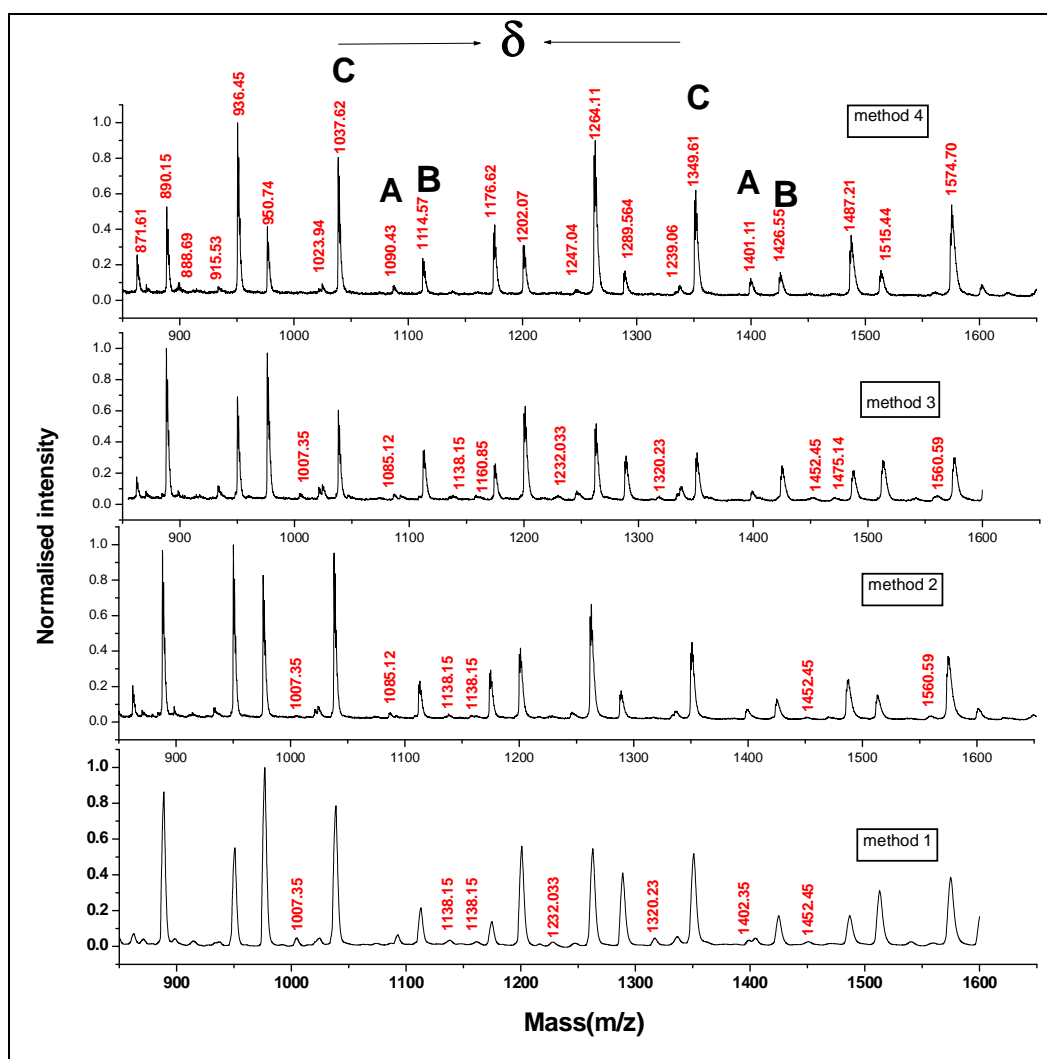
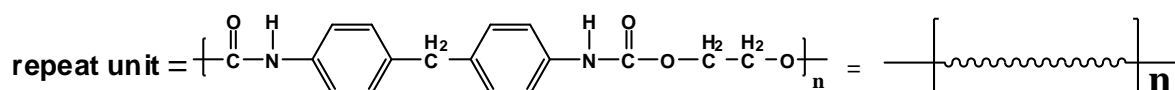


Figure 4.5: MALDI-TOF-MS results showing the comparison between the four different methods that were used to reduce the side reactions.

Figure 4.6 shows the full MALDI-TOF-MS of UM1 prepared by method 4 in a very dry system. MALDI-TOF-MS was carried out in linear mode. The recorded spectra reveal generally a high number of m/z signals with much diversified intensities; after a detailed analysis one can make signal-product pairs for the majority of the expected adducts. The calculated theoretical molecular weights of UM1 match with the locations of their corresponding signals in the MS spectra. Each sequence in the spectrum is made up of a specific sequence of signals arranged at the intervals of $m/z = 312.35$ from each other, which corresponds to the structural repeat unit (δ) of UM1.



Scheme 4.6: Repeat unit (δ) of UM1.

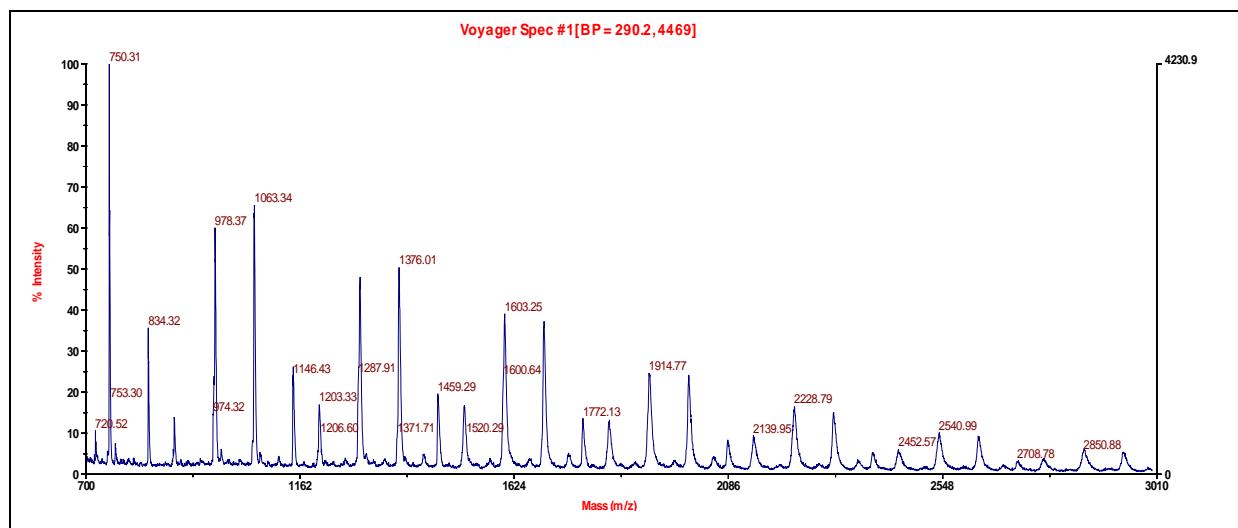


Figure 4.6: MALDI-TOF- MS of UM1 prepared using method 4.

Potassium trifluoro acetate (KTFA) was added as the cationizing agent hence all the chains in the rest of this work were cationized by KTFA. This accounted for 39.10 Da which is added to the experimental molar masses of synthesized UM1. For the sake of clarification of this work, an abbreviation was attributed to each possible chain end-group structure of UM1, taking into account the cationization nature and the number of urethane repeat units of the considered chain (Table 4.7).

Table 4.7: Abbreviations assigned to the main urethane macromonomers chains detected by MALDI-TOF-MS

Code*	Corresponding structures of UM1
C	$\text{H}_3\text{C}-\text{O}-\left[\text{---} \right]_n \text{MDI}-\text{O}-\text{CH}_3$
A	$\text{H}_2\text{C}=\text{HC}-\overset{\text{O}}{\parallel}{\text{C}}-\text{O}-\text{C}-\text{H}_2-\text{C}-\text{H}_2-\text{O}-\left[\text{---} \right]_n \text{MDI}-\text{O}-\text{CH}_3$
B	$\text{H}_2\text{C}=\text{HC}-\overset{\text{O}}{\parallel}{\text{C}}-\text{O}-\text{C}-\text{H}_2-\text{C}-\text{H}_2-\text{O}-\left[\text{---} \right]_n \text{MDI}-\text{O}-\text{C}-\text{H}_2-\text{C}-\text{H}_2-\text{O}-\overset{\text{O}}{\parallel}{\text{C}}-\text{C}=\text{CH}_2$
H	$\text{EG}-\overset{\text{O}}{\parallel}{\text{C}}-\text{N}-\text{H}-\text{PH}-\text{C}-\text{H}_2-\text{PH}-\overset{\text{O}}{\parallel}{\text{C}}-\text{N}-\text{H}-\text{PH}-\text{C}-\text{H}_2-\text{PH}-\overset{\text{H}}{\parallel}{\text{N}}-\overset{\text{O}}{\parallel}{\text{C}}-\text{O}-\text{C}-\text{H}_2-\text{C}-\text{H}_2-\text{O}-\left[\text{---} \right]_n \text{MDI}-\text{O}-\text{CH}_3$

* Abbreviations used

In general, MALDI-TOF-MS detects ions of the type $\{X-[M]_n-Y\} \dots C^+$, where the X is 2-HEA and Y is MeOH at the corresponding end groups, M is the repeat unit, n is the degree of polymerization and C⁺ is the cationizing ion. End group analysis can be done by plotting mass (m/z) against n to get a plot (as a straight line) of the type:

$$\text{Mass (m/z)} = (\text{MM})n + [(\text{MX} + \text{MY}) + \text{MC}^+]$$

The slope of the line gives MM, the molar mass of the repeat unit. The y-axis intercept, $[(MX + MY) + MC +]$, gives the combined masses of the end groups plus the cationizing ion, respectively.^{25,26}

Figure 4.7 shows the most useful range of the MS spectra of the UM1, doped with KTFA, obtained by means of MALDI-TOF-MS. The spectra show very similar distributions of the main peaks, which are separated by 312.45 mass units, corresponding to the repeat unit of UM1.

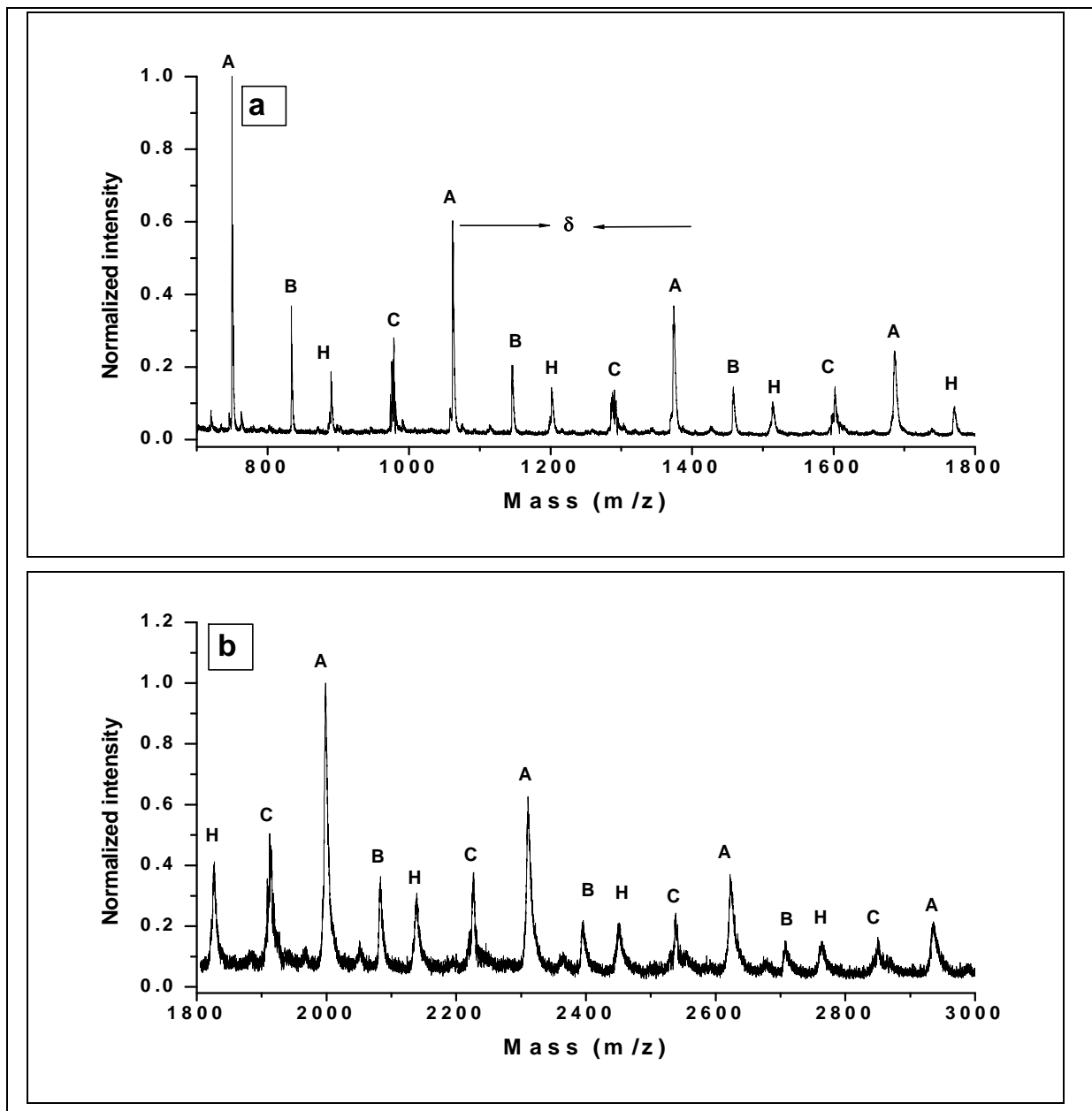


Figure 4.7: Enlarged region of mass spectra of UM1 (a) MALDI-TOF-MS of UM1 in the m/z region 700-1800 and n changed from n=1 to n=4 and (b) MALDI-TOF-MS of UM1 in the m/z region 1800-3000 and n changed from n=4 to n=8.

The spectra in Figure 4.7 show that four different series were observed, with a repeating unit of 312.35 Da, which clearly corresponds to UM1 (noted C, A, B, and H), with A being the predominant one (i.e. 2-HEA on one chain end and MeOH on the other). This confirms that the desired UM1 with only one polymerizable end group, i.e. 2-HEA on one chain end and MeOH on the other, was successfully synthesized. Series C corresponds to the attachment of a metal salt adduct to an undesirable product where MeOH has reacted on both chain ends of the urethane prepolymer, rendering the UM1 unreactive. Series B corresponds to the attachment of a metal salt adduct to undesirable product which occurs when 2-HEA reacts on both ends of the urethane prepolymers (urethane chain with excess isocyanate). This product will lead to branching of the copolymer as its concentration is too low to cause crosslinking. Series H, which occurs less than others reactions (as can be noted from the MALDI-TOF-MS), corresponds to the attachment of a metal salt adduct to an undesirable product where water has reacted with the forming urethane macromer causing an urea bond. All the results which summarize the monoisotopic masses of the ion peak series observed in MALDI-TOF-MS are shown in Table 4.8 which also shows an excellent agreement between the theoretical and the experimentally determined isotopic distributions, in which the difference between calculated mass and experimental mass differs only by between 0.05 and 0.66Da in all four structures that were formed during UM1 synthesis.

Table 4.8: Summary of monoisotopic masses of the ion peak series observed in MALDI-TOF-MS in Figure 4.7 (a) and (b)

Abbreviation	n*	Theory mass	Experimental mass	Difference**	Formula
C	1	665.30	665.20	0.10	CH ₃ O(C ₁₇ H ₁₆ N ₂ O ₄) _n C ₁₆ H ₁₅ O ₃ N ₂ K ⁺
	2	977.18	977.41	-0.13	
	4	1289.98	<u>1289.65</u>	0.33	
	4	1600.84	1600.54	0.40	
	5	1914.85	1914.65	0.20	
	6	2224.47	2224.10	0.37	
	7	2547.44	2547.01	0.43	
A	1	749.42	749.22	0.20	C ₅ H ₇ O(C ₁₇ H ₁₆ N ₂ O ₄) _n C ₁₆ H ₁₅ O ₃ N ₂ K ⁺
	2	1061.45	1061.44	0.01	
	4	1373.98	<u>1373.34</u>	0.44	
	4	1684.81	1684.56	0.27	
	5	1998.98	1998.67	0.31	
	6	2410.90	2410.78	0.12	
	7	2664.19	2764.15	0.04	
B	1	844.25	844.12	0.13	C ₅ H ₇ O(C ₁₇ H ₁₆ N ₂ O ₄) _n C ₂₀ H ₁₉ O ₅ N ₂ K ⁺
	2	1146.46	<u>1146.78</u>	-0.32	
	4	1459.47	1459.42	0.05	
	4	1772.58	1772.48	0.01	
	5	2084.70	2084.84	-0.14	
	6	2498.81	2498.79	0.02	
	7	2709.94	2709.42	0.52	
H	1	1201.16	1201.14	0.02	C ₃₃ H ₃₃ O ₆ N ₃ (C ₁₇ H ₁₆ N ₂ O ₄) _n C ₁₆ H ₁₅ O ₃ N ₂ K ⁺
	2	1514.47	1514.98	-0.39	
	4	1827.28	1826.64	0.62	
	4	2149.15	2148.76	0.39	
	5	2451.48	2450.87	0.61	
	6	2763.05	2762.98	0.07	

*n is UM1 repeat unit

**Difference between theoretical molecular weight values calculated using formula 4.1 Section 4.2.1 and molecular weight obtained by MALDI-TOF-MS

Figure 4.8 is an example which shows excellent agreement between the theoretical and the experimentally determined isotopic distributions.

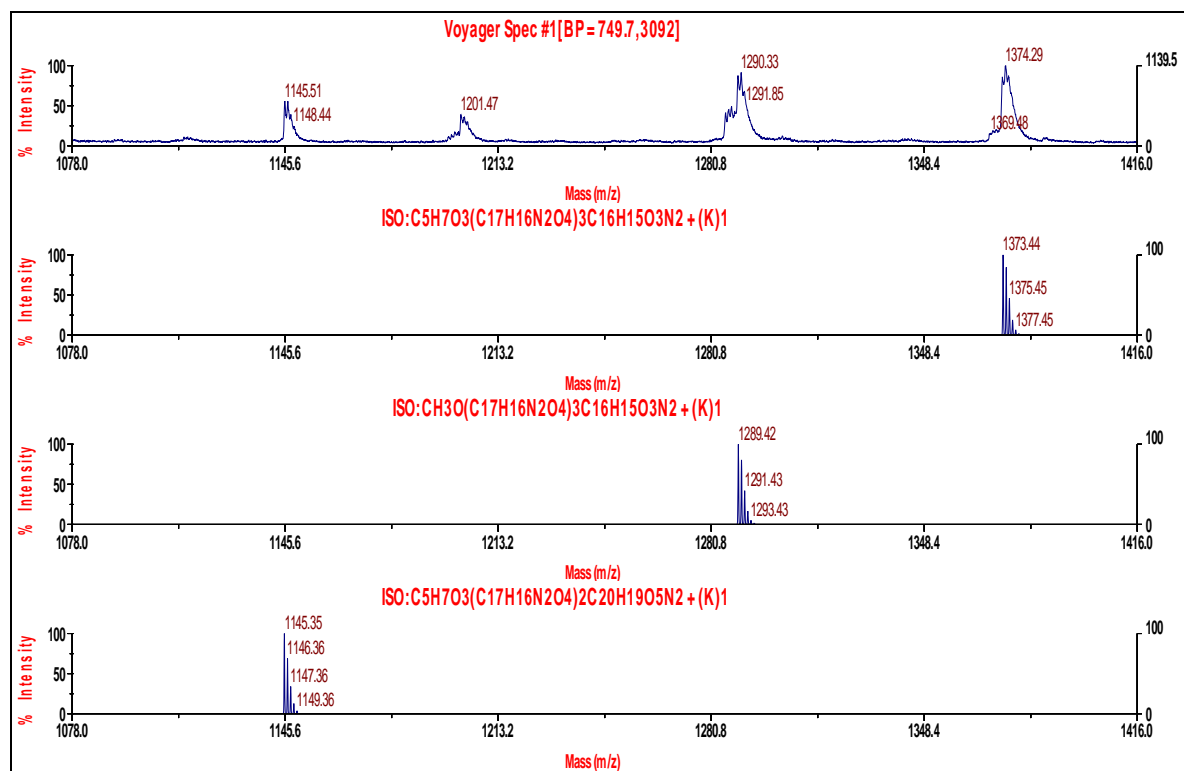


Figure 4.8: MALDI-TOF-MS of UM1, showing the experimental isotopic distribution (top) and the theoretical isotopic distribution (bottom) corresponding to structures (C, A and B) in Table 4.8.

4.5.1.3 $^1\text{H-NMR}$ analysis

UM1 structures were further analyzed by $^1\text{H-NMR}$. $^1\text{H-NMR}$ analysis was used to provide both qualitative and quantitative information of the UM1. Only UM1 with low degrees of polymerization were targeted in order to increase the concentration of end groups in the spectrum in order to avoid problems due to the low resolution of the end group signals. $^1\text{H-NMR}$ samples were run after making sure that formation of UM1 had been confirmed by FTIR and MALDI-TOF-MS. A typical $^1\text{H-NMR}$ spectrum of the UM1 prepared in this work is shown in Figure 4.9. Peak assignments were made based on the expected structure which is shown in the insert in Figure 4.9. These peaks were identified using NMR prediction software.

The large signals at 7.13 and 7.41 ppm are due to the aromatic ring protons of MDI,²⁷ whereas the resonance signal at $\delta = 4.35$ is due to the methylene protons of the EG.²⁸ Characteristic bands of urethane N-H protons appear at $\delta = 9.71$ ppm,²⁹ whereas the signal at $\delta = 3.82$ ppm is attributed to methylene protons between two aromatic rings,³⁰ and the peak at $\delta = 3.68$ ppm corresponds to the methyl groups of MeOH substitution. The important

characteristic signals of the vinyl-terminated protons in the UM1 are detected at $\delta = 5.95$, 6.25 and 6.47 ppm which prove the existence of acrylate groups in the UM1 structure.^{31,32}

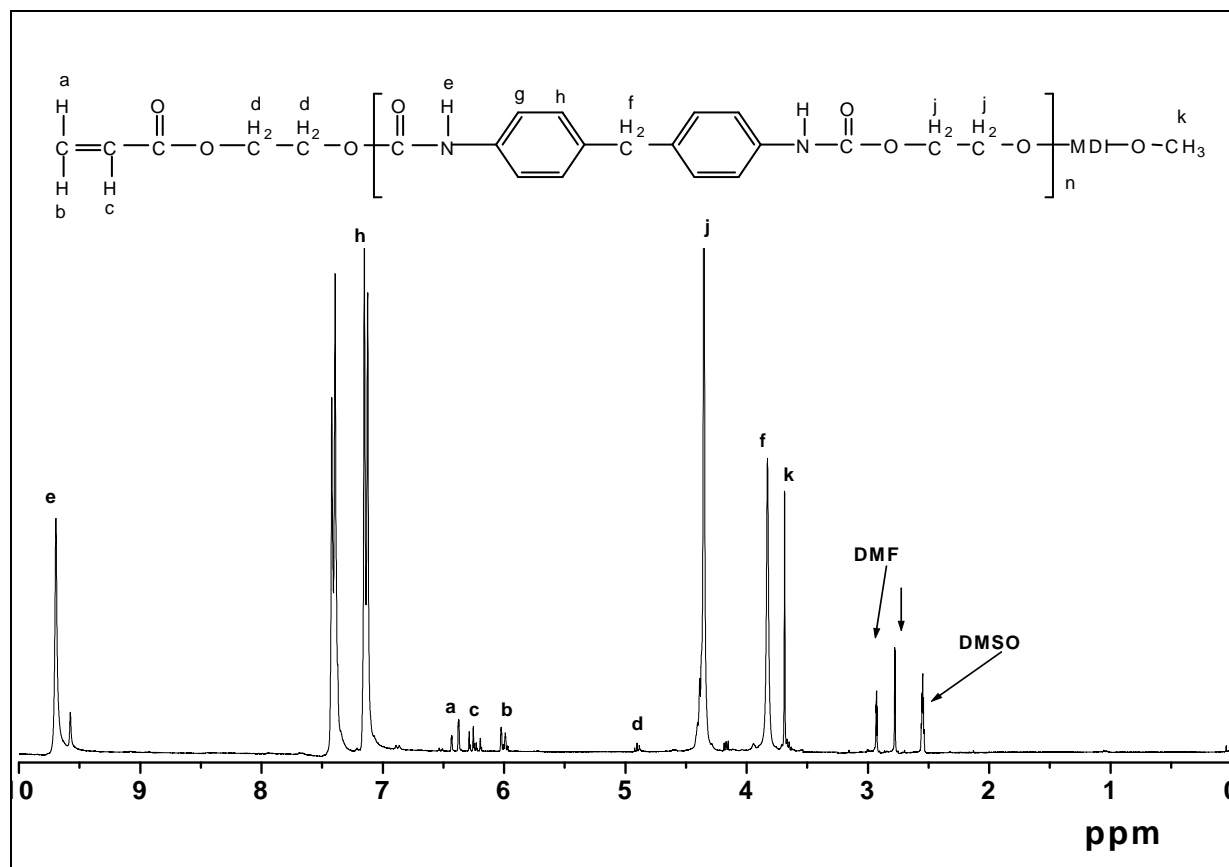


Figure 4.9: ¹H-NMR spectrum of UM1 dissolved in deuterated DMSO.

In addition, the ¹H-NMR analysis indicates that the end functionality, i.e., the number of methyl groups and vinyl end groups per molecule of product UM1, is nearly unity (0.92: 1.00) as determined by comparing the peak area of the methyl proton of MeOH at $\delta = 3.68$ ppm and that the vinyl protons of 2-HEA at $\delta = 5.95$, 6.25 and 6.47 ppm.

Moreover ¹H-NMR was used to calculate the average number of repeating units (n) for UM1 and number-average molecular weight (M_n). The integration signal of j at $\delta = 4.45$ which corresponding to EG in the UM1 repeat unit, is approximately four times that of the peak of k at $\delta = 3.68$ ppm, corresponding to MeOH, i.e the UM1 end group. This ratio between these two peaks gives the n of UM1. The calculation was done using the equation below:

$$\text{Average repeat unit } (n) = (j/4)/(k/3)$$

The integration value for signal j is divided by 4 and the integration value for signal k is divided by 3 so as to equal each other.

The average number of repeating units (n) which was calculated by ¹H-NMR was used to

calculate the number average molecular weight (M_n), by using the following formula:

$$M_n^{\text{NMR}} = \text{MeOH}-(\text{MDI-EG})_n\text{-MDI-2-HEA}$$

The result was 1646 g/mol

where the M_n of MeOH = 32, M_n of MDI = 250, M_n of EG = 62, M_n of 2-HEA = 116 and $n = 4$

4.5.1.4 ^{13}C -NMR analysis

^{13}C -NMR was also carried out to confirm the UM1 structure. A typical ^{13}C -NMR spectrum of the UM1 prepared in this work is shown in Figure 4.10. Peak assignments were made based on the expected structure, which is shown in the insert in Figure 4.10. The ^{13}C -NMR spectrum of the UM1 shows aromatic carbons at $\delta = 117.98$, 128.49, 134.84 and 136.71 ppm,³³ whereas the resonance signals for the methylene carbons of EG appear at $\delta = 61.77$ ppm.³⁴ The characteristic signal of the urethane ester appears at $\delta = 165.07$ ppm.³⁵ The methylene carbon between two aromatic rings of MDI shows a peak at $\delta = 42.04$ ppm,³⁶ whereas the peak at $\delta = 51.11$ ppm corresponds to the methyl groups of the methoxy group of the MeOH end of the synthesized UM1. The important characteristic signals of the vinyl-terminated group of the UM1 were detected at $\delta = 127.55$ and $\delta = 131.39$ ppm, which prove the existence of acrylate groups in the UM1 structures and confirms successful synthesis of the UM1.³⁴

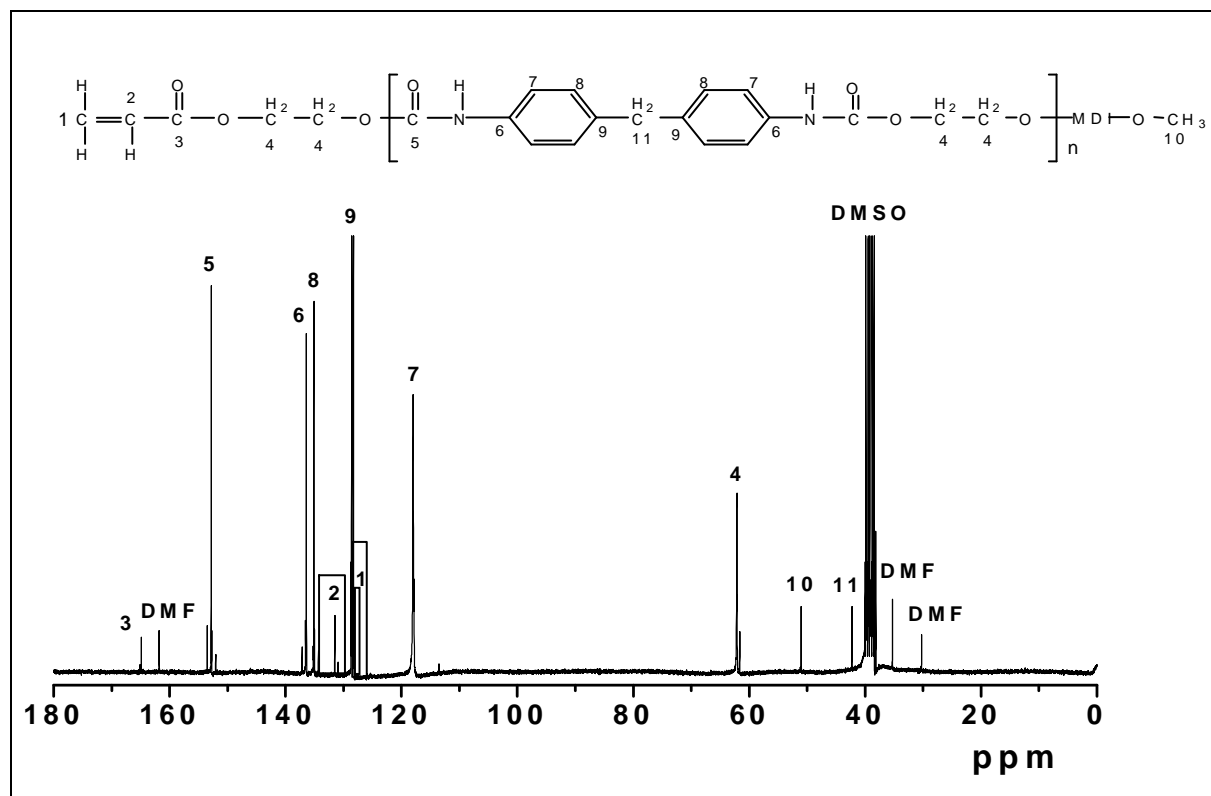


Figure 4.10: ^{13}C -NMR spectrum of UM1 dissolved in deuterated-DMSO.

4.5.1.5 SEC analysis

SEC analysis was performed to characterize the UM1. The SEC instrument was calibrated using linear polystyrene standards. Dimethylacetamide (DMAc) was used as solvent.

Figure 4.11 shows a SEC trace of UM1; it has a broad molecular weight distribution. This is expected, as polyaddition polymerization was used to synthesize the UM1.

The M_n values (experimental and predicted) and polydispersity obtained for the UM1 are summarized in Table 4.9. Here it shows that the synthesized UM1 has a relatively broad molecular weight distribution, and also that the actual molecular weight of the UM1 is close to the predicted one. The M_n and M_w of the UM1 obtained during SEC analysis was done according to polystyrene standards (PS) which does not represent the exact values. However, the values are very close, which indicates that the synthesized UM1 were designed and controlled, in other words, all polymerization conditions were controlled during polymerization.

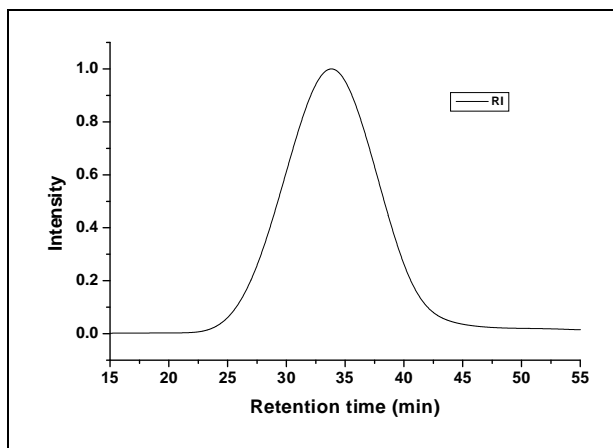


Figure 4.11: SEC chromatogram of UM1.

Table 4.9: M_n and polydispersity (M_w/M_n) of the UM1 of different chain lengths, as determined by SEC

Theoretical average chain length of UM1	Predicted molecular weight*	M_n by SEC	M_w by SEC	Polydispersity
5	1985	2205	5733	2.6

Theoretical molecular weight was calculated using Formula 4.1

4.5.2 Methacrylic-urethane graft copolymer formation

4.5.2.1 SEC analysis

The PMMA-g-UM1 and PnBMA-g-UM1 copolymers were synthesized by solution free radical polymerization, as described in Section 4.3.7. The molecular structure was confirmed using SEC with double detectors UV and RI.

The ability of UM1 to undergo copolymerization was determined using MMA and n-BMA respectively as comonomers. Different amounts of UM1 were copolymerized with different amounts of MMA and n-BMA under free radical copolymerization conditions. The resulting graft copolymers were isolated by precipitation from DMF solution into excess methanol.

Table 4.10 illustrates the formulations used to prepare the graft copolymer with different amounts of macromonomer. The yield was determined gravimetrically after extraction of the unreacted macromonomer. The yield of the PMMA-g-UM1 copolymers ranged between 70% and 84% and that of the PnBMA-g-UM1 copolymers range between 69% and 81% (all the calculations were done after extraction of the unreacted UM1, see Section 4.5.2.2).

Table 4.10 shows that all PMMA-g-UM1 and PnBMA-g-UM1 copolymers had molecular weights of about 70,000, which is higher than of the starting UM1 (Table 4.9). In addition to this, the molecular weight values of the graft copolymers obtained by SEC measurements were generally much lower than the absolute molecular weight because linear polystyrene has a much larger hydrodynamic volume than the corresponding graft copolymers of the same molecular weight.³⁷

Table 4.10: Formulation and characterization of graft copolymers

	Sample code	UM1 (g)	Acrylate (g)	Graft copolymer		PDI	Yield* % of graft copolymer
				Mn (g/mol)	Mw (g/mol)		
			MMA				
PMMA-g-UM1	G10M	0.50	4.50	7.39 X10 ⁴	1.15 X10 ⁵	1.56	84
	G25M	1.25	3.75	7.25 X10 ⁴	1.36 X10 ⁵	1.83	76
	G55M	2.75	2.25	7.13 X10 ⁴	1.47 X10 ⁵	2.07	70
			n-BMA				
PnBMA-g-UM1	G10B	0.50	4.50	7.02 X10 ⁴	1.17 X10 ⁵	1.68	81
	G25B	1.25	3.75	6.82 X10 ⁴	1.38 X10 ⁵	2.03	77
	G55B	2.75	2.25	6.34 X10 ⁴	1.47X10 ⁴	2.33	69

Yield of graft copolymer equals the amount of graft copolymer after extracting unreacted UM1 (g) divided by 5 (g) which is the total amount of UM1 and methacrylic monomer in the copolymerization feed.

Figure 4.12 shows SEC traces for UM1, PMMA and PnBMA, characterized by SEC with a UV detector (254 nm). The UV detected the UM1 but not the PMMA and PnBMA

absorptions, which were too small to detect at this wavelength. The UM1 has a strong UV absorption due to the aromatic ring in the polymer chain.

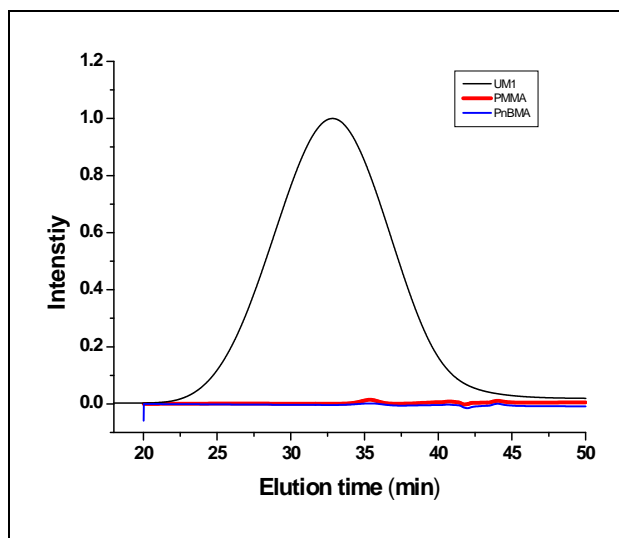


Figure 4.12: SEC traces of UM1, PnBMA and PMMA (UV detector).

Figure 4.13 and Figure 4.14 are examples of SEC traces of the graft copolymer of PMMA-g-UM1 and PnBMA-g-UM1 (25 wt % macromonomer), respectively, before extraction. A bimodal distribution curve was obtained after the copolymerization reaction. The first peak at a lower retention time is attributed to the graft copolymer. The red line represents the RI response corresponding to the graft copolymers PMMA-g-UM1 and PnBMA-g-UM1. The UV detector response is shown by the blue line, and the lower retention peak shows the presence and distribution of the UM1 in the PMMA or PnBMA backbone. The second peak is attributed to the presence of the unreacted UM1, since there is a strong UV response for this peak. This is expected as UM1 contains two terminated groups, see MALDI-TOF-MS structure C in Table 4.7.³ The presence of the macromonomers affects the degree of polymerization also in terms of increasing the viscosity, which results in a decrease in diffusion and limits incorporation.³⁸⁻⁴⁰

The segment and repeat unit density around the propagating radical site of the formed copolymer is relatively large, and increases with the degree of polymerization, making the insertion of the macromonomer more difficult. The incompatibility issue between the backbone and the branches also plays a large role in decreasing the reactivity of the macromonomer, as discussed by Ito and Kawaguchi,³ Hong et. al,⁴⁰ and Meijs and Rizzardo.⁴¹

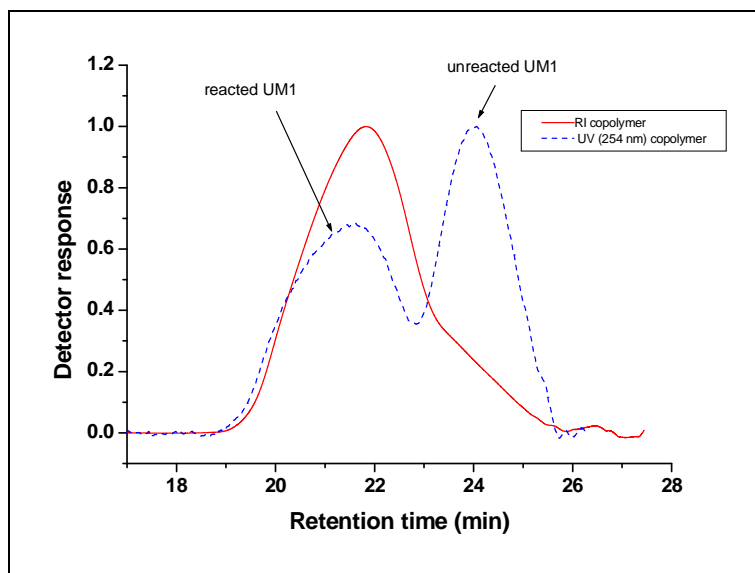


Figure 4.13: SEC traces of unextracted graft copolymer PMMA-g-UM1 (25 wt %). (RI and UV detector responses have been normalized.)

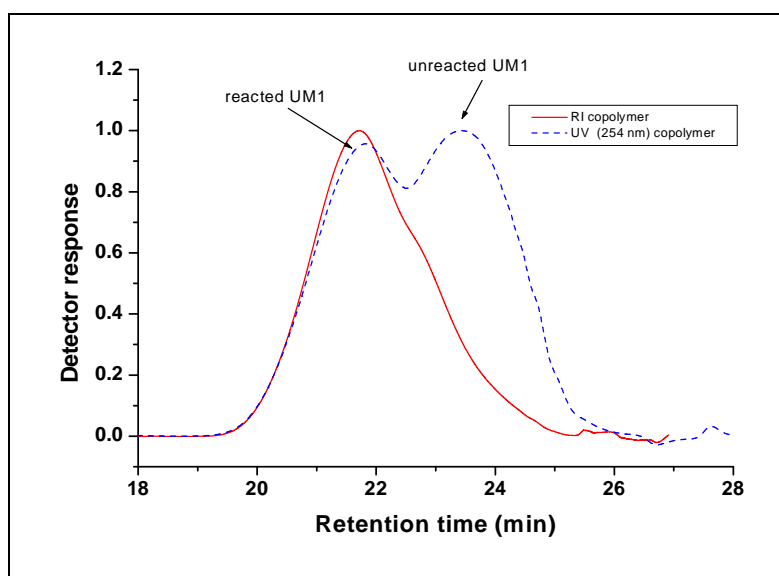


Figure 4.14: SEC traces of unextracted graft copolymer PnBMA-g-UM1. (Note: RI and UV detector responses have been normalized.)

The repeat unit density around the propagating radical site in the copolymer is relatively large, and increases with the degree of polymerization, making the insertion of the macromonomer more difficult. This is especially so if there is an incompatibility issue between the backbone and the graft as this will play a large role in decreasing the reactivity of the macromonomer, as discussed by Ito et al.³ Hong et al.,⁴⁰ Meijs and Rizzardo.⁴¹ This may not be a major issue as there is a large fraction of unreactive UM1 (see Section 4.5.1.2).

4.5.2.2 Extraction of unreacted macromonomer

Methanol is a nonsolvent for PMMA, PnBMA and the corresponding methacrylate-g-urethane copolymers. However, there is some unreacted UM1 (UM1 containing both MeOH end groups which cannot react during graft copolymerization or urea side reaction (H structure in

Table 4.7) and some unreacted UM1 (UM1 containing at least one 2-HEA end group, which did not react during graft copolymerization) were extracted by precipitation in methanol. However a little unreactive and unreacted UM1 also precipitated along with the graft copolymer, as indicated by the slight shoulder at low molecular weight in Figures 4.13 and 4.14.

The unreacted UM1 was further removed by precipitation using DMF as solvent and THF and MeOH as nonsolvent. A sample of about 0.5 g of graft copolymer was dissolved in about 10 ml DMF and precipitated in THF. The solution was filtered, and then precipitated again in MeOH. The resultant graft copolymer and PMMA or PnBMA homopolymers precipitated out of solution, while the unreacted macromer remained soluble. The extraction of the unreacted macromer was tracked using SEC with a RI detector, as shown in Figures 4.16 and 4.17. Figure 4.15 is an example of MALDI-TOF-MS showing (a) UM1 before using the UM1 in a free radical copolymerization and (b) extracted unreacted UM1 after using the UM1 in a free radical copolymerization. The percentage of graft formation was calculated gravimetrically after extraction of the unreacted macromer. The formulation and characterization of the grafts are tabulated in Table 4.10. The yields of the graft polymers were 69-84% and all the calculations were done after removing all unreacted macromer.

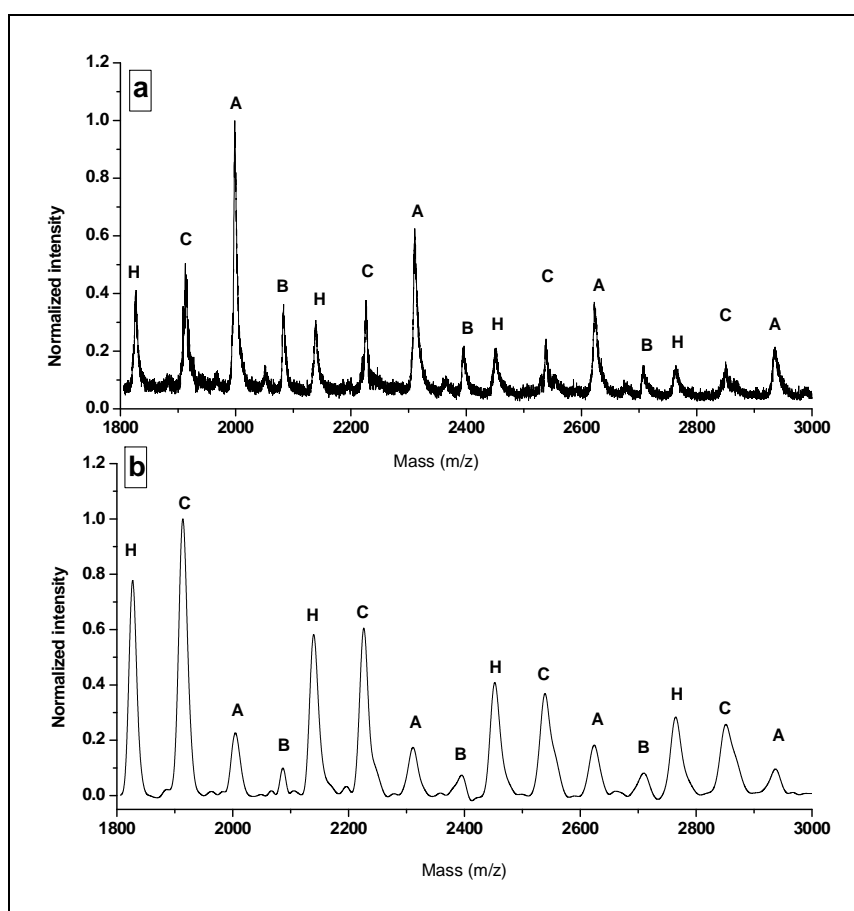


Figure 4.15: MALDI-TOF-MS (a) before using UM1 in free radical copolymerization and (b) extracted UM1 after free radical copolymerization.

4.5.3 Characterization of graft copolymers after extraction

4.5.3.1 SEC analysis

SEC equipped with a dual detector system (RI and UV) was used to characterize the graft copolymers. The UV detector was set up at a wavelength of 254 nm, which is suitable for detecting UM1 the aromatic rings. A UV response was observed for all the graft copolymers. The distribution of the UV response gives an idea of the branch content in the graft. Figures 4.16 and 4.17 are examples show the SEC of the graft copolymers PMMA-g-UM1 and PnBMA-g-UM1 after extraction of the unreacted macromer. The distribution of the UV response associated with the UM1 branches on the MMA or n-BMA backbones indicates that the UM1 branches are distributed evenly throughout the graft polymer, and no UV peaks for unreacted UM were observed at high retention time and also the retention time of the graft copolymer samples were shifted to lower time compared to the retention time of the starting materials (e.g. retention time of UM1). This result indicates that the molecular weights of the graft copolymer samples increased due to the grafting reaction. This was observed for all the synthesized grafts, with different macromonomer contents. In the two Figures below the UV response almost mirrors the RI response, but there is a significant difference at the longer retention times (note that the detector response has been normalized). This is an indication that there may not be a totally uniform distribution of the graft in the polymer.

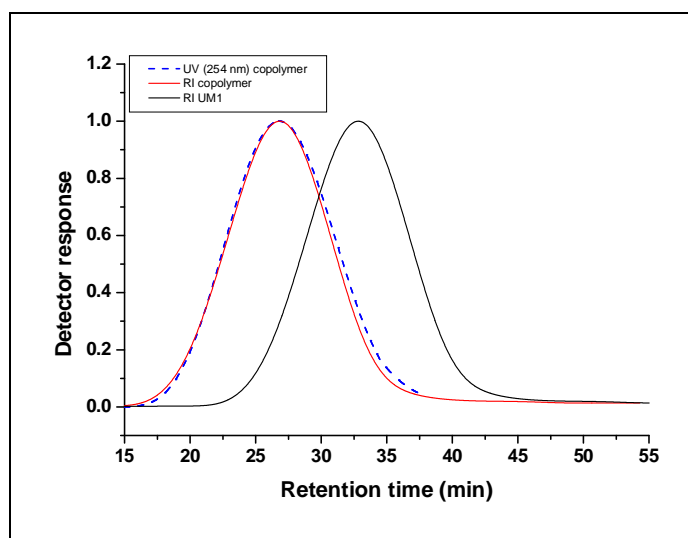


Figure 4.16: SEC traces of PMMA-g-UM1 (25 wt % UM1) illustrating the UM1 distribution.

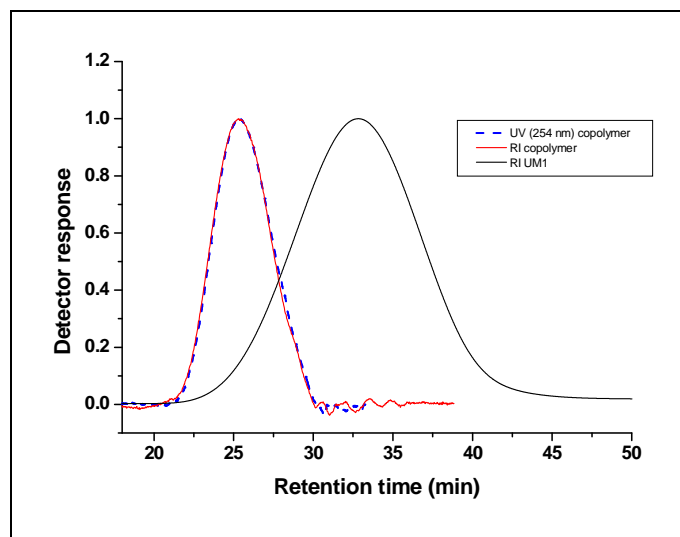


Figure 4.17: SEC traces of PnBMA-g-UM1 (25 wt % UM1) illustrating the UM1 distribution.

The yields of the copolymerization reactions for both PMMA-g-UM1 and PnBMA-g-UM1 copolymers are shown Table 4.10. The UM1 consists of four possible structures (as discussed previously in Section 4.5.1.2):

- (a) MeOH-(MDI-EG)_n-MDI- MeOH
- (b) MeOH -(MDI-EG)_n-MDI-2-HEA
- (c) 2-HEA-(MDI-EG)_n-MDI-2-HEA
- (d) Urea (structure H in Table 4.8) [(MDI-EG)_n-MDI-MeOH]

Due to the UM1 being encapped with a 60:40 mole ratio of MeOH:2-HEA during UM1 synthesis, the UM1 will consist of an unreactive fraction (structures (a) and (d) above). These unreactive UM1 fractions are the primary cause of the decreased percentage yield with an increase in the weight fraction of UM1 during copolymerization.

The yields of both PMMA-g-UM1 and PnBMA-g-UM1 copolymers decreased as the quantities of the UM1 are increased. This is because as the weight fraction is increased, so too does the weight fraction of the unreactive UM1 increase, which, after removal with methanol, resulted in a decrease in the percentage yield of the graft copolymers.

4.5.3.2 GPEC analysis

It is well known that graft copolymers synthesized, using a low molecular weight monomer and a macromonomer, by radical polymerization display heterogeneity in terms of both molecular mass and chemical composition. Therefore, the characterization of these materials by a single technique (for example SEC) is made difficult by the effects of both the molecular

mass and chemical composition on the separation mechanism. Techniques such as SEC, with selective detection, cannot be used to fully characterize copolymers due to the fact that the hydrodynamic volume, necessary for characterization, is dependent on the chemical composition. Gradient Elution High Performance Liquid Chromatography also known as Gradient Polymer Elution Chromatography (GPEC) is a good technique for separating via chemical composition.

Graft copolymers may contain ungrafted homopolymer and unreacted macromonomer, as well as copolymer that vary in composition. In this study GPEC was used to analyze the copolymers and monitor the extraction of unreacted macromonomer, as well as to determine the chemical composition distribution of synthesized graft copolymers.

HPLC analysis was performed with a combination of precipitation HPLC and adsorption or retention HPLC. By starting with a non-solvent and increasing the percentage of a good solvent, on a stationary phase possessing strong adsorption interactions with small-pore column packings, copolymer retention was achieved that resulted in compositional separations. In this study a Nucleosil C18; 100Å (25 x 0.46) column was used. A compromise between copolymer solubility and chromatographic solvent strength was used to ensure copolymer separation over a broad chemical composition distribution.

(a) GPEC of PMMA-g-UM1 copolymers

The premise on which the GPEC separation works can be explained as follows: PMMA homopolymer is completely soluble in chloroform and is therefore unretained on the silica packing. The graft copolymer however is insoluble in the starting solvent, chloroform. The mode of retention is therefore the governing factor in determining the actual separation. The retention process in the case of the PMMA-g-UM1 copolymer, using chloroform/DMF as solvent system over silica packing, relies on initial precipitation, followed by adsorption retention after redissolution of the graft copolymer in the solvent gradient.

Several gradients were tested before optimal separation was obtained. Variables that were investigated included: the rate at which the percentage of non-solvent to good solvent was added and the quantity of sample injected, furthermore both linear and non-linear gradients were tested. Figure 4.18 shows examples of some of the gradients that were tested (but not used, because they either resulted in bad separation or variable separation). Profile #1, for example, yielded good separation but results were not consistent and therefore this was unusable. For all profiles the quantity of sample injected on the GPEC column was varied from 8 µl to 20 µl. Profile #4 yielded good separation between PMMA, PMMA-g-UM1 copolymer and unreacted UM1, and more, importantly, results were consistent for multiple

runs. Here it was also found that a sample injection volume of 10 μl provided optimal results. Throughout the development of the gradient profile a sample flow rate of 1 mL/min was used.

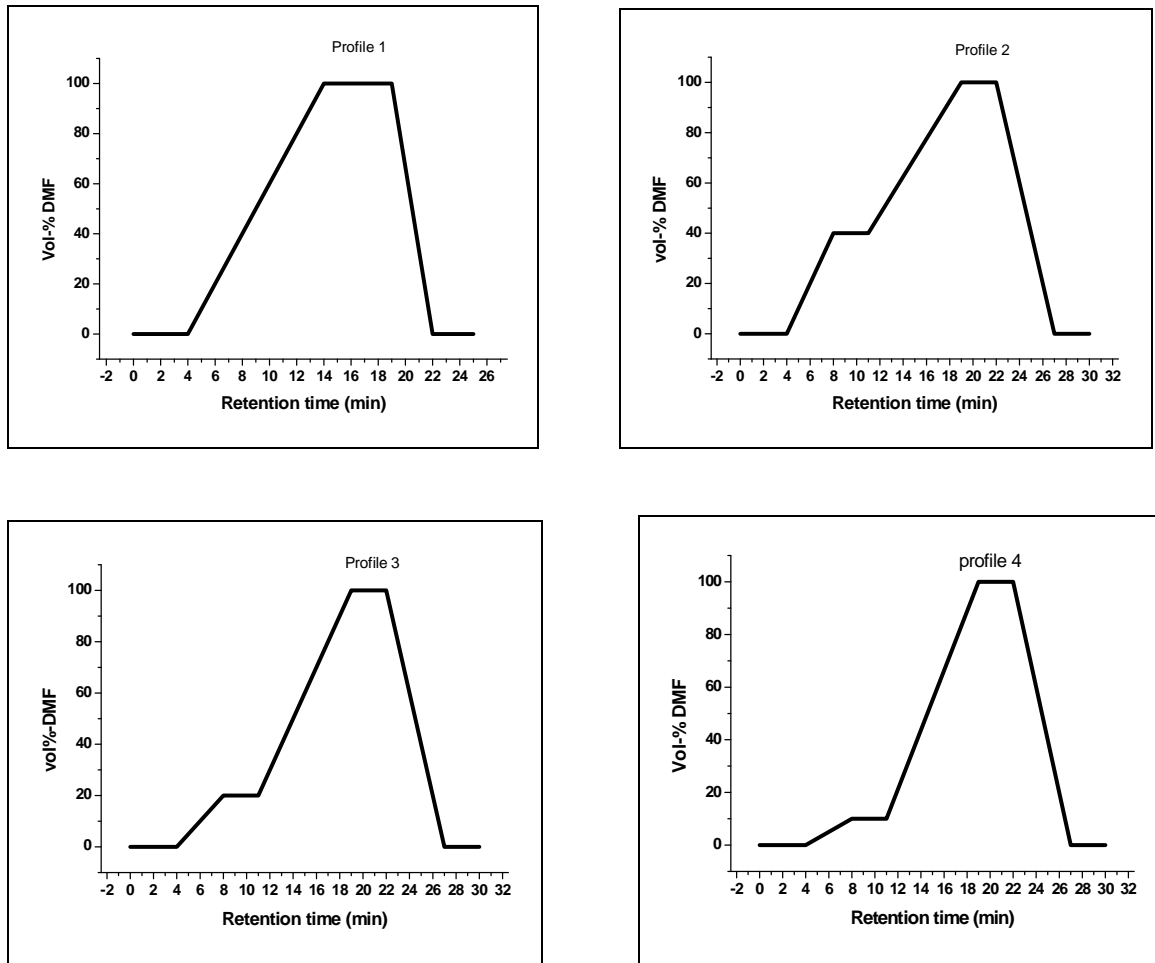


Figure 4.18: Example of gradient elution profiles considered for the separation of PMMA-g-UM1 copolymer: stationary phase: Nucleosil C18; 100Å; eluent:chloroform/DMF.

PMMA standard and UM1 synthesized in this study were used to identify their retention times in the elution profile. Figure 4.19 shows the retention times of these components. PMMA elutes between 2 and 4 min whereas UM1 elutes between 13 and 17 min.

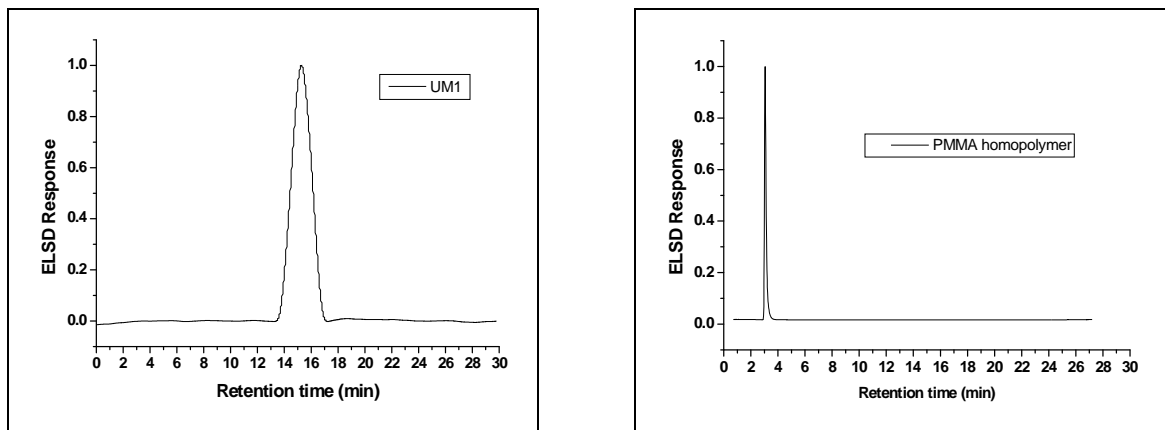


Figure 4.19: Gradient HPLC elution plots of UM1 and PMMA homopolymer.

The gradient HPLC chromatogram of the typical example of the PMMA-g-UM1 copolymer after gradient profile separation is presented in Figure 4.20. The assignment of the peaks was carried out by comparison with the chromatographic behaviour under similar conditions used for UM1 and PMMA separation using a reversed phase column (Nucleosil C18; 100Å). The first peak was assigned to PMMA homopolymer, followed by the graft copolymer PMMA-g-UM1, and finally unreacted UM1.

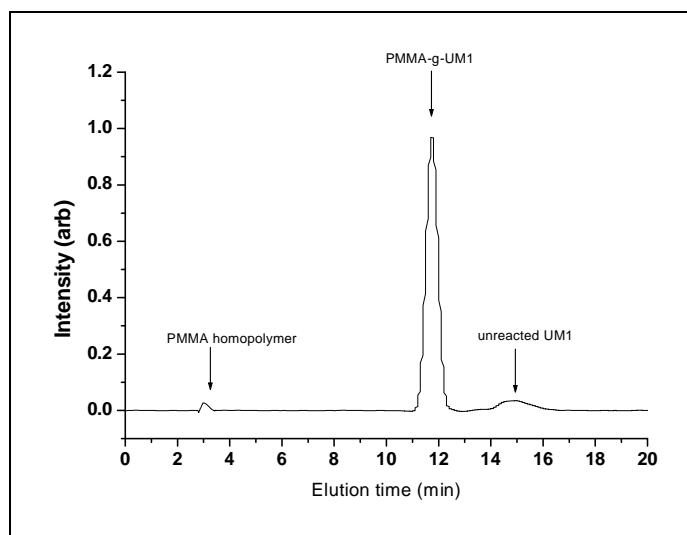


Figure 4.20: Gradient HPLC chromatogram of the PMMA-g-UM1 copolymer (G55M). (Stationary phase: Nucleosil C18; 100Å; eluent: chloroform/DMF; detector: ELSD).

(b) GPEC of PnBMA-g-UM1 copolymers

PnBMA homopolymer is completely soluble in toluene and is therefore not retained on the silica packing. The graft copolymer is however insoluble in the starting solvent toluene. The mode of retention is therefore the governing factor in determining the actual separation. In this case (PnBMA-g-UM1 copolymer), for the toluene/DMF system on silica the retention relies on initial precipitation, followed by adsorption retention after redissolution of the graft copolymer in the solvent gradient. Linear gradients were used here, as shown in Figure 4.21.

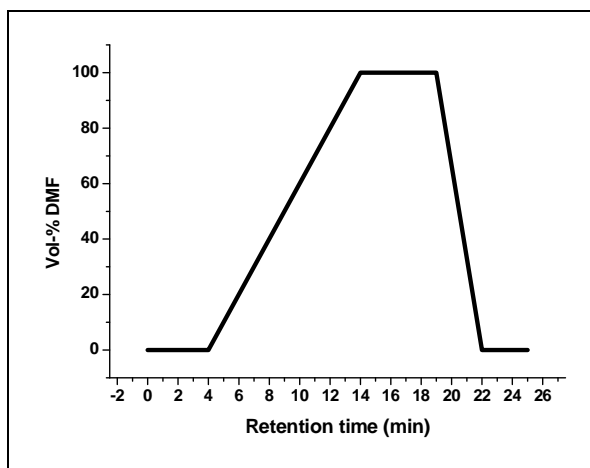


Figure 4.21: Gradient elution profiles considered for the separation of PnBMA-g-UM1 copolymer (Stationary phase: Nucleosil C18; 100Å, eluent: toluene/DMF.)

Separation is a function of component polarity. Here PnBMA is much less polar than UM1, therefore when using a reversed phase column (Nucleosil C18; 100Å) PnBMA is expected to elute first in a low polar solvent (toluene), followed by the UM1. PnBMA and UM1 were used to identify their retention times in the elution profile. Figure 4.22 shows the retention times of these components. PnBMA elutes between 2 and 4 min, whereas UM1 elutes between 15 and 18 min.

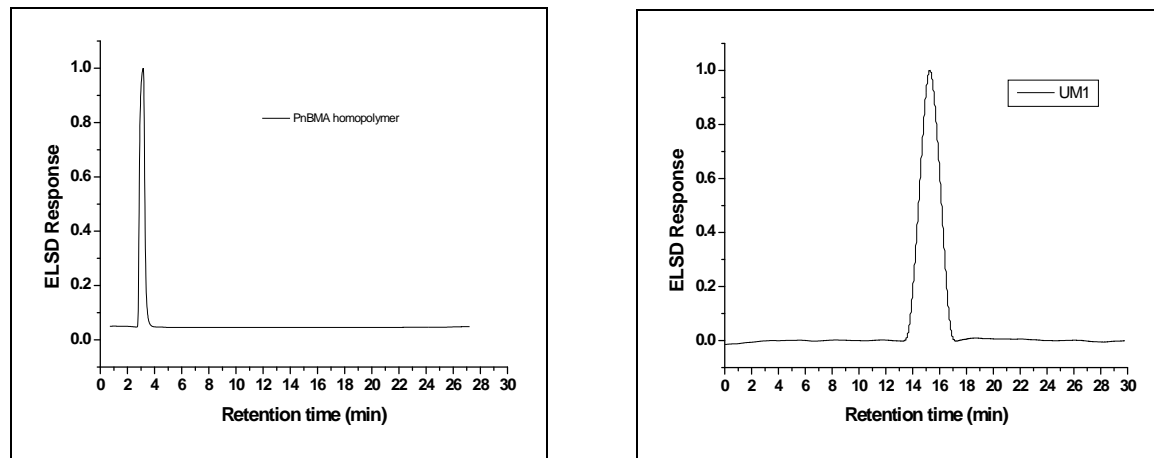


Figure 4.22: HPLC elution plots of UM1 and PnBMA homopolymer.

A gradient HPLC chromatogram showing a typical PnBMA-g-UM1 copolymer before extractions is illustrated in Figure 4.23. It shows that very good separation into three fractions was obtained. The assignment of the peaks was carried out by comparison with the homopolymer and chromatographic behaviour of UM1 and PnBMA homopolymer using a reversed phase column (Nucleosil C18; 100Å). The three elution peaks visible are assigned to the sample constituents PnBMA, UM1 and PnBMA-g-UM1. PnBMA is eluted quickly and leaves the column first. The second peak, which is significantly retained is PnBMA-g-UM1, and the third peak is assigned to unreacted UM1. As was expected, it is

retained the most on the stationary phase. A gradient HPLC chromatogram showing a typical PnBMA-g-UM1 copolymer after extracting almost all of the PnBMA homopolymer and unreacted UM1 is illustrated in Figure 4.24.

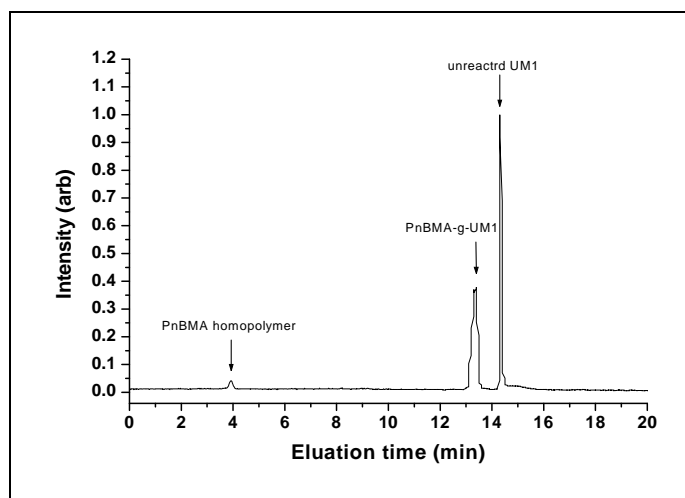


Figure 4.23: Gradient HPLC chromatogram of the PnBMA-g-UM1 copolymer (G55B) before extracting unreacted UM1 and PnBMA homopolymer. (Stationary phase: Nucleosil C18; 100Å; eluent: toluene /DMF; detector: ELSD.)

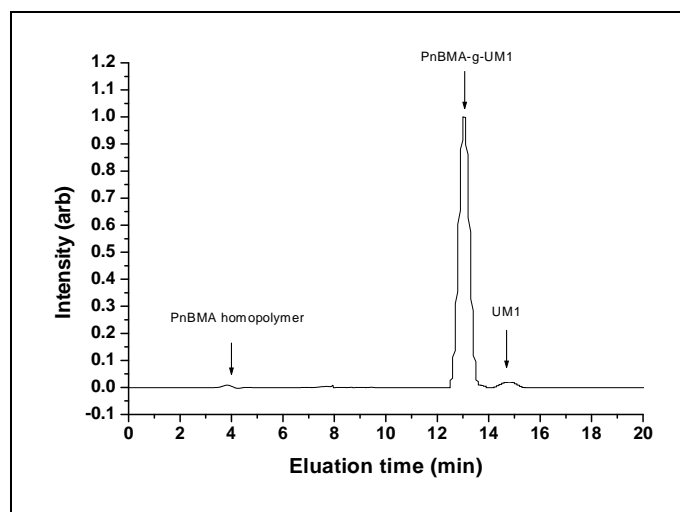


Figure 4.24: Gradient HPLC chromatogram of the PnBMA-g-UM1 copolymer (G55B) after extracting unreacted UM1 and PnBMA homopolymer. (Stationary phase: Nucleosil C18; 100Å; eluent: toluene /DMF; detector: ELSD.)

4.5.3.3 Light scattering

The graft copolymers were also characterized using a multi-angle light scattering detector (MALLS) to determine the absolute molecular mass, as the M_n result obtained from SEC calibrated with linear polystyrene standards could be misleading. These results are presented and discussed below. To be able to use the MALLS detector the specific refractive index increment, usually referred to as the dn/dc value, was determined for each of the individual graft copolymers in dimethylacetamide (DMAc), by calculating from the refractive

index detector signal and the concentration of the polymer solution. The molecular weights and molecular weight distributions (M_w/M_n) were calculated using Wyatt Technology Astra software. Peak areas were selected based on the width of the light-scattering peaks. Table 4.11 shows the weight average molecular weight and number average molecular weight of the graft copolymers obtained by MALLS. The molecular weight distributions of the graft copolymer were relatively narrower than those obtained from the normal SEC. The molar mass values obtained by MALLS are consistently higher than the molar mass obtained relative to polystyrene. This indicates a difference in molecular size of the graft copolymer in the better solvent for copolymers of same molar mass.

Table 4.11: The number average molar weight and weight average weight mass of the graft copolymers obtained via SEC-MALLS

	Sample code	dn/dc	Graft copolymer		PDI
			Mn (g/mol)	Mw (g/mol)	
PMMA-g-UM1	G10M	0.113	9.23×10^4	1.64×10^5	1.77
	G25M	0.133	9.14×10^4	1.85×10^5	2.02
	G55M	0.146	8.45×10^4	1.94×10^5	2.29
PnBMA-g-UM1	G10B	0.102	9.18×10^4	1.73×10^5	1.88
	G25B	0.141	9.07×10^4	1.78×10^5	1.96
	G55B	0.162	8.94×10^4	1.94×10^5	2.17

4.5.3.4 FTIR analysis

The FTIR spectra of the graft copolymers provide proof that the UM1 was actually grafted to PMMA or PnBMA through the double bond (which disappears) during free-radical copolymerization. After all the unreacted and unreactive UM1 (UM1 with MeOH in both chain ends and urea (structure H in Table 4.7)) were removed as confirmed by SEC (see Section 4.5.2.2), the graft copolymers samples were analyzed by FTIR.

(a) PMMA-g-urethane copolymers

Figure 4.25 shows a comparison of the FTIR spectra of the PMMA-g-UM1 copolymers and PMMA homopolymer. New peaks were observed in the spectra of the graft copolymers. The band at 3331 cm^{-1} is assigned to the hydrogen-bonded N-H stretching absorption peak of the urethane groups. The amide absorption peak appears at 1528 cm^{-1} and aromatic band of the MDI repeat unit at 1601 cm^{-1} . These results show that the UM1 was successfully incorporated into the PMMA polymer structure. This was also confirmed by GPEC and SEC.

The peaks at 936 cm^{-1} ascribed to the double bond in the UM1, disappear. This indicates that UM1 has fully reacted with MMA.

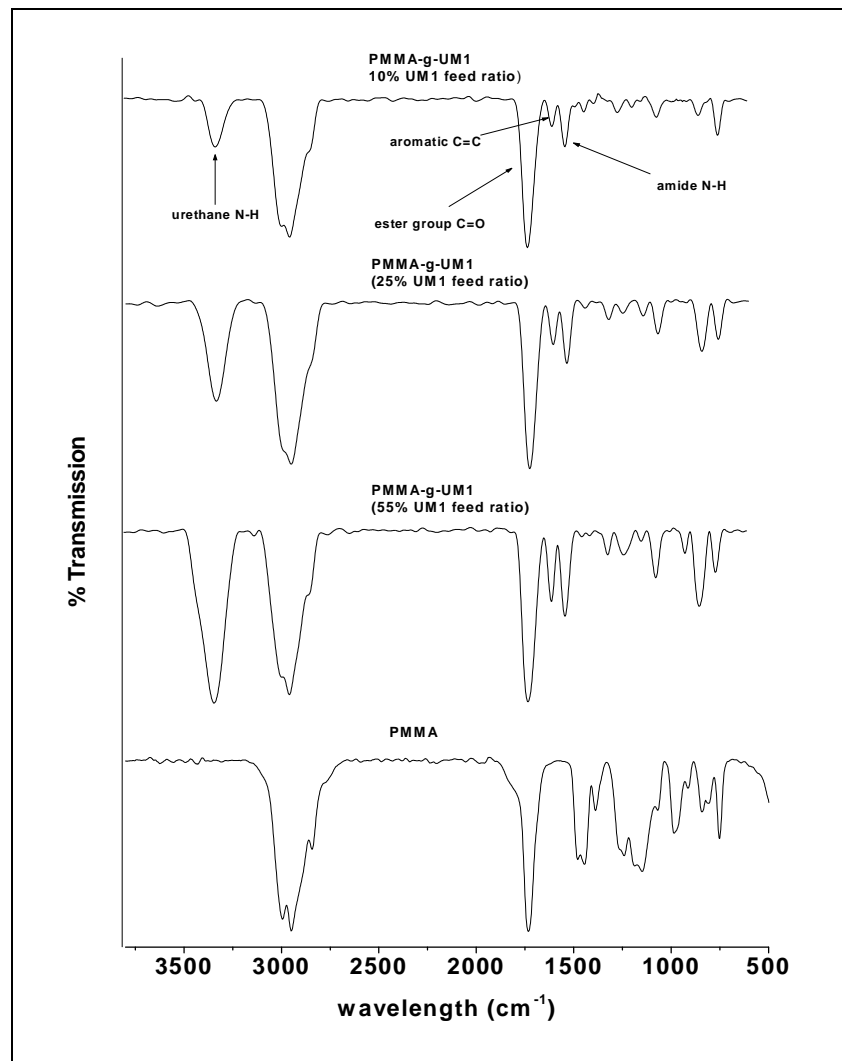


Figure 4.25: FTIR spectra showing comparisons between PMMA-g-UM1 and PMMA homopolymer.

(b) PnBMA-g-UM1 copolymers

Figure 4.26 shows a comparison of the FTIR spectra of the PnBMA-g-UM1 copolymers and the PnBMA homopolymer. New peaks were observed in spectra of the graft copolymers. The absorption peak at the 3329 cm^{-1} is assigned to the N-H stretching band of the urethane group. The amide vibration absorption peak appears at 1546 cm^{-1} and the aromatic absorption peak of the MDI repeat unit appears at 1605 cm^{-1} . These results show that the UM1 was successfully incorporated into the PnBMA polymer chain, which was also confirmed by GPEC and SEC. The peak at 936 cm^{-1} for the double bond in the UM1 disappears. This indicates that UM1 has fully reacted with n-BMA.

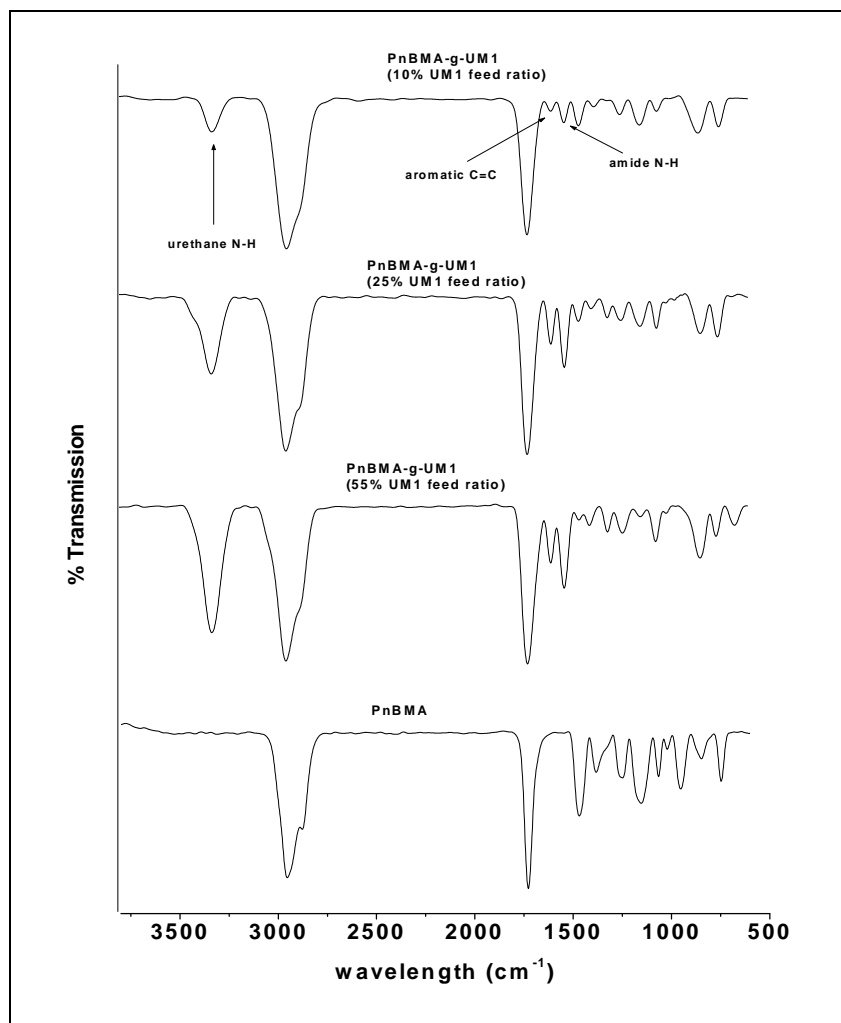


Figure 4.26: FTIR spectra showing comparisons between PnBMA-g-UM1 and PnBMA homopolymer.

(c) Effect of the UM1 content on copolymerization

Figures 4.25 and 4.26 above clearly show that as the amount of UM1 was increased in the feed of the copolymerization reactions, the percentage of UM1 being incorporated into the PMMA-g-UM1 and PnBMA-g-UM1 copolymers also increased. This is indicated by an increase in the intensity of the areas of the UM1 absorption peaks in these spectra, such as NH stretching at 3330 cm^{-1} , NH absorption at 1546 cm^{-1} , the aromatic absorption peak at 1605 cm^{-1} and C=O at 1742 cm^{-1} .

The weight percentages of UM1 incorporated into the graft copolymers were determined from FTIR spectra, using calibration curves. The calibration curves were drawn up by mixing different percentages of UM1 with PMMA and PnBMA homopolymers, respectively (without polymerization). The percentages of UM1 to PMMA and UM1 to PnBMA homopolymers that were used were: 9%, 12%, 21%, 32%, 43% and 51% by weight.

Figures 4.27 shows calibration curves for PMMA and PnBMA homopolymers which were separately mixed with different amounts of UM1. The calibration curves were obtained by

plotting the UM1 content on the X axis and the transmission area of the N-H area of the urethane groups at 3345 cm^{-1} on the Y axis.

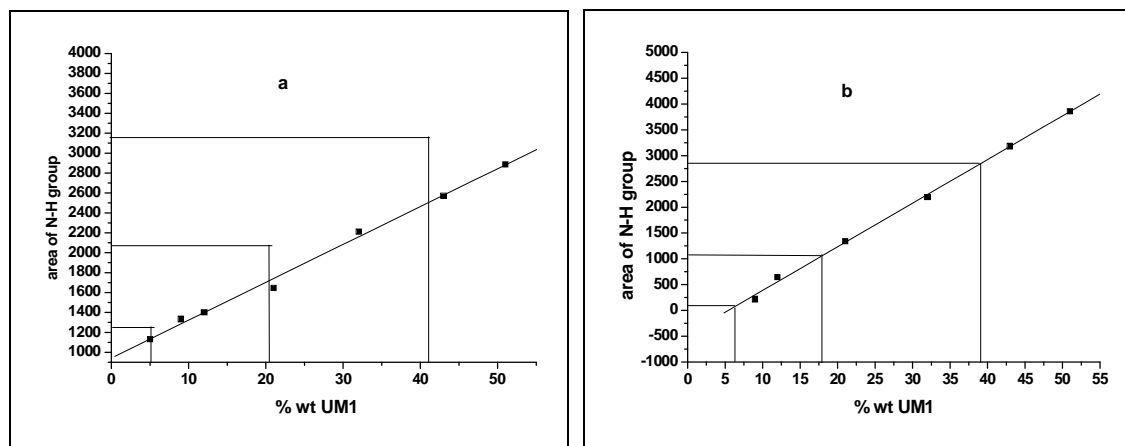


Figure 4.27: Calibration curve of (a) PMMA and (b) PnBMA mixed with different amounts of UM1.

From the calibration curves in Figures 4.27 (a) and (b), the weight percentages of UM1 calculated to be incorporated into both PMMA-g-UM1 and PnBMA-g-UM1 copolymers are shown in Table 4.12. It can be noted that as the amount of UM1 used during graft copolymerization increased, the weight percentages of UM1 incorporated into both PMMA-g-UM1 and PnBMA-g-UM1 copolymers also increased. This was also confirmed by UV-Vis and $^1\text{H-NMR}$ (see Sections 4.5.3.5 and 4.5.3.7, respectively).

Table 4.12: Weight percentages of UM1 incorporated into the graft copolymers, as calculated from FTIR data

	Sample code	UM1/MMA feed ratio (wt %)	NH absorption peak area in FTIR spectrum	UM1 incorporated into copolymers (wt %)
PMMA-g-UM1	G10M	10/90	1155	4.20
	G25M	25/75	1740	20.40
	G55M	55/45	2494	41.04
		UM1/n-BMA feed ratio (wt %)		
PnBMA-g-UM1	G10B	10/90	94.50	6.18
	G25B	25/75	1065	18.02
	G55B	55/45	2852	39.09

4.5.3.5 UV-Vis spectroscopy analysis

The graft copolymers were further characterized using UV-Vis spectroscopy, after extracting the unreacted macromer. UV spectroscopy is a method that is used to determine the absorption wavelength (λ_{\max}) of UV-absorbing species. Here UM1 was expected to absorb at 254 nm, where the aromatic ring of UM1 absorbs. The UV spectra of the UM1, PMMA, PnBMA, PMMA-g-UM1 and PnBMA-g-UM1 copolymers are presented in Figures 4.28 and 4.29.

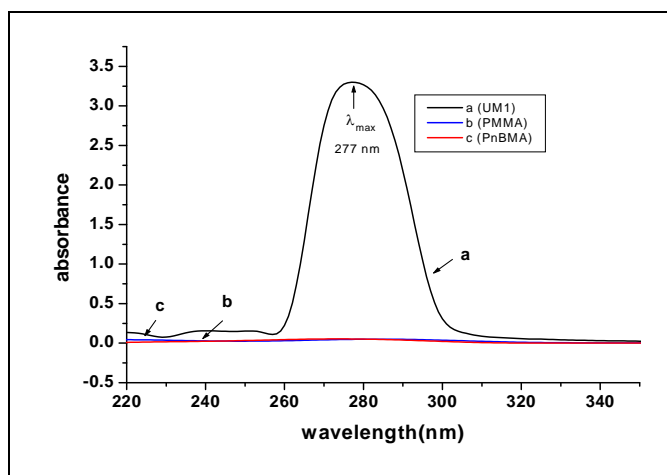


Figure 4.28: UV/Vis spectrum: (a) UM1 (b) PMMA and (c) PnBMA [DMF was used as solvent (UV-cutoff 200 nm)] wavelength.

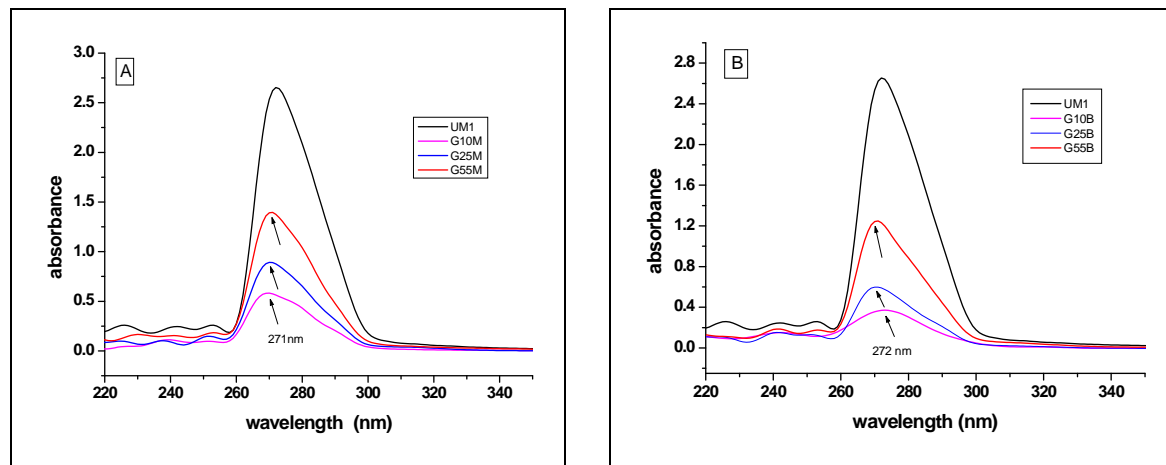


Figure 4.29: UV/Vis spectra of UM1 copolymerized with different amounts of acrylate [(A) PMMA and (B) PnBMA, DMF was used as solvent (UV-cutoff 200 nm)].

UV/Vis analysis of the PMMA-g-UM1 and PnBMA-g-UM1 copolymers (Figure 4.29) showed that graft copolymers had strong absorption peaks in the region where the UM1 absorbs. The strong absorption peak was absent in this region in the PMMA and PnBMA homopolymers (Figure 4.28).

A calibration curve was used to determine the equivalent amounts of the UM1 in the PMMA-g-UM1 and PnBMA-g-UM1 copolymers. Solutions of various concentrations of the UM1,

using DMF as solvent, were prepared and their UV absorbance measured. A plot of absorbance versus quantity of the UM1, in mg/mL, was constructed (Figure 4.30). Three samples of different known masses per each graft copolymer were dissolved in DMF and their absorbances were measured at a concentration of 0.2 mg/ml. The corresponding equivalent amount of UM1 in both copolymers was determined from the calibration curve (see Table 4.13).

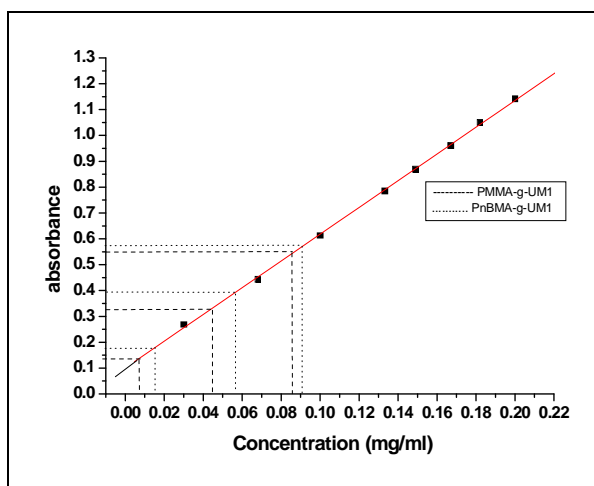


Figure 4.30: Calibration curve for the determination of percentage of UM1 incorporated into PMMA or PnBMA. [The dotted lines are extrapolation lines for PnBMA-g-UM1 copolymers and the dashed lines for PMMA-g-UM1 copolymers (see Table 4.14)].

Table 4.13: UV data for the determination of the weight percentages of UM1 incorporated into PMMA or PnBMA

	Sample code	Feed ratio		Absorbance	Equivalent amount of graft copolymer (mg/ml)	UM1 incorporated into copolymers (wt %*)
		UM1 (g)	MMA (g)			
PMMA-g-UM1	G10M	0.50	4.50	0.14	0.007	3.5
	G25M	1.25	3.75	0.33	0.045	22.0
	G55M	2.75	2.25	0.55	0.088	44.0
		UM1 (g)	n-BMA (g)			
PnBMA-g-UM1	G10B	0.50	4.50	0.18	0.015	7.5
	G25B	1.25	3.75	0.39	0.055	20.5
	G55B	2.75	2.25	0.57	0.091	44.5

* wt % UM1 was calculated by dividing the equivalent amount of graft copolymer by the equivalent amount of UM1, which is 0.2 mg/ml (absorbance of all graft copolymers was measured at this concentration.)

4.5.3.6 ^{13}C -NMR analysis

^{13}C -NMR analysis of graft copolymers after extraction was also used to confirm the presence of the branched UM1 in the graft copolymers.

(a) PMMA-g-UM1 copolymers

Figure 4.31 shows a comparison of the ^{13}C -NMR spectra of PMMA-g-UM1 copolymer to that of the PMMA homopolymer. New peaks were evident in the graft copolymer spectra. The peaks in the region between $\delta = 117$ and $\delta = 140$ ppm are mainly attributed to the aromatic carbons of the MDI in the UM1. The peaks at $\delta = 61.4$ ppm originate from methylene carbon of the EG in the UM1. In addition, the ^{13}C -NMR peaks ascribed to the vinylic carbon of the UM1 at $\delta = 127.55$ and $\delta = 131.49$ ppm were observed to have completely disappeared upon copolymerization with MMA. This result shows that the UM1 was successfully and totally incorporated into PMMA-g-UM1 copolymers, and confirms the results that of analysis by FTIR and SEC.

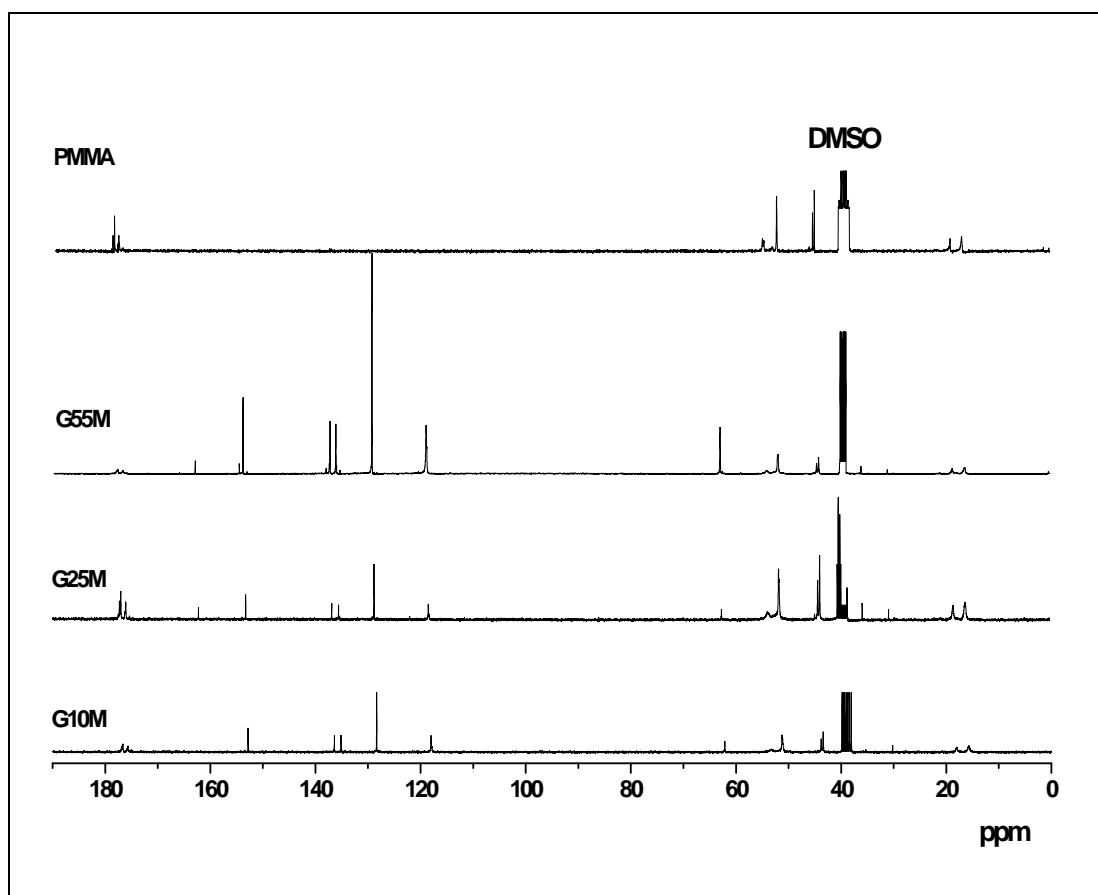


Figure 4.31: ^{13}C -NMR spectra of PMMA-g-UM1 copolymers and PMMA homopolymer dissolved in DMSO. (See Table 4.10 for explanation of G10M, G25M and G55M codes.)

(b) PnBMA-g-UM1 copolymers

Figure 4.32 shows a comparison of the ^{13}C -NMR spectra of PnBMA-g-UM1 copolymers and PnBMA homopolymer. New peaks were evident in the graft copolymer spectra. The peaks in

the region between $\delta = 117$ and $\delta = 140$ ppm are mainly attributed to the aromatic carbons of the MDI in the UM1. The peaks at $\delta = 62.5$ ppm originate from methylene carbons of the EG in the UM1. In addition, the ^{13}C -NMR peaks ascribed to the vinylic carbon of the UM1 at $\delta = 127.55$ and $\delta = 131.49$ ppm were observed to have completely disappeared upon copolymerization with n-BMA at all ratios used. This result shows that the UM1 was successfully and totally incorporated into PnBMA-g-UM1 copolymers, and confirms the results that of analysis by FTIR and SEC.

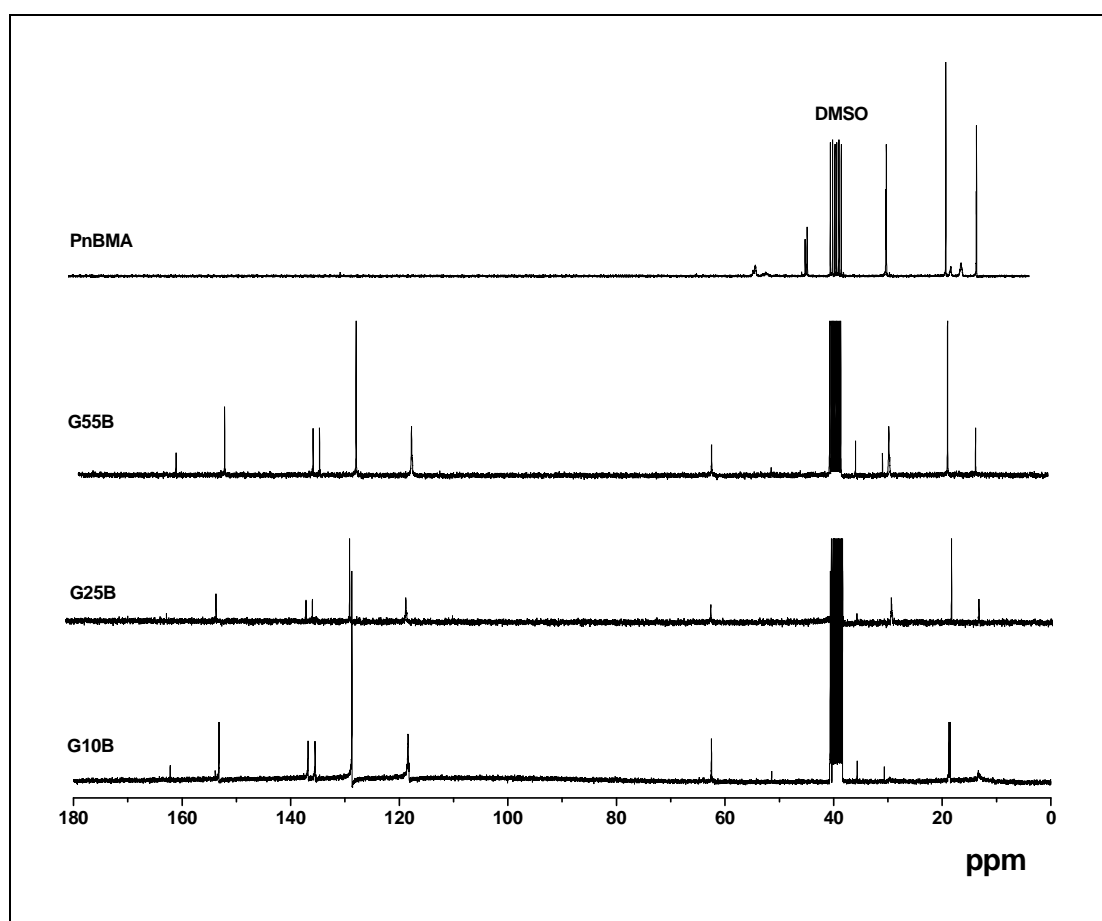


Figure 4.32: ^{13}C -NMR spectra of PnBMA-g-UM1 copolymers and PnBMA homopolymer dissolved in DMSO. (See Table 4.10 for explanation of G10B, G25B and G55B codes.)

4.5.3.7 ^1H -NMR analysis

Analysis of graft copolymers after extraction also confirmed the presence of the branched UM1 in the copolymers, and allowed the calculation of the percentage of UM1 incorporated into the graft copolymers.

(a) PMMA-g-UM1 copolymers

Figure 4.33 shows a typical ^1H -NMR spectrum of the graft copolymer, after extraction of the unreacted macromonomer, and PMMA homopolymer. The ^1H -NMR spectrum of PMMA-g-UM1 shows a characteristic peak at $\delta = 3.6$ ppm, which originates from the methoxy group ($\text{CH}_3\text{-O}$) of the methyl methacrylate. The appearance of peaks of MDI in regions of $\delta = 6.2$

ppm and $\delta = 7.5$ ppm which originate from the aromatic ring of UM1 indicates the presence of UM1 branches in the copolymer after extraction. In addition, the $^1\text{H-NMR}$ peaks ascribed to the vinylic protons of the UM1 at $\delta = 5.95$ ppm, $\delta = 6.25$ ppm and $\delta = 6.47$ ppm were observed to have disappeared upon copolymerization with MMA. These results show that the UM1 was successfully incorporated into PMMA-g-UM1 copolymers and confirm the FTIR, $^{13}\text{C-NMR}$ and SEC results.

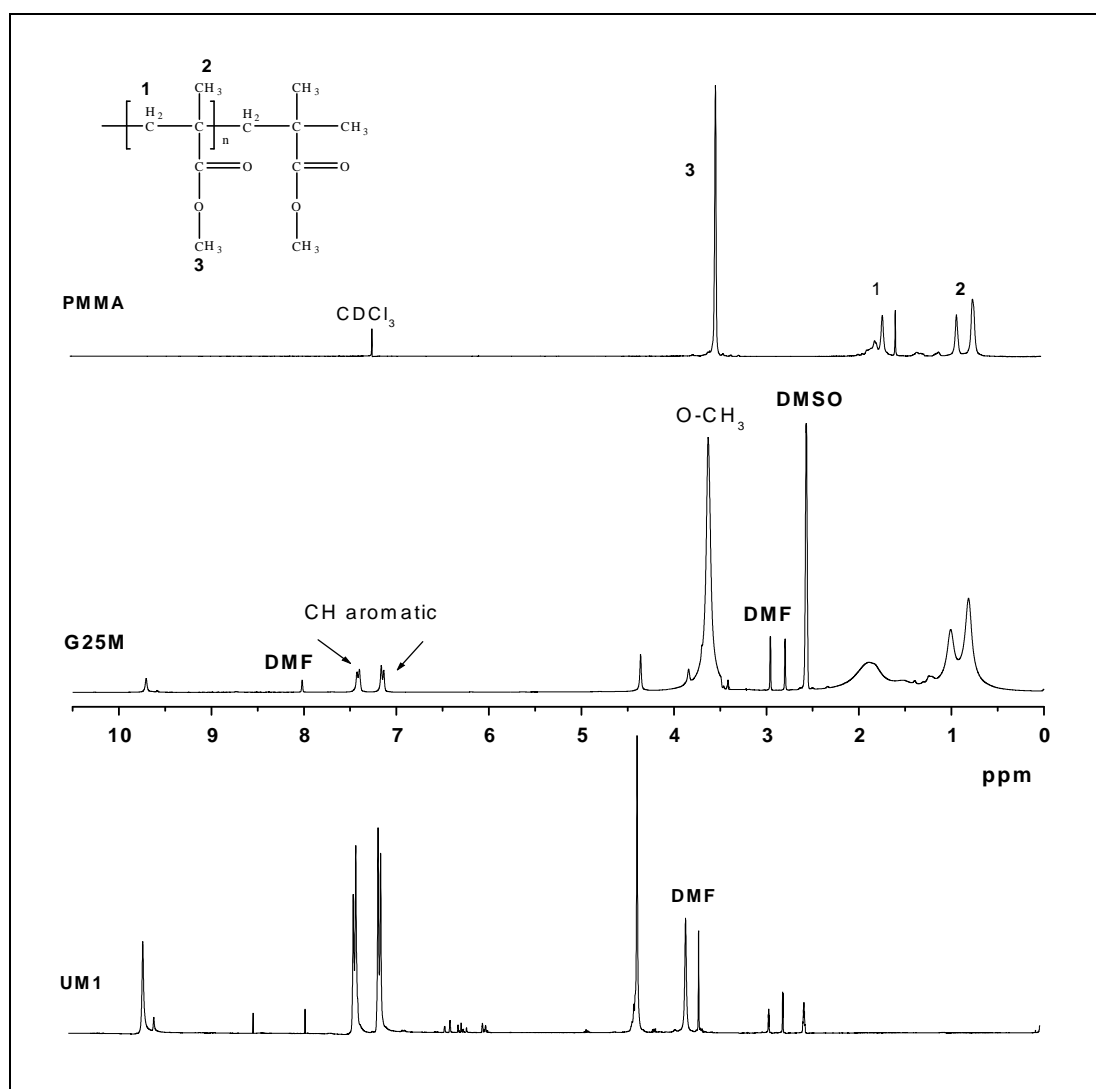


Figure 4.33: $^1\text{H-NMR}$ spectra of PMMA-g-UM1 copolymer, PMMA homopolymer and UM1 dissolved in DMSO.

(b) PnBMA-g-UM1 copolymers

Figure 4.34 shows a typical $^1\text{H-NMR}$ spectrum of the graft copolymer, after extraction of the unreacted macromonomer and PnBMA homopolymer. The spectrum of PnBMA-g-UM1 shows a characteristic peak at $\delta = 3.6$ ppm which originates from the methylene oxy group ($\text{CH}_2\text{-O}$) of the methyl methacrylate. The appearance of peaks of MDI in regions at $\delta = 6.2$ ppm and $\delta = 7.5$ ppm, which originate from aromatic ring of UM1, indicates the presence of UM1 branches in the copolymer after extraction. In addition, the $^1\text{H-NMR}$ peaks ascribed to

the vinylic protons of the UM1 $\delta = 5.95$ ppm, $\delta = 6.25$ ppm and $\delta = 6.47$ ppm were observed to have disappeared upon copolymerization with n-BMA. These results show that the UM1 was successfully incorporated into PnBMA-g-UM1 copolymers and confirm FTIR, ^{13}C -NMR and SEC results.

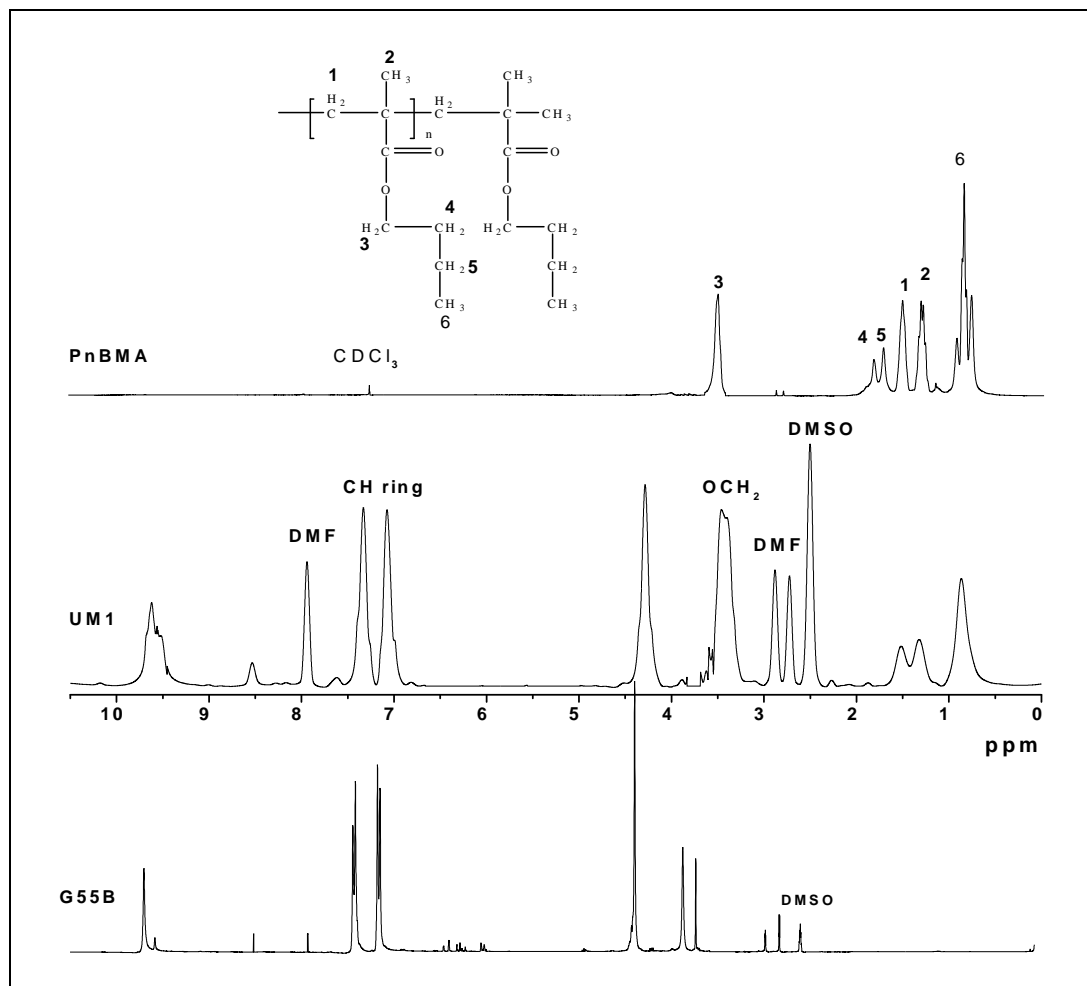


Figure 4.34: ^1H -NMR spectra of PnBMA-g-UM1 copolymer, PnBMA homopolymer and UM1 dissolved in DMSO.

(c) Determination of the UM1 percentage in the graft copolymers, using ^1H -NMR

The percentages of UM1 that were incorporated into the graft copolymers were determined from the ^1H -NMR spectra of each copolymer by the integration of the peaks for the methoxy group (at $\delta = 3.6$ ppm) for the PMMA (backbone) or methyleneoxy group for the PnBMA (backbone) versus the protons of the aromatic ring (at $\delta = 7.08$ and 7.29 ppm) of the UM1(branch),^{42,43} taking into account the number of protons in each peak.

$$UM1\% = \left[\frac{\frac{\delta_{ring}}{(N_{ring} * (n + 1))}}{\frac{\delta_{ring}}{(N_{ring} * (n + 1))} + \frac{\delta_{CH_3O}}{N_{CH_3O}}} \right] \times 100 \quad (4.2)$$

$$UM1\% = \left[\frac{\delta_{ring} / (N_{ring} * (n + 1))}{\delta_{ring} / (N_{ring} * (n + 1)) + \delta_{CH_2O} / N_{CH_2O}} \right] \times 100 \quad (4.3)$$

where UM1 % is the percentage of UM1 which was incorporated into graft copolymers.

δ_{ring} , δ_{CH_3O} and δ_{CH_2O} are the integration intensities of the aromatic ring, CH₃O and CH₂O protons.

N_{ring} , N_{CH_3O} and N_{CH_2O} are the number of protons in each group.

n is the average urethane macromonomer chain length equal to 4 as calculated using ¹H-NMR (see Section 4.5.1.3.)

Table 4.14 shows a summary of the graft copolymers synthesized and the corresponding mol % and wt % of UM2 incorporated into graft copolymers.

Table 4.14: Percentage UM1 incorporated into graft copolymers, as determined by ¹H-NMR

	Sample code	UM1 feed ratio (wt %)	Integration of CH ₃ O protons	Integration of aromatic ring protons	UM1 incorporated into copolymers (mol %)	UM1 incorporated into copolymers (wt %) <small>(Mw of UM1 by ¹H-NMR=1646 g/mol)</small>	UM1 incorporated into copolymers (wt %) <small>(Mw of UM1 by SEC=2218 g/mol)</small>
PMMA-g-UM1	G10M	10	1	0.061	0.44	4.26	6.91
	G25M	25	1	0.192	1.47	19.80	24.81
	G55M	55	1	0.687	4.96	40.44	47.57
			Integration of CH ₂ O protons	Integration of aromatic ring protons			
PnBMA-g-UM1	G10B	10	1	0.094	0.47	4.16	4.49
	G25B	25	1	0.400	1.96	18.81	24.65
	G55B	55	1	0.851	4.08	42.55	49.70

The results in Table 4.14 shows that the percentage of UM1 incorporated into both PMMA-g-UM1 and PnBMA-g-UM1 copolymers increased as the quantities of UM1 increased during graft copolymerization. The UM1 content in the graft copolymers, as determined by ¹H-NMR, was 4.26-40.44 by weight for PMMA-g-UM1 and 4.16-42.55 by weight for PnBMA-g-UM1. These results are close to the results that were determined by UV/Vis and FTIR using calibration curves.

4.5.4 Thermal and mechanical analysis

4.5.4.1 Thermogravimetric analysis (TGA)

Many different techniques have been used to study the thermal degradation of polymers, including pyrolysis mass spectroscopy and thermal volatilization analysis,⁴⁴ However, TGA analysis is the most widely used to investigate the thermal decomposition of a polymer.^{45,46} TGA analysis of dried samples was carried out to investigate the thermal stability of UM1 and methacrylate urethane graft copolymers.

(a) Thermal stability of urethane macromonomers (UM1)

The dominant factors that have an effect on the thermal stability of a polymer are the atomic bonding in the main and graft chains (primary and resonance bonding) and the environment of the given groups.⁴⁷ In a complex compound like PUs, the onset of degradation is governed by the weakest link in the chain, PUs with different backbones have different thermal stabilities.

Segmented PU materials are generally not very thermally stable, especially above their softening temperatures. The ester-based polyurethanes generally exhibit better thermal and oxidative stabilities than ether-based PUs do. Several studies have reported the results of the thermal degradation of ester- and ether-based thermoplastic polyurethanes (TPUs) carried out under vacuum, in air and nitrogen.⁴⁸⁻⁵⁰ The thermal degradation of PUs is very complicated. It has been suggested that PUs degrade by a combination of three independent pathways: (1) dissociation to the original diol and isocyanate; (2) formation of a primary amine, an alkene, and carbon dioxide; (3) formation of a secondary amine and carbon dioxide.⁵¹⁻⁵³

The thermal decomposition patterns of the UM1 were determined by TGA in a nitrogen atmosphere. A typical thermogram and derivative curve (DTG) are shown in Figure 4.35.

The three-stage thermal degradation of UM1 is noted. The first stage of degradation takes place in the temperature range 250–320 °C, and presents a maximum weight loss at 290 °C. The weight loss in this step will be due to pyrolysis of the urethane group, with carbon dioxide as the first volatile released.⁵⁴ The second stage of degradation takes place in the temperature range 320–500 °C, and presents a maximum weight loss at 364 °C. This is could be due to thermal decomposition of the aromatic residue of the UM1. In this step the weight loss may be due to liberation of HCN, nitriles and some aromatic carbons.⁵⁴ This stage leads to the third stage which ends with the loss of all volatile fractions and a mass loss that does not change much after 600 °C. This reduces the weight to 0% and will involve the loss of most aromatic type structure remaining.

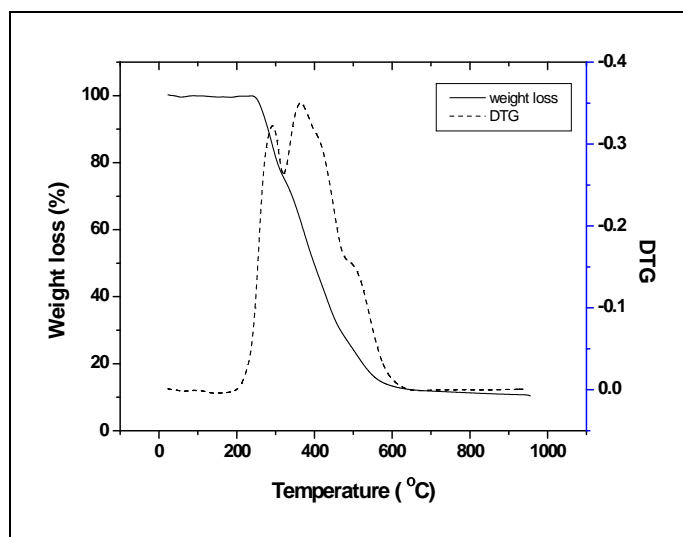


Figure 4.35: TGA thermogram of UM1 and its derivative curve.

(b) PMMA-g-UM1 copolymers

Polyacrylates are extremely resistant to oxygen, and only decompose very slowly under extreme conditions such as high temperature and in an oxygen-rich atmosphere. When heated, polyacrylates depolymerizes to monomers much less readily than the corresponding polymethacrylates do.⁵⁵ Polymethylacrylate decomposes at 290–400 °C to produce methanol and carbon dioxide. Volatile decomposition products of polybutylacrylate at 400–500 °C are butane, butanol and carbon dioxide.⁵⁶

Primary TGA curves for MMA copolymerized with different amounts of UM1, ranging from 0% to 55% by weight (according to MMA) is shown in Figure 4.36(a). The decomposition patterns for all the graft copolymers are similar. There was a slight improvement in thermal stability as the amount of UM1 increased. This might be due to optimum morphological interaction between PMMA and the UM1 segments. In other words, the graft copolymers degraded at a slower rate as the amount of UM1 incorporated in the graft copolymers was increased.

PMMA homopolymers prepared by free radical polymerization are known to begin degrading at approximately 175 °C. The degradation originates from the formation of sterically hindered linkages that result from head-to-head coupling during polymerization.^{57,58} Unsaturated end groups that form by disproportionation during polymerization begin to degrade at 225 °C, while the other possible saturated end groups are thermally stable in a nitrogen atmosphere up to 400 °C.⁵⁹ After formation of a polymeric radical, depolymerization occurs of PMMA to form the MMA monomer.⁶⁰

Figure 4.36(b) shows that PMMA degrades in three steps, and is virtually completely degraded by 465 °C. The first stage of degradation occurs in the temperature range 150–220 °C, which is attributed to cleavage of the weak links, e.g. head-to-head linkages.⁶¹ The second stage of degradation takes place in the temperature range 250–340 °C, and is attributed to a larger mass loss due to end chain unsaturation.⁵⁸ The third stage of degradation occurs in the range 340–465 °C, and which accounts for the majority of the degradation, is due to random scission.⁵⁸

The weight loss obtained from TGA thermograms for the various degradation steps, and the ash content are given in Table 4.15. Figure 4.36(c)-(f) revealed a three-step thermal degradation process for all PMMA-g-UM1 samples. The first stage of degradation took place in the temperature range 200–310 °C, with a weight loss of 4–12%. As the percentage of UM1 in the PMMA-g-UM1 increased, the onset decomposition temperature (T_i) shifted towards higher temperature.⁶² The weight loss during the first stage of degradation was found to decrease with the increase of the UM1 content in PMMA-g-UM1.

The second stage of the degradation of PMMA-g-UM1 took place in the temperature range 260–390 °C, with a weight loss of 24–42%. As the temperature ranges of the first and second stages of PMMA-g-UM1 fall in the temperature range of PMMA degradation, complete degradation of PMMA will occur in these two stages, with the weak links of UM1. This was evident from the fact that, as the composition of the PMMA increased in the PMMA-g-UM1, the net weight loss from steps I and II also increased.

The third stages of degradation of PMMA-g-UM1 took place in the temperature range 360–550 °C, with a weight loss of 61–64%. The third stage of thermal degradation of PMMA-g-UM1 and the second stage of degradation of UM1 lie in the same temperature range. The weight loss in this step is due to the aromatic residue of the UM1 in the PMMA-g-UM1. The above results are supported by the fact that as the UM1 content in the PMMA-g-UM1 decreased, the weight loss in this step also decreased.

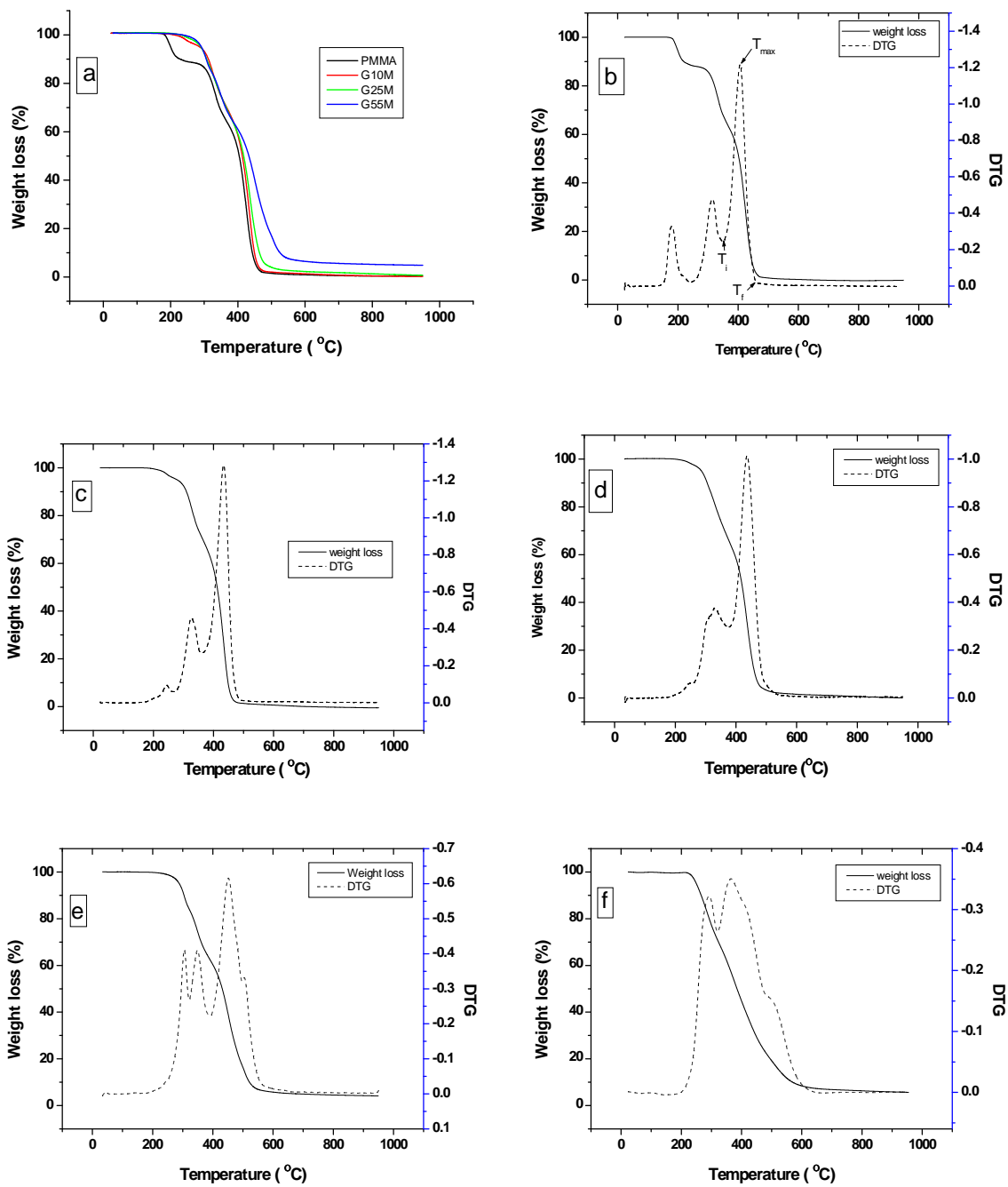


Figure 4.36: TGA thermograms: (a) TGA curves of MMA copolymerized with different amounts of UM1, (b) to (f) TGA thermograms and their derivative curves for 0/100, 10/90, 25/75, 55/45 and 100/0 UM1/MMA copolymers, respectively.

Table 4.15: Thermal data obtained from TGA scans for PMMA-g-UM1

Composition of UM1/PMMA (wt/wt)	Degradation stage	Temperature range (°C)			Weight loss (%)
		T _i	T _{max}	T _f	
0/100	1	150	181	220	12.4
	2	250	313	340	20.4
	3	340	406	465	67.0
	ash				0.4
10/90	1	200	244	268	4.4
	2	268	340	360	41.4
	3	360	420	480	61.4
	ash				1.6
25/75	1	205	304	310	4.4
	2	260	340	390	28.2
	3	390	448	550	64.1
	ash				4.9
55/45	1	260	304	310	12.0
	2	310	340	390	17.4
	3	390	451	550	64.9
	ash				6.1
100/0	1	220	292	300	24
	2	300	390	500	60
	3	500	520	570	8.7
	ash				4.5

(c) PnBMA-g-UM1 copolymers

Primary TGA curves of PnBMA homopolymer and PnBMA-g-UM1 graft copolymers are shown in Figure 4.37. The decomposition patterns of all the graft copolymers samples were similar. There was however a slight improvement in the thermal stability as the amount of UM1 in the graft copolymer increased, which might be due to better morphological interaction of the PnBMA by UM1 nanoinclusion (see TEM results, Section 4.5.5). The graft copolymers degraded at a slower rate as the amount of UM1 incorporated in the graft copolymers was increased.

The thermal degradation of PnBMA is well understood, and involves of three steps. In the first step it is attributed to the cleavage of weak links, i.e. head-to-head linkages. In the second step there is a larger mass loss due to chain end unsaturation. In the final step, which accounts for the majority of the degradation, there is random scission.

Figure 4.37(b) shows that PnBMA is degraded in three steps, and is virtually completely decomposed by 465 °C. The first stage of degradation occurs in the temperature range 200–275 °C, which is attributed to cleavage of the weak links, e.g. head-to-head linkages.⁶¹ The second stage of the degradation takes place in the temperature range 275–351 °C, which is attributed to a larger mass loss due to end chain unsaturation⁵⁸. The third stage of degradation occurs in the range 351–468 °C, and which accounts for the majority of the degradation, and is due to random scission.⁵⁸

The weight loss obtained from TGA thermograms for the various degradation steps, and the ash content, are given in Table 4.16. Figure 4.37 (c)-(f) revealed a three-step thermal degradation process for all PnBMA-g-UM1 samples. The first stage of degradation took place in the temperature range 200–280 °C, with a weight loss of 1–13%. As the percentage of UM1 in the PnBMA-g-UM1 is increased, the onset decomposition temperature (T_i) shifted towards higher temperature.⁶² The weight loss during the first stage of degradation was found to decrease with the increase of the UM1 content in PnBMA-g-UM1.

The second stage of the degradation of PnBMA-g-UM1 took place in the temperature range 280–350 °C, with a weight loss of 27–59%. As the temperature range of the first and second stages of degradations PMMA-g-UM1 falls in the temperature range of PnBMA degradation. complete degradation of PMMA will occur in these two stages, with the weak links in UM1. This was evident from the fact that, as the composition of the PnBMA increased in the PnBMA-g-UM1, the net weight loss from steps I and II also increased.

The third stages of degradation of PnBMA-g-UM1 took place in the temperature range 300–540 °C, with a weight loss of 17–64%. The third stage of thermal degradation of PnBMA-g-UM1 and the second stage of degradation of UM1 lie in the same temperature range. The weight loss in this step was mostly due to the PnBMA in the PnBMA-g-UM1. The above results are supported by the fact that as the UM1 content in the PnBMA-g-UM1 increased weight loss in this step decreased.

Table 4.16: Thermal data obtained from TGA scans of PnBMA-g-UM1

Composition of UM1/PnBMA (wt/wt)	Degradation stages	Temperature range (°C)			Weight loss (%)
		T _i	T _{max}	T _f	
0/100	1	200	255	275	7.0
	2	275	325	351	28.4
	3	351	402	491	64.2
	ash				0.3
10/90	1	201	218	248	3.2
	2	248	326	351	31.3
	3	351	400	538	63.3
	ash				2.7
25/75	1	205	241	260	2.6
	2	260	355	383	27.0
	3	383	429	567	64.1
	ash				4.9
55/45	1	213	299	322	12.0
	2	322	437	474	59.2
	3	374	502	600	19.0
	ash				8.2
100/0	1	220	292	300	24.0
	2	300	390	500	60.0
	3	500	520	570	8.7
	ash				4.5

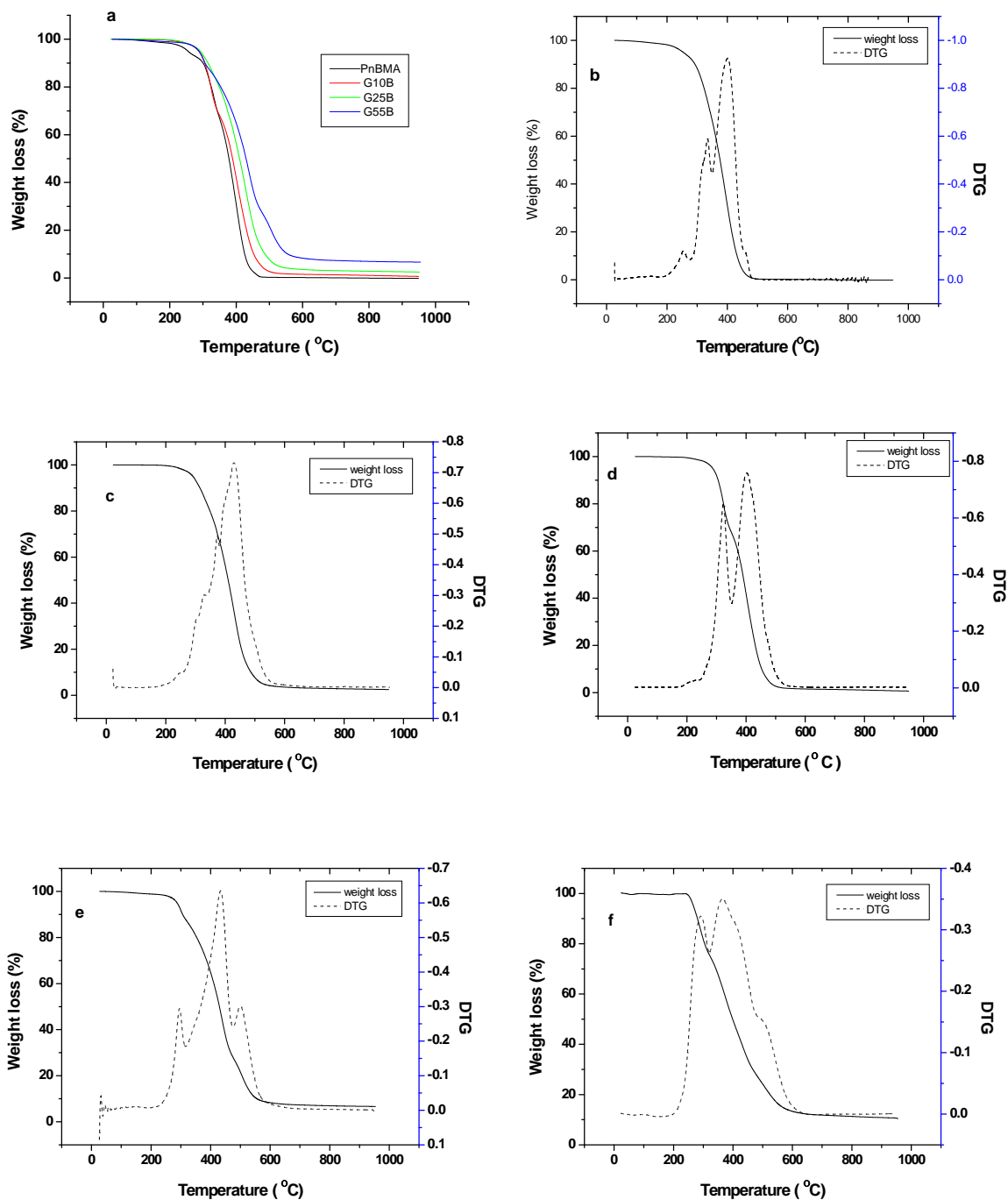


Figure 4.37: TGA thermograms: (a) TGA curves of n-BMA copolymerized with different amount of UM1, (b) to (f) TGA thermograms and their derivative curves for 0/100, 10/90, 25/75, 55/45 and 100/0 UM1/ n-BMA copolymers, respectively.

4.5.4.2 Dynamical mechanical analysis (DMA)

Dynamical mechanical analysis is a commonly used technique to study the mechanical and thermal properties of a polymer, largely due to its high sensitivity to different molecular rheology events. DMA provides information on transition temperatures, such as the glass-transition temperature (T_g), as well as the degree of phase separation and mechanical behaviour, such as loss (E'') and storage (E') moduli. DMA analysis is performed using a

stainless steel pan to support the material in the DMA apparatus and to enable turning and heating of the samples until melting without destroying the sample geometry or contaminating the instrument. DMA offers the possibility to follow the change in both elastic and viscous properties of a material as a function of temperature and the morphology of the polymers.⁶³

The structural differences between the soft and hard sections in graft copolymers normally result in phase separation. The degree of phase separation affects the properties of the copolymer.^{19, 64-67} Phase separated domains can be decreased by increasing the compatibility between the hard and soft segments.

The dynamic mechanical behaviour of copolymers depends on the miscibility of the polymer pair. The compatibility between pairs of polymers can be characterized by dynamic mechanical analysis. For incompatible copolymers the damping ($\tan \delta$) temperature curve shows the presence of two ($\tan \delta$) peaks corresponding to the glass transitions of the individual polymers, whereas in highly compatible copolymers only a single peak that is located in between the transition temperatures of the pure polymers is observed.⁶⁸ In the case of partially compatible copolymers, two broad separate peaks corresponding to the individual polymer components, or one broad peak, are observed but with their positions shifted closer to the single (compatible) peak, depending on the copolymers composition and the influence of their microstructures.⁶⁹⁻⁷¹

Occurrence of microphase separation depends on many factors, including segmental polarity difference, segmental length, and crystallizability of either segment, intra- and intersegment interactions such as hydrogen bonding, overall composition, and molecular weight. The elasticity, toughness, and other physical properties of copolymers are largely determined by the size, crystallinity, and interconnectivity of the hard domains as well as the nature of the domain interface and the mixing of hard segments in the soft segment phase.⁷²⁻⁷⁸

From a molecular standpoint, the glass transition temperature is viewed as the temperature above which large-scale chain segments develop mobility that permits conformational rearrangements of the chain backbones.⁴⁷ There are several factors that affect the mobility of a polymer chain or backbone flexibility such as pendent groups like “fish hooks”, and “boat anchors”, as pendent groups like “elbow room”.⁷⁹ The more flexible the backbone chain the lower its T_g value will be.

In this study DMA analysis was used firstly to determine the T_g of graft copolymer samples, secondly to investigate the phase separation between urethane and acrylate segments of the

synthesized methacrylate-g-urethane copolymers, and thirdly to study mechanical behaviour such as loss and storage modulus.

(a) PMMA-g-UM1 copolymers

The temperature dependence of DMA of graft copolymers as a function of composition yields particular insight into the structure of graft copolymers. The DMA results in Figures 4.38 and 4.39 clearly show that two-phase separations took place in the PMMA-g-UM1 copolymeric system; this two-phase character is seen by the appearance of two $\tan \delta$ peaks, which indicate to microphase separation.

PMMA has a glass transition, resulting in a larger change in E' as the material softens from a hard plastic to viscous material, which corresponds to the onset of long range coordinated motion, and the $\tan \delta$ peak exhibits a sharp damping peak. The $\tan \delta$ curve of PMMA (Figure 4.38) shows the start of the peak beginning of at 108 °C due to a transition arising from the transitional motion (All T_g values in this study were measured as onset temperature values.) This corresponds to the T_g of PMMA. At the $\tan \delta$ peak there is optimum energy absorption of the viscoelastic structure with no movement below T_g and very little energy absorption near a T_g .⁸⁰ UM1 shows T_g at 182 °C, as shown by the onset of the $\tan \delta$ peak in Figure 4.38.

Figure 4.38 also shows that the $\tan \delta$ curves of the PMMA-g-UM1 copolymers of the other ratio show two relaxation peaks (T_g), for the PMMA and UM1. These results show that the PMMA and UM1 segments in PMMA-g-UM1 copolymers are nano- or microphase separated. This could be due to a segmental polarity difference between the PMMA and UM1 segments. The T_g values (T_g defined here as to the onset of the peak of $\tan \delta$) of all the synthesized PMMA-g-UM1 copolymers are summarized in Table 4.18.

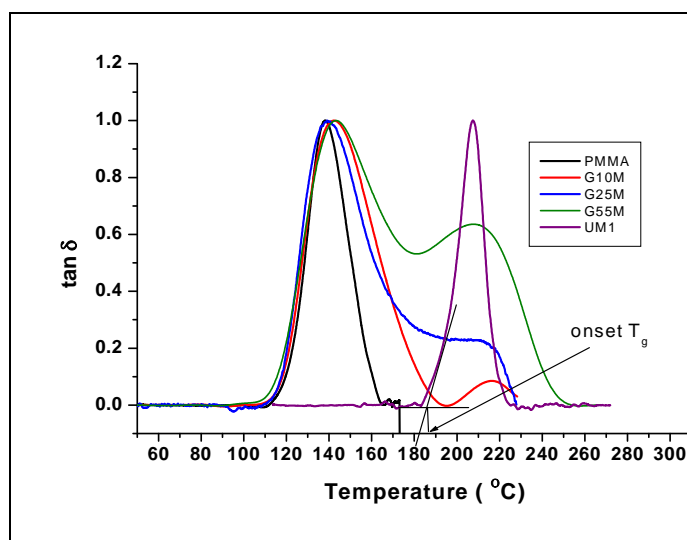


Figure 4.38: Tan δ traces of PMMA, UM1 and the PMMA-g-UM1 copolymers.

Figure 4.39 is an example showing the loss modulus curve for the PMMA-g-UM1 copolymer that contains 40.44 wt % UM1 (according to $^1\text{H-NMR}$ calculations), which shows the presence of loss maxima at 120 °C and 210 °C, respectively, for PMMA and UM1. These results confirm nano- or microphase separation between PMMA and UM1 segments.

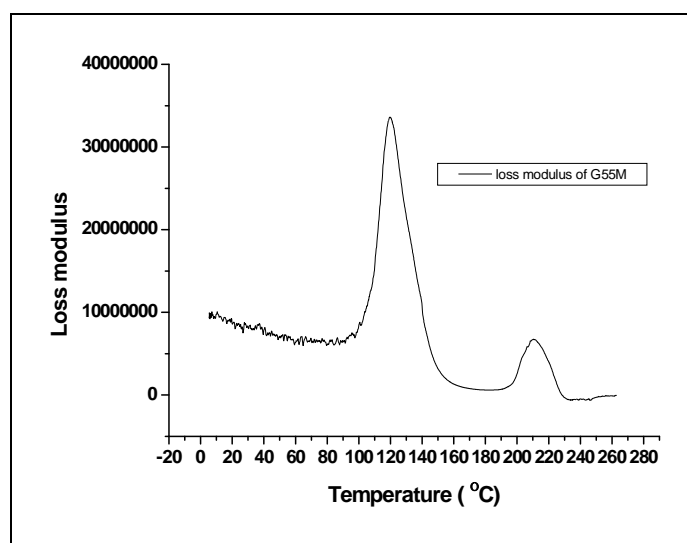


Figure 4.39: Loss modulus of the PMMA-g-UM1 copolymer containing 40.44 wt % UM1.

Figure 4.40 shows the storage modulus (E') curves of the PMMA and PMMA-g-UM1 copolymer which show a great change in modulus with increasing temperature. The decrease in signifies changes in the elastic contribution to the properties. There is one notable change observed in the storage modulus (E') curve at around 110 °C. This change corresponds to an increase in the free volume of the sample with temperature, which enables segmental motion of the PMMA chain backbone, and this change is referred to as the glass transition (T_g). The T_g which was also observed in the tan δ curve Figure 4.38. Also seen in this figure is that the PMMA-g-UM1 copolymers show dramatic increases in modulus as the

amount of UM1 incorporated into graft copolymers increases (Figure 4.40). For example, the sample containing 40.44 wt % UM1 (according to $^1\text{H-NMR}$ calculations) shows a storage modulus about 4 times that of PMMA. Overall DMA analysis reveals that the PMMA-g-UM1 copolymers are much stiffer and can withstand higher temperatures compared to the PMMA the homopolymer.

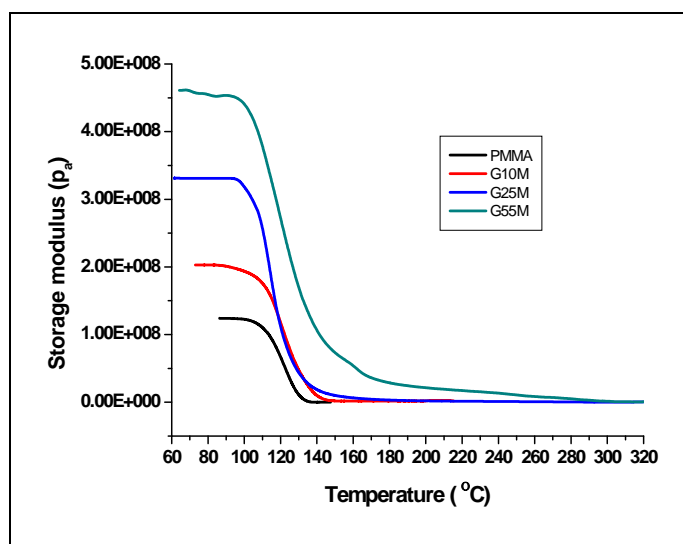


Figure 4.40: Storage modulus traces of PMMA and PMMA-g-UM1 copolymers.

(b) PnBMA-g-UM1 copolymers

Figure 4.41 displays the $\tan \delta$ and Figure 4.42 storage modulus (E') curves as a function of temperature for PnBMA homopolymer and PnBMA-g-UM1 copolymers that were synthesized in this study. The $\tan \delta$ curve shows a peak starting at 25-35 °C due to the a transition arising from the segmental motion (T_g is defined here as to the onset peak of $\tan \delta$). This corresponds to the glass transition temperature (T_g) of the PnBMA homopolymer. On other hand, UM1 shows a glass transition temperature at 182 °C, as shown previously by the $\tan \delta$ peak in Figure 4.38.

The $\tan \delta$ curves of PnBMA-g-UM1 copolymer show two relaxations peaks (T_g) of the PnBMA and UM1 segments close to 34 °C and 182 °C, respectively. These results show that PnBMA and UM1 segments in PnBMA-g-UM1 copolymers are microphase separated, which is due to the degree of mixing brought about by the segmental polarity difference between PnBMA and UM1 segments and segmental length of branching of the graft copolymers (UM1). The T_g values of all the synthesized PnBMA-g-UM1 copolymers are summarized in Table 4.17.

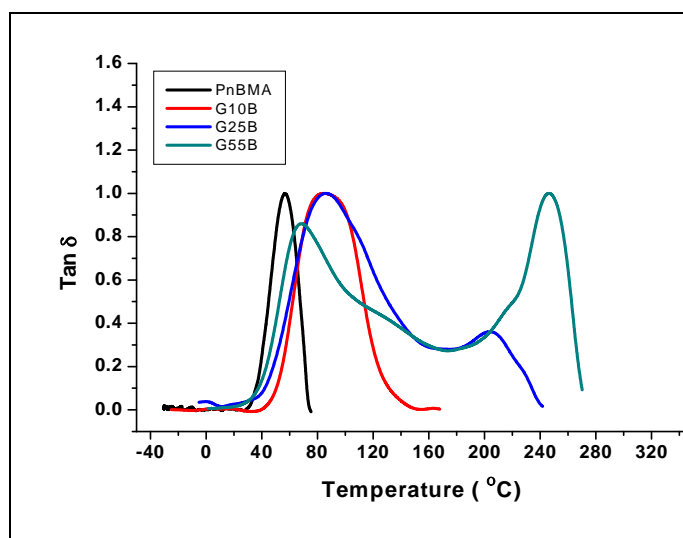


Figure 4.41: Tan δ traces of PnBMA and the PnBMA-g-UM1 copolymers.

Figure 4.42 shows the storage modulus (E') curves of PnBMA and PnBMA-g-UM1 copolymers, which show a great change in modulus with increasing temperature; the decrease signifies changes in the elastic contribution to the properties. There is one notable change observed in the storage modulus (E') curve at around 25 °C. This change corresponds to an increase in the free volume of the sample with temperature, which enables segmental motions of the PnBMA chain backbone and this change referred to as the glass transition (T_g). It is also observed that the PnBMA-g-UM1 copolymers show a dramatic increases in modulus i.e. more than doubling in modulus as the amount of UM1 incorporated into graft copolymers is increased (Figure 4.42). For example, the sample containing 42.55 wt % UM1 (according to calculations) shows a storage modulus about 2.5 times that of PnBMA. Overall, DMA analysis reveals that the PnBMA-g-UM1 copolymers are much stiffer and can withstand higher temperatures compared to the PnBMA homopolymer. Since the two phases are separate (two tan δ peaks) there must be an anchoring of the PnBMA segment by closely packed hard segment (tan δ , 186 °C) which, according to being tethered and of limited length, must mean a second phase which is nano in size. But not all the particles are the same size as there is a spread of the graft length made by polyaddition.

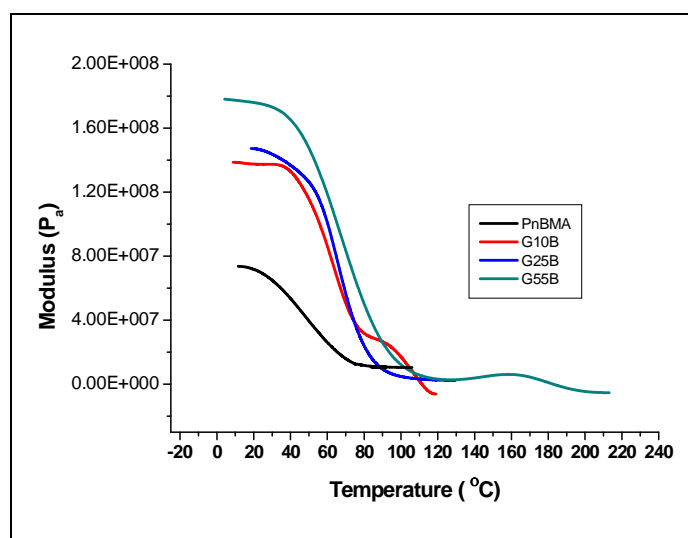


Figure 4.42: Storage modulus traces of PnBMA and PnBMA-g-UM1 copolymers.

Table 4.17: DMA results for PMMA-g-UM1 and PnBMA-g-UM1 copolymers at varying UM1 ratio in the polymerization feed

	Sample code	UM1 feed ratio (wt %)	UM1 incorporated into copolymers as calculated by ¹ H-NMR (wt %)	T _g (°C) at onset	T (°C) at max peak height	E'X10 ⁸ (Pa)
PMMA-g-UM2	PMMA	0	-	108	133	1.3
	G10M	10	5.3	110,195	141,216	2.1
	G25M	25	19.8	112,189	139,212	3.3
	G55M	55	40.4	109,185	135,209	4.7
PnBMA-g-UM2	PnBMA	0	-	34	56	0.8
	G10B	10	4.2	42	68	1.3
	G25B	25	18.8	36,184	184,220	1.4
	G55B	55	32.6	34,186	63,235	1.8

4.5.4.3 Differential Scanning Calorimetry (DSC)

Differential scanning calorimetry (DSC) is a commonly used tool to determining molecular organization changes, such as phase separation and glass transition. As mentioned earlier in Chapter 2, both the mechanical and thermal properties of the graft copolymer can be affected dramatically by the degree of phase mixing. Interaction between the soft and hard segments can increase the a glass transition temperature (T_g) of the soft segment and decrease the T_g of the hard segments. The T_g of the graft copolymer and the macromonomers were determined using DSC. Table 4.18 shows T_g for all graft copolymers. UM1 shows a glass transition temperature (T_g) at 174 °C which is considerably higher than

the T_g of PMMA (110 °C) and the T_g of PnBMA (44 °C).

The DSC results of both the PMMA-g-UM1 and PnBMA-g-UM1 copolymers, especially with high UM1 content, show the presence of two T_g values, that indicates the formation of phase separation, where the UM1 region aggregates separately from methyl methacrylate and from normal butyl methacrylate. The phase separation was obtained also with low macromonomer content. These results correspond well with those results measured by DMA analysis (Table 4.18). From the thermal properties of the grafts, the T_g is only slightly affected by the macromonomer content.

Table 4.18: DSC results for PMMA-g-UM1 and PnBMA-g-UM1 copolymers at varying UM1 ratio in the polymerization feed

	Sample code	UM1 feed ratio (wt %)	UM1 incorporated into copolymers as calculated by $^1\text{H-NMR}$ (wt %)	T_{g1} (°C)	T_{g2} (°C)
PMMA-g-UM2	PMMA	0	-	110	-
	G10M	10	5.26	121	183
	G25M	25	19.80	124	180
	G55M	55	40.43	116	171
PnBMA-g-UM2	PnBMA	0	-	34	-
	G10B	10	4.16	34	-
	G25B	25	18.81	38	176
	G55B	55	32.55	36	173

Figure 4.43 and Figure 4.44 are examples of DSC results for PMMA-g-UM1 and PnBMA-g-UM1 copolymers, respectively. The two T_g values that appeared in the graft copolymers are almost the same as values for PMMA and UM1 (Figure 4.44) or PnBMA and UM1 (Figure 4.44). This provides additional evidence for the incorporation of UM1 into the graft copolymers, and their total phase separation.

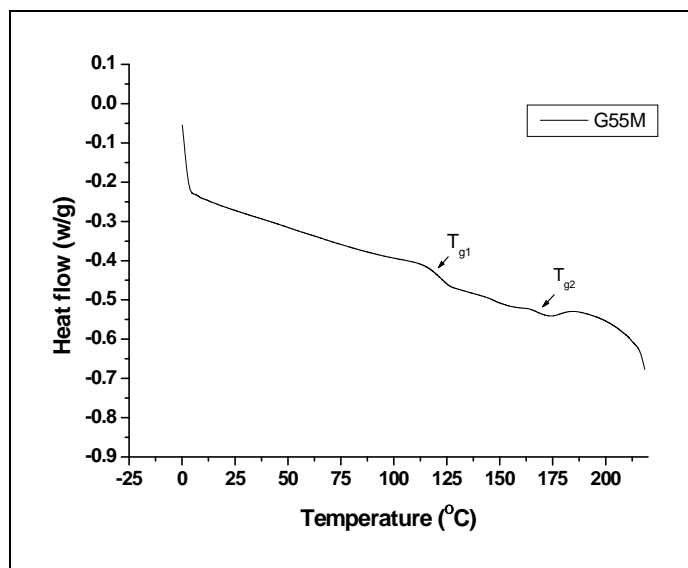


Figure 4.43: DSC of PMMA-g-UM1 copolymer containing 40.44 wt % UM1.

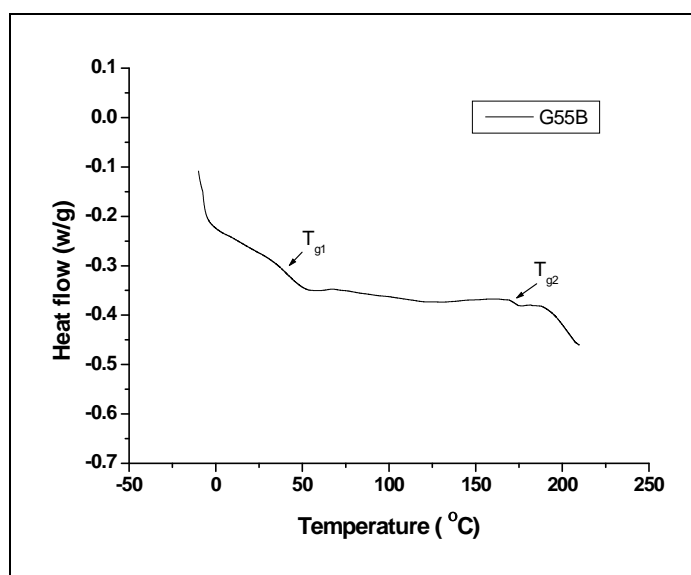


Figure 4.44: DSC of PnBMA-g-UM1 copolymer containing 42.55 wt % UM1.

4.5.5 Transmission electron microscopy

The presence of a two-phase nature was strongly indicated from the DSC and DMA results given above. In order to confirm this hypothesis more fully, transmission electron microscopy was conducted. TEM images in Figures 5.45 and 5.46, show evidence of phase segregated morphologies for both graft copolymers PMMA-g-UM1 and PnBMA-g-UM1. In the images the difference in the electron densities of the PMMA, PnBMA and UM1 components in the graft copolymer allow the various components to be distinguished by TEM. UM1 is more electro-dense due to the aromatic backbone and will tend to show darker regions, which appear in the form of spheres. PMMA and PnBMA are less electro dense and appear lighter in the image. The images in Figure 5.44 and 5.45 show evidence of darker and lighter regions, which would suggest phase segregation.

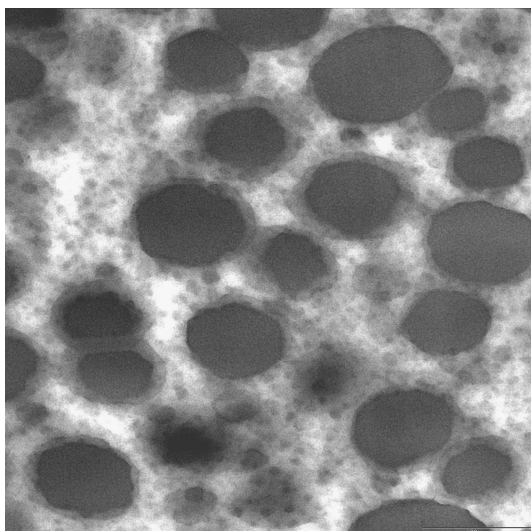


Figure 4.45: A typical TEM image of PMMA-g-UM1 copolymer containing 40.44 wt % UM1 as calculated using $^1\text{H-NMR}$ analysis. The sample was coated with tetroxide. The light regions are soft PMMA domains and the dark regions are hard urethane domains. Bar 100 nm.

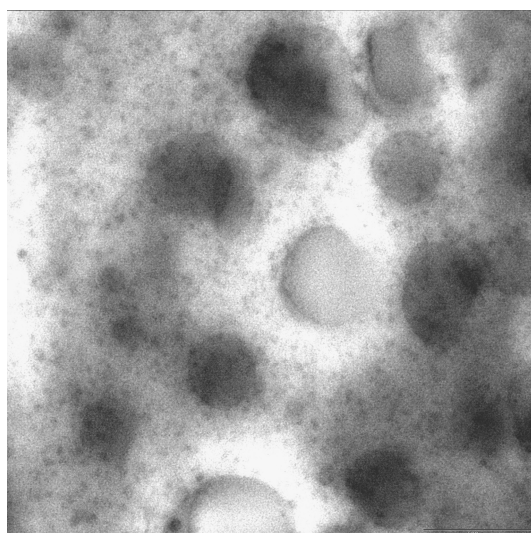


Figure 4.46: A typical TEM image of PnBMA-g-UM1 copolymer containing 42.55 wt % UM1 as calculated using $^1\text{H-NMR}$ analysis. The sample was coated with osmium tetroxide. The light regions are soft PnBMA domains and the dark regions are hard urethane domains. Bar 100nm.

4.6 Conclusions

A novel urethane macromonomer, predominantly monofunctional was successfully synthesized by polyaddition using the prepolymer method and the structure confirmed (using FTIR and MALDI-TOF-MS analysis). This novel urethane macromonomer was then used in solution free-radical copolymerization with MMA and with n-BMA. The existence of the grafted urethane macromonomer with PMMA and PnBMA, respectively was confirmed using FTIR, and SEC (with UV and RI detectors), HPLC, DSC, TEM and DMA. The yield of both graft copolymers decreased as the concentration of the urethane macromonomers in the

copolymerization feed increased. As the concentration of urethane macromonomer in the copolymerization feed increased, more urethane macromonomer was incorporated into the PMMA and PnBMA backbones, and better thermal stability and storage modulus was detected in both PMMA-g-UM1 and PnBMA-g-UM1 copolymers. In most of the graft copolymers a large measure of incompatibility was observed, evident from DSC and DMA results. Two glass transition temperatures, corresponding to the PnBMA or PMMA and UM1 fractions, were found. The result also indicated that PnBMA or PMMA and UM1 moieties exhibited nanophase separation especially at high level incorporation of UM1 into both the respective graft copolymers, as confirmed by DMA, DSC and TEM.

4.7 References

1. Dreyfuss, P.; Quirk., R. P.; Mark, H. F.; Bikales, N. M.; Overberger, C. C.; Menges, G.; Kroschwitz, J. I., *Encyclopedia of Polymer Science and Engineering*, 2nd ed. Wiley-Interscience: New York, 1987; Vol. 7, p 551.
2. Pitsikalis, M.; Pispas, S.; Mays, J.; Hadjichristidis, N. *Adv. Polym. Sci.* **1998**, 1, 135.
3. Ito, K.; Kawaguchi, S. *Adv. Polym. Sci.* **1999**, 142, 129.
4. Burchard, W. *Adv. Polym. Sci.* **1999**, 143, 113.
5. Beyer, F. L.; Gido, S. P.; Buschl, C.; Latrou, H.; Uhrig, D.; Mays, J. W. *Macromolecules* **2000**, 33, 2039.
6. Xenidou, M.; Beyer, F. L.; Hadjichristidis, N.; Gido, S. P.; B.Tan, N. *Macromolecules* **1998**, 31, 7659.
7. Pakula, T. *Macromol. Symp.* **2004**, 214, 307.
8. Harjunalanen, T.; Lahtinen, M. *Eur. Polym. J.* **2003**, 39, 817.
9. Schmitt, F.; Wenning, A.; Weiss, J. *Prog. Org. Coat.* **1998**, 34, 227.
10. Saunders, J.; Frisch, K., *Polyurethane Chemistry, Part I*. Wiley-Interscience: New York, 1962.
11. Renault, B.; Tassaing, T.; Cloutetl, E.; Cramail, H. *J. Polym. Sci. Part A: Polym. Chem.* **2007**, 45, 5649.
12. Ito, K. *Prog. Polym. Sci.* **1998**, 23, 581.
13. Christensen, S. F.; Everland, H.; Hassager, O.; Almdal, K. *Int. J. Adhes.* **1998**, 18, 131.

14. Mori, S.; H.Taziri. *J. Liq. Chromatogr.* **1994**, 17, 305.
15. Cools, P.; Herk, A.; Staal, W.; German, A. *J. Liq. Chromatogr.* **1994**, 17, 3133.
16. Philipsen, H. A.; Klumpermann, B.; German, A. L. *J. Chromatogr. A.* **1996**, 13, 727.
17. Otts, D.; Dutta, S.; Zhang, P.; Smith, O.; Thames, S.; Urban, M. *Polymer* **2004**, 45, 6235.
18. Garrett, J.; Xu, R.; Cho, J.; Runt, J. *Polymer* **2003**, 44, 2711.
19. Kuran, W.; Sobczak, M.; Listos, T.; Debek, C.; Florjanczyk, Z. *Polymer* **2000**, 41, 8531.
20. Dutta, S.; Karak, N. *Prog. Org. Coat.* **2005**, 53, 147.
21. Jayakumar, R.; Nanjundan, S. *Eur. Polym. J.* **2005**, 41, 1623.
22. Vargun, E.; Usanmaz, A. *J. Polym. Sci. Part A: Polym. Chem.* **2005**, 43, 3957.
23. Wang, J.; Lin, M.; Wang, C.; Chu, F. *J. Appl. Polym. Sci.* **2009**, 113, 3757.
24. Alshuiref, A. MSc thesis, University of Stellenbosch, Stellenbosch, December 2006.
25. Hickner, R. A.; Judd, C. I.; Bakke, W. W. *J. Org. Chem.* **1967**, 32, 729.
26. Montaudo, G.; Samperi, F.; Montaudo, M. S. *Prog. Polym. Sci.* **2006**, 31, 277.
27. Ma, C.; Du, Y.; Wang, F.; Wang, H.; Yang, J. *J. Appl. Polym. Sci.* **2002**, 83, 1875.
28. Kim, Y.; Kim, H.; Yoo, J.; Hong, J. *Surf. Coat. Technol.* **2002**, 157, 40.
29. Shim, S. E.; Jung, H.; Lee, K.; Lee, J. M.; Choe, S. *J. Colloid Interface Sci.* **2004**, 279, 464.
30. Wen, T.; Du, Y.; Digar, M. *Eur. Polym. J.* **2002**, 38, 1039.
31. Zhou, P.; Frisch, H. *J. Polym. Sci. Part A: Polym. Chem.* **1992**, 2577.
32. Ma, C.; Du, Y.; Wang, F.; Wang, H.; Yang, J. *J. Appl. Polym. Sci.* **2002**, 83, 962.
33. Arun, R.; Nanjundan, S.; Pakula, T.; Klapper, M. *Eur. Polym. J.* **2004**, 40, 1767.
34. Dzunuzovic, E.; Tasic, S.; Bozic, B.; Babic, D.; Dunjic, B. *Prog. Org. Coat.* **2005**, 52, 136.
35. Asha, S.; Thirumal, M.; Kavitha, A.; Pillai, C. *Eur. Polym. J.* **2005**, 41, 1343.
36. Okamoto, T.; Cooper, L.; Root, W. *Macromolecules* **1992**, 25, 1068.
37. Dzunuzovic, E.; Tasic, S.; Bozic, B.; Babic, D.; Dunjic, B. *Prog. Org. Coat.* **2005**, 52, 136.

38. Tsukahara, Y.; Mizuno, K.; Segawa, A.; Yamashita, Y. *Macromolecules* **1989**, *22*, 1546.
39. Tsukahara, Y.; Tsutsumi, K.; Yamashita, Y.; Shimada, S. *Macromolecules* **1990**, *23*, 5201.
40. Hong, S. C.; Jia, S.; Teodorescu, M.; Kowalewski, T.; K. Matyjaszewski; Gottfried, A. C.; Brookhart, M. *J. Polym. Sci. Part A: Polym. Chem.* **2002**, *40*, 2736.
41. Meijs, G.; Rizzardo, E. *Macromol. Sci. Rev: Macromol. Chem. Phys.* **1990**, *C30*, 305.
42. Al-Muallem, H. A.; Knauss, D. M. *J. Polym. Sci. Part A: Polym. Chem.* **2001**, *39*, 3547.
43. Brink, M.; Pepers, M.; Herk, A.; German, A. *Polym. React. Eng.* **2001**, *9*, 101.
44. Wilkie, C. *Polym. Degrad. Stab.* **1999**, *66*, 301.
45. Chang, T.; Shen, Y.; Chiu, S.; Sy, H. *Polym. Degrad. Stab.* **1995**, *49*, 353.
46. Pticek, A.; Hrnjak-Murgic, Z.; Jelencic, J.; Kovacic, T. *Polym. Degrad. Stab.* **2005**, *90*, 319.
47. Chang, T.; Shen, Y.; Chiu, S.; Sy, H. *Polym. Degrad. Stab.* **1997**, *57*, 7.
48. Petrovic, Z.; Zavargo, Z.; Flynn, J. *J. Appl. Polym. Sci.* **1994**, *51*, 1087.
49. Shieh, Y.; Chen, H.; Liu, K.; Twu, Y. *J. Polym. Sci. Part A: Polym. Chem.* **1999**, *37*, 4126.
50. Pattanayak, A.; Jana, S. *Polym. Degrad. Stab.* **2005**, *46*, 5183.
51. Wang, F. PhD dissertation, Virginia Polytechnic Institute and State University, USA, April 1998.
52. Elvers, B.; Hawkins, S.; Russey, W., *Ullmann's Encyclopedia of Industrial Chemistry*. VCH Publishers: New York, 1993; Vol. B6, p 4.
53. Wilks, E., *Industrial Polymer Handbook*. John Wiley and sons: New York, 1988; Vol. 1, p 578.
54. Herrera, M.; Matuschek, G.; Kettrup, A. *Polym. Degrad. Stab.* **2002**, *78*, 323.
55. Zeng, M.; Zhang, L.; Kennedy, J. *Polymer* **2005**, *60*, 399.
56. Elvers, B.; Hawkins, S.; Schulz, G., *Ullmann's Encyclopedia of Industrial Chemistry*. John Wiley and sons: New York, 1992; Vol. 21A, p 158.

57. Manring, L.; Soguh, D.; Cohen, G. *Macromolecules* **1989**, 22, 4652.
58. Kashiwagi, T.; Inaba, A.; Brown, J.; Hatada, K.; Kitayama, T.; Masuda, E. *Macromolecules* **1986**, 19, 2160.
59. Kashiwagi, T.; Hirata, T.; Brown, J. *Macromolecules* **1985**, 18, 131.
60. Manring, L. *Macromolecules* **1989**, 22, 2673.
61. Holland, B.; Hay, N. *Polym. Degrad. Stab.* **2002**, 77, 435.
62. Goswami, S.; Chakrabarty, D. *J. Appl. Polym. Sci.* **2004**, 93, 2764.
63. Ioan, S.; Grigorescu, G.; Stanciu, A. *Eur. Polym. J.* **2002**, 38, 2295.
64. Sheth, J.; Aneja, A.; Wilkes, G.; Yilgor, E.; Atilla, G.; Yilgor, I.; Beye, F. *Polymer* **2004**, 45, 6919.
65. Zhu, G.; L.Tao. *Eur. Polym. J.* **2005**, 41, 1090.
66. Garrett, J.; Runt, J. *Macromolecules* **2000**, 33, 6353.
67. Hq, A.; Liu, H.; Huang, D.; Guo, S. *Eur. Polym. J.* **2001**, 37, 497.
68. Thomas, S.; George, A. *Eur. Polym. J.* **1992**, 28, 145.
69. Malaika, S.; Kong, W. *Polymer* **2005**, 46, 209.
70. George, S.; Neelakantan, N.; Varughese, K.; Thomas, S. *J. Polym. Sci: Polym. Phys.* **1997**, 35, 2309.
71. Singh, D.; Malhotra, V.; Vats, J. *J. Appl. Polym. Sci.* **1999**, 71, 1959.
72. Sung, C. S.; Hu, C. B.; Wu, C. S. *Macromolecules* **1980**, 13, 111.
73. Sung, C. S.; Smith, T. W. *Macromolecules* **1980**, 13, 117.
74. John, A. M.; Kirk, K. S. *Macromolecules* **1985**, 18, 32.
75. Qin, Z. Y.; Macosko, C. W.; Wellinghoff, S. T. *Macromolecules* **1985**, 18, 553.
76. Lee, D.; Richard, A.; Yang, C. *Macromolecules* **1988**, 21, 998.
77. Koberstein, J. T.; Galambos, A. F.; Leung, L. M. *Macromolecules* **1992**, 25, 6195.
78. Tien, Y. I.; Wei, K. H. *Macromolecules* **2001**, 34, 9045.
79. www.psrc.usm.edu/macrog/tg.htm> (25/03/2009).
80. Tang, E.; Cheng, G.; Ma, X. *Powder Tech.* **2005**, 161, 209.

Chapter 5

Synthesis and characterization of a novel urethane macromonomer (UM2) methacrylic-urethane copolymer

5.1 Synthesis of urethane macromonomers (UM2)

5.1.1 Introduction

The UM2 was synthesized with better solubility in common chromatographic solvents and compatibility with the polymethacrylates backbone.

Polyaddition polymerization was used to synthesize UM2 using a prepolymer method to introduce a polymerizable functional group into the urethane polymer chain end. The experimental procedures used to synthesize the urethane macromonomer are described in this chapter. Theoretically the UM2 was to have the following Formula:



where NPG is Neopentylglycol

5.1.2 Raw materials

The raw materials used for the synthesis of UM2 are tabulated in Table 5.1. The synthesis of UM2 requires that all monomer reagents, solvents and intermediates be free from moisture. This was achieved as described in Section 4.2.2

Table 5.1: Reagents used to synthesize UM2

Raw material	Chemical structure	Supplier
4,4'-diphenylmethane diisocyanate(MDI)		Sigma-Aldrich
neopentylglycol (NPG)		Sigma-Aldrich
2-hydroxyethyl acrylate (2-HEA)		Sigma-Aldrich
methanol (MeOH)	CH ₃ OH	Sigma-Aldrich

5.1.3 Experimental setup

The following equipment was used for the UM2 synthesis: a 250-ml three-neck flask, nitrogen gas inlet, oil bath, reflux condenser, temperature controller unit, magnetic stirrer, bubbler, glass syringe, packed column with molecular sieve, and calcium chloride to prevent any moisture entering the reactor vessel/flask.

5.1.4 Urethane macromonomer formulations

Formulations for the preparation of the UM2 are tabulated in Table 5.2. The formulations were determined according to formula 5.1, assuming 100% conversion, and average chain lengths of $n = 5$.

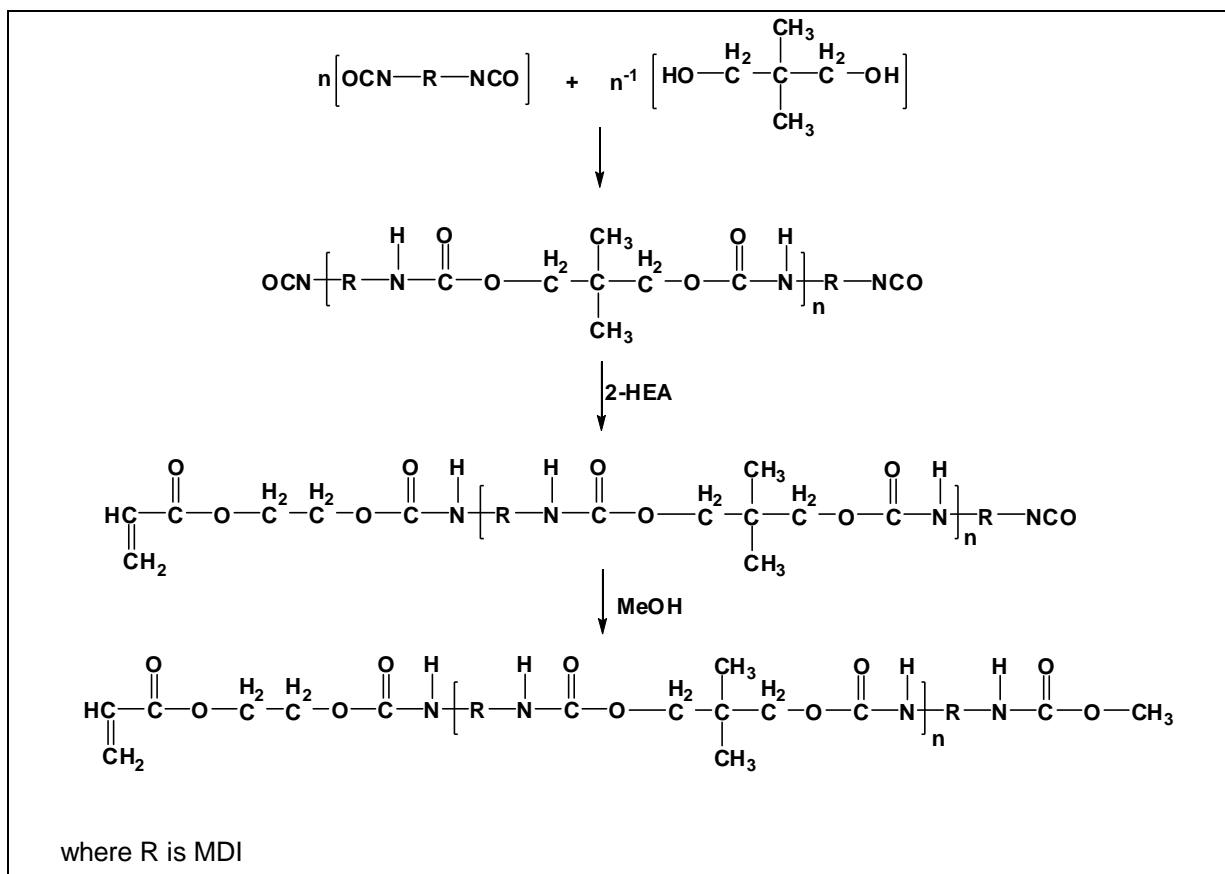
Table 5.2: Formulation used for the preparation of polyurethane macromonomers

MDI (g)	NPG (g)	2-HEA (g)	MeOH (g)	Total mass (g)	Excess of MeOH (g)	[OH]/[NCO]
13.84	4.79	1.07*	0.30*	20.00	0.14	1.04

* The quantities of 2-HEA, MeOH, MDI and NPG used to synthesize UM2 were calculated as mole % according to Formula 5.1, at [OH]/[NCO] mole ratio 1:1, in which 2-HEA was calculated as 40 mole % of the UM2 chain end and methanol was calculated as 60 mole % of the UM2 chain end.

5.1.5 Experimental procedure

MDI in excess and NPG were added together, dropwise, to the reaction flask containing dried DMF and heated to 50 °C under stirring for 40-60 min. In the second step, the reaction temperature was reduced to 37 °C and 2-HEA was added all at once. The reaction was allowed to run for 60 min. In the final step, the MeOH was added at 37 °C over 30 min, and then the reaction temperature was increased to 55 °C to ensure that all previously unreacted isocyanate reacted. The degree of the reaction was monitored by measuring the isocyanate group (2275 cm^{-1}) that disappears as result of reaction with an hydroxyl group, using IR spectroscopy. The isocyanate group was no longer visible in the IR spectrum of the reaction product. The obtained UM2 was dried in a vacuum oven at 50 °C for 24 hours then stored in a desiccator until required for use in further polymerization. The formation of UM2 is shown in Scheme 5.1.



Scheme 5.1: Formation of urethane macromonomer (when 2-HEA reacts at one side and MeOH at the other side of the UM2).

Besides the desired UM2 with only one polymerizable end group, i.e. 2-HEA on one chain end and MeOH on the other, the obtained UM2 can also have undesirable side products. One such undesirable product occurs when 2-HEA reacts on both ends of the urethane pre-polymer (urethane chain with excess isocyanate). A second undesirable product is formed when MeOH reacts on both chain ends of the urethane pre-polymer. Thus it is very important to optimize reaction conditions in an attempt to maximize the yield of the desired product that has 2-HEA on one chain end and MeOH on the other.

5.2 Synthesis of methacrylic-urethane graft copolymers

Most graft copolymers are formed by the reaction of a parent polymer, containing reactive sites (macromonomer technique), with a second type of monomer. UM2 was grafted with MMA and with n-BMA, respectively. All the graft copolymers were synthesized by using solution free radical copolymerization in which various quantities of UM2 were copolymerized with various amounts of MMA, and with various quantities of n-BMA, respectively. The procedure that was used to synthesize novel methacrylic-urethane graft copolymer was described earlier (Section 4.2.5).

5.2.1 Methacrylic-urethane copolymer formulations

Formulations used of the preparation of the different PMMA-g-UM2 and PnBMA-g-UM2 copolymers are shown below in Table 5.3

Table 5.3: Formulations for the preparation of PMMA-g-UM2 and PnBMA-g-UM2 graft copolymers

Reagents	Mass of reagents used in various experiments			
	EXP.1* (g)	EXP.2* (g)	EXP.3* (g)	EXP.4* (g)
MMA	5.00	4.50	3.75	2.25
AIBN**	0.05	0.045	0.037	0.025
UM2	0.00	0.50	1.25	2.75
DMF	35.12	35.10	35.15	35.13
nBMA	5.00	4.50	3.75	2.25
AIBN**	0.05	0.045	0.037	.025
UM2	0.00	0.50	1.25	2.75
DMF	35.32	35.19	35.14	35.12

*The concentrations of the UM2 were between 0 and 50 wt % (relative to MMA), and the amounts of urethane macromonomer and MMA in all copolymerization feeds were based on 5 g.

** The concentration of initiator (AIBN) was varied between 0.7 to 1% by weight according to n-BMA. This is however actually considered slightly high, and will affect the molecular weight of graft copolymers.

5.3 Characterization methods

Many different analytical techniques were used to analyze and characterize UM2 and its graft copolymers with acrylate. All these techniques were described Section 4.4.

5.4 Results and Discussion

As stated earlier, graft copolymers enable us to combine various properties of different materials into a single material. Here, it is described how the structure of UM2 was characterized using Fourier-transform infrared spectroscopy (FTIR), matrix-assisted laser mass spectrometry (MALDI-TOF-MS), nuclear magnetic resonance spectroscopy (NMR), size exclusion chromatography (SEC). The graft copolymer was then characterized using SEC with double detectors (UV and RI), NMR, FTIR, gradient elution liquid chromatography (HPLC). The thermal and mechanical properties of graft copolymers were characterized by thermogravimetric analysis (TGA), dynamic mechanical analysis (DMA), differential scanning calorimetry (DSC) and transmission electron microscopy (TEM).

5.4.1 Formation of urethane macromonomers (UM2)

5.4.1.1 Fourier-transform infrared spectroscopy

FTIR analysis was employed firstly to monitor the isocyanate (NCO groups) consumption during the UM2 synthesis, and secondly to characterize the UM2 itself.

(a) NCO content

The presence of the free –NCO of MDI during the synthesis of the UM2 pre-polymer is seen in the FTIR spectrum of the UM2 at 2275 cm^{-1} in Figure 5.1a. The absence of the characteristic NCO peak at 2275 cm^{-1} in Figure 5.1b indicates that all the isocyanate had reacted with NPG, MeOH and 2-HEA during polymerization. It is very important that no NCO groups remain, because if there is any moisture present, unwanted crosslinked structures will form (especially during the copolymerization stage). The absorption band at 3540 cm^{-1} in the FTIR spectrum (Figure 5.1a) represents the OH groups of the UM2 prepolymer during addition of NPG. These OH bands disappear in the UM2 as seen in the FTIR spectrum (Figure 5.1b). A strong N-H stretching band of the urethane groups appears at about 3326 cm^{-1} .

(b) Characterization of the urethane macromonomers

FTIR analysis of UM2 was done using a photo-acoustic cell (PAS). Figure 5.1(b) shows the FTIR spectrum of the UM2. The important characteristic signals of the vinyl-terminated group of the UM2 were detected at about 935 cm^{-1} , which correspond to C=C, indicating the formation of the UM2. A complete list of FTIR group's of UM2 is given in Table 5.4.

Table 5.4: FTIR peak assignment of the UM2¹⁻⁷

Wavelength number (cm^{-1})	Assignment	Reference
3334	Stretching vibration of the urethane N-H bond	2
3045, 2966 and 2902	Stretching vibration of the aliphatic C-H bond	1
1719	Amide I, stretching vibration of the of the ester C=O bond	3
1602	Stretching vibration of the aromatic ring C-C	5,6
1527	Amide II, stretching vibration of the benzene ring	1
1450	Bending vibration of the aliphatic C-H bond	1
1468	Stretching vibration of the benzene C-C	1,2
1327	Parallel vibration of C-H bond in CH_2	1
1067	Symmetric stretching vibration of the CO-O-C	1
935	Out-of- plane bending of CH in $\text{RCH}=\text{CH}$	7
823	Vibration of aromatic CH	2
757	Vibration of aromatic CH	2

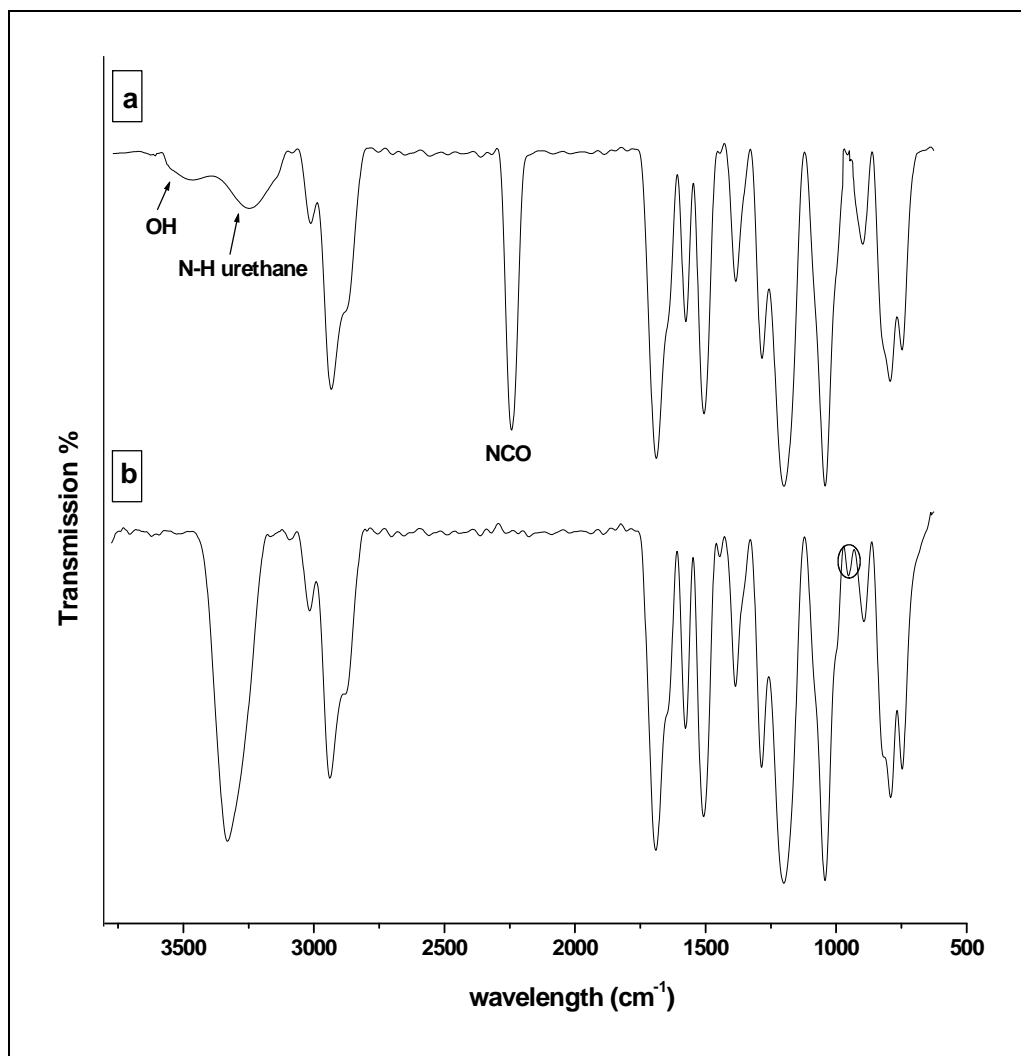


Figure 5.1: FTIR spectra of UM2 (a) before and (b) after addition of MeOH + 2-HEA.

5.4.1.2 MALDI-TOF-MS

MALDI-TOF-MS was carried out in linear mode to confirm the formation of the UM2 structure. Figure 5.2 shows a typical MALDI-TOF-MS spectrum of a UM2 prepared as described in Section 5.1.5.

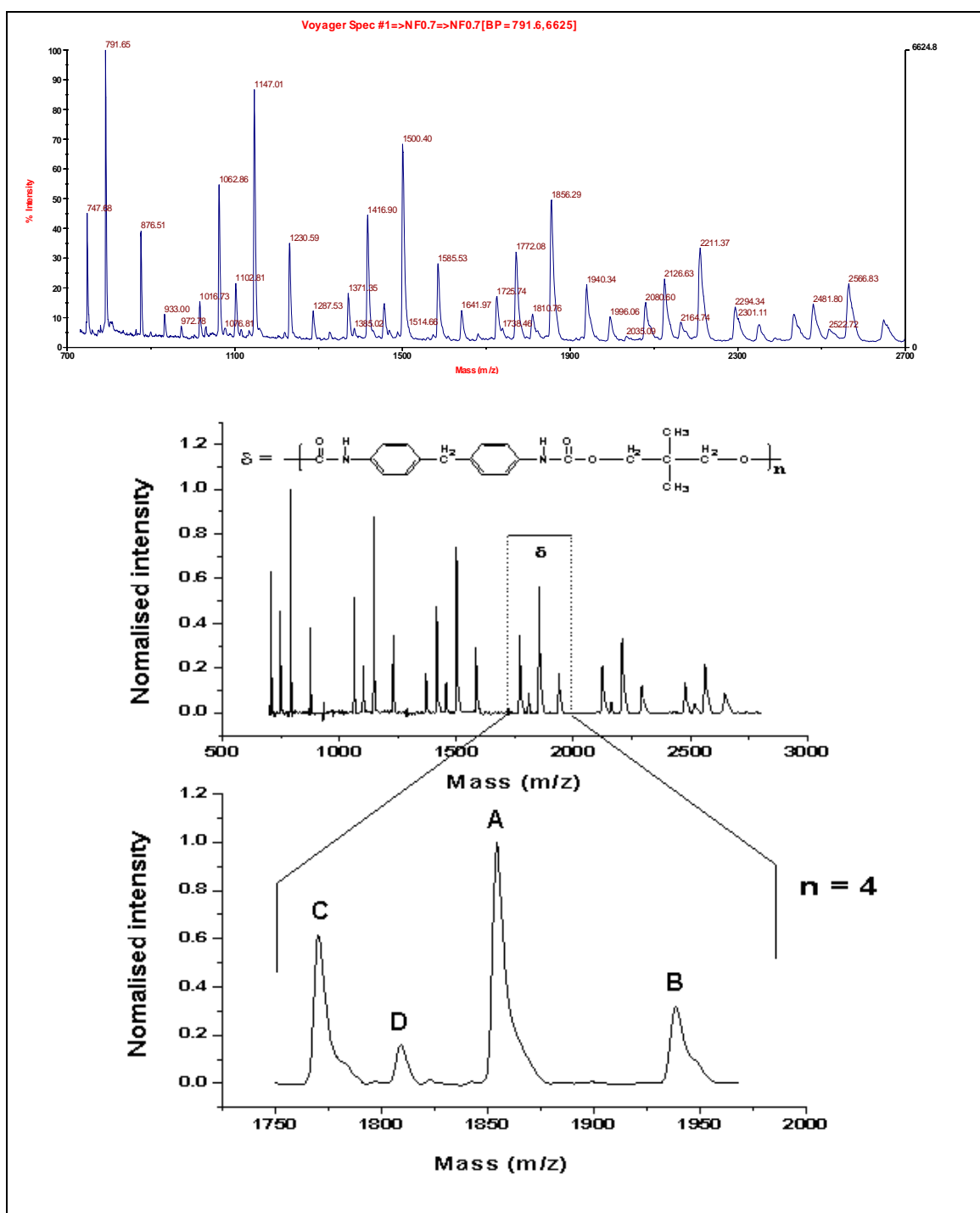
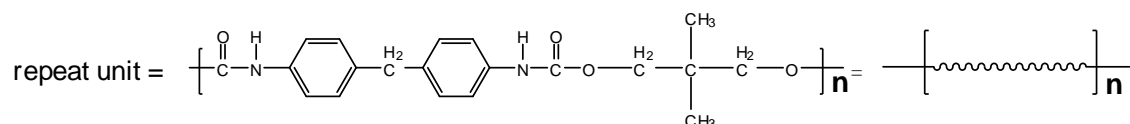


Figure 5.2: Enlarged region of MALDI-TOF-MS of UM2 (a) in the m/z region 500-3000 Da (b) experimental isotopic distribution of UM2 in m/z region 1750-1955 Da.

The peaks in the main distribution, in Figure 5.2, are at intervals of 354.35 mass units from each other, which corresponds to the molar mass of the repeat unit (δ) of UM2:



Scheme 5.2: repeat unit (δ) of UM2.

KTFA was added as the cationizing agent hence all the chains reflected, in the spectrum in Figure 5.2, were cationized by potassium. This accounts for 39.10 Da of the experimental molar masses.

The m/z region 1750–1970 Da in the Figure 5.2, expanded for illustrative purposes, shows that there were four signals, of varying intensity. These four signals correspond to the structures of UM2 products: C, A, B and D. The structures of UM2 which are corresponding to these signals are shown in Table 5.5.

Table 5.5: Abbreviations of main urethane macromonomers chain detected by MALDI-TOF-MS (possible scheme corresponding to signals in Figure 5.2)

Abbreviation	Corresponding structures of UM2
C	$\text{H}_3\text{C}-\text{O}-\left[\text{---} \right]_n \text{MDI}-\text{O}-\text{CH}_3$
A	$\text{H}_2\text{C}=\underset{\text{H}}{\text{C}}-\overset{\text{O}}{\parallel}{\text{C}}-\text{O}-\overset{\text{H}_2}{\text{C}}-\overset{\text{H}_2}{\text{C}}-\text{O}-\left[\text{---} \right]_n \text{MDI}-\text{O}-\text{CH}_3$
B	$\text{H}_2\text{C}=\underset{\text{H}}{\text{C}}-\overset{\text{O}}{\parallel}{\text{C}}-\text{O}-\overset{\text{H}_2}{\text{C}}-\overset{\text{H}_2}{\text{C}}-\text{O}-\left[\text{---} \right]_n \text{MDI}-\text{O}-\overset{\text{H}_2}{\text{C}}-\overset{\text{H}_2}{\text{C}}-\text{O}-\overset{\text{O}}{\parallel}{\text{C}}-\underset{\text{H}}{\text{C}}=\text{CH}_2$
D	$\left[\text{---} \right]_n$

Figure 5.3(a) and (b) shows MALDI-TOF-MS of the UM2 mention this in figure caption doped with KTFA. The spectra show very similar distributions of the main peaks. The peaks separated by 354.35 mass units, which corresponds to the repeat unit of UM2.

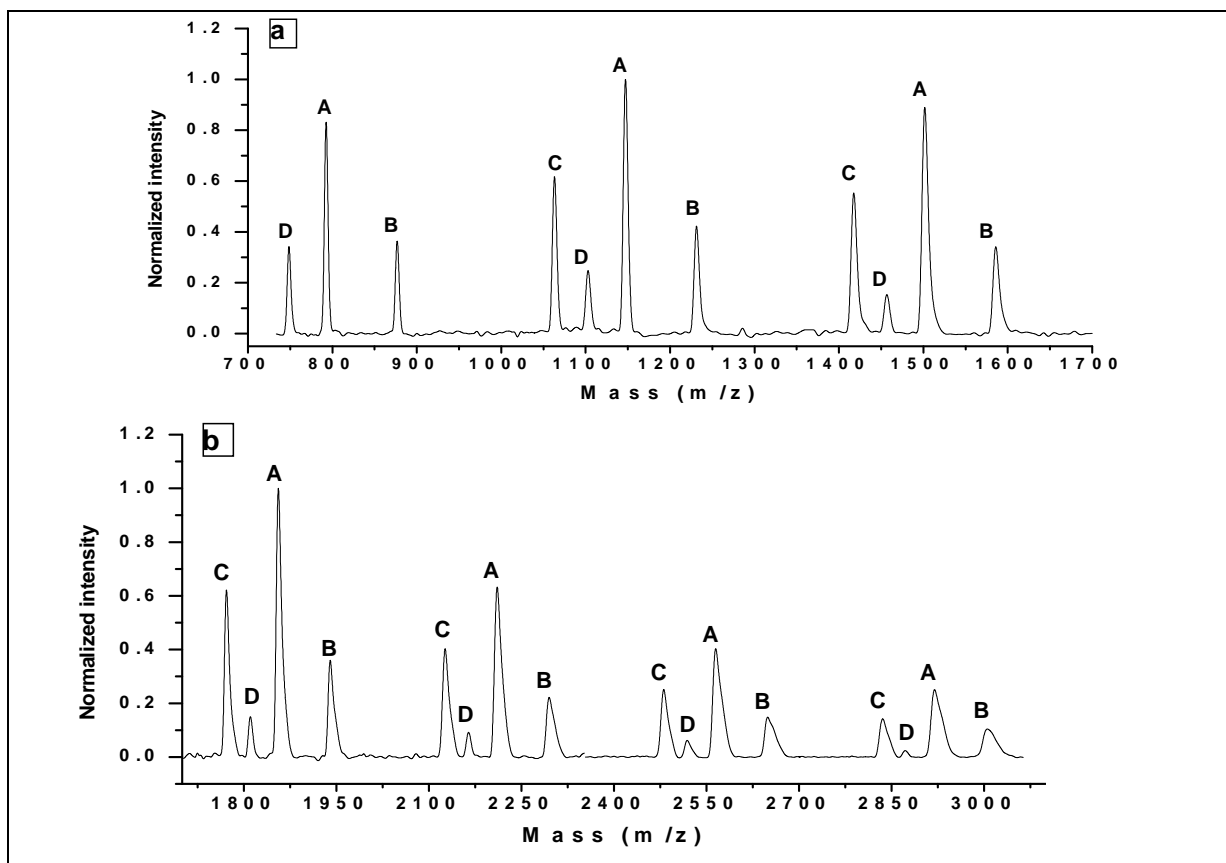


Figure 5.3: Enlarged region of mass spectra of UM2 (a) MALDI-TOF-MS of the UM2 in the m/z region 700-1800 Da and n changed from $n=1$ to $n=3$, and (b) MALDI-TOF-MS of the UM2 in the m/z region 1800-300 Da and n changed from $n=4$ to $n=7$.

The MALDI-TOF-MS of UM2 is similar to that of the MALDI-TOF-MS of UM1 (Section 4.5.1.2) except there is a new series D that appears in MALDI-TOF-MS of UM2 instead the H which had appeared in the MALDI-TOF-MS of UM1. Figure 5.3 shows that there are four different series are observed with a repeating unit of 354.36 Da (which clearly corresponds to UM2). These are noted as C, A, B, and D, with A being the predominant one (i.e. 2-HEA on one chain end and MeOH on the other) which confirms that the desired UM2 with only one polymerizable end group, i.e. 2-HEA on one chain end and methanol on the other was successfully synthesized. Series D is the least prominent. This series corresponds to the attachment of a metal salt adduct to an undesirable product corresponding to a cyclization reaction, which can occur if there are traces of moisture present during the reaction. All the results which summarize the monoisotopic masses of the ion peak series observed in MALDI-TOF-MS of UM2 are shown in Table 5.6.

Table 5.6: Summary of the monoisotopic masses of the ion peak series observed in MALDI-TOF-MS in Figure 5.3 (a) and (b)

Abbreviation	n*	Theoretical mass	Experimental mass	Difference**	Formula
C	1	708.25	-	-	CH ₃ O(C ₂₀ H ₂₂ N ₂ O ₄) _n C ₁₆ H ₁₅ O ₃ N ₂ K ⁺
	2	1062.44	1062.88	-0.44	
	3	1417.57	1417.45	0.12	
	4	1772.73	1772.11	0.62	
	5	2126.89	2126.70	0.19	
	6	2482.05	2483.03	0.02	
	7	2837.99	2837.87	0.12	
	8	3193.37	3193.00	0.37	
	9	3546.52	3546.38	0.14	
A	1	791.65	791.27	0.38	C ₅ H ₇ O(C ₂₀ H ₂₂ N ₂ O ₄) _n C ₁₆ H ₁₅ O ₃ N ₂ K ⁺
	2	1147.43	1147.01	0.42	
	3	1501.59	1501.58	0.01	
	4	1856.75	1856.27	0.48	
	5	2211.91	2211.37	0.54	
	6	2566.99	2566.91	0.08	
	7	2923.23	2923.08	0.15	
	8	3278.39	3278.59	-0.20	
	9	3633.54	3633.32	0.22	
B	1	876.29	876.62	-0.33	C ₅ H ₇ O(C ₂₀ H ₂₂ N ₂ O ₄) _n C ₂₀ H ₁₉ O ₅ N ₂ K ⁺
	2	1231.45	1231.03	0.42	
	3	1586.63	1586.61	0.02	
	4	1940.77	1940.40	0.37	
	5	2296.93	2296.68	0.25	
	6	2653.09	2653.03	0.06	
	7	2008.99	2008.87	0.11	
	8	3358.41	3358.24	0.17	
D	1	394.12	-	-	(C ₂₀ H ₂₂ N ₂ O ₄) _n K ⁺
	2	747.28	747.19	0.09	
	3	1102.44	1102.19	0.25	
	4	1456.98	1456.80	0.18	
	5	1810.76	1810.61	0.15	
	6	2166.82	2166.21	0.61	
	7	2522.33	2522.25	0.08	
	8	2873.68	2873.53	0.15	
	9	3231.69	3231.51	0.18	

*n is the UM2 repeat unit

**Difference between theoretical molecular mass value which was calculated using Formula 5.1 and molecular mass obtained by MALDI-TOF-MS.

In addition, Table 5.6 also shows an excellent agreement between the theoretical and the experimentally determined isotopic distributions; the difference between calculated mass and experimental mass is at most 0.01-0.61 Da for all four structures that were formed during UM2 synthesis.

5.4.1.3 $^1\text{H-NMR}$ analysis

UM2 structures were further analyzed by $^1\text{H-NMR}$. $^1\text{H-NMR}$ analysis provided both qualitative and quantitative information on the UM2. $^1\text{H-NMR}$ samples were run after the formation of UM2, which had been confirmed by FTIR and MALDI-TOF-MS. A typical $^1\text{H-NMR}$ spectrum of the UM2 prepared in this work is shown in Figure 5.4. Peak assignments were made based and labeled on the expected structure which is shown in the upper insert in Figure 5.4.

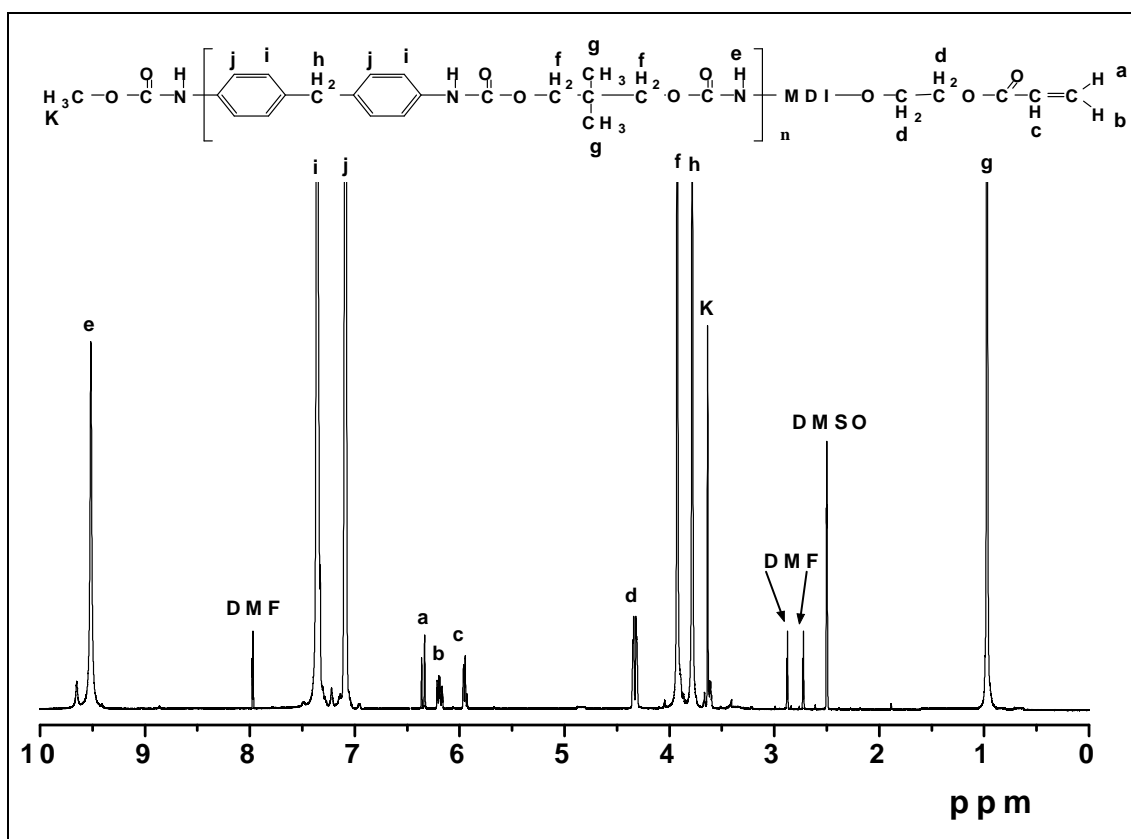


Figure 5.4: $^1\text{H-NMR}$ spectrum of urethane macromonomer UM2 dissolved in DMSO.

The peak at about $\delta = 9.51$ ppm is due to the N–H protons of urethane the linkages.⁸ The peak corresponding to the aromatic protons from MDI units are observed at $\delta = 7.34$ and $\delta = 7.08$ ppm.⁹ The methyl protons of the NPG unit appear at about $\delta = 0.96$ ppm,¹⁰ whereas the $-\text{O}-\text{CH}_2$ adjacent to urethane groups is observed around at $\delta = 3.90$ ppm.¹⁰ The signals at $\delta = 3.78$ ppm is attributed to methylene protons between two aromatic rings,¹¹ whereas the presence of resonance peaks around 3.61 ppm is attributed to O-CH₃ of the MeOH end group. The important characteristic signals of the vinyl-terminated protons in the UM2 are

detected at $\delta = 6.95, 6.18$ and 6.32 ppm, which proves the existence of acrylate groups in the UM2 structure.^{12,13}

In addition, the $^1\text{H-NMR}$ spectroscopic analysis indicates that the end functionality, i.e., the number of methyl groups and vinyl end groups per molecule of product UM2 is nearly unity (0.94:1.00) as determined by comparing the integration peak area of the methyl proton of MeOH at $\delta = 3.61$ ppm and the vinyl protons of 2-HEA at $\delta = 6.95, 6.18$ and 6.34 ppm.

$^1\text{H-NMR}$ can also be used to calculate the average repeating unit (n) for UM2 and number-average molecular weight (M_n). The integration signal of g at $\delta = 0.96$, which corresponds to NPG of the UM2 repeat unit, is approximately four times that of the peak of k at $\delta = 3.61$ ppm, which corresponds to the MeOH of the UM2 end group, and the multiple relationship between these two peaks is identical to the average chain length (n) of UM2. The calculation was done using the equation below:

$$\text{Average repeat unit } (n) = (j/6)/(k/3)$$

The integration value for signal j is divided by 6 and the integration value for signal k is divided by 3 so as to equal to each other. The number average chain length (n) which was calculated by $^1\text{H-NMR}$ was used to calculate the number-average molecular weight (M_n), which was 1814 g/mol, using the following equation:

$$M_n^{\text{NMR}} = \text{MeOH} + (n-1) \times (\text{MDI} + \text{NPG}) + \text{MDI} + 2 \times \text{HEA}$$

where the M_n of MeOH = 32, M_n of MDI = 250, M_n of NPG = 104, M_n of 2-HEA = 116, and $n = 4$

5.4.1.4 $^{13}\text{C-NMR}$ analysis

$^{13}\text{C-NMR}$ was also carried out to confirm the synthesis of the UM2 structure. A typical $^{13}\text{C-NMR}$ spectrum of the UM2 prepared in this work is shown in Figure 5.5. Peak assignments were made based on the expected structure, which is shown in the insert in Figure 5.5. The important characteristic signals of the vinyl-terminated group of the UM2 were detected at $\delta = 127.55$ and 131.62 ppm, which prove the existence of methacrylate groups in the UM2 structure and which confirm the synthesis of UM2.

Table 5.7: ^{13}C -NMR peak assignments for UM2¹⁴⁻¹⁷

Peak location (ppm)	Corresponding carbon bond (component)
20.85	(-C-(CH ₃) ₂) methyls (NPG)
36.50	(- C -) carbon (NPG)
68.44	(- CH ₂ -C(CH ₃) ₂ -) methylene (NPG)
42.37	methylene (-Ph- CH ₂ -Ph-) from MDI
118.32	ring carbons meta to MDI methylenes (hard segment)
128.80	ring carbons ortho to MDI methylene (hard segment)
136.15	ring carbons para to MDI methylene (hard segment)
136.72	ring carbons attached to MDI methylene (hard segment)
152.58	urethane (-OC= O NH-) carbonyl (hard segment)
50.72	methyl O- CH ₃ from MeOH
127.53	vinyl = CH ₂ from 2-HEA
131.62	vinyl CH = CH ₂ from 2-HEA

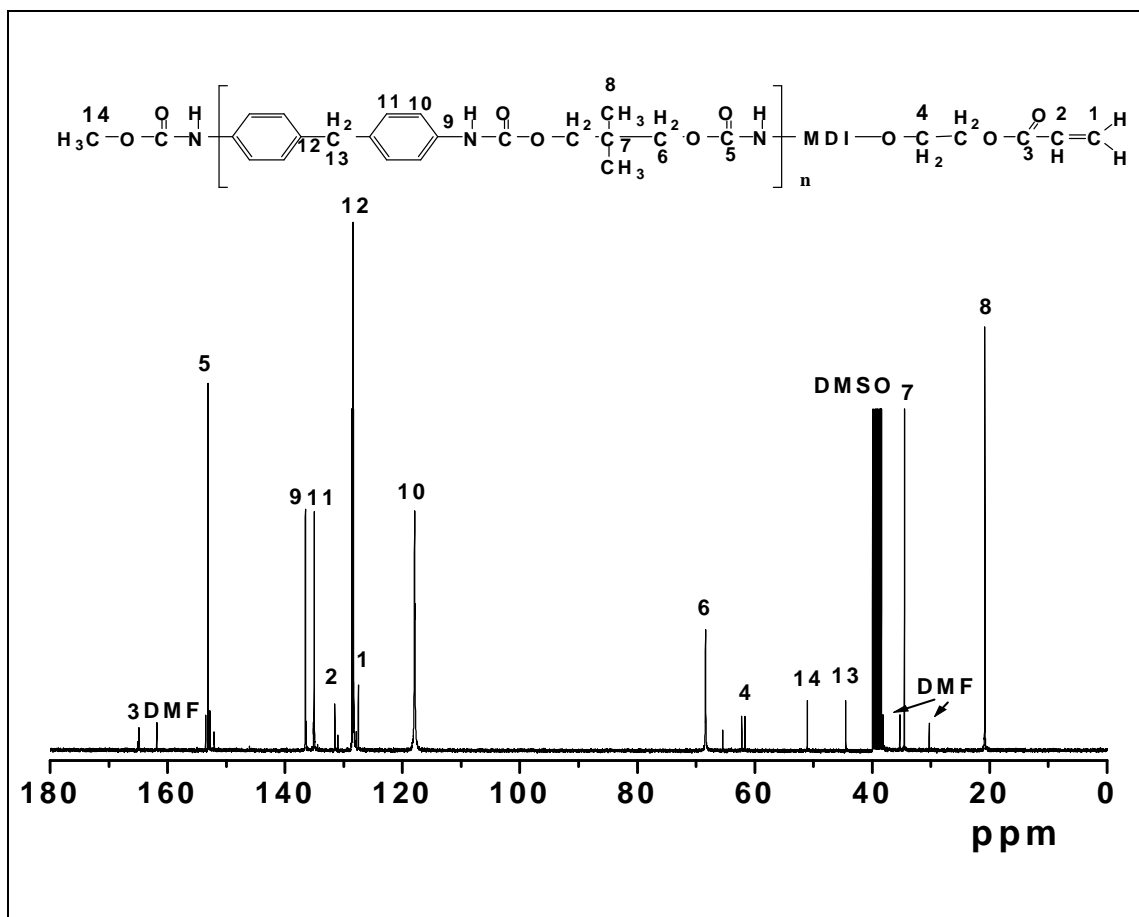


Figure 5.5: ^{13}C -NMR spectrum of urethane macromonomer UM2 dissolved in DMSO.

5.4.1.5 SEC analysis

SEC analysis was done to characterize the UM2. The SEC instrument was calibrated using linear polystyrene standards. Tetrahydrofuran (THF) was used as solvent. Figure 6.6 shows the SEC trace of the UM2, which has a shoulder on the low molecular mass side. This is due to low molecular weight fractions. Polyaddition polymerization was used to synthesize the UM2, which could lead to broad molecular weight distribution on the low molecular mass side.

The number average molecular weight (M_n) (experimental and predicted) and polydispersities obtained for the UM2 with $n = 5$ of UM2 are summarized in Table 5.8. It shows that synthesized UM2 has a relatively narrow molecular weight distribution, and also that the actual molecular weight of the UM2 is close to the predicted one (calculated based on Formula 5.1). Although SEC calibration was with polystyrene standards, which does not offer the exact values. The values nonetheless are close. This indicates that the synthesized UM2 was successfully synthesized, to provide a specific controlled urethane macromonomer.

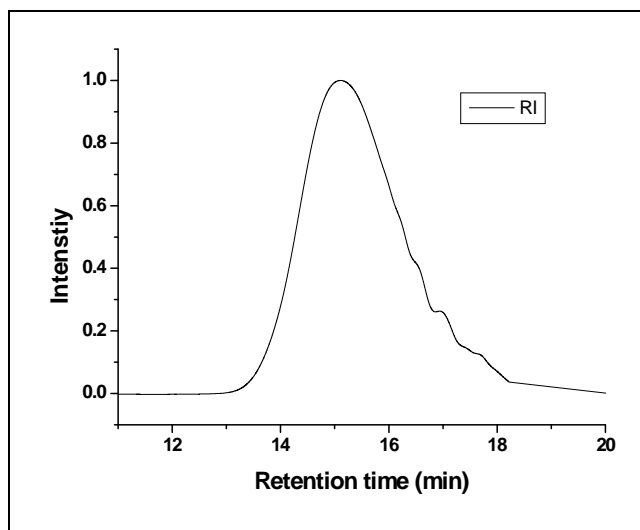


Figure 5.6: SEC chromatogram of UM2.

Table 5.8: Number average molecular weight (M_n), and polydispersity (M_w/M_n) the UM2 of different chain lengths, as determined by SEC

Theoretical urethane length (n)	Theoretical molecular weight*	M_n by SEC	M_w by SEC	Polydispersity
5	2128	2353	5412	2.3

Theoretical molecular weight, calculated using formula 5.1

5.4.2 Methacrylic-urethane graft copolymer formation

The copolymerization of UM2 with MMA or n-BMA to form graft structures was performed with different feed compositions of the macromonomer to MMA or n-BMA monomer (10, 25, and 55 wt %). The copolymerization reaction was carried out in freshly dried DMF at 75 °C for 24h. AIBN was used (1 wt %) as the initiator. The amount of DMF was determined so that the polymer would constitute 15 weight percent. The resulting graft copolymers were isolated by precipitation from DMF solution into methanol.

Table 5.9 illustrates the formulation and SEC characterization of graft copolymer with different amount of macromonomer. Methanol was a non-solvent for PMMA, PnBMA and the corresponding methacrylate-g-urethane copolymers, whereby the molecular structure was confirmed using SEC having UV (254 nm, which only detects the UM2 at this wavelength due to aromatic ring in its structure) and RI double detectors and THF was used as solvent. The yield was determined gravimetrically after extraction of the unreacted macromonomer.

Table 5.9 shows that all PMMA-g-UM2 and PnBMA-g-urethane copolymers had molecular weights of about 80000, which was higher than those of the starting UM2. In addition to this point, the molecular weight values of the graft copolymers obtained by SEC measurements are generally much lower than the absolute molecular weight.¹⁷

Table 5.9: Formulation and characterizations of PMMA/UM2 and PnBMA/UM2 graft copolymers

	Sample code	UM2 (g)	Methacrylic (g)	Graft copolymer		PDI	Yield of graft copolymer (%)
				Mn (g/mol)	Mw (g/mol)		
			MMA				
PMMA-g-UM2	G10M	0.50	4.50	7.11×10^4	1.69×10^5	2.38	78
	G25M	1.25	3.75	8.78×10^4	2.23×10^5	2.55	74
	G55M	2.75	2.25	7.65×10^4	1.85×10^5	2.42	65
			n-BMA				
PnBMA-g-UM2	G10B	0.50	4.50	7.73×10^4	1.73×10^5	2.24	82
	G25B	1.25	3.75	7.46×10^4	1.78×10^5	2.39	72
	G55B	2.75	2.25	7.31×10^4	1.92×10^5	2.60	67

5.4.2.1 Extraction of unreacted macromonomer

Methanol is a non-solvent for PMMA, PnBMA and the corresponding methacrylate-g-urethane copolymers. However, it was expected that some unreactive (structures C and D in Table 5.5) and unreacted UM2 (structures A and B in Table 5.5) might precipitate along with the graft copolymer, as shown in the SEC trace in the Figure 5.7 by a small shoulder at low molecular weight (high retention time). This may be expected, due the difference in the reactivity between macromonomers and methacrylic monomers.¹⁸⁻²² Attempts to separate unreacted and unreactive UM2 from the copolymers were made by precipitation using THF as solvent and toluene and MeOH as non-solvents.

A sample of about 0.80 g UM2 was dissolved in about 10 ml THF and precipitated in toluene. The solution was filtered, and then precipitated, again in MeOH. The resultant graft copolymer and PMMA or PnBMA homopolymers precipitated out of solution, while the unreacted macromonomer remained soluble in the solution. The extraction of the unreacted macromonomer was tracked using SEC with double detector UV (254 nm) and RI, as shown in Figure 5.8. The percentage of graft formation was calculated gravimetrically after extraction of the unreacted macromonomers. The formulation and characterization of the grafts are tabulated in Table 5.9. The yield of the graft copolymers was 69–84%.

Figure 5.7 shows examples of a SEC trace of the graft copolymer of PMMA-g-UM2 and PnBMA-g-UM2 before extraction. A bimodal distribution curve was obtained after the copolymerization reaction, which shows that the unreacted UM2 (in the low molecular weight

region) is still present, whereas these unreacted and unreactive UMs were completely removed after precipitation using THF as solvent and toluene and MeOH as non-solvent, as shown in Figure 5.8.

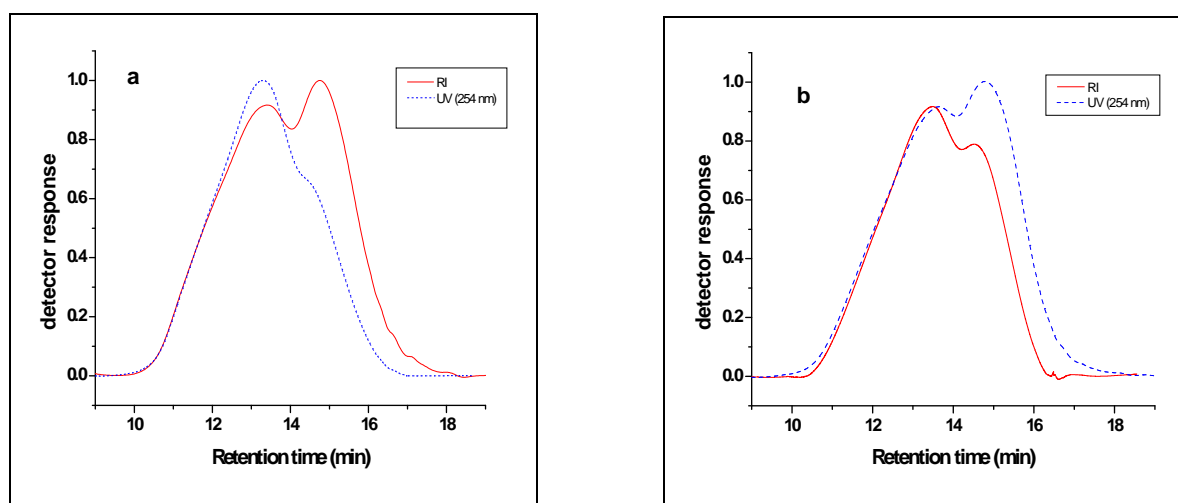


Figure 5.7: SEC traces of unextracted graft copolymer (a) PMMA-g-UM2 (25 wt %) and (b) PnBMA-g-UM2 (25 wt %) (Note: RI and UV detector response have been normalized).

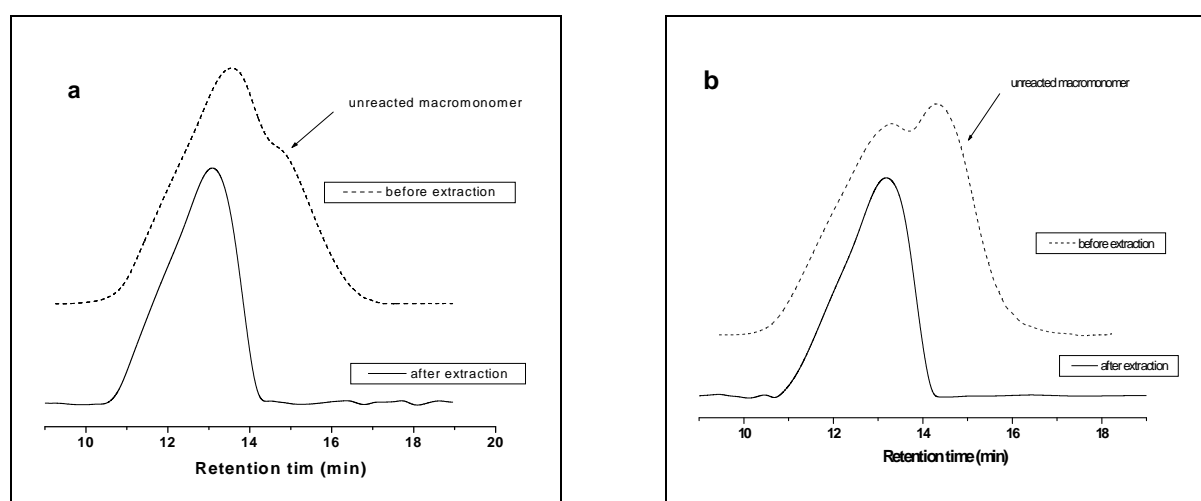


Figure 5.8: SEC trace of (a) PMMA-g-UM2 (25 wt %) and (b) PnBMA-g-UM2 (25 wt %) showing the efficiency of the extraction procedure (RI detector).

5.5 Characterization of graft copolymers after extraction

5.5.1 SEC analysis

As was mentioned previously in Section 4.5.2.1, the UV detector only detects the UM2 at 254 nm due to the absorption by the aromatic ring in the polymer chain, hence SEC with double detectors was used to prove the syntheses of PMMA-g-UM2 and PnBMA-g-UM2 copolymers. Figures 5.9 and 5.10 are examples of SEC traces showing the extracted graft copolymers of PMMA-g-UM2 and PnBMA-g-UM2 copolymers, respectively, after all the unreacted and unreactive UM2 had been removed. They showed that no UV peaks for

unreacted UM2 were observed at low molecular weight and also that the retention times of the graft copolymer samples were shifted to lower time compared to the retention time of the of UM2. This result indicates that the molecular weights of the graft copolymer samples were increased due to the grafting reaction, and also that no homopolymers of PMMA or PnBMA, or UM2, were present. In the absence of unreacted UM2, the UV response almost mirrors the RI response in all graft copolymers, which indicates the compositional homogeneity of UM grafts onto the graft copolymers.

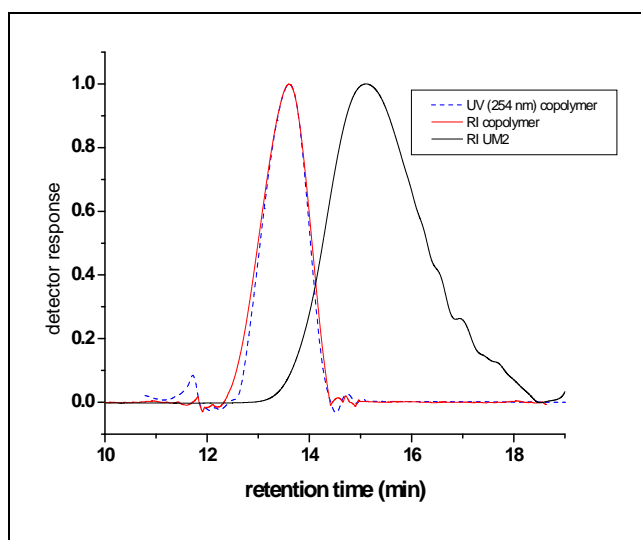


Figure 5.9: Example of SEC traces of PMMA-g-UM2 (25 wt % UM2) illustrating the UM2 distribution.

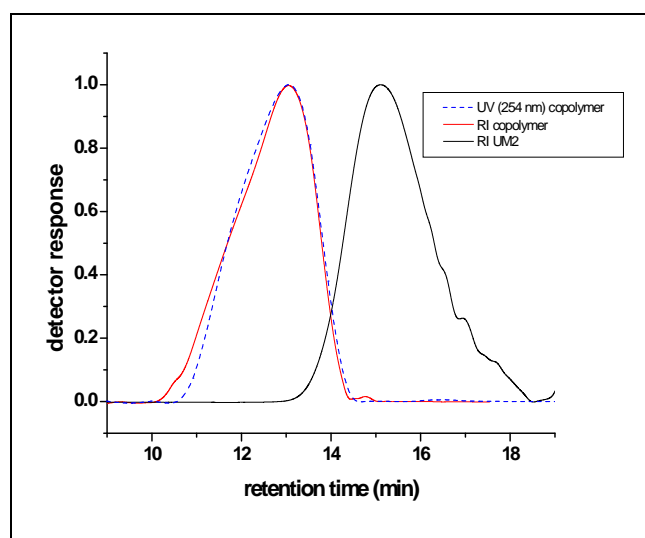


Figure 5.10: Example of SEC traces of PnBMA-g-UM2 (25 wt % UM2) illustrating the UM2 distribution.

The yields of the copolymerization reactions for both PMMA-g-UM2 and PnBMA-g-UM2 copolymers are included in Table 5.9. The UM2 consists of four possible structures A, B, C

and D (as discussed previously in Section 5.3.1.2). Due to the UM2 being endcapped with 60:40 mole ratio of MeOH: 2-HEA during UM1 synthesis, the UM2 will consist of an unreactive fraction (structures C and D). These unreactive UM2 fractions are the partially the cause of the decreased percentage % yield when the weight fraction of UM2 is increased during copolymerization. In other words, the yields of both PMMA-g-UM2 and PnBMA-g-UM2 copolymers decreased as the quantities of the UM2 are increased. This is because as the weight fraction is increased, so too does the weight fraction of the unreactive UM2 increase, which, after removal with methanol, results in a decrease in the percentage yield of the graft copolymers.

5.5.2 Gradient elution HPLC

The graft reaction of UM2 with MMA and with n-BMA was investigated by gradient HPLC. When UM2 is grafted with MMA or n-BMA the reaction product contains: residual ungrafted UM2, the graft copolymer PMMA-g-UM2 or PnBMA-g-UM2, and PMMA or PnBMA homopolymers. In order to carry out a detailed analysis the components must first be separated from each other by stable chromatographic techniques. Gradient HPLC is the most useful technique for the separation of copolymers according to chemical composition. The gradient HPLC separation mechanism is based on the differences in solubility between copolymer fractions with different chemical compositions.^{23,24} Hence a method was developed for the complete separation of all components by gradient HPLC. Gradient Elution Chromatography (GPEC) was used to analyze the copolymers and monitor the extraction of unreacted macromonomer as well as to determine the chemical composition distribution.

HPLC analysis was performed with a combination of precipitation HPLC and adsorption or retention HPLC. In this part of the study a Nucleosil C18; 100 Å (25 x 0.46) columns was used. A compromise between copolymer solubility and chromatographic solvent strength was used to ensure copolymer separation over a broad chemical composition distribution.

5.5.2.1 GPEC of PMMA-g-UM2 copolymers

PMMA homopolymer is completely soluble in chloroform and is therefore unretained on the silica packing. The graft copolymer is however insoluble in the starting solvent, chloroform. The mode of retention is therefore the governing factor in determining the actual separation. The retention process in the case of the PMMA-g-UM2 copolymer using the chloroform /THF system on silica relies on initial precipitation, followed by adsorption retention after redissolution in the solvent gradient of the graft copolymer.

Several gradients were tested before obtaining optimal separation. Both linear and non-linear gradients were tested. Figure 5.11 below is an illustration of the gradient that gives a good

separation between PMMA, PMMA-g-UM2 copolymer and unreacted UM2. In this profile sample injection volume was 11 μ l and the flow rate 1 mL/min.

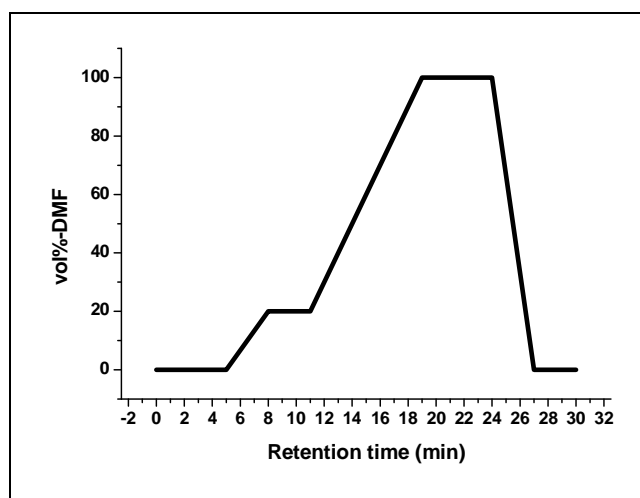


Figure 5.11: Gradient elution profile used for chemical composition for the separation of PMMA-g-UM2 copolymer constituents. (stationary phase: Nucleosil C18; 100Å, eluent: chloroform/THF.)

A PMMA standard and UM2 were used to identify their retention times in the elution profile. Figure 5.12 shows the retention times of these components. PMMA elutes between 2 and 3 min whereas UM2 elutes between 9 and 24 min.

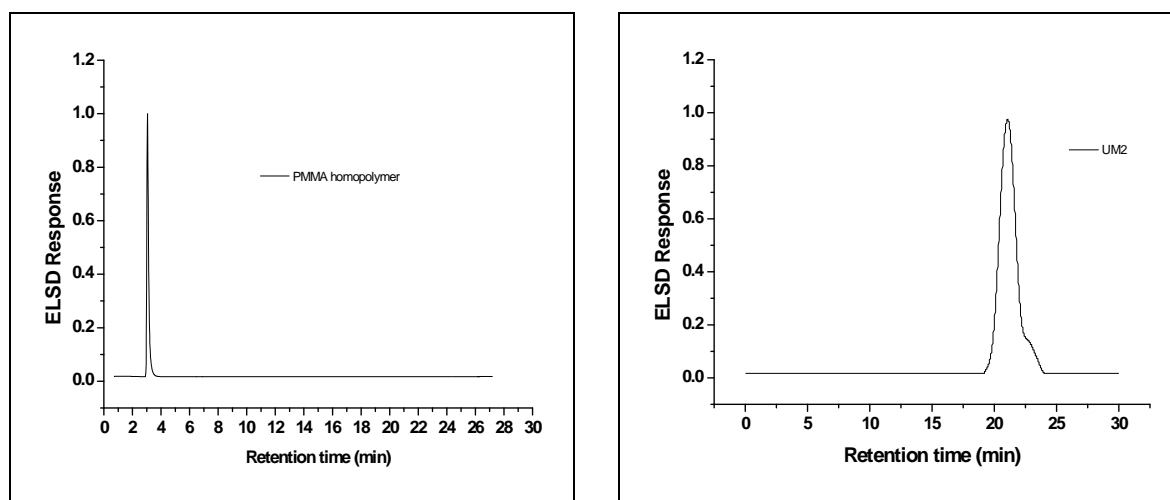


Figure 5.12: HPLC elution plots of UM2 and PMMA homopolymer.

A typical example of a gradient HPLC chromatogram for a PMMA-g-UM2 copolymer before extraction of the unreacted UM2 is presented in Figure 5.13. It can be seen that the PMMA homopolymer elutes at 4 min followed by the graft copolymer at 17 and lastly the unreacted UM2 at 20 min. The assignment of the peaks was carried out by comparison with the

chromatographic behaviour when using a reversed phase column (Nucleosil C18; 100Å) of UM2 and PMMA under same conditions.

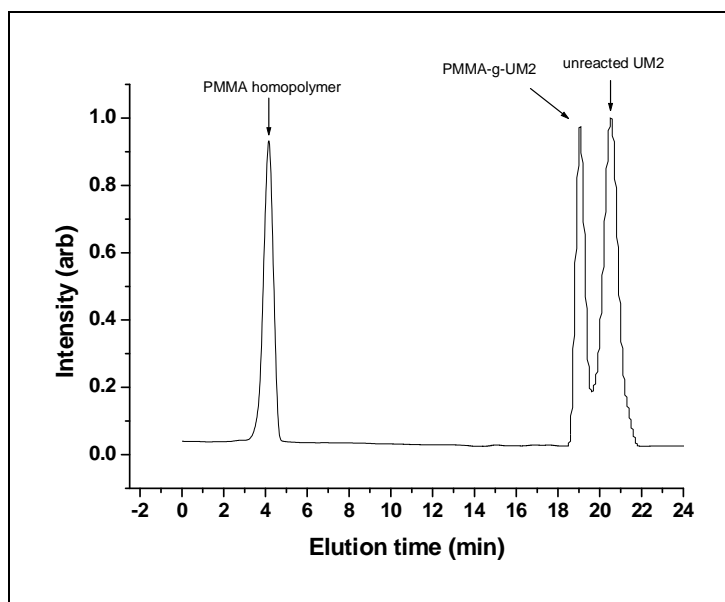


Figure 5.13: Gradient HPLC chromatogram of the PMMA-g-UM2 copolymer (G55M) before extraction of the unreacted UM2. (Stationary phase: Nucleosil C18; 100Å; eluent: chloroform /THF; detector: ELSD.)

Figure 5.14 shows a typical gradient elution analysis of a PMMA-g-UM2 copolymer (G55M) after extraction of the unreacted UM2 and PMMA homopolymers. Here it can be seen that almost all of the unreacted UM2 and PMMA homopolymers were removed.

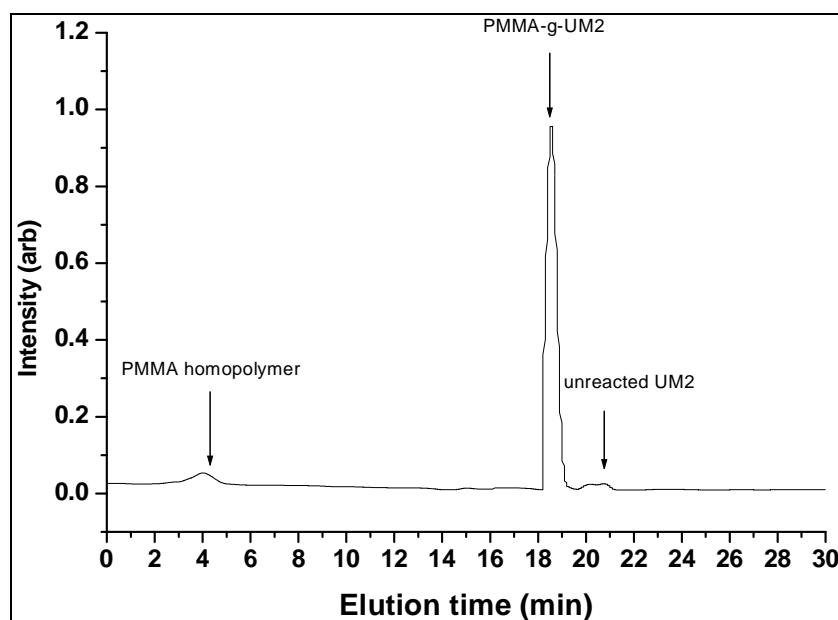


Figure 5.14: Gradient HPLC chromatogram of the PMMA-g-UM2 copolymer (G55M) after extraction of the unreacted UM2 and PMMA homopolymers. (Stationary phase: Nucleosil C18; 100Å; eluent: chloroform /THF; detector: ELSD.)

GPEC of PnBMA-g-UM2 copolymers

PnBMA homopolymer is completely soluble in toluene and is therefore unretained on the silica packing. The graft copolymer is however insoluble in the starting solvent toluene. The retention process in the case of the PnBMA-g-UM2 copolymer using toluene/THF system on silica relies on initial precipitation, followed by adsorption retention after redissolution in the solvent gradient of the graft copolymer. Linear gradients were used here as shown in Figure 5.15.

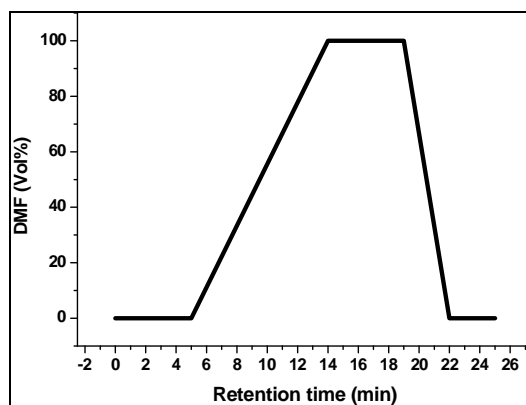


Figure 5.15: Gradient elution profile used for chemical composition for the separation of PnBMA-g-UM2 copolymer constituents. (stationary phase: Nucleosil C18; 100Å, eluent: toluene/THF.)

Separation is a function of component polarity. Therefore when using a reversed phase column (Nucleosil C18; 100Å) PnBMA is expected to elute first in a low polar solvent (toluene) followed by the UM2. PnBMA and UM2 were used to identify their retention times in the elution profile. Figure 5.16 shows the retention times of these components. PnBMA elutes between 2 and 3 min whereas UM2 elutes between 15 and 20 min.

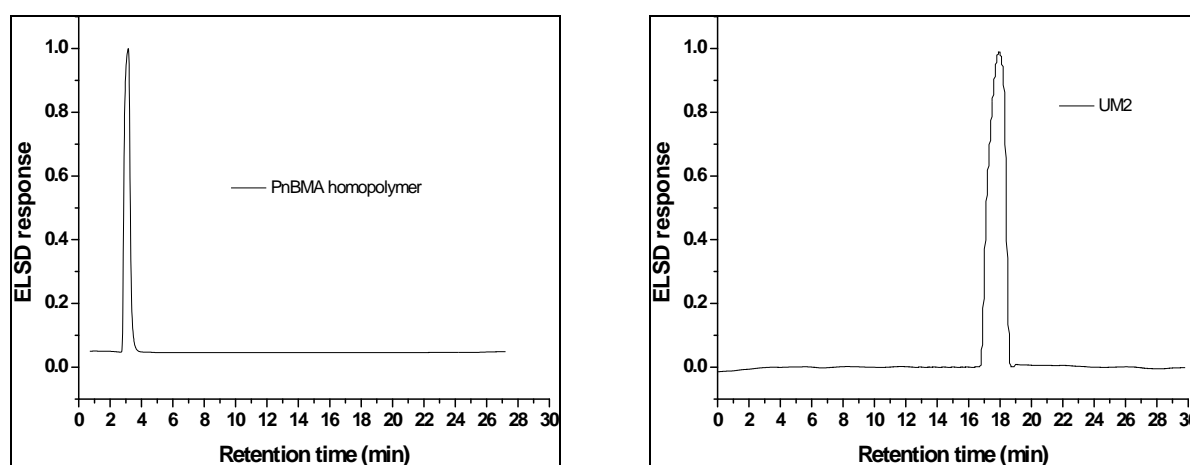


Figure 5.16: HPLC elution plots of UM2 and PnBMA homopolymer.

A typical example of the HPLC chromatogram for PnBMA-g-UM2 copolymer before extraction of the unreacted UM2 is presented in Figure 5.17. The result shows that a very good separation into three fractions was obtained. The assignment of the peaks was carried out by comparison with the chromatographic behaviour of UM2 and the PnBMA homopolymer using a reversed phase column (Nucleosil C18; 100Å) under the same conditions. The three elution peaks visible can be assigned to the sample constituents PnBMA, PnBMA-g-UM2 and UM2 respectively. Figure 5.18 shows the extracted product (PnBMA-g-UM2 graft copolymer).

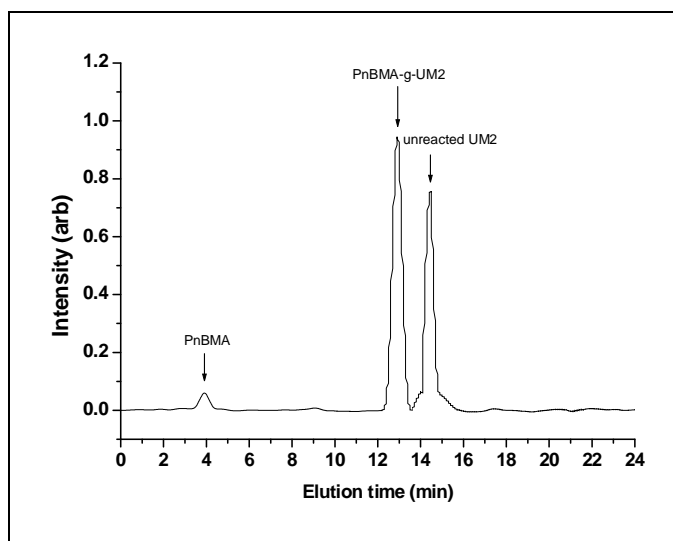


Figure 5.17: Gradient HPLC chromatogram of the PnBMA-g-UM2 copolymer (G55B) before extraction of the unreacted UM2 and PnBMA homopolymer. (Stationary phase: Nucleosil C18; 100Å; eluent: toluene /THF; detector: ELSD.)

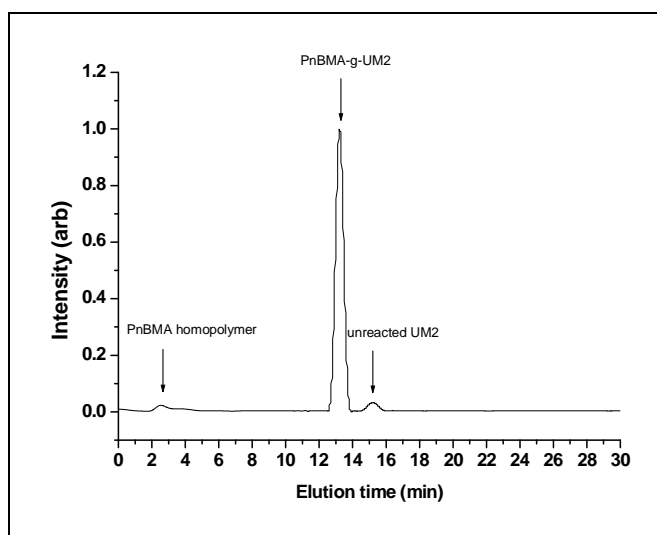


Figure 5.18: Gradient HPLC chromatogram of the PBMA-g-UM2 copolymer (G55B) after extraction of the unreacted UM2 and PnBMA homopolymers. (Stationary phase: Nucleosil C18; 100Å; eluent: toluene /THF; detector: ELSD.)

5.5.3 Light scattering

The graft copolymers were also characterized using a multi-angle light scattering detector (MALLS) to determine the absolute molecular mass, as the M_n result obtained from SEC calibrated with linear polystyrene standards does not represent the exact values. These results are presented and discussed below. To be able to use the MALLS detector the specific refractive index increment, usually referred to as the dn/dc value, was determined for each of the individual graft copolymers in THF. The molecular weights and molecular weight distributions (M_w/M_n) were calculated using Wyatt Technology Astra software. Table 5.10 shows the weight average molecular weight and number average molecular weight of the graft copolymers obtained by MALLS. The molecular weight distributions of the graft copolymer were relatively narrower than those obtained through the normal SEC. The molar mass obtained by MALLS is consistently higher than the molar mass obtained relative to polystyrene.

Table 5.10: The number average molar mass and weight average molar mass of the graft copolymers obtained via SEC-MALLS

	Sample code	dn/dc ml/g	Graft copolymer		PDI
			M_n (g/mol)	M_w (g/mol)	
PMMA-g-UM1	G10M	0.096	1.01×10^5	1.84×10^5	1.83
	G25M	0.12	1.09×10^5	2.21×10^5	2.04
	G55M	0.14	1.05×10^5	2.61×10^5	2.48
PnBMA-g-UM1	G10B	0.093	1.09×10^5	1.48×10^5	1.35
	G25B	0.102	1.07×10^5	1.38×10^5	1.54
	G55B	0.119	8.59×10^4	1.25×10^5	2.08

5.5.4 FTIR analysis

After all the unreacted (structures A and B) and unreactive UM2 (structures C and D) were removed as confirmed by SEC (see Section 5.4.2.1), the graft copolymers samples were analyzed by FTIR. The FTIR was run to prove that the UM2 had actually grafted to PMMA or PnBMA through the double bond (which disappears) during free-radical copolymerization.

5.5.4.1 PMMA-g-UM2 copolymers

Figure 5.19 compares the FTIR spectra of PMMA-g-UM2 copolymer and the PMMA homopolymer. The new peaks observed in the graft copolymer spectra are very similar to the FTIR results of PMMA-g-UM1 which was discussed in the previous chapter (Section 4.5.3.4). A complete list of FTIR group assignments of the PMMA-g-UM2 copolymers is given in Table 5.11. The peak at 935 cm^{-1} for the double bond in the UM2 disappears, which implies that

UM has fully reacted with MMA. This result and the result in Table 5.11 show that the UM2 was successfully incorporated into the PMMA polymer structure, which was also confirmed by $^1\text{H-NMR}$ and $^{13}\text{C-NMR}$ and SEC.

Table 5.11: IR absorption data for PMMA-g-UM2 copolymer

Wavelength number (cm^{-1})	Assignment
3345	Stretching vibration of the urethane N-H bond
2991, 2955 and 2839	Stretching vibration of the aliphatic C-H bond
1730	Stretching vibration of the of the ester C=O bond
1605	Stretching vibration of the aromatic ring C-C
1530	Amide II, stretching vibration of the benzene ring
1450	Bending vibration of the aliphatic C-H bond
1327	Parallel vibration of the C-H bond in CH_2 Symmetric deformation of aliphatic CH_3
1246	C-O Stretching
1129	C-(C=O)-O Stretching
1067	Symmetric stretching vibration of the CO-O-C
916	Out-of-plane bending of CH in the benzene ring
896	Vibration of aromatic CH
839	Vibration of aromatic CH
757	Vibration of aromatic CH

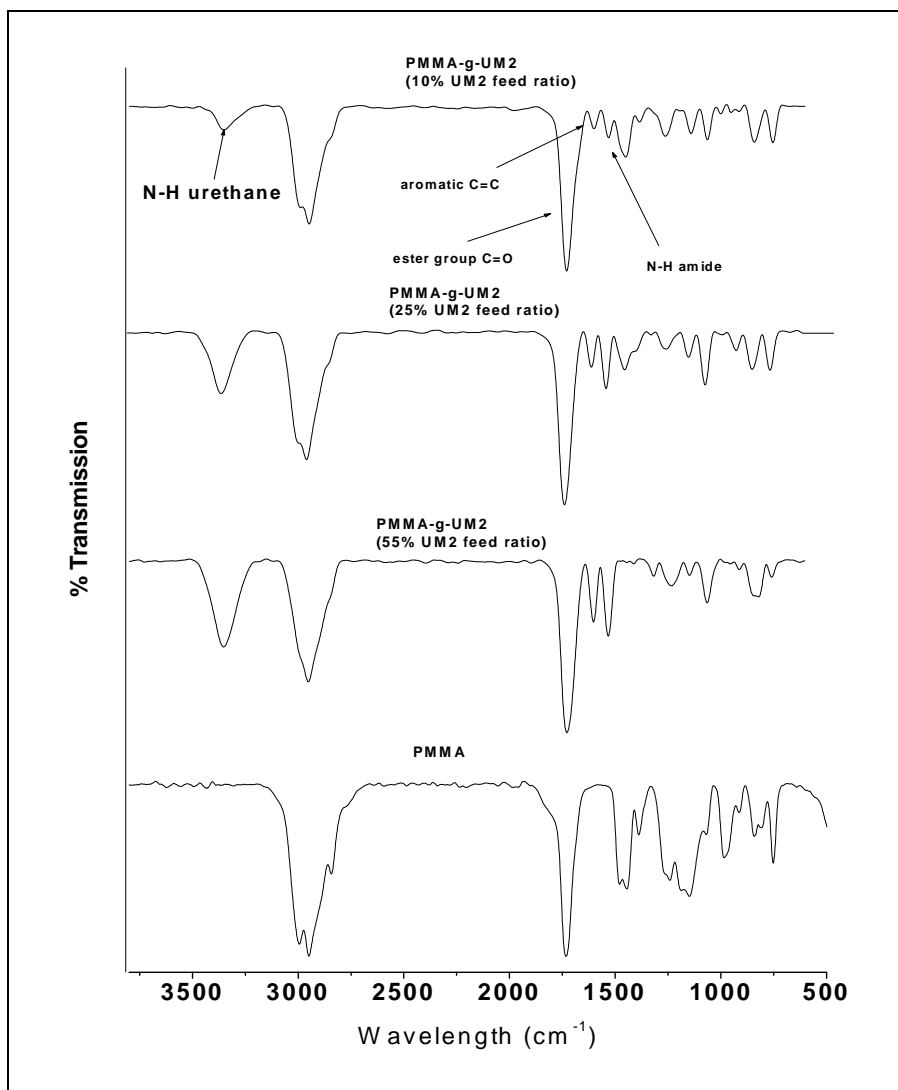


Figure 5.19: FTIR spectra of PMMA-g-UM2 copolymers and PMMA homopolymer.

5.5.4.2 PnBMA-g-UM2 copolymers

Figure 5.20 compares the FTIR spectra of PnBMA-g-UM2 copolymers to the spectrum of the PnBMA homopolymer. New peaks were observed in the graft copolymer spectra which are similar to FTIR results of PnBMA-g-UM1 (Section 4.5.3.4). A complete list of the FTIR group assignments of PnBMA-g-UM2 copolymers is given in Table 5.12. The peak at 935 cm^{-1} for the double bond in the UM2 disappears, which implies that the UM2 has fully reacted with n-BMA. This results and the result in Table 5.12 show that the UM2 was successfully incorporated into the PnBMA polymer structure, which was also confirmed by $^1\text{H-NMR}$ and $^{13}\text{C-NMR}$ and SEC.

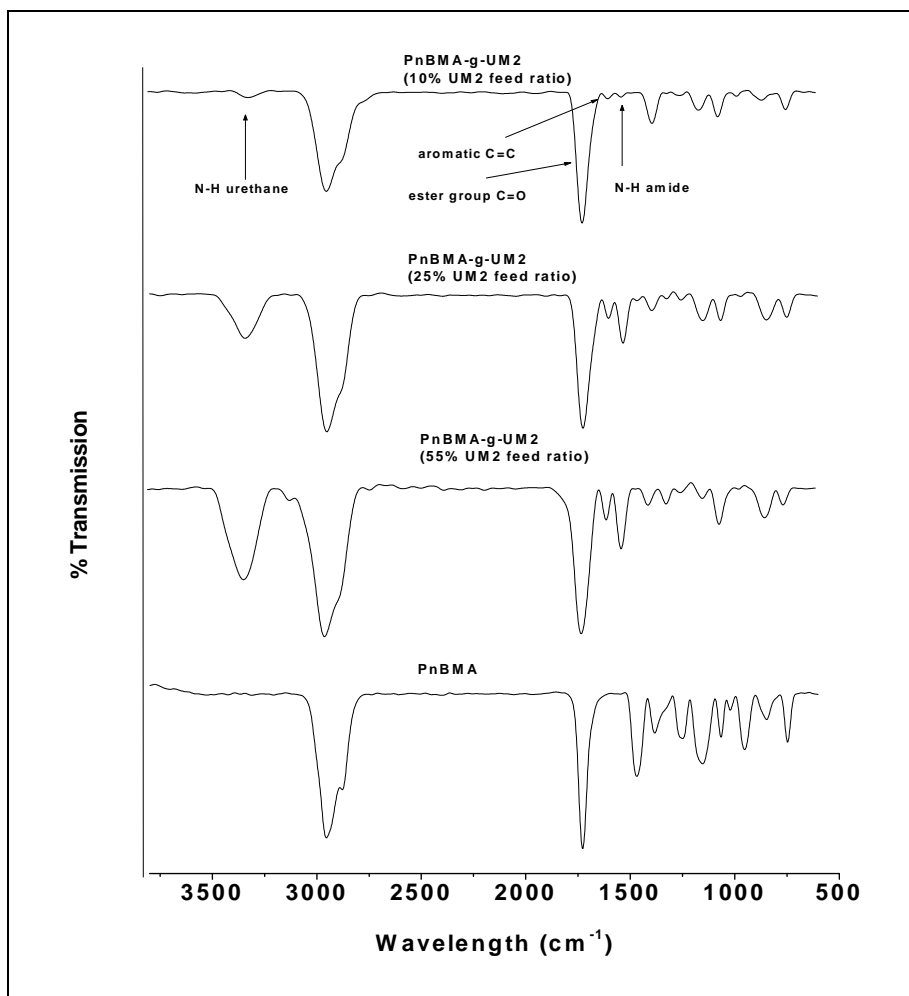


Figure 5.20: FTIR spectra of PnBMA-g-UM2 copolymers and PnBMA homopolymer.

Table 5.12: IR absorption data for PnBMA-g-UM2 copolymer

Wavelength number (cm^{-1})	Assignment
3329	Stretching vibration of the urethane N-H bond
2959 and 2875	Stretching vibration of the aliphatic C-H bond
1726	Amide I, stretching vibration of the ester C=O bond
1605	Stretching vibration of the aromatic ring C-C
1536	Amide II, stretching vibration of the benzene ring
1450	Bending vibration of the aliphatic C-H bond
1368	Parallel vibration of the C-H bond in CH_2 Symmetric deformation of aliphatic CH_3
1148	C-(C=O)-O stretching
1067	Symmetric stretching vibration of the CO-O-C
1009	Out-of-plane bending of CH in the benzene ring
978	Vibration of aromatic CH
839	Vibration of aromatic CH
748	Vibration of aromatic CH

5.5.4.3 Effect of the UM2 content on copolymerization

Figures 5.21 clearly show that as the amount of UM2 in the feed to the copolymerization was increased, the percentage of UM2 be incorporated into the PMMA-g-UM2 and PnBMA-g-UM2 copolymers also increased. This was indicated by an increase in the intensity or the areas of the UM2 peaks in these spectra.

In addition, the percentage of UM incorporated into the graft copolymers was determined by FTIR using calibration curves. The percentages of UM2 to PMMA and UM2 to PnBMA used were 9%, 12%, 21%, 32%, 43% and 51 % by weight.

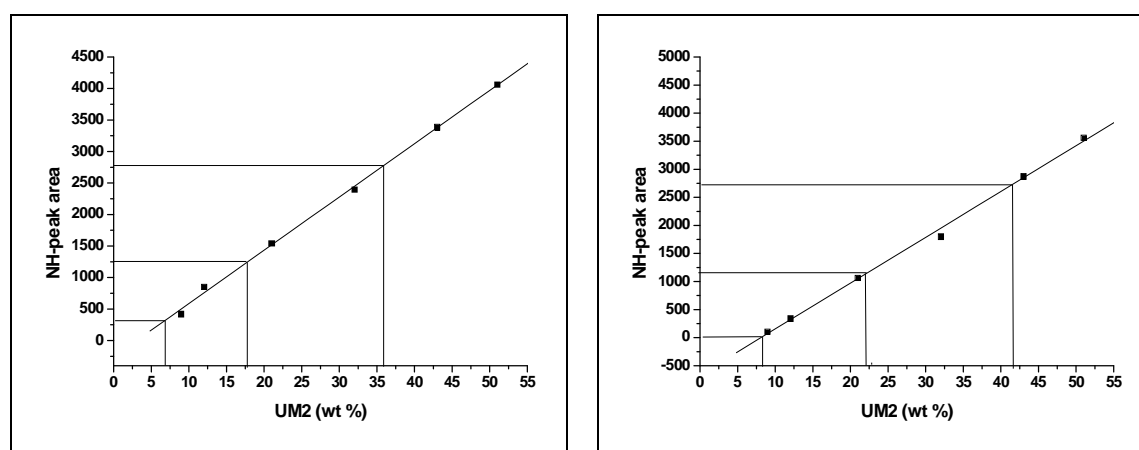


Figure 5.21: Calibration curve of (a) PMMA (b) PnBMA mixed with different quantities of UM2

From the calibration curves in Figures 5.21 (a) and (b), the percentages of UM2 that was incorporated into PMMA-g-UM2 and PnBMA-g-UM2 copolymers are given in Table 5.13. It can be noted that as the amount of UM2 used during graft copolymerization increased, the percentages of UM2 incorporated into both PMMA-g-UM2 and PnBMA-g-UM2 copolymers also increased, which was also confirmed by ¹H-NMR (see Section 5.5.7).

Table 5.13: Percentages UM2 incorporated into the graft copolymers as calculated from FTIR data

	Sample code	UM2/MMA feed ratio by weight	N-H absorption area in FTIR spectrum	UM incorporated into copolymers (wt %)
PMMA-g-UM2	G10M	10/90	31	8.3
	G25M	25/75	1157	22.2
	G55M	55/45	2795	41.6
		UM2/n-BMA feed ratio by weight		
PnBMA-g-UM2	G10B	10/90	300	6.9
	G25B	25/75	1254	17.9
	G55B	55/45	2763	36.7

5.5.5 UV-Vis spectroscopy analysis

UV spectroscopy is a method that is used to determine the absorption wavelength (λ_{\max}) of UV-absorbing species. UM2 were expected to absorb between 254 nm and 300 nm, where the aromatic ring of MDI in UM2 absorbs. The UV spectra of the UM2, PMMA-g-UM2 and PnBMA-g-UM2 copolymers are presented in Figures 5.22 and 5.23.

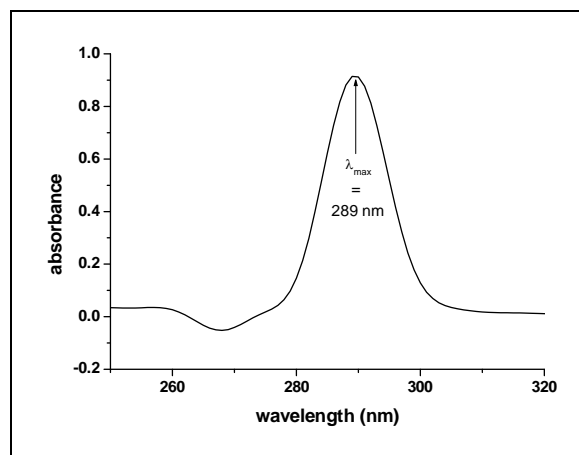


Figure 5.22: UV/Vis spectrum of UM2. THF was used as solvent (UV-cutoff 350 nm).

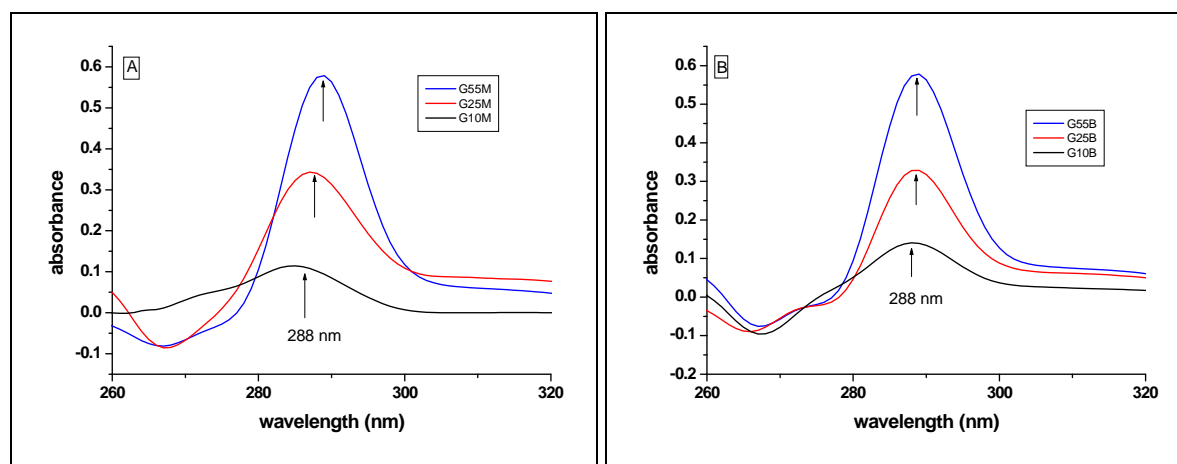


Figure 5.23: UV/Vis spectra of UM2 copolymerized with different quantities of acrylate [(A) PMMA and (B) PnBMA]. THF was used as solvent (UV-cutoff 200 nm).

UV/Vis analysis of the PMMA-g-UM2 and PnBMA-g-UM2 copolymers (Figure 5.23) showed that both graft copolymers have a strong absorption peak in the region where the UM2 absorbs (see Figure 5.22).

A calibration curve was used to determine the equivalent amount of the UM2 in the PMMA-g-UM2 and PnBMA-g-UM2 copolymers. Solutions of various concentrations of the UM2 in DMF were prepared and their UV absorptions measured. A plot of absorbance versus quantity of the UM2, in mg/mL, was constructed (Figure 5.24). Three samples of different known

masses of each graft copolymer were dissolved in THF and their absorbance was measured at a concentration of 0.2 mg/ mL. The corresponding equivalent amounts of UM2 in both copolymers were determined from the calibration curve (see Table 5.14).

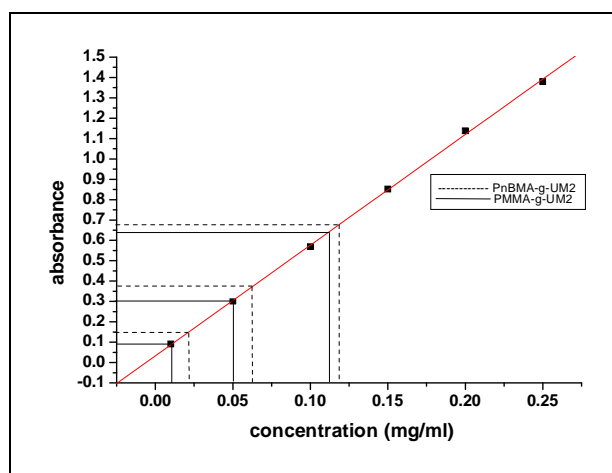


Figure 5. 24: Calibration curve for the determination of the percentage of UM2 incorporated into PMMA or PnBMA. [The dotted lines are extrapolation lines for PnBMA-g-UM2 copolymers and the dash lines for PMMA-g-UM2 copolymers (see Table 5.14)].

Table 5.14: UV/Vis data for the determination of the percentage of UM2 incorporated into PMMA or PnBMA

	Sample code	Feed ratio		Absorbance	Equivalent amount of graft copolymer (mg/mL)	UM2 incorporated into copolymers (wt %*)	
		UM2 (g)	MMA (g)			UV	FTIR
PMMA-g-UM2	G10M	0.50	4.50	0.09	0.011	4.4	8.3
	G25M	1.25	6.75	0.30	0.051	20.4	22.2
	G55M	2.75	2.25	0.65	0.113	46.3	41.6
		UM2(g)	n-BMA(g)				
PnBMA-g-UM2	G10B	0.50	4.50	0.14	0.119	6.5	6.9
	G25B	1.25	6.75	0.38	0.063	24.3	19.9
	G55B	2.75	2.25	0.67	0.021	47.7	36.7

* wt % UM2 was calculated by dividing the equivalent amount of graft copolymer by the equivalent amount of UM2 which is 0.2 mg/mL (all absorbance of graft copolymers in Figure 5.17 were measured at this concentration). The small discrepancies can be due the fact the extraction did not totally remove unreacted UM2 and a small peak remained in the HPLC plots (see Section 5.5.2).

Figures 5.23 and Table 5.14 clearly show that as the amount of UM2 increased during copolymerization, the percentage of UM as incorporated into the PMMA-g-urethane and PnBMA-g-urethane copolymers also increased, indicated by an increase in the absorbance peak areas of the UM2 peaks in the spectra.

5.5.6 ^{13}C -NMR analysis

^{13}C -NMR analysis of graft copolymers after extraction also confirmed the presence of the branches of UM2 in the copolymers.

5.5.6.1 PMMA-g-UM2 copolymers

Figure 5.25 compares the ^{13}C -NMR spectra of PMMA-g-UM2 copolymers to the spectrum that of the PMMA homopolymer. The ^{13}C -NMR spectra of PMMA-g-UM2 copolymers show all carbon peaks that originate from the PMMA in addition to new peaks which correspond to the UM2 carbon peaks (see Section 5.4.1.4). Aromatic carbon peaks from MDI appeared in the region between $\delta = 117$ and $\delta = 140$ ppm. The carbon peak of the methylene which originates from the NPG in the UM2 appeared at $\delta = 61.3$ ppm. In addition, the ^{13}C -NMR peaks ascribed to the vinylic carbon of the UM2 at $\delta = 127.55$ and $\delta = 131.39$ ppm were observed to have completely disappeared upon copolymerization with MMA. These results show that the UM2 was successfully incorporated into PMMA and confirm the results of analysis by FTIR and SEC.

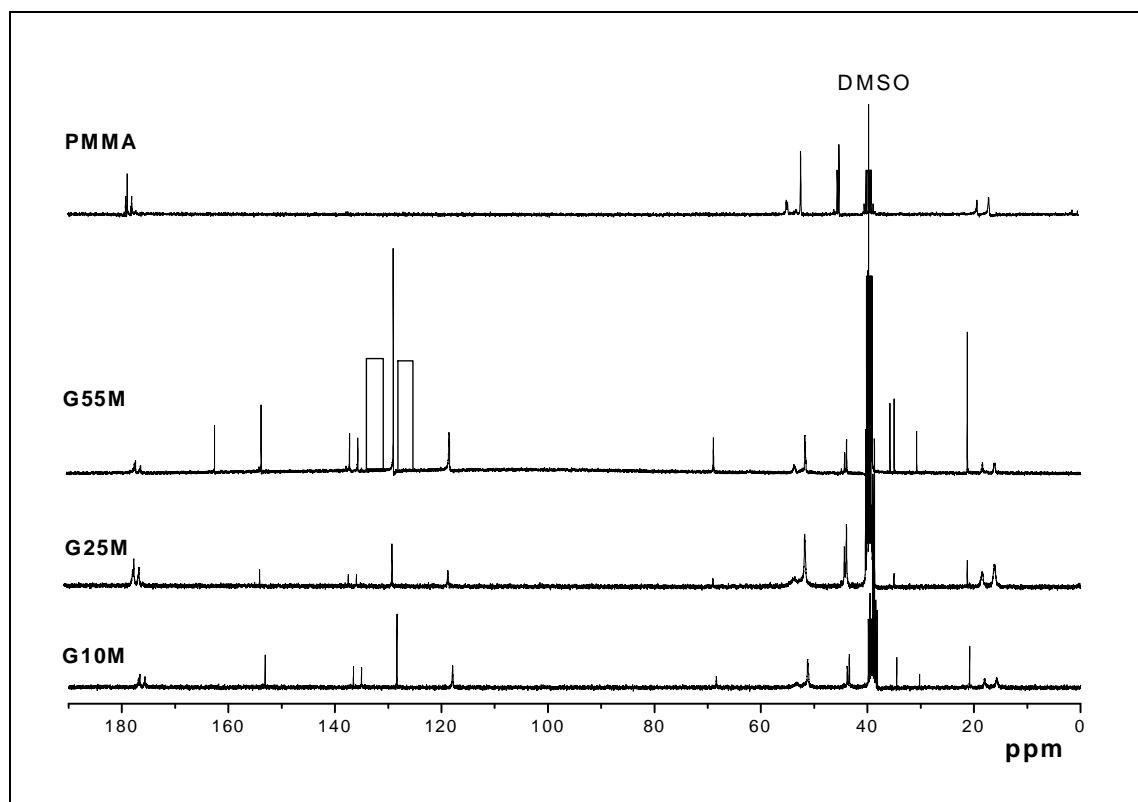


Figure 5.25: ^{13}C -NMR spectra of PMMA-g-UM2 copolymers and PMMA homopolymer dissolved in DMSO. (See Table 5.9 for explanation of codes G10M, G25M and G55M.)

5.5.6.2 PnBMA-g-UM2 copolymers

Figure 5.26 compares the ^{13}C -NMR spectra of the PnBMA-g-UM2 copolymers to that of the spectrum of the PnBMA homopolymer. The ^{13}C -NMR spectra of the PnBMA-g-UM2 copolymers show all carbon peaks originate from the PnBMA as well as new peaks which correspond to the UM2 carbon peaks (see Section 5.4.1.4), namely the aromatic carbons peaks from MDI which appear in the region between $\delta = 118$ and $\delta = 139$ ppm. The carbon peak of the methylene which originates from the NPG in the UM2 appeared at $\delta = 62.5$ ppm. In addition, the ^{13}C -NMR peaks ascribed to the vinylic carbon of the UM2 at $\delta = 127.55$ and $\delta = 131.39$ ppm were observed to have completely disappeared upon copolymerization with MMA. These results show that the UM2 was successfully incorporated into PMMA and confirm the results of FTIR and SEC.

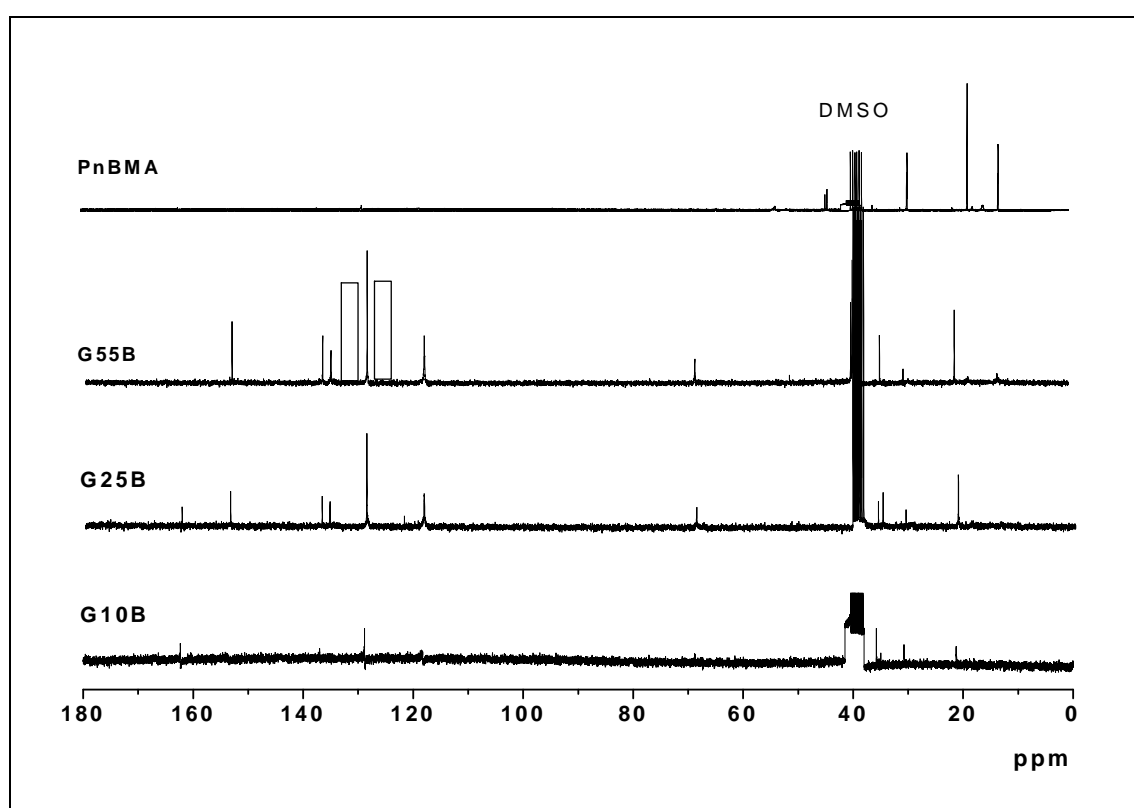


Figure 5.26: ^{13}C -NMR spectra of PnBMA-g-UM2 copolymers and PnBMA homopolymer dissolved in DMSO. (See Table 5.11 for explanation codes of G10B, G25B and G55B.)

5.5.7 ^1H -NMR of methacrylic-urethane graft copolymers

^1H -NMR analysis was also carried out to confirm the formation of the graft copolymers and to calculate the percentages of UM2 incorporated into the graft copolymers. Samples of synthesized graft copolymers were taken to run in the ^1H -NMR instrument after all the unreacted and unreactive UM2 removed, as was confirmed by SEC (see Section 5.4.2.1)

5.5.7.1 PMMA-g-UM2 copolymers

Figure 5.27 presents a typical comparison of the $^1\text{H-NMR}$ spectrum of PMMA-g-UM2 to that of the PMMA homopolymer. The $^1\text{H-NMR}$ spectrum of the PMMA-g-UM2 copolymer shows all the proton peaks that originate from the PMMA, e.g. the peak at $\delta = 3.45$ ppm which corresponds to methyl proton of the O-CH₃ of PMMA in addition to new peaks which corresponding to UM2 proton peaks (see Section 5.4.1.3), and new integrated peaks of UM2 appear in the PMMA-g-UM2 spectrum. The aromatic protons from the MDI appeared at $\delta = 7.05$ ppm and $\delta = 7.33$ ppm, urethane protons were observed at $\delta = 9.5$ ppm and the methylene protons from MDI were assigned to the peak at 3.72 ppm. The methylene protons from NPG were assigned to the peaks at $\delta = 0.96$ ppm. This shows that the UM2 was successfully incorporated into the graft copolymer system. In addition, the peaks ascribed to the vinylic protons of the UM2 in the region $\delta = 6.18$ ppm to $\delta = 6.94$ ppm were observed to have completely disappeared upon copolymerization of MMA.

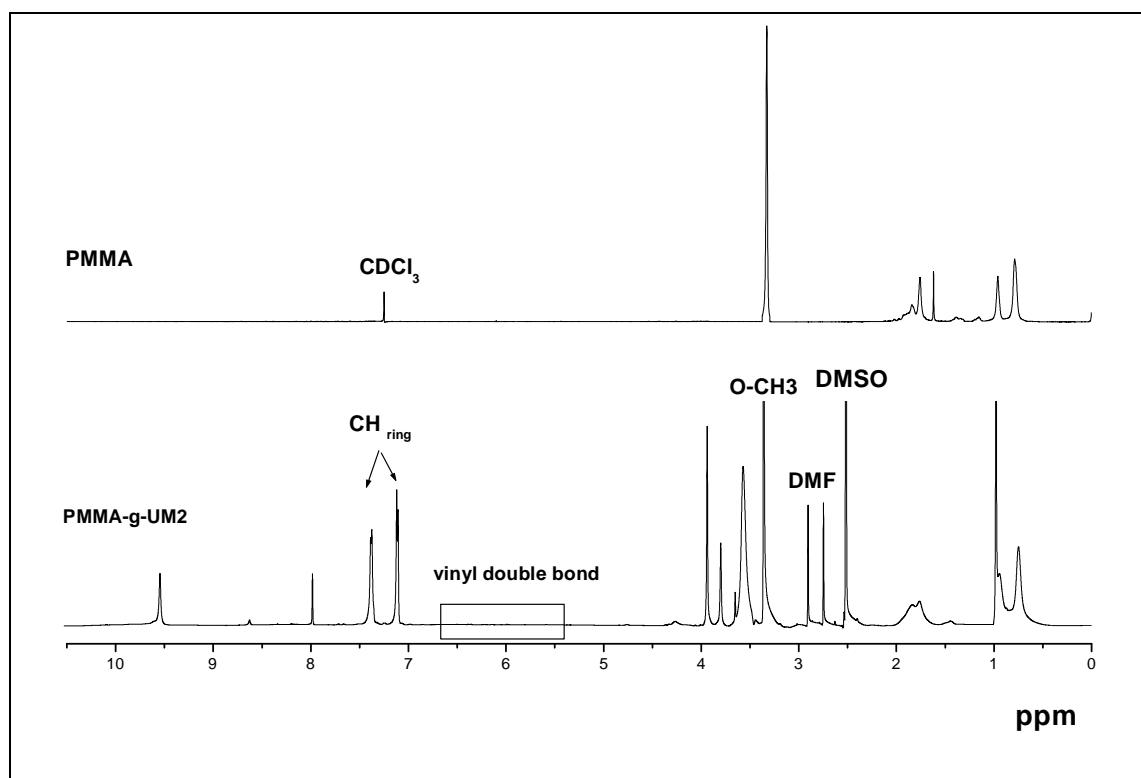


Figure 5.27: $^1\text{H-NMR}$ spectrum of PMMA-g-UM2 copolymer (G55M), dissolved in DMSO.

5.5.7.2 PnBMA-g-UM2 graft copolymers

Figure 5.28 compares the $^1\text{H-NMR}$ spectra of PnBMA-g-UM2 copolymers to that of a PnBMA homopolymer, showing integration of peaks in the graft copolymer spectrum. The two peaks $\delta = 7.05$ ppm and $\delta = 7.33$ ppm of the graft copolymers are mainly attributed to the aromatic protons of MDI in the repeat unit of UM2, and the peak at $\delta = 3.41$ ppm corresponds to the methylene proton of the O-CH₂ of PnBMA. These results show that the UM2 was successfully incorporated into the PnBMA polymer chain. In addition, the peaks ascribed to

the vinylic protons of the UM2 in the region $\delta = 6.18$ ppm to $\delta = 6.94$ ppm were observed to have completely disappeared upon copolymerization of n-BMA.

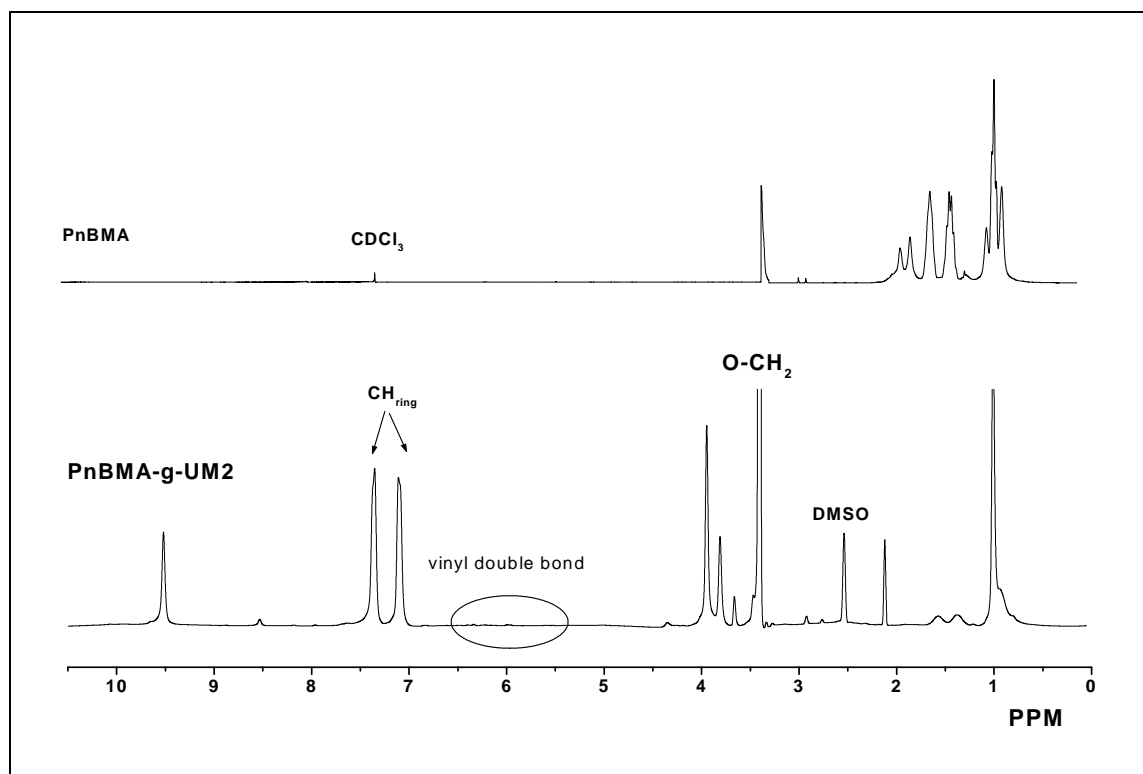


Figure 5.28: ¹H-NMR spectrum of PnBMA-g-UM2 copolymer (G55B) and PnBMA homopolymer dissolved in DMSO.

5.5.7.3 Determination of the percentage UM2 in the graft copolymers using a ¹H-NMR technique

The amount of the UM2 that was incorporated into the two copolymers was determined by ¹H-NMR spectroscopy. Calculation was based on the integration of the proton of the aromatic ring of the UM2 ($\delta = 7.05$ ppm and $\delta = 7.33$ ppm) in both graft copolymers versus the methoxy group of PMMA ($\delta = 3.45$ ppm) in the PMMA-g-UM2 copolymers, and the methylene-oxy of PnBMA ($\delta = 3.41$ ppm) in the PnBMA-g-UM2 copolymers. These calculations were performed for both graft copolymers by using equations 5.1 and 5.2, respectively. Results are given in Table 5.15.

$$UM2\% = \left[\frac{\delta_{ring}/(N_{ring}*(n+1))}{\delta_{ring}/(N_{ring}*(n+1)) + \delta_{CH_3O}/N_{CH_3O}} \right] \times 100 \quad (5.1)$$

$$UM2\% = \left[\frac{\delta_{ring}/(N_{ring}*(n+1))}{\delta_{ring}/(N_{ring}*(n+1)) + \delta_{CH_2O}/N_{CH_2O}} \right] \times 100 \quad (5.2)$$

where UM2% is the mole percentage of UM2 that was incorporated into the graft copolymer, δ_{ring} , δ_{CH_3O} and δ_{CH_2O} are the integration intensities of the aromatic ring, CH₃O and CH₂O protons, N ring, N CH₃O and N CH₂O are the number of protons and n is the average urethane macromonomer chain length, which equals 4, as calculated using ¹H-NMR (see Section 5.4.1.3)

Table 5.15: Percentage UM2 incorporated into graft copolymers, as determined by ¹H-NMR

	Sample code	UM2 feed content (wt %)	Integration area of CH ₃ O protons	Integration area of aromatic ring protons	UM2 incorporated into copolymers (mol %)	UM2 incorporated into copolymers (wt %) (Mw of UM2 by ¹ H-NMR=1816 g/mol)	UM2 incorporated into copolymers (wt %) (Mw of UM2 by SEC=2353 g/mol)
PMMA-g-UM2	G10M	10	1	0.008	0.25	3.11	4.18
	G25M	25	1	0.030	1.24	20.43	26.16
	G55M	55	1	0.120	4.34	36.50	43.07
			Integration area of CH ₂ O protons	Integration area of aromatic ring protons			
PnBMA-g-UM2	G10B	10	1	0.010	0.23	6.21	6.63
	G25B	25	1	0.080	1.11	17.08	20.90
	G55B	55	1	0.18	3.26	37.99	44.28

Table 5.15 shows that as the amount of UM2 increased during graft copolymerization, the mole and weight percentages of UM2 incorporated into both PMMA-g-UM2 and PnBMA-g-UM2 copolymers also increased. The UM2 content in the graft copolymers, as determined by ¹H-NMR, was 3.1–36.50 wt % for PMMA-g-UM2 and 6.2–38.0 by weight for PnBMA-g-UM2. These results confirm the UV-Vis and FTIR results that were recorded earlier in this study.

5.6 Thermal and mechanical analysis

5.6.1 Thermogravimetric analysis (TGA)

TGA was performed in order to evaluate the effect of the UM2 content on the decomposition patterns and thermal stability of the polyacrylate copolymers.

5.6.1.1 Thermal stability of urethane macromonomer (UM2)

As was mentioned in section 4.5.4.1, a complex compound like polyurethanes has the onset of degradation of Pus governed by the weakest link in the chain, whereas the most available group in the chain is the dominant factor for overall thermal stability. Pus with different backbones have different thermal stabilities.

The thermal decomposition patterns of UM2 were determined by TGA. Typical thermograms along and its derivative curve (DTG) were recorded in a nitrogen atmosphere and results shown in Figure 5.29.

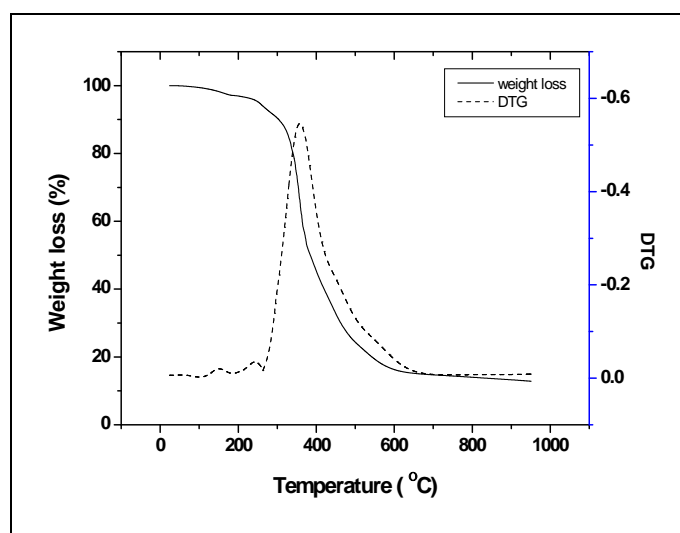


Figure 5.29: TGA thermogram of UM2 and its derivative curve.

Figure 5.29 indicates the three-stage thermal degradation of UM2. The first stage and second stage degradation are very small, and took place in the range 105–160 °C and 160–264 °C respectively. The weight loss in these two steps was 2% and 1% respectively which might be due to some water and unreacted raw martial still present in the UM2 sample. The third stage degradation in the temperature range 264–623 °C occurred with a weight loss of 92%. This could be due to thermal decomposition of all the segments of UM2. In this step the weight loss may be due to liberation of HCN, nitriles or aromatic carbon and ethers.²⁵ This stage ends with the loss of all volatile fractions, and a mass loss that does not change much after 603 °C.

5.6.1.2 PMMA-g-UM1 copolymers

Primary TGA curves for MMA copolymerized with different amounts of UM2, in the range from 0–55% by weight according to MMA, are shown in Figure 5.30(a). The decomposition patterns for all the graft copolymer samples were similar. There was a slight improvement in thermal stability as the amount of UM1 increased, which might be due to optimum morphological interaction between PMMA and the urethane segments.

PMMA degrades in three steps, and is virtually completely destroyed by 465 °C. The first stage of degradation occurs in the temperature range 205–290 °C, which is attributed to depolymerization after cleavage of weak links, i.e., head-to-head linkages.²⁶ The second stage of the degradation takes place in the temperature range 290–390 °C, which is attributed to a larger mass loss due to end chain unsaturation²⁷. The third stage of degradation occurs in range 390–450 °C which accounts for the majority of the degradation, and is due to random scission.²⁷ The TGA curve and its derivative are shown in Figure 5.30(b).

The weight loss obtained from TGA thermograms for different degradation steps and the ash content are given in Table 5.16. Figure 5.30(b)-(f) revealed three-step thermal degradation process for all PMMA-g-UM2 copolymers. The explanation for this three-step thermal degradation process for all PMMA-g-UM2 copolymers is similar to that for the three-step thermal degradation process for all PMMA-g-UM1 copolymers (See Section 4.5.4.1).

Table 5.16: Thermal data obtained from TGA scans for PMMA-g-UM2

Composition of UM1/PMMA (wt/wt)	Degradation stages	Temperature range (°C)			Weight loss (%)
		Ti	Tmax	Tf	
0/100	1	133	181	241	12.3
	2	241	313	347	20.4
	3	347	406	465	67
	ash				0.3
10/90	1	207	282	318	6.3
	2	318	349	409	31.3
	3	409	474	536	61.4
	ash				1.7
25/75	1	243	285	333	4.3
	2	263	328	377	28.2
	3	377	438	538	63.1
	ash				2.5
55/45	1	263	255	330	12
	2	300	400	438	17.4
	3	438	483	607	63.9
	ash				6.4
100/0	1	105	135	160	24
	2	160	239	264	68.7
	ash				6.3

Table 5.16 shows that the copolymers, especially in the low temperature range (where PMMA starts at 133 °C and UM2 at 105 °C), are very much more stable; the first signs of degradation appear at 263 °C for the 55/45 copolymer.

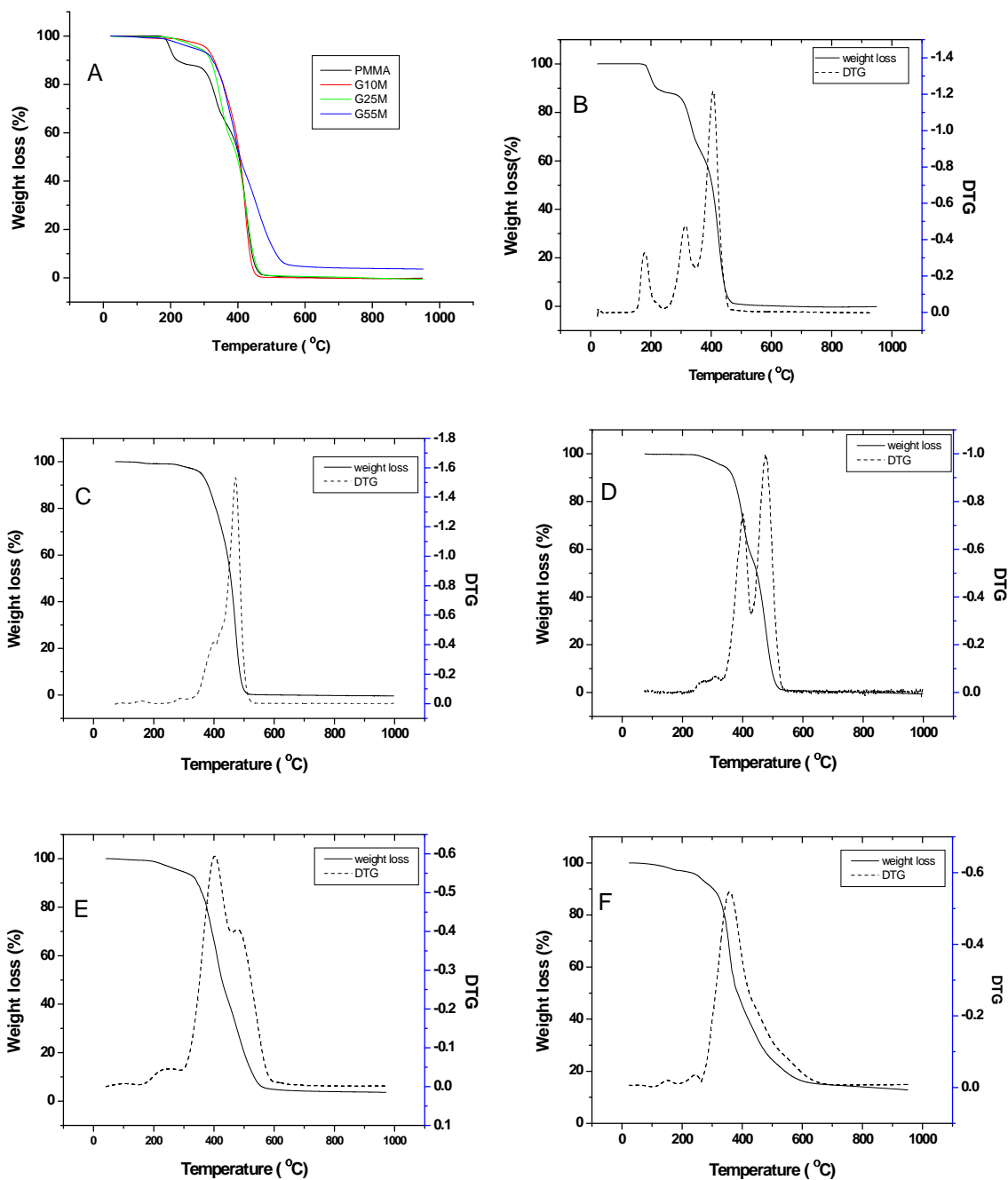


Figure 5.30: TGA thermograms and their derivate curves for: (A) TGA curves of MMA copolymerized with different amounts of UM1, (B) 0/100, (C) 10/90, (D) 25/75, (E) 55/45, and (F) 100/0 UM2/MMA copolymers.

5.6.1.3 PnBMA-g-UM2 copolymers

Primary TGA curves for n-BMA copolymerized with different amounts of UM2 are shown in Figure 5.31(a). The decomposition patterns for all graft copolymers samples were similar. There was however a slight improvement in thermal stability as the amount of UM2 in the graft copolymer increased, which might be due to better morphological interaction between PnBMA and UM2 segments.

Figure 5.31(b) shows that PnBMA is degraded in three steps. An explanation for this is given in Section 4.5.1.4.1

The weight loss obtained from TGA thermograms for different degradation steps and ash content are given in Table 5.17. Figure 31 (b)-(f) revealed a two-step thermal degradation process for PnBMA-g-UM2 copolymers. The first stage of degradation occurs in the temperature range 255–390 °C occurred with a weight loss of 38–57%. As the percentage of UM2 in the PnBMA-g-UM2 is increased the onset decomposition temperature (T_i) is shifted towards higher temperature. The weight loss during the first stage of degradation was found to decrease with the increase in PnBMA content in the PnBMA-g-UM2. The second stage of degradation of PnBMA-g-UM2 in the temperature range 355–549 °C occurred with a weight loss of 57–71%. The above observation was supported by the fact that as the UM2 content in the PnBMA-g-UM2 copolymer decreased, weight loss in this step was increased.

Table 5.17: Thermal data obtained from TGA scans for PnBMA-g-UM2

Composition of UM1/PnBMA (wt/wt)	Degradation stages	Temperature range (°C)			Weight loss (%)
		T_i	T_{max}	T_f	
0/100	1	190	255	275	7
	2	275	334	351	28.4
	3	351	402	491	64.2
	ash				0.3
10/90	1	255	326	355	38
	2	355	395	497	60.3
	ash				1.7
25/75	1	261	356	377	47.7
	2	377	397	519	49.7
	ash				2.5
55/45	1	265	366	390	57.1
	2	390	414	549	40.4
	ash				6.5
100/0	1	105	138	163	2
	2	163	237	264	1
	3	264	353	603	91
	ash				6.9

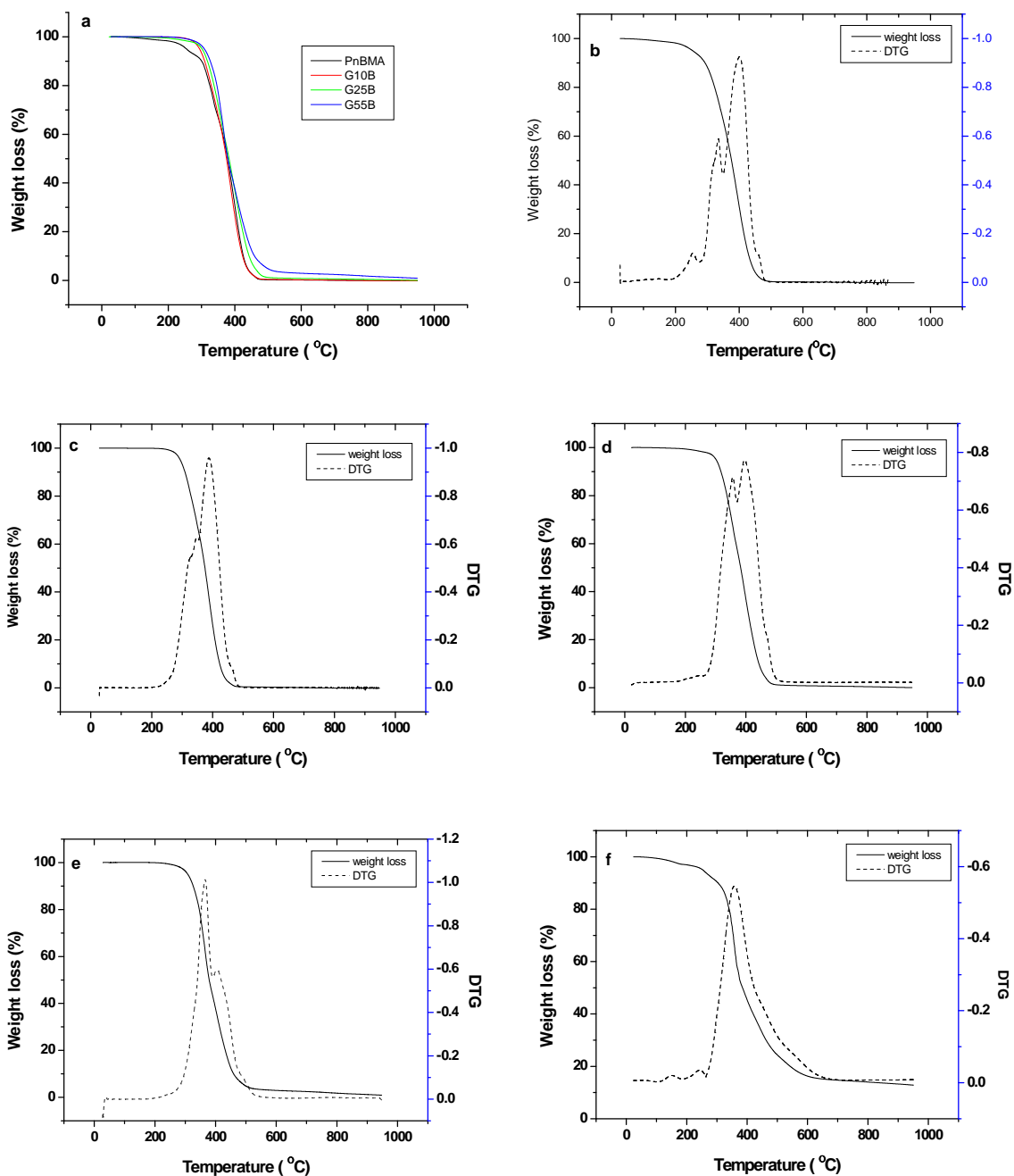


Figure 5.31: TGA thermograms and their derivate curves for: (a) TGA curves of n-BMA copolymerized with different amounts of UM2, (b) 0/100, (c) 10/90, (d) 25/75, (e) 55/45, and (f) 100/0 UM2/n-BMA copolymers.

5.6.2 DMA analysis

The dynamic mechanical behaviour of a graft copolymer depends on the miscibility of the polymer pair. If the polymer pair is miscible, only one phase is formed and one sharp glass transition will be observed. Conversely, if two polymers are totally immiscible, two glass transitions will be observed, that is, at the glass transitions of the homopolymers.

As in Section 4.5.4.2, the structural differences between soft and hard blocks normally result in phase separation. The degree of phase separation affects the properties of the

polymer.^{3,28-31} Phase separated domains can be decreased by increasing the compatibility between the hard and soft segments.

In this study, different quantities of UM2 were incorporated into the acrylate backbone. For incompatible copolymers the damping temperature ($\tan \delta$) curve shows the presence of two peaks corresponding to the glass transitions of the individual polymers, whereas in highly compatible copolymers only a single peak that is located in between the transition temperatures of the pure polymers is observed.³² In the case of partially compatible copolymers, two separate broad peaks corresponding to the individual polymer components or one broad peak are observed, but with their positions shifted closer to the single (compatible) peak, depending on the copolymer composition and the influence of the microstructure.³³⁻³⁵

5.6.2.1 PMMA-g-UM2 copolymers

The dynamic mechanical properties such as $\tan \delta$, and storage modulus (E') versus temperature of the homopolymers and graft copolymer are shown in Figures 5.32 and 5.33. $\tan \delta$, and the storage modulus shows a transition arising at 100–110 °C due to the segmental motion. This corresponds to the T_g of PMMA. UM2 shows a glass transition temperature at 147 °C. When MMA was copolymerized with UM2 the T_g of the copolymer shifted to a higher temperature, to between the T_g values of the UM2 and PMMA. This indicates a measure of compatibility and mixing where, because of the varying sequence length of the MMA in the backbone and the spread from a couple of units to many urethane units in the side chains, one can expect short side chains to mix. The $\tan \delta$ traces and storage modulus (E') of the graft copolymer showed only a single peak between the PMMA and UM2 peaks, which also suggests a homogeneous (i.e. not phase separated) material. The T_g was measured as the onset temperature, and the T_g values of the PMMA-g-UM2 copolymers varied between 105 and 116 °C. It was also observed that the T_g values of PMMA-g-UM2 copolymers had single T_g values and that the value increased with increasing UM2 content incorporated. This confirmed that the UM2 and PMMA segments were largely compatible and that copolymers were formed. The T_g values of all the synthesized PMMA-g-UM2 copolymers are tabulated in Table 5.18 (T_g defined here as extrapolated onset temperature peak of the $\tan \delta$).

When the amount of UM2 was increased to 55 wt % during copolymerization (at 36.50 wt % UM2 incorporation into the graft copolymers), microphase separation occurred. Two T_g values are observed in all $\tan \delta$, loss modulus (E'') and storage modulus traces (107 °C, and 147 °C), which are due to the PMMA and harder UM2, respectively (Figures 5.32-5.34) This indicated that there was a degree of microphase separation. Detection of glass transition temperatures associated with each of the respective homopolymers indicated that the UM2

segments and PMMA segments in the above case were partially separated (microphase separation). This partial phase separation will be due to the degree of mixing and is extended beyond the interface region between the PMMA and UM2 microdomain.

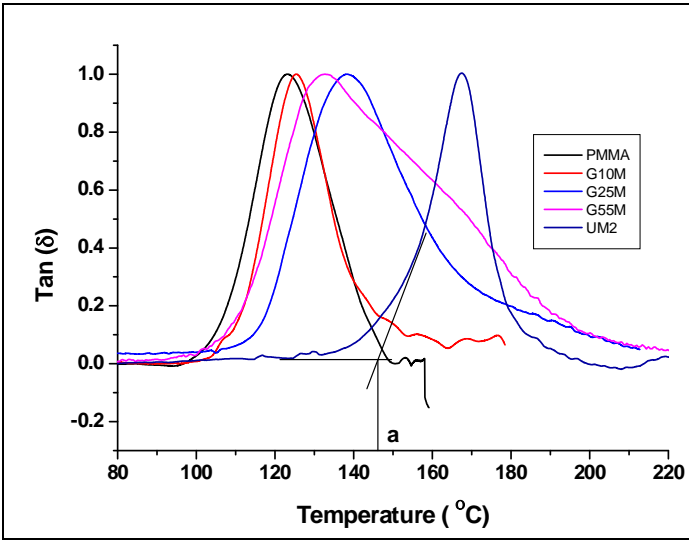


Figure 5.32: tan δ traces of PMMA, UM2 and PMMA-g-UM2 copolymers. Note (a: extrapolated T_g at onset of UM2 tan δ.)

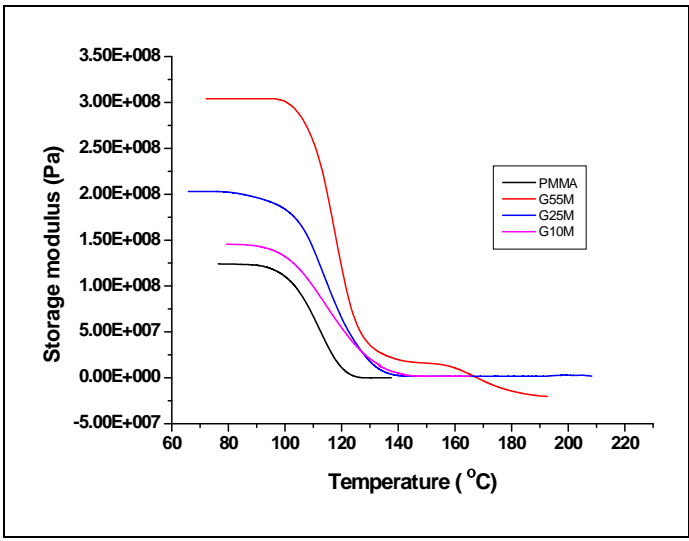


Figure 5.33: Storage modulus traces of PMMA and PMMA-g-UM2 copolymers.

Figure 5.33 shows that G55M has partial compatibility when incorporation is low while for 36.1 wt % incorporation of UM2 onto the graft copolymers there is a small secondary storage modulus at 107 °C to 145 °C, where separation reoccurred. Figure 5.33 also shows dramatic increases in modulus as the amount of UM2 incorporated into the graft copolymers was increased for example, the sample containing 36.50 wt % UM2 (according to $^1\text{H-NMR}$ calculations) shows a storage modulus that is about 2.35 greater than that of PMMA. Overall, DMA analysis reveals that the PMMA-g-UM2 copolymers are much stiffer and can withstand higher temperatures compared to the PMMA homopolymer. The effect of the amount of UM2

that was incorporated into the PMMA-g-UM2 copolymer and that affects the storage modulus value, is shown in Table 5.18

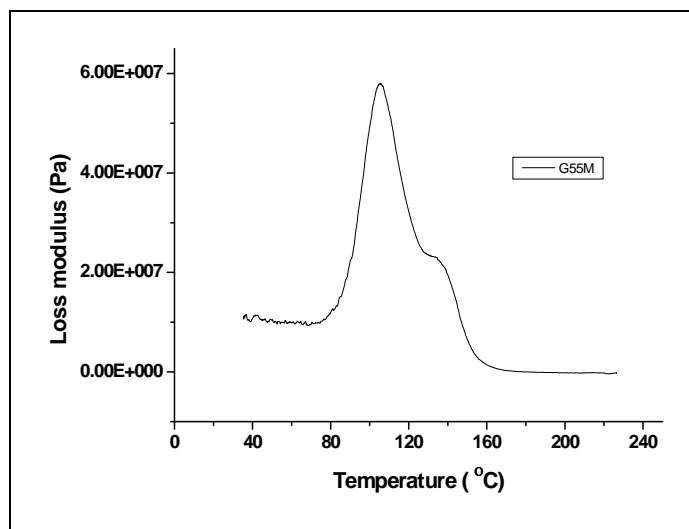


Figure 5.34: Loss modulus of PMMA-g-UM2 copolymer containing 36.50 wt % UM2.

Figure 5.34 shows the loss modulus of PMMA-g-UM2 copolymer containing 36.50 wt % UM2, which confirms a significant degree of mixing, especially at the interfacial areas of two phases, as a peak containing a single shoulder is found, not two peaks.

5.6.2.2 PnBMA-g-UM2 copolymers

The variation of dynamic mechanical properties such as $\tan \delta$, and storage modulus versus temperature of the homopolymers and graft copolymer are shown in Figures 5.35 to 5.37. The $\tan \delta$, storage modulus, and loss modulus show a transition arising at 40-45 °C due to the segmental motion. This corresponds to the glass-transition temperature (T_g) of PnBMA. UM2 shows a glass transition temperature at 135 °C as shown in the extrapolated peak in Figure 5.35. When n-BMA was copolymerized with UM2 the T_g of the copolymer shifted to a higher temperature, to between the T_g values of the UM2 and PnBMA. The $\tan \delta$ traces and storage modulus (E'') of graft copolymer showed only a single peak between the PnBMA and UM2 peaks, which suggested a homogeneous (i.e. not phase separated) material. The T_g was measured as the onset temperature, and the T_g values of the PnBMA-g-urethane copolymers varied between 38-45 °C. It was also observed that the T_g values of PnBMA-g-UM2 graft copolymers had single T_g values and that the value increased with increasing UM2 content. This confirmed that the UM and PnBMA segments were largely compatible and that copolymers were formed. The T_g values of all the synthesized PnBMA-g-UM2 copolymers are tabulated in Table 5.18. (T_g defined here as extrapolated onset peak of $\tan \delta$).

When the amount of UM2 added was increased to 55 wt % during copolymerization (to give 37.99% UM2 incorporation into the graft copolymers), partial microphase separation occurred. Two T_g values are observed in all $\tan \delta$, loss modulus (E'') and storage modulus

traces (45 °C, 130 °C), which are due to the PnBMA and harder UM2, respectively. This indicated that there was a degree of microphase separation. Detection of glass transition temperatures associated with each of the respective homopolymers indicated that the UM2 segments and PnBMA segments in the above case were locally separated (microphase separation) into distinct regions. However, the increase in the onset T_g over 34 °C of PnBMA shows minor mixing, due to short backbone sequences and short branch sequences (a result of the addition synthesis).

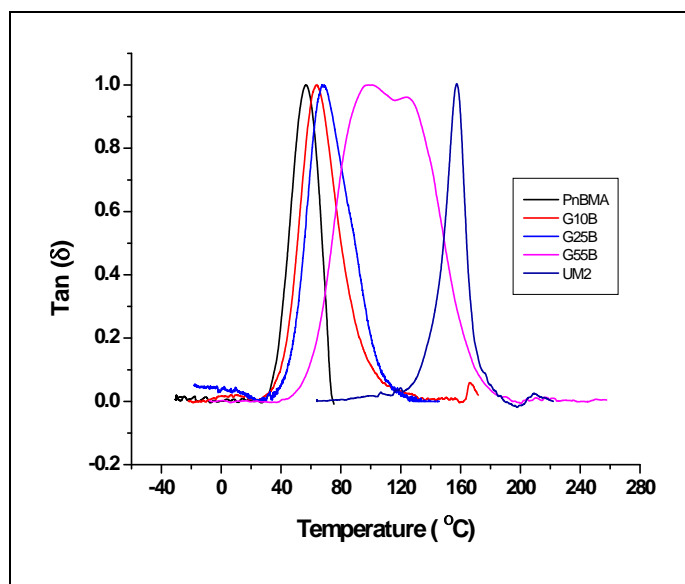


Figure 5.35: $\tan \delta$ traces of PnBMA, UM2 and PnBMA-g-UM2 copolymers.

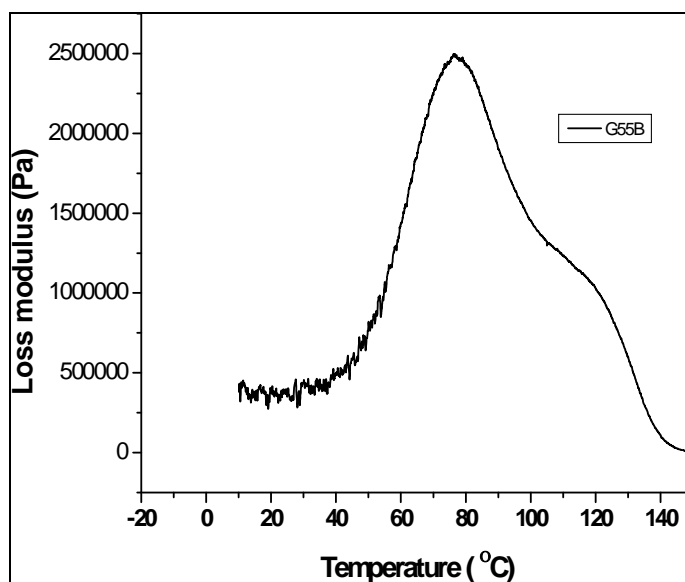


Figure 5.36: Loss modulus of PMMA-g-UM2 copolymer containing 37.99 wt % UM2.

On other hand, the PnBMA-g-UM2 copolymers show dramatic increases in modulus as the amount of UM2 incorporated into graft copolymers was increased (Figure 5.37). For example, the sample containing 37.99 wt % UM2 (according to $^1\text{H-NMR}$ calculations) shows a storage modulus about 3.73 times that of PnBMA. This modulus increase shows partial

compatibility and matches the increases in the T_g . The overall DMA analysis reveals that the PMMA-g-UM2 copolymers are much stiffer and can withstand higher temperatures compared to PMMA homopolymer. The effect of the amount of UM2 that was incorporated into PMMA-g-UM2 into the storage modulus value is shown in Table 5.18.

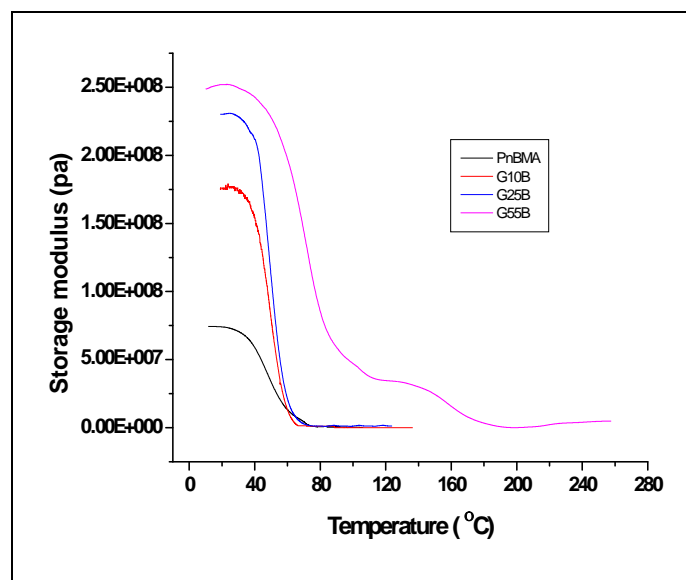


Figure 5.37: Storage modulus traces of PnBMA and PnBMA-g-UM2 copolymers.

Table 5.18: DMA results for PMMA-g-UM2 and PnBMA-g-UM2 copolymers at varying UM2 ratio in polymerization feed

	Sample code	UM2 feed ratio (wt %)	UM2 incorporated into copolymers as calculated by $^1\text{H-NMR}$ (wt %)	T_g ($^{\circ}\text{C}$) at onset	T_g ($^{\circ}\text{C}$) at max peak height	$E' \times 10^8$ (Pa)
PMMA-g-UM2	PMMA	0	-	108	125	1.3
	G10M	10	3.09	113	136	1.5
	G25M	25	20.35	115	138	2.0
	G55M	55	36.50	107, 147	132	3.0
PnBMA-g-UM2	PnBMA	0	-	34	56	0.7
	G10B	10	6.16	37	63	1.8
	G25B	25	16.96	40	68	2.2
	G55B	55	37.99	45, 130	90	2.5

5.6.3 Differential scanning calorimetry (DSC)

Differential scanning calorimetry (DSC) is a commonly used tool to determine molecular organization changes, such as phase separation, and glass transition. As mentioned earlier in Chapter 3, both the mechanical and thermal properties of the copolymer can be affected dramatically by phase mixing. Interaction between the soft and hard segments can increase the glass transition temperature of the soft segment and decrease the T_g of the hard segment. The glass transition temperatures of the graft copolymer and the macromonomers were determined using DSC. The results for all graft copolymers and macromonomers are shown in Table 5.19. UM2 showed T_g at 150 °C, the T_g of the PMMA is about 108 °C) and the T_g of PnBMA is about 34 °C.

The DSC results of both PMMA-g-UM2 and PnBMA-g-UM2 copolymers with high UM2 content shows the presence of two T_g values, which indicates the formation of phase separation, where the UM2 region aggregates separately from methyl methacrylate and from n-butyl methacrylate. These results correspond well with the DMA results (Table 5.19). The T_g decreased with a decrease in the macromonomers content. This is expected, due to an decrease in the number of (hard chain) UM2 chains which have relatively high T_g .

This decrease in the T_g could be explained as follows. At low macromonomer content there are less very long chain branches which can assimilate and form a separate phase. In the case of the high macromonomer content the longer grafts in the copolymer can better find themselves and can assimilate more resulting in high T_g . From the thermal properties of grafts, the T_g is affected by the macromonomer content and here there are sufficient short branches and sterically hindered branches that form mixing.

$$T_g \text{ mix} = \alpha_{\text{PMMA}} T_{g \text{ PMMA}} + \alpha_{\text{UM2}} T_{g \text{ PMMA}}$$

where α is volume present

Table 5.19: DSC results for PMMA-g-UM2 and PnBMA-g-UM2 copolymers at varying UM2 ratios in polymerization feed.

	Sample code	UM2 feed ratio (wt %)	UM2 incorporated into copolymers as calculated by ¹ H-NMR (wt %)	T _{g1} (°C)	T _{g2} (°C)
PMMA-g-UM2	PMMA	0	-	118	-
	G10M	10	3.09	113	-
	G25M	25	20.35	115	-
	G55M	55	36.50	117	148
PnBMA-g-UM2	PnBMA	0	-	34	-
	G10B	10	6.16	37	-
	G25B	25	16.96	40	-
	G55B	55	37.99	57	150

Figures 5.38 and 5.39 show DSC results for the PMMA-g-UM2 and PnBMA-g-UM2 copolymers, respectively. The two T_g values of the graft copolymers are similar to those PMMA and UM2, or PnBMA and UM2 (measured by DMA). This offers additional evidence for incorporation of UM2 into the graft copolymers, and their phase separation.

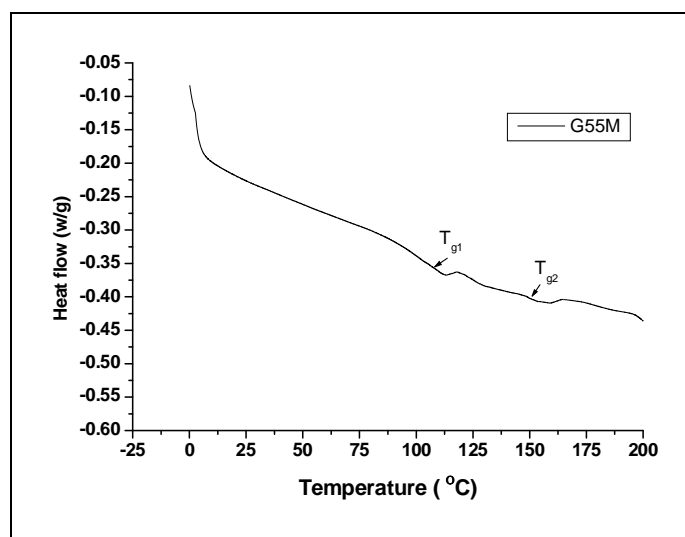


Figure 5.38: DSC trace of PMMA-g-UM2 copolymer containing 37.99 wt % UM2.

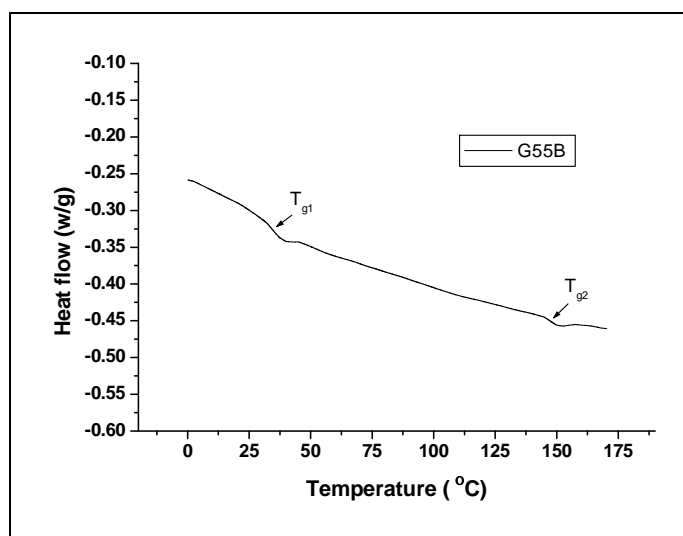


Figure 5.39: DSC trace of PnBMA and PnBMA-g-UM2 copolymer containing 36.50 wt % UM2.

5.7 Transmission electron microscopy

The presence of a two-phase nature has been strongly confirmed from the DSC and DMA results listed above. In order to confirm this hypothesis more directly, transmission electron microscopy was conducted. As shown in Figures 5.40 and 5.41, TEM images below show evidence of phase segregated morphologies on both graft copolymers PMMA-g-UM2 and PnBMA-g-UM2 copolymers. In the images the difference in the electron densities of the PMMA, PnBMA and urethane components in the graft copolymer allow the various components to be distinguished by TEM. UM2 is more electrodense due to the aromatic backbone and will tend to show darker regions in the TEM which appear to form a spherical phase. PMMA and PnBMA are less electro dense and show lighter in the image. The images in Figures 5.40 and 5.41 show evidence of darker and lighter regions which strongly suggest results of nanophase segregation.

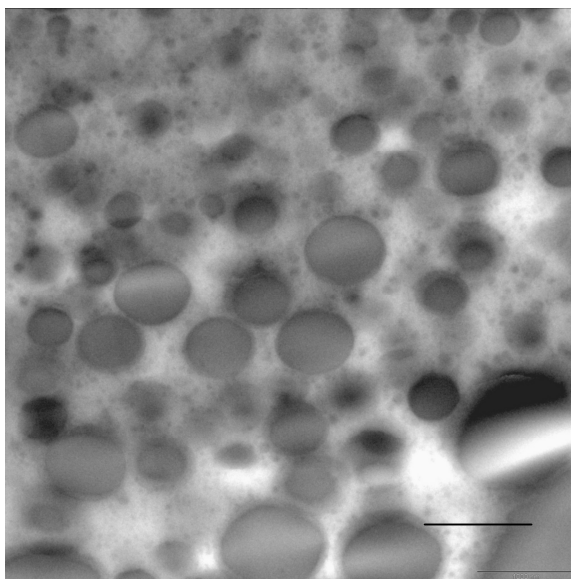


Figure 5.40: TEM image of PMMA-g-UM2 copolymer containing 37.99 wt % UM2 tinted with osmium tetroxide. The light regions are soft PMMA domains and the dark regions are hard urethane domains. Bar = 100 nm.

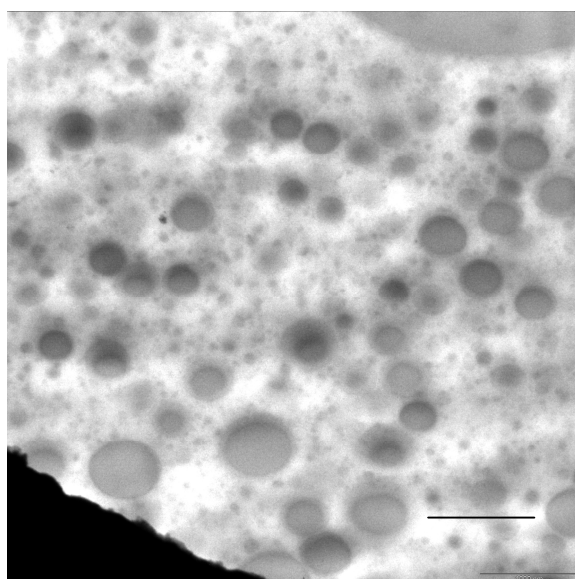


Figure 5.41: TEM image of PnBMA-g-UM2 copolymer containing 36.50 wt % UM2 tinted with osmium tetroxide. The light regions are soft PnBMA domains and the dark regions are hard urethane domains. Bar = 100 nm.

5.8 Conclusions

Novel urethane macromonomers (UM2), predominantly monofunctional, were successfully synthesized by polyaddition using the pre-polymer method, and their structures confirmed by FTIR and MALDI-TOF-MS, NMR and SEC. UM2 then were used in solution free-radical copolymerization of MMA and n-BMA. The existence of the grafted urethane macromonomer with PMMA and PnBMA was confirmed using FTIR, $^1\text{H-NMR}$, and SEC (with UV and RI

detectors), HPLC, DSC and DMA. The yield of both graft copolymers decreased as the concentration of the urethane macromonomers in the copolymerization feed increased. As the concentration of urethane macromonomer in the copolymerization feed increased, more urethane macromonomer was incorporated into the PMMA and PnBMA backbones, and better thermal stability was found in both PMMA-g-UM2 and PnBMA-g-UM2. In most of the graft copolymers a large measure of compatibility was observed, as was evident from in DSC and DMA results. The T_g values increased as the concentration of urethane macromonomer was increased in the PnBMA-g-UM2 copolymer. A single peak, indicating compatibility, was observed in most of the graft copolymers. Yet in the case of the copolymer with the high UM2 content (both PMMA-g-UM2 a PnBMA-g-UM2 copolymers) there were two glass transition temperatures, corresponding to the PMMA or PnBMA, and UM2 fractions, respectively. The result also indicated that the PMMA or PnBMA and UM2 moieties exhibited partial nanophase separation, as confirmed by TEM.

5.9 References

1. Garrett, J.; Xu, R.; Cho, J.; Runt, J. *Polymer* **2003**, 44, 2711.
2. Otts, D.; Dutta, S.; Zhang, P.; Smith, O.; Thames, S.; Urban, M. *Polymer* **2004**, 45, 6235.
3. Kuran, W.; Sobczak, M.; Listos, T.; Debek, C.; Florjanczyk, Z. *Polymer* **2000**, 41, 8531.
4. Dutta, S.; Karak, N. *Prog. Org. Coat.* **2005**, 53, 147.
5. Jayakumar, R.; Nanjundan, S. *Eur. Polym. J.* **2005**, 41, 1623.
6. Guelcher, S.; Gallagher, K.; Didicr, J.; Klinedinst, D. *Acta/Biomaterialia.* **2005**, 1, 471.
7. Xu, G.; Shi, W. *Prog. Org. Coat.* **2005**, 52, 110.
8. Rosbu, D.; Ciobanu, C.; Casăcaval, C. N. *Eur. Polym. J.* **2001**, 37, 587.
9. Cordeiroa, N.; Belgacemb, M. N.; Gandini, A.; Netoc, C. P. *Ind. Crops Prod.* **1999**, 10, 1.
10. Zagar, E.; Zigon, M. *Polymer* **1999**, 40, 2727.
11. Suresh, S.; Chandure, S. *Chem. Eng. J.* **2008**, 142, 65.
12. Zhou, P.; Frisch, H. *J. Polym. Sci. Part A: Polym. Chem.* **1992**, 2577.
13. Ma, C.; Du, Y.; Wang, F.; Wang, H.; Yang, J. *J. Appl. Polym. Sci.* **2002**, 83, 962.
14. Okamoto, T.; Cooper, L.; Root, W. *Macromolecules* **1992**, 25, 1068.
15. Meadows, M.; Christenson, P.; Howard, L.; Harthcock., A.; Guerra, E.; Turner, B.

- Macromolecules* **1990**, 23, 2440.
16. Weisberg, M.; Gordon, B.; Rosenberg, G.; Snyder, A.; Benesi, A.; Runt, J.
Macromolecules **2000**, 33, 4380.
 17. Dzunuzovic, E.; Tasic, S.; Bozic, B.; Babic, D.; Dunjic, B. *Prog. Org. Coat.* **2005**, 52, 136.
 18. Ito, K.; Kawaguchi, S. *Adv. Polym. Sci.* **1999**, 142, 129.
 19. Tsukahara, Y.; Mizuno, K.; Segawa, A.; Yamashita, Y. *Macromolecules* **1989**, 22, 1546.
 20. Tsukahara, Y.; Tsutsumi, K.; Yamashita, Y.; Shimada, S. *Macromolecules* **1990**, 23, 5201.
 21. Hong, S. C.; Jia, S.; Teodorescu, M.; Kowalewski, T.; K. Matyjaszewski; Gottfried, A. C.; Brookhart, M. *J. Polym. Sci. Part A: Polym. Chem.* **2002**, 40, 2736.
 22. Meijs, G.; Rizzardo, E. *Macromol. Sci. Rev: Macromol. Chem. Phys.* **1990**, C30, 305.
 23. Pasch, H.; Trathnigg, B. *HPLC of Polymers*. Berlin: Springer, 1999.
 24. Degoulet, C.; Perrinaud, R.; Ajdari, A.; Prost, J.; Benoit, H.; Bourrel, M.
Macromolecules **2001**, 34, 2667.
 25. Herrera, M.; Matuschek, G.; Kettrup, A. *Polym. Degrad. Stab.* **2002**, 78, 323.
 26. Holland, B.; Hay, N. *Polym. Degrad. Stab.* **2002**, 77, 435.
 27. Kashiwagi, T.; Inaba, A.; Brown, J.; Hatada, K.; Kitayama, T.; Masuda, E.
Macromolecules **1986**, 19, 2160.
 28. Sheth, J.; Aneja, A.; Wilkes, G.; Yilgor, E.; Atilla, G.; Yilgor, I.; Beye, F. *Polymer* **2004**, 45, 6919.
 29. Zhu, G.; L.Tao. *Eur. Polym. J.* **2005**, 41, 1090.
 30. Garrett, J.; Runt, J. *Macromolecules* **2000**, 33, 6353.
 31. Hq, A.; Liu, H.; Huang, D.; Guo, S. *Eur. Polym. J.* **2001**, 37, 497.
 32. Thomas, S.; George, A. *Eur. Polym. J.* **1992**, 28, 145.
 33. Malaika, S.; Kong, W. *Polymer* **2005**, 46, 209.
 34. George, S.; Neelakantan, N.; Varughese, K.; Thomas, S. *J. Polym. Sci: Polym. Phys.* **1997**, 35, 2309.

35. Singh, D.; Malhotra, V.; Vats, J. *J. Appl. Polym. Sci.* **1999**, *71*, 1959.

Chapter 6

Surface and adhesion properties of methacrylic/urethane graft copolymers

6.1 Introduction

Adhesion is the intermolecular action at the interface of two surfaces.¹ It is a multi-disciplinary topic which includes surface chemistry, physics, rheology, polymer chemistry, stress analysis polymer physics and fracture analysis. Describing the mechanism of adhesion in simple terms is difficult due the complexity and evolving understanding of the subject. There is a range of adhesion mechanisms are based variously on diffusion, mechanical, molecular and chemical and thermodynamic adhesion phenomena.²⁻⁵

Applications for polyacrylate homopolymers and polyurethanes have shown remarkable growth over the last years. Many industrial applications require good adhesion properties. It is well known that the favourites general purpose adhesives are: the monomeric acrylates, such as super glue, which cure from monomer to polymer; the acrylics in solvent,⁶ Pu in solvent^{7,8} or a moisture curing grade of Pu; two part epoxy resins^{9, 10} and finally emulsion based polyvinyl acetates,¹¹ commonly known as wood glue.¹²

The major market is, however, solvent based and is dominated by acrylics with a low temperature solvent such as a MEK solvent mixture. Pu require a higher boiling solvent, which can be as exotic as n-methyl-2-pyrrolidone (NMP), where the solvent is mostly evaporated, the urethane heated and the two surfaces joined. This is a difficult high-tech glue to use, and not generally accepted for household use.

In this study the graft copolymer has the properties of both an acrylic and a urethane. Then to increase the solubility of the urethane in a common solvent, is pulled into solution by the acrylic part of the molecule. As the solvent evaporates two phases form and either phase can be continuous. For cost reasons preferable, but it is preferentially for price to have a continuous acrylic phase with nano inclusions of Pu, which means that either the acrylic or the urethane phase can associate with the surface to be glued. This has been proved previously in rolled steel research, by mixing three urethanes with different functionality and finding enrichment of the correct one at the adhesive surface phase and enrichment of the correct one at the air surface phase and modulus improvement of the entire adhesive film by enrichment of the high modulus component in between these.¹³ This has also been proven in early polycarbonate bullet proof-transparent sheets, where the soft silicone rubber required

needs to be soft, but bond securely to the polycarbonate.¹⁴ Block polymers of polycarbonate with silicone were used with excellent bullet-stopping effects, and no easy delamination.

A further advantage of the nano/micro inclusions are that they increase the modulus of the glue, as has been described earlier in this study (see Sections 4.6.1 and 5.6.1) and this relates directly to the strength of the adhesive bond. The fact that the acrylic is the larger component of the two phases means that poorly soluble urethane is drawn into solution by ether or ketone solvents, such as THF or MEK, which dissolve the acrylic and swell the urethane.

6.2 Surface properties

6.2.1 Introduction

The surface is the crucial part of a material in various applications, since it is the first contact with the environment. Therefore, the properties of the surface such as chemical structure, homogeneity, crystallinity, and the level of cohesive attractions between atoms and molecules, as well as the physical shape, provides much information about its reactions toward its surroundings.^{15,16}

Adhesion is strongly influenced by surface wettability; the adhesive spreads better (i.e. wetting the surface is better) on a more hydrophilic surface.¹⁷

Wetting is the extent or angle to which a liquid makes contact with a surface. This is characterized by the degree of direct interfacial contact and the ease with which it is achieved. Adhesion is the intimate sticking together of surfaces so that stress can be transmitted between the phases. It can be quantified by the amount of work required to pull the interface apart, when pulling the two separate surfaces. The surface wettability influences both adhesion and permeation.¹⁸⁻²¹

The surface free energy of solids is a characteristic factor which affects the surface properties and interfacial interactions such as adsorption, wetting, adhesion, etc.^{22,23} The surface free energy therefore is of interest in the field of adhesive technology, biomedical applications, cleaning procedures, or for the wettability of tribological systems.²⁴

6.2.2 Theoretical and background

For any material, the molecules in the bulk have no net force acting on them, while the ones at the surface encounter a net force inward. For solids, this force is called as “surface free energy” (SFE) or surface tension, and is defined as the amount of energy required to change the surface area of a material by one meter square. Knowing the SFE or not value of a material, one can predict whether the material is wettable by a certain liquid. Solids, which

have a similar SFE to or higher SFE than a liquid's SFE are wettable by that liquid.²⁵ The contact angle (θ) of a liquid drop is the angle formed by the surface and the tangent of the drop at the point that it touches the surface. A contact angle indicates the strength of non covalent forces between the liquid and the first monolayer of the material. The liquid drop spreads on the solid and wets the surface, in the case of strong interactions between phases.²⁶ A zero contact angles mean a strong interaction between the phases and complete wetting by the liquids.

SFE values can be determined by different methods.²⁷ All these methods are based on contact angle measurements, but they may have discrepancies in the results.^{15,27} In this study the harmonic mean approaches was used to measure the surface tension of UM and its graft copolymers.

In the harmonic mean approach the surface tension of a polymer can be divided into a non-polar dispersion component, γ^d , and a polar component, γ^p , $\gamma = \gamma^d + \gamma^p$

The harmonic mean is given in equation (1)

$$(1 + \cos \theta_i) \gamma_i = 4 \left[\frac{\gamma_i^d \gamma_s^d}{\gamma_i^d + \gamma_s^d} + \frac{\gamma_i^p \gamma_s^p}{\gamma_i^p + \gamma_s^p} \right] \quad (1)$$

If the subscript 1 expresses water, the surface tension, dispersion component, and polar components of water are: $\gamma_1 = 72.8, \gamma_1^d = 22.1, \gamma_1^p = 50.7$. If the subscript 2 expresses glycerol, the surface tension, dispersion component, and polar component of glycerol are: $\gamma_2 = 64, \gamma_2^d = 34, \gamma_2^p = 30$.

According to the above parameters and the contact angle θ_i of water on the surface of polymer and glycerol on the surface of polymer as well as the harmonic mean equation (1), two simultaneous equations can be obtained, one from the polymer and water, the other from the polymer and glycerol. The dispersion component γ_s^d and polar component γ_s^p of each polymer can be determined by solving the two simultaneous equations.

The contact angle (θ_i) for a sessile drop, is defined by the tangent at the air /liquid/ solid line of contact and line of contact and line through the base of liquid drop where it contacts the solid.²⁸ The contact angle of each polymer was calculated by the following equation:

$$\text{Contact angle } (\theta) = 2 \times \tan^{-1}(h/r) \quad (2)$$

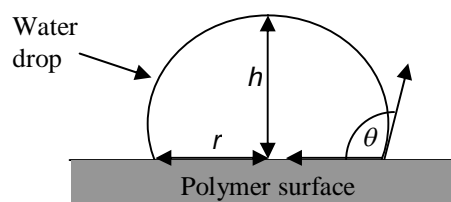


Figure 6.1: Image of a water drop showing the height and radius used in determination of the contact angle θ .

6.2.3 Experimental

6.2.3.1 Materials

Any consideration of adhesion mechanisms requires information about the physical and chemical properties of the adhering surfaces and the delamination surfaces in cases where adhesion has failed in use or as a result of mechanical testing. Urethane macromonomers (UM1 and UM2) and all their graft copolymers (PMMA-g-UM and PnBMA-g-UM2) were described previously in Chapters 4 and 5. Glycerol was product of Merck, deionized water (DDI), were obtained from a Millipore milli-Q purification system, and silicon oil was supplied by SA Silicones.

6.2.3.2 Optical contact measurement

Sample films of graft copolymer were prepared by melt pressing at temperatures between 40 and 200 °C. A 1 μL drop of water or glycerol was placed onto the sample film and the magnified image was captured using a Nikon SMZ-2T (Japan), model VCC 250C, digital video camera. Figure 6.1 shows a cartoon of a captured image. Included on the image are the parameters used to determine the static contact angle according to the relationship in Equation 1 below. PVR- plus software was used for imaging along with an Able Image analyzer (μ -labs) version V3.6, which enabled determination of the lengths associated with contact angle calculation. For the statistical approach, at least five (generally 8) values were measured for each liquid. Drops that had unsymmetrical forms (difference between the angles at both sides being higher than 5°) were excluded. The temperature of the environment was fixed at 20 °C. The contact angle results are given in Table 6.1.

6.2.3.3 Surface energy measurement

The surface energy of urethane macromonomers and methacrylic/urethane graft copolymer was determined via the measurement of contact angles of several of testing liquids (i.e. redistilled water, glycerol). The drop of the testing liquid ($V = 1 \mu\text{L}$) was placed on the polymer surface, and a contact angle of the testing liquid was measured. The surface energies of the polymer were evaluated using harmonic mean equation (1). In the calculations two simultaneous equations can be obtained, one from the polymer and water, the other from the polymer and glycerol. Windows Excel program was used.

In general, a polar and non-polar liquid are dispensed onto the sample surface with the angle that the liquid makes with the surface (as measured through the liquid) being recorded. Smaller contact angles indicate a more wetting surface with a higher surface energy and therefore a greater work of adhesion.²⁹ As surface energy and wettability are related to adhesion, OCA provides an indirect measure of adhesion, allowing for the comparison between the work of adhesion and direct adhesion methods.

6.2.4 Results and discussion

Optical contact angle analysis (OCA) is a surface sensitive technique which allows the surface energy of the investigated sample to be measured. The contact angle results are given in Table 6.1.

Table 6.1: Contact angle values of synthesized polymer

Sample code	UM% (wt %)*	Contact angle (θ_1) H ₂ O
UM1	100	74.2
PMMA	0	96.2
G10M1 (PMMA-g-UM1, 10 wt % UM1 feed ratio)	4.3	91.2
G25M1	19.2	83.5
G55M1	40.4	72.9
PnBMA	0.0	95.1
G10B1 (PnBMA-g-UM1, 10 wt % UM1 feed ratio)	4.2	89.1
G25B1	18.8	81.3
G55B1	42.6	75.0
UM2	100	75.1
PMMA	0	96.2
G10M2 (PMMA-g-UM2, 10 wt % UM2 feed ratio)	3.1	90.1
G25M2	20.4	85.2
G55M2	36.5	79.5
PnBMA	0	95.1
G10B2 (PnBMA-g-UM1, 10 wt % UM2 feed ratio)	6.2	90.1
G25B2	17.0	87.6
G55B2	38.0	78.8

* All the weight percentages were calculated using the ¹H-NMR technique, as described in section 4.5.3.7 and section 5.5.7.

Figure 6.2(a-d) shows the contact angles of re-distilled water deposited on the surface of graft copolymer surface films vs the UMs content. The contact angles of water decreased when the amount of UM was incorporated into the PMMA or PnBMA backbones was increased. The contact angles of PMMA-g-UM1 copolymers decrease from 96.19° for only PMMA, to 72.91° for 40.4 wt % UM1 in the graft copolymer, and the contact angle of PnBMA-

g-UM1 copolymers decrease from 95.13° for only PnBMA, to 75.02° for 42.55 wt % UM1 in the graft copolymer. On other hand the contact angles of PMMA-g-UM2 copolymers decreased from 96.19° for only PMMA, to 79.46° for 36.50 wt % UM2 in the graft copolymer and the contact angle of PnBMA-g-UM1 copolymers decreased from 95.1° for only PnBMA, to 78.84° for 38.00 wt % UM2 in the graft copolymer. Since the surface energies of PMMA and PnBMA are lower than the surface energies of UM1 and UM2, the PMMA or PnBMA segments migrate away from the top surface to leave a hydrophilic-enriched layer, which can interact with the water. Micro-phase separation in graft copolymers occurs even at relatively low UMs content due to dissimilarity between the chemical structures of the PMMA or PnBMA, and UMs as has been proven by DMA and TEM results (see DMA and TEM results in Chapters 4 and 5).

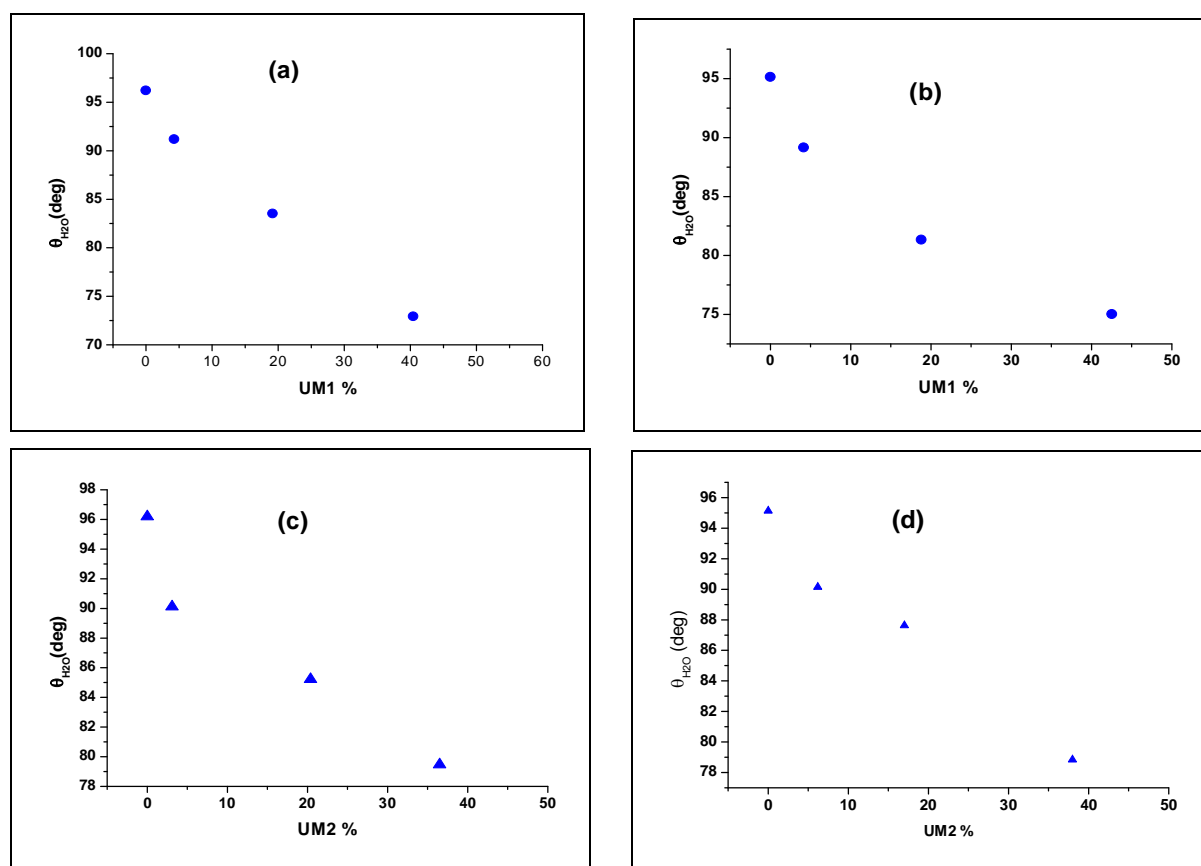


Figure 6.2: Contact angles of water vs the content of the urethane macromonomer in graft copolymerization (a) contact angles of water vs. UM1/MMA content, (b) contact angles of water vs. UM1/n-BMA content (c) contact angles of water vs. UM2/MMA feed ratio (d) contact angles of water vs. UM2/n-BMA content.

The surface energy of the graft copolymers was determined by the harmonic mean method vs. the content of the UMs incorporated in the graft copolymer are shown in Table 6.2. This table lists the surface tensions of each polymer measured by the contact angle method, where the subscript 1 expresses water, and the subscript 2 expresses glycerol.

Table 6.2: Contact angles and surface tensions synthesized graft copolymers

Sample code	θ_1	θ_2	γ_s^d	γ_s^p	γ_s (mN.m ⁻¹)
UM1	74.2	62.2	26.1	9.8	35.9
PMMA	96.19	84.5	20.7	2.4	23.1
PnBMA	95.13	83.2	21.6	2.5	24.1
G55M1	72.91	73.4	4.9	26.5	31.4
G55B1	75.02	74.5	5.8	23.4	29.2
UM2	75.13	67.2	21.7	11.2	32.9
G55M2	79.46	75.9	9.1	25.5	25.5
G55B2	78.84	78.7	4.8	21.6	26.4

Table 6.2 shows that, the surface energy of all synthesized graft copolymer increases significantly with the concentration of UMs. The surface energy of PMMA-g-UM1 copolymers increases from 23.14 mN.m⁻¹ for only PMMA, to 31.42 mN.m⁻¹ for 40.44 wt % of UM1 in the graft copolymer and the surface energy of PnBMA-g-UM1 copolymers increases from 24.07 mN.m⁻¹ for only PnBMA, to 29.23 for 42.55 wt % of UM1 in the graft copolymer. On the other hand the surface energy of the PMMA-g-UM2 copolymers increase from 23.14 mN.m⁻¹ for only PMMA, to 25.52 mN.m⁻¹ for 36.50 wt % of UM2 in the graft copolymer and the surface energy of the PnBMA-g-UM1 copolymers increase from 24.07 mN.m⁻¹ for only PnBMA, to 26.43 mN.m⁻¹ for 38.0 wt % of UM2 in the graft copolymer. This indicates that the phase separated phases need much longer relaxation times for the urethane component to play a decisive role by rising to the surface.

In addition, the increase in the polar and decrease in the dispersive forces of surface energy for all graft copolymer samples in much the same order,. It says that the surfaces become more hydrophilic with increasing polar share, as expected, i.e. the contact angle of water drops falls due to the better wetting (as the UM content into graft copolymer increases). High energy values are favourable for wetting a surface. Polar interactions due to dipoles also have much higher bonding energies than dispersion forces; so that one can also expect high polar energy contributions to lead to a good adhesion. In other words, smaller contact angles indicate a more wetting surface with a higher surface energy and therefore a greater work of adhesion.

6.3 Adhesive properties

6.3.1 Introduction

An adhesive is defined as a material which, when applied to a substrate surface, can join two surfaces together and resist separation. Adhesive is the general term, and includes cement, glue, paste, etc. These terms are all used essentially interchangeably. Various description adjectives are often applied to the term adhesive to indicate certain characteristics, for example, its physical form, e.g. liquid adhesive, film adhesive; its chemical form, e.g. epoxy adhesive; to indicate the materials bonded, e.g. metal-to-metal adhesive, paper adhesive; or to show the conditions of use, e.g. cold-setting adhesive, solvent-based adhesive.

On other words, adhesion is the bond strength measurement of a coating to a substrate. When an adhesive is bonded to an item or surface, numerous physical, mechanical and chemical forces come into play, which may have an affect on each other. These need to be tested before a product can be used.

Many direct measurements provide qualitative data but tests such as T-peel and pull tests provide a quantitative measure of adhesion. Repetition is required to provide consistent results.

6.3.2 Theoretical background

The T-peel test has been used for many years by the adhesives industry to measure the energy required to separate two bonded layers. Proper interpretation of the test requires knowledge of how much energy is required to plastically deform the peeled foil. Aluminum foils are sometimes used, whose deformation behavior can be modeled as ideally plastic, and several models have been developed to account for the work of deformation based on that behaviour.^{30,31}

The peel test is an excellent example of an adhesion test whose values are only useful in a relative sense. Adhesive tape is placed and pressed on the surface of the sample to be tested. Peel strength, or adhesion energy (GIC), is generally used to measure the adhesive bond strength of a material, which is typically an adhesive. Figure 6.3 shows a typical graph of a peel strength test.

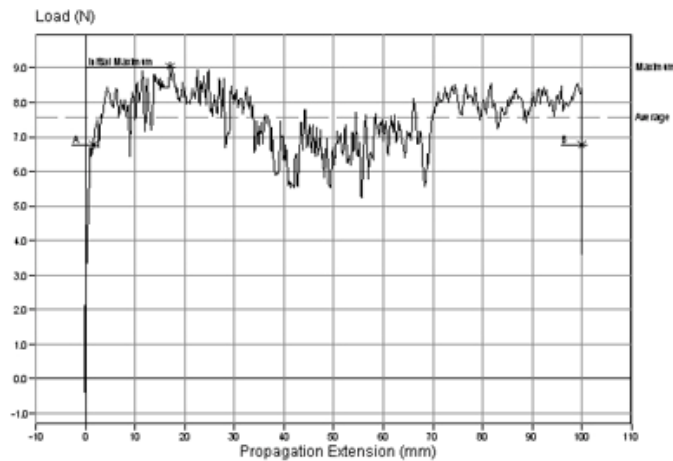


Figure 6.3: Typical graph showing the results of a T-peel strength test.

Several typical peel tests have been used to measure the peel strength. Usually the peel angle θ is kept constant during the test. Various mixed loadings can be obtained at different angles. The T-peel test is the most widely used method by industry for determining the relative peel resistance of adhesive bonds between flexible adherents. This test geometry has been adopted by most standards bodies and is widely used by industry to evaluate the environmental durability of adhesively bonded systems. The simplicity and low costs associated with specimen manufacture, testing and data analysis has contributed to the widespread use of this method. Figure 6.4 shows a schematic view of a T-peel test for the measurement of peel strength.

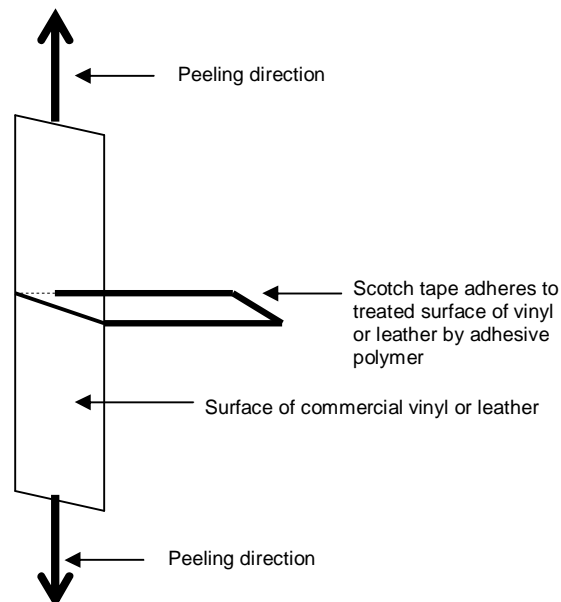


Figure 6.4: Schematic view of the set-up used for the T-peel test, for the measurement of peel strength.

In the T-peel test, the peel strength or peel energy is the average load per unit width of bond line required to separate bonded materials.

$$\text{Peel energy} = 2F/W \quad (3)$$

where the F is average peel force and W is the width of the adhesive bond i.e leather or vinyl

6.3.3 Experimental

6.3.3.1 Adhesive preparation

Test samples were prepared by dissolving PMMA, PnBMA, and their graft copolymers (which have high percentages of UM2 content [UM1 copolymer only dissolved in a strong solvent like NMP i.e. MEK was/is not a good solvent for this adhesive]) into a solvent comprising 50 wt % THF, 25 wt % acetone and 25 wt % ethanol. The solid content of the sample was 35 wt %.

6.3.3.2 Peel test

The substrates used for T-peel tests i.e. commercial leather or vinyl, were cut to dimensions of 8 cm x 2 cm. The adhesive coating area was 6 cm long. The sample of copolymer/solvent glue was then placed on the commercial leather or vinyl to form the testing sample, which was then conditioned at room temperature using a pressure of a 5 kg weight on the test piece.

A T-peel test was carried out using a Universal Testing Machine (UTM) (LLOYD Instruments-Model LRX 5) at a rate of 50 mm/min at room temperature. Scotch tape (width 2.5 cm) was stuck over a length of 4.0 cm on the sample polymer film. Care was taken to ensure that there were no air gaps or wrinkles. The sample kept under a pressure of 1.0 kg for 10 min. The T-peel test was carried out after fixing one end of the sample in one jaw of the instrument and the Scotch tape end with other piece of sample adhered to it in the other jaw, as in Figure 6.4. T-peel strengths are reported as force of peel per millimeter of sample width. For better accuracy of results the T-peel test was repeated five times for each sample and the average T-peel strength was recorded. Table 6.3 shows the results of calculations of peel strength of commercial vinyl and leather for the two synthesized graft copolymers containing different amounts of UM2.

6.3.4 Result and discussion

Figure 6.5 shows the dependence of the T-peel strength of the adhesive joint of the methacrylate/urethane graft copolymer vs. content of UM2, using commercial vinyl or leather as substance in the T-peel test. It is seen that the peel strength of the adhesive joint of the methacrylate/urethane graft copolymer increases with an increases in UM2 content over the entire concentration range. The fact that peel strength of the adhesive joints increases with

an increase in UM2 content reflects the modulus increase of the adhesion. Figure 6.5(a) shows the dependence of the peel strength of the adhesive joint PMMA/UM2 graft copolymer vs. content of UM2 using commercial vinyl or leather as substance in the T-peel test. A maximum value is observed for the PMMA/UM2 graft copolymer at 36.5 wt % of UM2 in both leather and vinyl. Comparing PMMA with PMMA-g-UM2 copolymer containing 36.5% of UM2 shows that the peel strength of the adhesive joint to commercial vinyl or leather increased 1.4 and 1.9 times respectively. The increase of peel strength to the maximum value is attributed to the modulus increase as well as the increasing wettability of the adhesive which enhances the peel adhesion property of the adhesive. The final increase in the UM2 content decreases the compatibility of copolymer parts of PMMA and UM2 as reflected by the higher peel strength. Similar observations are also obtained for PnBMA/UM2 graft copolymer. Figure 6.5(b) shows the dependence of the peel strength of the adhesive joint of the PnBMA/UM2 graft copolymer vs. content of UM2 using commercial vinyl or leather as substance in the T-peel test. Comparing PnBMA homopolymer with PnBMA-g-UM2 copolymer containing 0.0% of UM2 shows that the peel strength of adhesive joint to commercial vinyl or leather increased 1.2 and 1.2 times, respectively. This increase in the peel strength is due to increasing wettability of the adhesive which enhances the peel adhesion property of the adhesive. All the peel strength results for all the synthesized PnB-methacrylate/UM2 graft copolymers which contain different amounts of UM2 are shown in Table 6.3. The main increase is probably because of the modulus (stiffness) increase as the UM2 content increases.

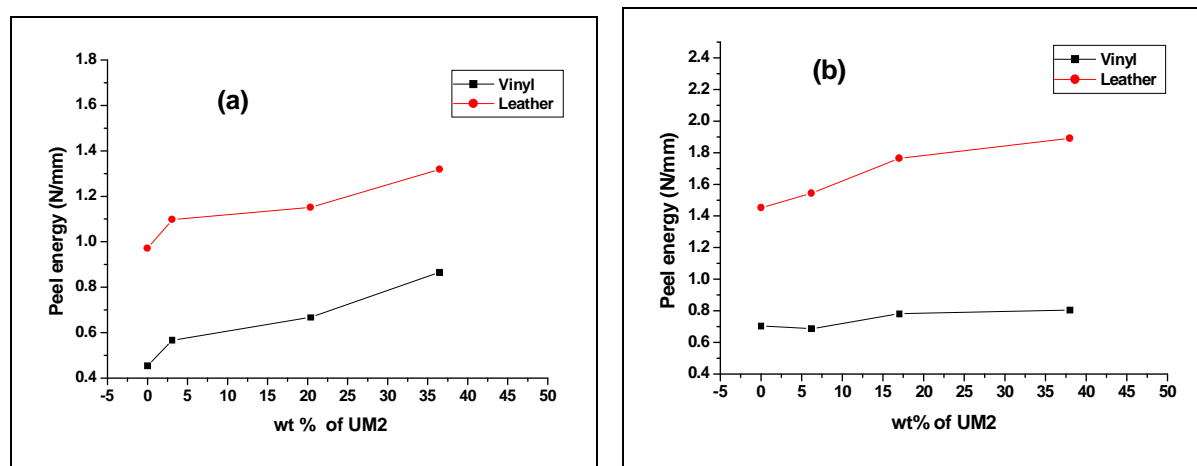


Figure 6.5: Peel strength of (a) PMMA-g-UM2 and (b) PnBMA-g-UM2 versus UM2 content.

Table 6.3: Peel energy of commercial vinyl and leather for synthesized graft copolymer containing different amount from UM2.

	Sample code	UM2 incorporated into copolymers as calculated by ¹ H-NMR (wt %)	Force (N) (vinyl)	width	Peel energy (N/mm)	Force (N) (Leather)	width (mm)	Peel energy (N/mm)
PMMA-g-UM2	PMMA	-	4.545	20.2	0.455	10.39	21.4	0.971
	G10M	3.1	5.870	20.7	0.567	11.09	20.2	1.098
	G25M	20.4	7.230	21.0	0.668	11.98	20.8	1.151
	G55M	36.5	9.576	22.1	0.866	13.33	20.1	1.319
PnBMA-g-UM2	PnBMA	-	6.950	19.7	0.705	14.34	19.7	1.452
	G10B	6.2	7.320	21.3	0.687	15.82	20.5	1.543
	1025B	17.0	7.850	20.1	0.781	16.91	20.2	1.764
	G55B	38.0	9.130	22.8	0.805	19.58	20.7	1.891

6.4 Conclusions

The surface, modulus (stiffness) and the adhesive properties improved as the amount of the UM incorporated in the methacrylate/ urethane graft copolymer increased.

(a) Values of the contact angles of the water decreased by increasing the urethane macromonomer content in the methacrylate/urethane graft copolymer i.e. wets easier, more hydrophilic and stiffer.

(b) Surface tension increased by increasing the urethane macromonomer content in methacrylate/ urethane graft copolymer.

(c) A maximum value of peel strength is also observed with the maximum UM2 content in the methacrylate/urethane graft copolymer.

6.5 References

1. Poisson, C.; Hervais, V.; Lacrampe, M.; Krawczak, P. *J. Appl. Polym. Sci.* **2006**, 101, 118.
2. Beholz, B.; Aronson, C.; Zand, A. *Polymer* **2005**, 46, 4604.
3. Qin, R.; Schreiber, H. *Colloids Surf.* **1999**, 156, 85.
4. Lippert, T.; Dickinson, J. *Chem. Rev.* **2003**, 103, 453.
5. Sathyanarayana, M.; Yaseen, M. *Progr. Org. Coat.* **1995**, 26, 275.
6. Dunky, M.; Pizzi, A. *Appl. Surf. Chem.* **2002**, 23, 1039.
7. Somani, K.; Kansara, S.; Patel, N.; Rakshit, A. *Int. J. Adhes. Adhes.* **2003**, 23, 269.
8. Desai, S.; Patel, J.; Sinha, V. *Int. J. Adhes. Adhes.* **1990**, 10, 225.
9. Raftery, G.; Harte, A.; Rodd, P. *Int. J. Adhes. Adhes.* **2009**, 29, 580.

10. Davis, G. *Int. J. Adhes. Adhes.* **1990**, 10, 263.
11. Haaga, A.; Geeseya, G.; Mittleman, M. *Int. J. Adhes. Adhes.* **2006**, 26, 177.
12. Frihart, C. R., *Hand book of Wood Chemistry and Wood Composites*, CRC: USA, 2005; p 216.
13. Mequanint, K. MSc thesis, University of Stellenbosch, South Africa, December 1997.
14. Biron, M., *Thermoplastics and Thermoplastic Composites*. Elsevier Science Publishing Company 2007; p 217.
15. Shimizu, R.; Demarquatte, R. *J. Appl. Polym. Sci* **2000**, 76, 1831.
16. Valsesia, A.; Silvan, M.; Ceccone, G.; Rossi, F. *Surf. Sci.* **2004**, 560, 121.
17. Callow, A.; Callow, M.; Ista, L.; Lopez, G.; Chaudhury, M. *J. R. Soc. Interface* **2005**, 2, 319.
18. Kallish, K., Annual Technical Conference, Society of Plastics Engineers. Washington D.C., May 1985.
19. Hansen, C., *Chemtech*, September 1972; p 547.
20. Krevelen, D., *Properties of Polymers*. Elsevier Science Publishers B.V: Amsterdam, 1990; p 228.
21. Breiggs, D., *Industrial Adhesion Problems*. UK, Oxford, 1985.
22. Lugscheider, E.; Bobzin, K.; Moeller, M. *Thin Solid Films* **1999** 355, 367.
23. Luner, P.; Oh, E. *Colloids Surf., A* **2001**, 181, 31.
24. Lugscheider, E.; Bobzin, K. *Surf. Coat. Technol.* **2001**, 142, 755.
25. Cantin, S.; Bouteau, M.; Benhabib, F.; Perrot, F. *Colloids Surf.* **2006**, 276, 107.
26. Kaczmarek, H.; Kowalonek, J.; Szalla, A.; Sionkowska, A. *Surf. Sci.* **2002**, 507, 883.
27. Ozcan, C.; Hasirci, N. *J. Appl. Polym. Sci.* **2007**, 108, 438.
28. Bascom, W. D. *Adv. Polym. Sci.* **1988**, 85, 89.
29. Maier, G., Operating manual OCA, Germany: Dataphysics Instruments, 2002.
30. Crocombe, A.; Adams, R. *J. Adhesion* **1982**, 13, 241.
31. Crocombe, A.; Adams, R. *J. Adhesion* **1981**, 12, 127.

Chapter 7

Conclusions and Recommendations

7.1 Conclusions

1. Two types of linear UMs were successfully synthesized by the polyaddition polymerization of 4,4'-methylenediphenyl diisocyanate (MDI) with ethylene glycol (EG) and MDI with neopentylglycol (NPG) via the prepolymer method and successfully terminated with 2-hydroxy ethylacrylate (2-HEA) and methanol (MeOH), to yield predominantly monofunctional UMs, as was confirmed by MALDI-TOF-MS.
2. Three different synthesis methods were used to eventually obtain the desired structure of urethane macromonomers (where 2-HEA reacts from one side and MeOH reacts from the other side). In the first method, 2-HEA was added to urethane prepolymer all at once, followed by the addition of MeOH. In the second method, 2-HEA was added dropwise to the urethane prepolymer, followed by MeOH. In the third method, 2-HEA and MeOH were added together to the urethane prepolymer, in fractions. The first method was eventually considered the best method as it gave the highest yield of both graft copolymers, PMMA-g-urethane and PnBMA-g-urethane. Exhaustive drying allowed optimization of the structures of UMs as seen by MALDI-TOF-MS.
3. Detailed analysis revealed successful preparation of both UMs. MALDI-TOF-MS analysis prove that the major product is the 2-HEA chain end/methoxy chain end but that the di methoxy gives sizable peak while only a small di-HEA peak is present. The successful synthesis of the desired structures of UM1 and UM2 were then confirmed by FTIR, $^{13}\text{C-NMR}$, $^1\text{H-NMR}$ and SEC analysis.
4. The PMMA-g-urethane and PnBMA-g-urethane copolymers were successfully synthesized by the macromonomer technique in solution free radical polymerization (in which AIBN was used as initiator and DMF as the solvent).
5. The obtained graft copolymer molecular structures were fully characterized by SEC with double detectors (UV and RI), FTIR, $^1\text{H-NMR}$, $^{13}\text{C-NMR}$, HPLC, after removing nonfunctional (unreactive) as well as unreacted urethane macromonomers.
6. The weight percentages of the graft copolymers (containing urethane macromonomers), after unreacted urethane macromonomers had been removed, were determined by $^1\text{H-NMR}$, UV/Vis and FTIR (calibration curves were used for the

later two techniques). The weight percentages calculated for $^1\text{H-NMR}$, UV/Vis, and FTIR agreed well. Weight percentages of urethane macromonomer increased with increase in the macromonomer weight percentage in the feed.

7. Thermal stability, determined by TGA, of PMMA-g-urethane and PnBMA-g-urethane copolymers improved as the amount of urethane macromonomer increased in the polymerization feed, due to higher incorporation of the urethane macromonomer.
8. Storage modulus (stiffness) of all synthesized PMMA-g-urethane and PnBMA-g-urethane copolymers increased as the concentration of urethane macromonomer in the copolymerization feed increased, due to more urethane macromonomer incorporation into the PMMA and PnBMA backbones.
9. Phase separation:
 - In the case of PMMA-g-UM1 and PnBMA-g-UM1 copolymers, two glass transitions temperatures corresponding to the PMMA or PnBMA and UM1 fractions, respectively, were recorded using DMA. This indicated that the PMMA or PnBMA and UM1 moieties exhibit microphase separation. This result was confirmed by DSC and TEM images.
 - In the case of the PMMA-g-UM2 and PnBMA-g-UM2 copolymers a large measure of compatibility was observed. This result was confirmed by DMA and DSC. The T_g value increased as the concentration of urethane macromonomer increased, in both the PMMA-g-UM2 and PnBMA-g-UM2 copolymers.
 - In the case of one of the PMMA-g-UM2 and PnBMA-g-UM2 copolymers, two glass transitions temperatures were observed, corresponding to the PMMA or PnBMA and UM2 fractions, respectively. The result also indicated that PMMA or PnBMA and UM2 moieties can exhibit microphase separation. This result was found when the amount of this UM used in the copolymerization feed was increased to 55 wt %. This result was confirmed by DMA, DSC and TEM .
10. Surface and adhesive properties were improved as the amount of UM2 content increased in the graft copolymer. Smaller contact angles result giving a surface with a higher surface energy and increase in T-peel strength was observed as the amount of UM2 content in the graft copolymer increased.

7.2 Recommendations

- ❖ Improve the desired phase separation properties obtained from the synthesized urethane macromonomers especially in terms the monomers used and their cost.
- ❖ Investigate possible applications for PMMA-g-urethane and PnBMA-g-urethane products, both in compatible and incompatible forms.
- ❖ Synthesize the graft copolymers in emulsions for use as coatings and for glue.

Patent aspects and publishes during this study

PROVISIONAL PATENT

Title

Solvent based adhesive formulation

Motivation

It is known that in general purpose adhesives, the favourites are: the monomeric acrylates, such as super glue, which cure from monomer to polymer, the acrylics in solvent, polyurethane in solvent or a moisture curing grade of polyurethane; two part epoxy resins and finally emulsion based polyvinyl acetates, commonly known as wood glue.

Where now can one look for newer materials?

There is an industrial adhesive and pigment based binder based on urethane acrylics, which cure to do the job required. These are also advances in the patent literature for polyurethanes with polyacrylic end groups in emulsion as polyester replacement in rolled steel coating and rolled aluminium coating.

The major market however, is solvent based and is dominated by acrylic using a low temperature solvent such as a MEK solvent mixture. The urethane requires a higher boiling solvent, which can be as exotic as NMP. Here the solvent is mostly evaporated, the urethane heated and the two surfaces joined. This is a difficult high-tech glue to use, not generally accepted for household use. So where lies the obvious solution?

This is to macromolecular engineer a graft or block polymer that has the properties of both an acrylic and a urethane and then to increase the solubility of the urethane by it being pulled into solution by the acrylic part of the molecule.

Now the adhesive molecule will show the following advantages:

1. Two phases and it can be chosen to make either phase continuous, but it is preferentially for price to have a continuous acrylic phase with nano inclusions of polyurethane. What does this mean? It means that either the acrylic or the urethane phase can associate with the surface to be glued. This we have proved previously in rolled steel research by mixing three urethanes with different functionality and finding enrichment of the correct one at the adhesive phase and enrichment of the correct one at the surface phase and modulus improvement of the entire adhesive film by enrichment of the high modulus component in between these.

This has also been proven in early polycarbonate bullet proof transparent sheets, where the soft silicone rubber required needed to be soft, but bond securely to the polycarbonate. Here block polymers of polycarbonate with silicone were used with excellent bullet stopping effects, no easy delamination. It is this concept that is being used.

A further advantage is the nano inclusions increase the modulus of the glue and this relates directly to the strength of the adhesive bond.

The fact that the acrylic is in the larger component of the two phase's means that poorly soluble urethane is drawn into solution by ether or ketone solvents, such as THF or MEK.

Claim 1: Preparation of polyurethane macromers with a large percentage of monofunctionality. A macromer of urethane can be four to 32 units long, preferably, although longer to 100 is possible, and 16 to 32 is preferred. The ends will incorporate and isopropyl dead terminated group and an acrylic reactive group. There will be urethane, which is not active, present in the mixture and a small percentage of urethane with two reactive groups, but in a too small a quantity to cause gelling during polymerisation.

Claim 2: The isocyanates used include TDI, MDI, The alcohol used is dimethylene diglycol, ethylene glycol, For good phase separation we have found that MDI plus dimethyl diglycol tends to give better phase separation and better crystallisation of the urethane domains.

Claim 3: A process whereby the macromonomer is polymerised with butyl acrylate, methyl methacrylate or styrene or with other monomers added at their effective loadings up to 8% generally for special adhesive purposes, e.g. for ceramic tiles. These monomers are added to the macromer in the ratio required and the polymerisation is carried out.

Two types of glue are now possible, a more technical glue, where unreacted macromers are removed (simple solvent process) or a general purpose adhesive where they are not removed with not too much detriment to properties (since the polyurethanes cocrystallise).

Claim 4: To dissolve the urethane acrylic graft polymer in a suitable mixed ether or ketone solvent offering a range of volatilities to best suite a general purpose adhesive.

Claim 5: The fact that the polyurethane phase can wet a surface often better than the acrylic phase will mean that it both assembles at the surface for better adhesion and crystallises out as a second phase which is highly reinforcing for the glue, especially because the phase is a crystalline nanophase.

Claim 6: That this glue now expands the applicability of the acrylic from paper, card board, leather, wood, metal, etc. into the field of polyurethanes which covers all these and bonds to soft and hard vinyl. This material is best described in the following examples of synthesis of the polyurethane, of the graft copolymers, of SEM micrographs of the two phases, the surface tension of the glue and the adhesive tests of the glue based on enhancing and receding contact angles as well as Instron data measured in the tear strength mode of adhesive testing.